



The neuroendocrine control of animal size, body proportion and symmetry

Memoria de Tesis Doctoral presentada por
Sergio Juárez Carreño

Thesis director:

María Domínguez Castellano

Thesis Co-director:

Javier Morante Oria



INSTITUTO DE NEUROCIENCIAS



**EXCELENCIA
SEVERO
OCHOA**

Centro de Excelencia
«Severo Ochoa»
2014-2018



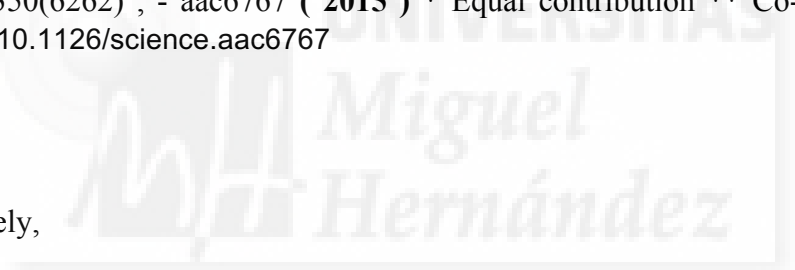
San Juan de Alicante, 28 of May 2018

To whom it may concern:

The doctoral thesis developed by me, Sergio Juárez Carreño, with the title: The neuroendocrine control of animal size, body proportion and symmetry, is a compendium of publications and includes the following publication in which I am the first author:

-Vallejo DM.* , Juárez-Carreño S.* , Bolívar J., Morante J.** , Domínguez M.** " *A brain circuit that synchronizes growth and maturation revealed through Dilp8 binding to Lgr3.* " **Science** . 350(6262) , - aac6767 (2015) * Equal contribution ** Co-corresponding authors. doi: 10.1126/science.aac6767

Yours sincerely,



Sergio Juárez Carreño

San Juan de Alicante, 28 of May 2018

To whom it may concern:

The doctoral thesis developed by me, Sergio Juárez Carreño, with the title: The neuroendocrine control of animal size, body proportion and symmetry, includes the following publication in which I am the first author and I declare that these publications will not be used in any other thesis and the agreement with my director Maria Dominguez and Co-director Javier Morante:

-Vallejo DM.* , Juarez-Carreño S.* , Bolivar J., Morante J.** , Dominguez M.** " *A brain circuit that synchronizes growth and maturation revealed through Dilp8 binding to Lgr3.* " **Science** . 350(6262) , - aac6767 (**2015**) * Equal contribution ** Co-corresponding authors. doi: 10.1126/science.aac6767

Yours sincerely,

Fdo:Sergio Juárez Carreño

Fdo: Maria Dominguez Castellano

Fdo: Javier Morante Oria

D^a María Domínguez Castellano, Profesor de Investigación del Consejo Superior de Investigaciones Científicas (CSIC),

AUTORIZA la presentación de la Tesis Doctoral titulada: `` The neuroendocrine control of animal size, body proportion and symmetry´´ , realizada por D^o Sergio Juárez Carreño, bajo mi inmediata dirección y supervisión como directora de su tesis Doctoral en el instituto de Neurociencias (CSIC-UMH) y que presenta para la obtención del grado de Doctor por la Universidad Miguel Hernández.

Y para que conste, a los efectos oportunos, firma el presente certificado en San Juan de Alicante.

Fdo. María Domínguez Castellano



Dº Javier Morante Oria, Científico titular del Consejo Superior de Investigaciones Científicas (CSIC),

AUTORIZA la presentación de la Tesis Doctoral titulada: `` The neuroendocrine control of animal size, body proportion and symmetry´´ , realizada por Dº Sergio Juárez Carreño, bajo mi inmediata dirección y supervisión como co-director de su tesis doctoral en el instituto de Neurociencias (CSIC-UMH) y que presenta para la obtención del grado de Doctor por la Universidad Miguel Hernández.

Y para que conste, a los efectos oportunos, firma el presente certificado en San Juan de Alicante.

Fdo. Javier Morante Oria



El catedrático Miguel Valdeolmillos López, Director del programa de doctorado en Neurociencias del Instituto de Neurociencias de Alicante, centro mixto de la Universidad Miguel Hernández (UMH) y de la Agencia Estatal Consejo Superior de Investigaciones Científicas (CSIC),

CERTIFICA:

Que la Tesis Doctoral titulada: `` The neuroendocrine control of animal size, body proportion and symmetry`` ha sido realizada por D^o Sergio Juárez Carreño, bajo la dirección de D^a María Domínguez Castellano como directora y D^o Javier Morante Oria, como co-director y da su conformidad para que sea presentada a la comisión de Doctorado de la Universidad Miguel Hernández.

Y para que conste, a los efectos oportunos, firma el presente certificado en San Juan de Alicante.

Fdo. Miguel Valdeolmillos López



A mi padre, madre y hermana



AGRADECIMIENTOS

Año 2012, cuando me encontraba acabando la carrera de biología tenía que ir pensando en qué hacer con mi futuro y plantearme como conseguirlo. Lo único que tenía claro, incluso antes de empezar la carrera, era que mi objetivo era la investigación, y la forma de llegar a ello era hacer un doctorado.

En Octubre del 2012, llegue al Instituto de Neurociencias para cursar mi Master. Comencé en el laboratorio de Javier Sáez, lugar en el que me sentí muy bien recibido, pero me di cuenta que no era exactamente lo que buscaba ... me encontraba muy cerca de un laboratorio que conocía desde hace años, y por alguna razón que aun hoy no se explica, nunca me atreví a escribir para solicitar un puesto de doctorado. Pensaba que en ese laboratorio yo no estaría a la altura, como muchos profesores de la Universidad de Alicante se hartaban de decirme. Pero como soy una persona de convicción y con valentía, en un seminario, en enero del 2013 decidí ir a hablar con su investigadora principal. Ella era María Domínguez, y es justo ahí donde empezó toda la historia que estoy a punto de terminar.

En primer lugar, y como no podía ser de otra manera, agradezco a María Domínguez que me recibiera aquel día con los brazos abiertos y con total sinceridad. Me dijo que no habría problema en que pudiese realizar mi Trabajo Fin de Master en su laboratorio, y que podría empezar en febrero del 2013. Me encantaba todo de ese laboratorio, la genética con *Drosophila*, la biología molecular y, sobre todo, lo bien acogido que me sentí por todos mis compañeros. Por fin encontré un lugar donde me sentía cómodo. Cuando María me propuso que hiciera mi Doctorado en su laboratorio no dude ni un momento en decirle que sí, que me quedaba, y cinco años después tengo mucho que agradecerle. Me siento orgulloso de la confianza que depositó en mí, ya que me propuso como tema de tesis un proyecto muy ambicioso y competitivo, tanto dentro como fuera de mis fronteras. Le agradezco que me haya dejado ser libre en la toma de decisiones en los experimentos y la dirección que ha tomado mi proyecto de tesis doctoral. También le agradezco que me haya ayudado a cumplir unos cuantos sueños que tenía en mente desde que era joven, como poder viajar a EEUU. Aún recuerdo nuestra llegada a Chicago, nunca se me olvidara, y es que fue extremadamente divertida la situación que nos encontramos. Pero sobre todo le agradezco que me diera la oportunidad de haber podido vivir en Nueva York durante cuatro meses, haciendo la estancia en una de mis universidades más deseadas, Rockefeller University, que sin lugar a dudas ha sido una de las mejores experiencias de mi vida y que me ha marcado. En definitiva, le agradezco que me haya llevado a lo que soy hoy en día. María, te agradezco que me hayas dado la oportunidad de empezar mi tesis doctoral y que ello me haya llevado a empezar este camino, que a saber dónde me acabara llevando.

Gracias a Javier Morante, que se ha convertido en uno de mis grandes apoyos en esta etapa. Le agradezco, ante todo, su compromiso conmigo y con mi trabajo. Él ha sido una de las personas que, en mis momentos bajos, ha estado dispuesto a escucharme, a aconsejarme cómo atajar el problema, y a explicarme cómo funciona este mundo y esta vida. En Javier he encontrado un ejemplo de lucha y superación. Le agradezco su tiempo en la discusión sobre experimentos y discusión de resultados, y su ayuda en la corrección de esta Tesis Doctoral que me dispongo a defender. Te agradezco tu actitud cercana y que me hayas comprendido en los momentos buenos y en los malos, que eso es algo difícil de encontrar en un compañero de trabajo. En definitiva, te agradezco que me hayas ayudado a acabar esta pequeña historia.

Por otro lado, tengo mucho que agradecer a mis compañeros de laboratorio, a los que me encontré cuando empecé y a los que fueron llegando en mitad de camino. En primer lugar me vienes tú a la mente, Verónica Miguela. No hay ni habrá espacio suficiente para poder escribir todo lo que te agradezco, así que intentaré ser breve, aunque me cueste. Cuando llegué al laboratorio sentí una química especial contigo. Tú fuiste una de las personas que me hizo sentir uno más nada más aterrizar en el *labo*. Enseguida me sentí muy cómodo contigo, te contaba todo lo que me ocurría, mis *eureka*, y mis fracasos y frustraciones... que ha habido muchas como ya sabes, pero siempre estabas ahí para animar y compartir las penas como una verdadera amiga. Recuerdo con mucha nostalgia cuando, a las 7 de la tarde, teníamos nuestro momento *Crystal Fighters* y su *Love Natural*. Echo mucho de menos esos momentos contigo, o poder irme a tomarme una birra y ahogar las penas que nos generaban de vez en cuando. Recuerdo como me recibisteis Edu y tú en Nueva York y todo lo que me ayudasteis. Gracias a vosotros el primer día allí fue memorable. Me llevasteis a la que sería mi casa durante mi estancia y me hicisteis la mejor ruta turística que alguien puede tener por Midtown... fue imposible tener a unos anfitriones mejores. También te agradezco que, aunque te fuiste para continuar tu camino, sigues ahí para seguir aconsejándome, ayudándome en mis momentos más bajos y, sobre todo, para ayudarme con la corrección de la tesis. Supongo que la experiencia compartida, a parte del cariño personal que me tienes, hace que puedas comprenderme en tantas cosas. Aun así, no he conocido persona más auténtica que tú, y me hace inmensamente feliz decirte que para mí eres una amiga de verdad y espero que sea para siempre.

A Diana Vallejo, le agradezco su ayuda y el apoyo que me transmitió en el trabajo que desarrollamos juntos durante mis dos primeros años de doctorado. Eres un claro ejemplo de cómo funciona la colaboración entre dos personas, y creo que ambos podemos estar muy orgullosos de ello. A Zeus Antonello, que su motivación y esfuerzo eran inspiradores. A Irene Gutiérrez, que eras otra de mis compañeras predilectas. Tú eres una de las personas con la que más tiempo he compartido dentro del laboratorio, y de ti he aprendido la constancia, la buena actitud ante las

cosas malas que ni controlamos, ni dependen de nosotros, y a volvernos locos por las tardes para descargar frustraciones. Eres un claro ejemplo de lucha y eso me motiva a seguir para adelante. A Pol Ramón, que eres todo un bonachón. Ya te expliqué que envidio tu forma de tomarte la vida, con tanta filosofía. Gracias por acompañarme durante cuatro largos años y por compartir conmigo pensamientos mutuos para levantarnos la moral. Eres todo un grande!!!!

A los que vinieron después. Lucía García, fuiste como un soplo de aire fresco en la laboratorio. A mi entender, no podemos ser más afines, nuestra locura, nuestras bromas y situaciones comunes en la vida te han hecho ser para mí una de las mejores cosas de este lugar en el que trabajamos. Me alegras las mañanas y las tardes. Como nos descuidemos, incluimos los ``findes''... Tú intentas hacerme ver el lado bueno de las cosas, y eso es de gran ayuda en este camino. A ti, Roberto, aunque no haya tenido el placer de conocerte mucho, te agradezco la perspectiva de no perder el tiempo en preocuparse por cosas que no dependen de uno mismo. Virginie Roure, te agradezco tus consejos sobre la vida científica y nuestras charlas sobre la vida, siempre con esa sonrisa característica que alegra el día en cuanto se te mira. A Dolors Ferres-Marco, gracias por tu espontaneidad. Cuando volviste de Rockefeller University, descubrí a una buena compañera, con mucha experiencia, la cual no ha dudado en echarme una mano cuando la he necesitado, y te agradezco, ante todo, tu apoyo en las malas rachas y tus consejos para mi futura estancia en Nueva York.

A mis chicas, las técnicas de laboratorio. A tí, Mari Martínez, como ya te he dicho, eres la abuela que siempre habría deseado tener. Me encanta que, con tu edad, seas tan comprensiva, moderna e intentes siempre aprender más. Eso, es algo que quiero recordar de ti cuando los años vayan sumando, porque al igual que tú, no quiero perder las ganas de superarse siempre a mi mismo. Te agradezco tu comprensión, tus ganas infinitas de escucharme y aconsejarme siempre desde la experiencia, por nuestras conversaciones sobre mi vida, que a ti te hacen reír tanto y a mi desahogarme sin ningún tipo de censura. En definitiva, te has convertido en alguien de mi familia. A Esther Ballesta, gracias por tu ayuda, por nuestras risas sobre la conducción de las personas (que ha sido un tema recurrente), y por nuestras charlas sobre la vida cotidiana y mis historietas, que siempre nos hemos echado unas buenas risas. Has sido una compañera maravillosa. Laura Mira, te agradezco tu constante positividad a la hora ver las cosas. A ver si es verdad que siendo así atraigo las cosas buenas, como siempre nos dices. Irene Oliveira, gracias por los consejos y por las experiencias compartidas.

Por ultimo quería darte las gracias a ti, Rosa Sánchez, por tu ayuda administrativa, tu forma imparcial de tratar diversos asuntos conmigo, y por ayudarme cada vez que pedía tu ayuda.

Te agradezco que me hayas comprendido, aunque a veces haya sido imposible por mi punto de vista opuesto.

Llegados a este punto, no me puedo olvidar de los amigos que se hacen en el instituto. Hay mucha gente a la que echare de menos. No podía empezar por otra persona que no fueras tú, Noelia Antón Bolaños. Uno hecha la vista atrás y se da cuenta de quienes son personas auténticas. Has estado a mi lado en los mejores momentos y en los peores (cuantas frustraciones compartidas ¿verdad?), compartiendo dudas y sueños futuros. Me alegro de que hayamos recorrido juntos este camino de principio a fin, de haber podido ver y vivir como te has hecho cada vez más fuerte y que me muestres que quien lucha consigue lo que se propone, aunque las piedras en el camino hagan mucho daño. Te mereces lo mejor, mi rubia!. Michal Lipinski, recuerdo como al principio no querías hablar conmigo en español...y ahora no paras!. De ti me llevo la tranquilidad y el lado positivo de todas las cosas. La verdad es que hace falta mucha más gente con tu punto de vista, y por ello es imposible no agradecerle a la vida el cruzarse en el camino con gente como tú. A Rocío González Martínez, que llegaste en febrero de 2016 a mi vida, justo en el momento que necesitaba un cambio en mi rutina. Desde ese día te hiciste indispensable en mi vida, sobre todo porque nunca en nuestra relación el trabajo era algo de lo que hablaríamos. Compartíamos más cosas vitales y ajenas a la tesis, las cuales nos han unido y no nos han separado (de hecho, quiero que te vengas conmigo a NY!). Te agradezco que me hayas dado tantos empujones hacia delante y nunca hacia atrás. Hay mucha más gente a la que agradecer, como Ana María de Torres Jurado, Sandra Manzanero Ortiz, Fran Gutiérrez Aviño, Rafael Susin Carmona, Alejandro Sempere, Irene Huerga Gómez, y Abraham Andreu entre otros. Gracias por hacerme la vida mas amena entre estas paredes y fuera de ellas.

En cuarto lugar a mi familia (Mis padres Jesús Juárez y Mari Carmen Carreño, y mi hermana Pilar Juárez). Ellos son mi sustento en este camino. Son los que realmente me aguantan, en mi mal humor, en mi alegría, en mis ambiciones. Ellos son los que realmente conocen como me afectan la frustración y la mayor de las alegrías... y es que no tengo término medio. Ellos saben que siempre estoy agradecido por esos sacrificios a los que han tenido que hacer frente para ayudarme a llegar donde quiero ir, aunque a veces no me comprendan. Simplemente, decirles que son lo mejor que tengo en la vida y, gracias infinitas a su apoyo incondicional. En especial, quería agradecer a mi hermana Pilar el haber convivido conmigo 30 años de nuestras vidas (básicamente toda nuestra vida). Ahora me toca irme lejos, pero espero que esta nueva etapa que nos toca sea igual de buena que la vivida hasta ahora. Os quiero!!!!

Por último, no me podía olvidar de mi segunda familia: Mis amigos. Ellos me han acompañado en esta vida y en este viaje profesional. Bangla, Fátima, y Ana, os agradezco que

aunque la vida nos separó hace ya 12 años, siempre hagáis que, cuando vuelvo a casa, todo sea como en nuestra adolescencia y que estéis orgullosas de mi desarrollo profesional. También a los amigos que me han estado acompañando desde la universidad y aún continúan en mi vida. José Ángel Ramírez, persona tranquila, paciente, tolerante y ante todo ``mi mejor amigo de la universidad``(cuanta guerra con esto). A Javier Torregrosa, que has sido y eres un ejemplo de superación, eres alguien indispensable en mi día a día, me alegras la vida en nuestras tertulias y, es un regalo el poder el hablar sin secretos sobre nosotros mismos y nuestras circunstancias. Serás algo muy grande el día de mañana (aunque para mí a día de hoy ya lo eres!!!). A Sara Yagüe, que no entiendo cómo me puedes comprender tanto titi. Me encanta que te rías de lo cínica y disparatada que es mi vida (ya sabes bien de lo que hablo). Me alegras en los malos momentos y potencias todos los buenos. A Laura Martínez, que llegaste de la mano de José Ángel y te has convertido en una más. He de decir que he disfrutado mucho con tu alegría y desparpajo. Sería imperdonable olvidarme de Sandra Moreno, con la que compartí muchas noches de series y rajes máximos, como cuando nos quedamos atascados en los pupitres de clase de Fisiología Animal, eres una crack!. A Cheche Martínez y sus artes de fotomontajes, a Guillermo Follana, que estará viviendo la vida en Mallorca, a Nuria Padilla con su ``en ciencias!!!``. A Ruth Planelles y su ``mediterráneamente``. A Juan Carlos Muñoz y sus disparates frikis. Y para acabar, a Oliver Klawitter, un compañero de viaje que me acompañó durante el final de mi carrera y el principio del doctorado, y ahora como un buen amigo en la distancia, decirte que siempre me acordare de tu apoyo, de tu serenidad, y de los diferentes puntos de vista sobre las circunstancias de la vida. En definitiva, gracias por tu total y absoluto apoyo en mis decisiones y por tu confianza plena en mí.

A todos vosotros, estaré siempre agradecido...

Key abbreviations:

IIS: insulin/insulin-like growth factor signalling

DILP: *Drosophila* Insulin Like Peptide

InR: Insulin receptor

FOXO: Forkhead box, sub-group O transcription factor

4e-bp: The initiation factor 4e-binding protein

IPCs: Insulin producing cells

20E: 20-hydroxyecdysone

JH: Juvenile hormone

PTTH: Prothoracicotropic hormone

CA: Corpora allatum

PG: Prothoracic gland

Met: Methoprene

Kr-h1: Krüppel-homolog 1

JHAMT: juvenile hormone acid O-methyltransferase

EcR: Ecdysone receptor

PDF: Pigment dispersing factor

PDFR: Pigment dispersing factor receptor

E75B: Ecdysone-induced protein 75B

SREBP: Sterol regulatory element binding protein

Ascl: Acetyl-CoA carboxylase

ACC: Acetyl-CoA carboxylase

Bgm: Bubblegum

fas: Fatty acid synthase

dib: Disembodied

phm: Phantom

Hex-C: Hexokinase-C

PGM: Phosphoglucose mutase

bmm: Brummer

Lpin: Lipin

pepck: Phosphoenolpyruvate carboxykinase

TAG: Triglycerides acids

Lgr3: Leucine-rich repeat-containing G protein-coupled receptor 3

Lgr4: Leucine-rich repeat-containing G protein-coupled receptor 4





INDEX

ABSTRACT/RESUMEN	A
INTRODUCTION	1
Chapter I: Key factors involve in growth control during development and metamorphosis in <i>Drosophila melanogaster</i>	3
1. Background and context	5
1.1. What is fluctuating asymmetry?	5
1.2. Fluctuating asymmetry as an indicator of genetic noise and enviromental stress	6
2. Asymmetric flies: <i>Drosophila melanogaster</i> for studies of developmental stability	7
2.1. Life cycle of <i>Drosophila melanogaster</i>	8
2.2. The imaginal disc of <i>Drosophila melanogaster</i>	9
3. The control of organ growth is largely autonomous	9
3.1. Organ-intrinsic control	10
3.2. Hormonal control of growth	11
3.2.1. Insulin-like peptides (DILPs) and insulin receptor signalling	12
3.3. Hormonal control of metamorphosis: PTTH, 20-hydroxyecdysone and juvenile hormone	14
3.3.1. The juvenile hormone receptors and signalling	15
3.3.1.1. Role of Metoprene-tolerant (Met) in larval development and growth control	16
3.3.1.2. The Kruppel-homolog 1, a JH-dependent regulator of larval development	17
3.3.1.3. How are JH levels regulated to facilitate metamorphic molt?	18
3.3.2. 20-Hydroxyecdysone (20E) and ecdysone	19
3.3.2.1. PTTH receptor and signalling cascade in the Prothoracic gland	21
3.3.2.2. Nutritional control of metamorphosis and biosynthesis of ecdysone	22
Chapter II: Dilp8 signalling coordinates growth with developmental timing	27
1. Coordination of growth with developmantal timing: the discovery of Dilp8	29
1.1. Classical regeneration studies suggested a negative feedback signal from imaginal disc	29
1.2. Dilp8 is a universal signal produced by growth perturbed imaginal disc	29
1.3. Trade-Offs between Dilp8-mediated developmental homeostasis on late-life fitness or reproductive output?	31
Chapter III: Circadian clock: linking growth, lipids metabolims, and metamorphosis	33
1. Circadian clock control of growth and metabolims. An overview	35
1.1. PDF and circadian regulation of developmental transition in insect	35
1.2. Evidence of regulation of metamosphosis by circadian clock	36
Chapter IV: Body weight, growth, and developmental timing	39
1. The critical weght hypothesis of ``puberty``	41
1.1. Fat body-derived factors controls insulin secretion, body size and weight	42
OBJECTIVES	45

MATERIALS AND METHODS	49
RESULTS	59
PART I: A brain circuit that synchronizes growth and maturation revealed through Dilp8 binding to Lgr3	61
PART II: Trade-Offs between Dilp8-Lgr3-mediated homeostatic growth control and fitness response to stress and modulation by circadian clock	89
PART III: Role of Dilp8-Lgr3 neural circuit in adult flies	111
PART IV: A sema-1a/Leptin-like sensor for body fat times reproductive maturation	119
DISCUSSION	129
A brain circuit that synchronizes growth and maturation revealed through Dilp8 binding to Lgr3	131
Trade-Offs between Dilp8-Lgr3-mediated homeostatic growth control and fitness response to stress and modulation by circadian clock	133
Role of Dilp8-Lgr3 neural circuit in adult flies	137
A sema-1a/Leptin-like sensor for body fat times reproductive maturation	139
CONCLUSION	141
BIBLIOGRAPHY	147





ABSTRACT/RESUMEN



ABSTRACT

Understanding how animals control their size is of fundamental importance in biology and clinical research. It is known that juvenile organisms can adjust their size in response to changes in their environment (plastic response), therefore they produce adults with correct size by counteracting growth anomalies. It is currently unclear exactly how immature animals (including children) compensate these potentially substantial variations in their size. Such compensatory mechanism delays the onset of the reproductive stage of adulthood until a correct size has been reached. This process slows down the growth of normal tissues in order to maintain body and organ proportions within the normal range.

However, the neural mechanism of such homeostatic size regulation has yet to be fully defined in any species. In *Drosophila*, body size is controlled by two prominent neuronal populations: the prothoracicotropic hormone (PTTH)-expressing neurons, which are analogous to the gonadotropin-releasing hormone (GnRH) neurons in mammals; and the neurons located in the *pars intercerebralis* (called insulin-producing cells, IPCs) which produce insulin-like peptides and regulate tissue growth, metabolism and developmental timing. Experiments in which the activity of each of these neurons is altered have shown that these neurons operate independently, albeit both regulate maturation time resulting in larger or smaller adults. Thus, it is now apparent that the activity of these neuronal populations operating independently might not be sufficient to explain the reliable size control, which in turn may require more complex or synchronized regulatory circuits.

Previous studies have established that the insulin/relaxin-like peptide 8 (Dilp8) controls homeostasis size in *Drosophila*, although its receptor and site of action remained uncharacterized. In the present thesis project, I employed a candidate approach to demonstrate that the orphan relaxin receptor Lgr3 acts as a Dilp8 receptor. Lgr3 receptor is activated by nanomolar concentrations of Dilp8 hormone and results in a robust production of cyclic AMP. Furthermore, using a biochemical readout of Lgr3 response to Dilp8 *in vivo*, I identified that a pair of neurons acutely respond to Dilp8 signal. I unveiled that these neurons have extensive axonal arborizations (hub-like structure) and connect with both PTTH-producing neurons and the IPCs.

Functional relevance of connectivity between Lgr3/PTTH-producing neurons and Lgr3/IPCs were evaluated using several genetical approaches as perturbing neural activity, and/or assessing changes in transcription of genes in postsynaptic targets. Regarding to this, I identified Dilp3 and Dilp5 and the Juvenile hormone signalling as output pathways of this circuit for growth compensation through IPCs. Moreover, I demonstrated the ecdysone inhibition through PTTH-producing neurons as output pathway of this circuit for developmental timing regulation.

Accordingly with previous studies, the circadian clock regulates the onset of maturation in animals. To clarify the role of circadian clock in Dilp8/lgr3 neural circuit, I characterized the role of the master clock neurons (PDF neurons) and the synaptical connections with Lgr3-positive neurons, and PTHH-producing neurons (where PDF receptor or PDFR is expressed to mediate the function of PDF neuropeptide). I demonstrated the Dilp8-Lgr3 homeostatic growth control circuit in collaboration with circadian clock during development has an impact in the lipogenic larval metabolism and adult fitness, providing a better performance upon inanition conditions.

In adult female flies, Lgr3-positive neurons are connected synaptically with IPCs, controlling the expression levels of *insulin-like peptides 2* and *5* (*dilp2* and *dilp5*). Previous studies have postulated that Dilp2, Dilp3 and Dilp5 could be involve in courtship behaviour and metabolism. Furthermore, the Lgr3-positive neurons have been involved in courtship behaviour. Nevertheless, the activation of Lgr3-positive neurons by Dilp8 do not show impact neither in mating behaviour, nor in the offspring generated.

On the other hand, I colaborated with Javier Morante PhD in an independent project to clarify the potential role of Sema1a as a sensor of fat content during development, since this receptor is necessary to detect the critical weight and surpase the juvenile stages to puberty. *sema1a* depletion in the prothoracic gland allows the larvae to extent the growth period, followed by the inhibition of the ecdysis. The extension of this growth period in *sema1a* mutants generates as consequences larvae with aberrant lipid content, disproportionate weight, and bigger sizes. Finally, *sema1a* depletion in the prothoracic gland shows higher insulin and juvenile hormone signalling, disrupting the critical weight detection necessary to promote the ecdysone synthesis.

Resumen

La comprensión de cómo los animales controlan su tamaño es fundamental en la investigación biológica y clínica. Es conocido que, los organismos en fases juveniles pueden ajustar su tamaño en respuesta a cambios ambientales (respuesta plástica), generando en consecuencia animales de tamaños diferentes (mayores o menores). Actualmente, no está claro como animales en fase de desarrollo (inclusive niños) compensan variaciones sustanciales en el tamaño. Estos mecanismos compensatorios del crecimiento están involucrados en el retraso de la adquisición de los caracteres sexuales para la reproducción de los organismos hasta que el tamaño correcto es adquirido. A su vez, es desconocido como los ratios de crecimiento son mantenidos, a través de los diferentes órganos durante las fases de desarrollo, para el mantenimiento de las proporciones y simetría características de las especies.

Sin embargo, los mecanismos neuronales de la regulación homeostática están aún por ser definidos en cualquier especie animal. En *Drosophila*, el tamaño del cuerpo es controlado por dos poblaciones neuronales: las neuronas productoras del neuropéptido PTTH, las cuales son análogas a las neuronas secretoras de gonadotropina (GnRH) en mamíferos y, que controlan el tiempo de desarrollo, y las neuronas del *par intercerebralis* (llamadas células productoras de insulina, IPCs), que producen los péptidos de insulina y que regulan el crecimiento de los tejidos, metabolismo y el tiempo de desarrollo. Experimentos en los cuales la actividad neuronal de cada uno de estos tipos de neuronas se altera de forma independiente regula la maduración y crecimiento de los tejidos resultando en adultos de mayor o menor tamaño (respuesta plástica). Por ello, estos fenotipos producidos por las modificaciones de las poblaciones neuronales, explicadas anteriormente, parecen actuar de forma independiente. Por lo tanto, estas neuronas conocidas (neuronas productoras de PTTH y/o las células productoras de péptidos de insulina), que trabajan de manera independiente, no pueden explicar cómo son mantenidos los tamaños finales de las moscas adultas, sus proporciones correctas y el crecimiento sincrónico entre las diferentes partes del cuerpo generando una perfecta simetría bilateral.

Estudios previos han establecido que el péptido perteneciente a la familia hormonal de insulina/relaxina Dilp8 controla el tamaño homeostático en *Drosophila*, aunque su receptor y sitio de acción permanece siendo una incógnita. En la presente tesis doctoral, he desarrollado una aproximación genética con receptores candidatos para demostrar que el receptor Lgr3 actúa como receptor de Dilp8. El receptor Lgr3 se activa en concentraciones nanomolares de la hormona Dilp8, generando un incremento de AMP cíclico. Además, usando genes reporteros en respuesta a la interacción de Dilp8 con Lgr3 *in vivo*, he identificado un par de neuronas que responden a la señal de Dilp8. A su vez, estas neuronas Lgr3 positivas, extienden sus axones hacia las neuronas productoras

del neuropéptido PTTH y las células productoras de insulina.

La relevancia funcional de la conexión entre las neuronas Lgr3 y las neuronas productoras del neuropéptido PTTH, y las neuronas Lgr3 con las neuronas productoras de insulina, fue evaluada usando diversas aproximaciones genéticas, como la manipulación de la actividad neuronal y/o por medición de la actividad transcripcional de los genes en las neuronas postsinápticas del circuito que forman las neuronas Lgr3 positivas. De este modo, identifiqué Dilp3 y Dilp5 junto a la señalización de la hormona juvenil como respuesta a la interacción de Dilp8/Lgr3 para compensar el crecimiento desde las células productoras de insulina, y la inhibición de la síntesis de ecdisoma desde las neuronas productoras del neuropéptido PTTH.

Por otro lado, previos estudios han demostrado la implicación del ritmo circadiano en la maduración de los organismos. Para poder comprender el papel del ritmo circadiano en el circuito formado por las neuronas Lgr3 positivas con las neuronas productoras de PTTH y las células productoras de péptidos de insulina, caractericé la función de las neuronas que controlan el ciclo circadiano (neuronas PDF). Las neuronas PDF hacen sinapsis con las neuronas Lgr3 positivas, y con las neuronas productoras del neuropéptido PTTH (donde el receptor de PDF o PDFR se expresa para mediar la función del neuropéptido PDF). De este modo he observado que el crecimiento homeostático mediado por Dilp8-Lgr3 en colaboración con el ciclo circadiano, durante el desarrollo, tiene un impacto en el metabolismo de lípidos en las fases juveniles (larva) y en la supervivencia de los individuos adultos bajo condiciones de inanición.

Estudios anteriores postulan que, los diferentes péptidos de insulina (Dilp2, Dilp3 y Dilp5), controlan el apareamiento y metabolismo de las moscas de *Drosophila*. A su vez, otro estudio reciente muestra como las neuronas Lgr3 positivas controlan también el apareamiento. Curiosamente, en hembras adultas, las neuronas Lgr3 positivas siguen conectadas sinápticamente con las células productoras de las insulinas, controlando la transcripción de los péptidos de insulina 2 y 5. Sin embargo, la regulación en la expresión de los péptidos de insulina, a través de la señalización de Dilp8-Lgr3 en las hembras adultas, no tiene ningún impacto en el apareamiento y generación de descendencia por parte de la hembra.

Por otro lado, he colaborado con Javier Morante PhD en un proyecto independiente para clarificar el papel de Sema1a como sensor del contenido en grasa durante el desarrollo, indispensable para la detección del peso crítico necesario para hacer la transición a la pubertad. La eliminación de *sema1a* en la glándula protorácica permite a las larvas extender el periodo de crecimiento mediante la inhibición en la producción de ecdisona. La extensión de esta etapa de crecimiento genera como consecuencia la acumulación aberrante de lípidos en la larva, un aumento del peso desproporcionado

y mayor tamaño. La eliminación de *semala* muestra una mayor actividad de la vía de señalización de las insulinas y de la hormona juvenil, indicando la pérdida de la detección del peso crítico necesario para la inducción de la síntesis de ecdisona.



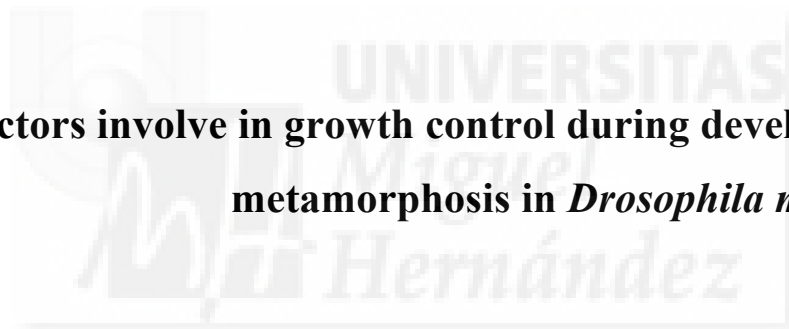


INTRODUCTION



Chapter I

Key factors involve in growth control during development and metamorphosis in *Drosophila melanogaster*



Animal size within a specie is remarkable robust. This precision of organ and body size is crucial for survival and the reproductive success. A fundamental question in developmental biology is thus how developing animals attain the correct final size, proportion and body symmetry of the body even in the face of perturbances. In spite of great progress on our understanding of genes and pathways controlling organ growth, we still know very little about how individual cells, the organs and the organism (and its brain) know when to stop growing? In this Thesis work, I am addressing the inter-organ communication system that helps to synchronise growth across the body to maintain the proper size, proportions and perfect symmetry despite environmental and genetic perturbations.

1. Background and Context

The robustness and phenotypic invariance of animals, including humans, is remarkable considering the noisiness of development and gene expression dynamics, the molecular variation among individuals, and the potential negative impact of environmental influences such as pollutants, extreme temperature and toxics. This phenotypic robustness to perturbation evolved through stabilizing selection for robust developmental processes and it involves buffering mechanisms and cellular surveillance mechanisms that detect and counteract such variation (Møller 1997; Hood 1999). Unilateral malformations in paired organs and variability in the incidence of familial diseases, such as cancer, frequently show no clear Mendelian inheritance pattern, even when there is strong evidence of underlying genetic components (Adams & Niswander 1967). Following these observations, Waddington coined the notion of ‘canalization’ to account for how populations and individuals maintain a constant phenotype across different genetic backgrounds and environments (WADDINGTON 1942). Pioneering studies in the fruit fly *Drosophila melanogaster* defined the first specific ‘canalising genes’, whose primary function is to buffer development against morphological changes and to mask the effects of hidden genetic mutations (Garelli et al. 2012). As such, phenotypic variability in isogenic stocks and unilateral malformations in humans, such as a failure of an eye to develop or the discrepancy in the length of the legs, reflect the incapacity of an individual to cope with genetic variations or environmental perturbations. Thus, these homeostatic systems are of major clinical relevance as potential therapeutic targets of human malformations and familial diseases including cancer syndromes.

1.1. What Is Fluctuating Asymmetry?

Most animals exhibit perfect bilateral symmetry with most humans, for example, displaying less than a 2% of size difference between their left and right arms. Fluctuating asymmetry is defined as small random deviations from perfect symmetry of bilaterally paired traits. Fluctuating asymmetry

measures both deviations as results of developmental and genetic noise and those caused by environmental stress experienced by individuals during development. Fluctuating asymmetry can be measured by a fluctuating asymmetry index (FAi) (Palmer 1994) and the greater the FA of an individual the lesser capacity of the individual to cope with genetic or environmental noise and to buffer variations. Fluctuating asymmetry has attracted a great deal of attention because bilaterally symmetrical traits are extremely common in nature and because the failure to produce bilaterally symmetrical traits such as legs, wing, the eyes, ears, and other paired organs can profoundly impact the performance and overall fitness of the individual (Hendrickx et al. 2003).

Asymmetry of an individual is measured as the right minus the left value of the bilaterally paired trait. In addition to random (fluctuating) asymmetry, directional asymmetry, and antisymmetry can be observed to occur in some individual but these types of asymmetry are not the focus of this study as they involve mainly patterning defects associated with mammalian specification of left-right asymmetry for internal organ position. Moreover, directional symmetry and antisymmetry are developmentally controlled and therefore likely to have adaptive significance. In contrast, fluctuating asymmetry are not likely to be adaptive as bilateral symmetry and the mechanism that ensures such precision in size control are expected to promote the ideal state and the size that best fits to the organism (Valen 1962; Palmer 1994; GangestadThornhill 1999).

1.2. Fluctuating Asymmetry as an Indicator of Genetic Noise and Environmental Stress

Interest in fluctuating asymmetry originated because in most animal species phenotypes are remarkable stable and robust to perturbations despite the extreme genetic variation of the population. This robustness reflects the existence of buffering mechanisms that are at play during development to ensure variations are counterbalanced (Wagner 2008; Bergman & Siegal 2003; Siegal & Bergman 2002). The origin of this phenotypic invariance or robustness has attracted a great deal of interest over the past 50 years but remains nevertheless ill-defined at the molecular level. Recently, much interest has also been devoted to the analysis of fluctuating asymmetry as an indicator of individual quality (Debat et al. 2011; Debat & Peronnet 2013; Garelli et al. 2012). For example, several studies pointed out that individual with greater fluctuating asymmetry, or less buffered, are more prone to diseases. In humans, around 50 syndromes have associated with asymmetric growth (e.g. children with syndromes such as Silver Russell).

The invariance of phenotype and size implies that homeostatic mechanisms exist that buffer variations such as that produced by genetic variance and as such cryptic mutations can accumulate overtime in the population (Bar-Even et al. 2006; Raser & O'Shea 2005; Balázsi et al. 2011).

Mutations in buffering genes can unmask these cryptic mutations resulting in the generation of phenotypic variation and individuals with imperfect left-right symmetry (Debat et al. 2011). There are also other factors, for example injuries, which can create variation and that requires regeneration to repair or regrowth the missing parts, as well as mechanisms that ensure stability and synchrony between the damaged and the undamaged parts. Injury induced regeneration is particularly useful to investigate the developmental mechanisms buffering variations that arise from perturbation and whether different mechanisms specifically buffer different sources of variation or whether there is a universal basis for the buffering mechanisms (Garelli et al. 2012). By studying the invariance of size of *Drosophila melanogaster* we have discovered a signalling pathway that buffer variations of different origin, environmental stress and genetic variation. Our experimental work integrates different levels of analysis to identify the mechanisms by which this signal buffers variation (measured as fluctuating asymmetry), the receptor of the signal, the site of action, and the potential impact that such developmental homeostatic process can have in another fitness parameters.

2. Asymmetric flies: *Drosophila melanogaster* for studies of developmental stability

The fruit fly *Drosophila melanogaster* has been extensively studied for over a century as a model organism for genetic investigations. The invariance of size of the fruit fly wings and eyes, for example, have served as favourite experimental models for genetic studies of size regulation and patterning (B. Cohen et al. 1993). These structures develop from imaginal discs that have remarkable capacity to regenerate after damage (Hadorn 1963; Bryant 1971; Schubiger 1971). The powerful genetics tools in this animal model have helped to elucidate the genetic and signalling pathways involved in organ size control and regeneration (Brand & Perrimon 1993; Smith-Bolton et al. 2009; Bergantiños et al. 2010) and also as a powerful tool for discovering molecular mechanisms underlying cancer initiation and progression (Ferres-Marco et al. 2006). Recently, fruit flies have also been used for the studies of fluctuating asymmetry (Debat et al. 2011; Garelli et al. 2012). However, our understanding of the molecular mechanism that buffers size variation is still in its infancy.

Recent studies from our laboratory and others showed that a gene called *dilp8* (*drosophila insulin-like peptide 8*) is essential to mediate developmental stability in response to genetic noise and environmental stress including injuries (Colombani et al. 2012; Garelli et al. 2012). A better understanding of the buffering mechanisms in fruit flies may provide insights into how organisms ensure robustness and invariance phenotypes despite perturbations that could help to develop new diagnostic tools and interventions for growth problems and asymmetric syndromes in humans.

2.1. Life cycle of *Drosophila melanogaster*

Fruit flies are relatively simple organisms with a short life-cycle that involves different developmental stages (**Figure 1A**): egg, larva (3 instars), pupa, and adult stage.

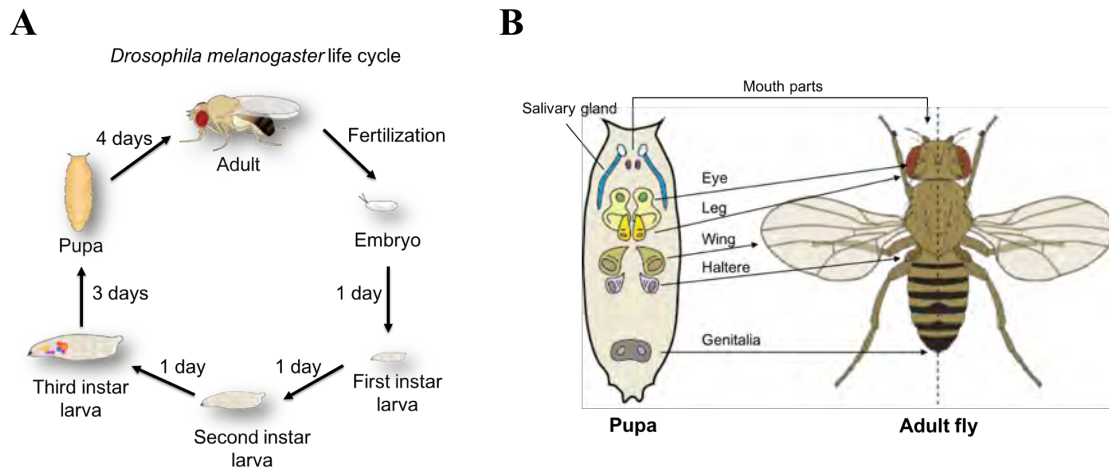


Figure 1: The life cycle of *Drosophila melanogaster* and the anatomy relationship between the larval imago discs and adult body. (A) Scheme of the life cycle of *Drosophila*. At 25° C it takes 10 days approximately to go from the fertilized egg to the sexually mature adult. During the larva stages, the larvae increases its size exponentially and upon acquiring the critical weight the third instar larva switches from a foraging behaviour to wandering behaviour and leaves the food to seek for a dry site to form pupation. The metamorphosis starts at pupation and lasts 4-5 days until the new adult fly emerge from the pupal case (B) Representation of the 10 pairs of larval imago disc and the corresponding parts in the adult fly.

An adult *Drosophila* fruit fly can live between 60 to 90 days, depending on culturing conditions (food) and genetic backgrounds. Females are larger than males, and the size is highly invariant among individuals with the same genetic background and reared in the same environmental conditions and food. Size is influenced by two main parameters: the rate of growth and the duration of growth period. The rate of growth is different for each body parts and these differences explain why the wings are larger than the halteres, and the different shape and size of the anterior and posterior parts of a wing, for example (Martin & Morata 2006). All organs and body parts of the adult fly grow during a similar period of time (the juvenile or larval stage). Genetic variations and environmental conditions such as starvation, without compensatory changes in the rate growth, can influence the length of the growth period and will produce animals that are smaller or larger than normal (Shingleton et al. 2005). Genetic variations that influence the rate of growth will generally influence the length of the larval period to compensate and ensure that animals attain the most optimal size, closer to the genetically determined size (Halme et al. 2010; Parker & Shingleton 2011). These variations produce animals that are of variable size but well proportionated and symmetrical. In contrast, genes that act locally on growth control will produce animals with particular organs that are smaller or larger than normal, without affecting the other body parts (Dominguez & de Celis 1998). Finally, genes that buffer size variations against perturbations would be expected to generate

dramatic variation of all types. As the main function of ‘buffering’ genes is to mask variations of any source, the prediction is that mutations in a buffering gene will generate individuals of greater than normal varied size and imperfect left-right symmetry, and that the variance in phenotypes can be influenced by environmental stress (Garelli et al. 2012).

2.2. The imaginal discs of *Drosophila melanogaster*

The adult of *Drosophila* derives from 9 pairs of imaginal discs and a single genital disc. The imaginal discs are discreet epidermal sheets that are set-aside during the embryonic stage (Bate & Arias 1991). Each paired discs (wing, eye, and leg discs) grow separately at each side of the larvae without any apparent communication and each disc grows to attain its characteristic size and shape (**Figure 1B**), with paired discs (e.g. left and right wing discs) attaining perfect mirror image shape and identical size (Averof & S. M. Cohen 1997; B. Cohen et al. 1991; Wieschaus & Gehring 1976). At metamorphosis, the wing imaginal discs undergo a last division and all imaginal discs will complete their terminal differentiation and fuse to form the adult epidermis, and external organs such as the eyes and the limbs (**Figure 1B**).

3. The control of organ growth is largely autonomous

Classical transplantation experiments in vertebrates and insect imaginal discs revealed that the majority of organs possess organ-autonomous size information and thus can grow in a host and achieve the ‘almost’ correct size (Schubiger et al. 1969; Stern & Emlen 1999). However, such ‘blind’ control of growth is not sufficient to account for how organisms recover from injury or for how symmetric growth ensures paired organs such as eyes and limbs can maintain perfect symmetry even though they grow separately. We have argued that communication between growing organs is required for coordinating growth and ensuring perfect symmetry and body proportions in particular in the face of perturbations. The strongest candidate to date for a buffering mechanism that preserves bilateral symmetry is the gene *drosophila insulin-like peptide 8 (dilp8)* (Garelli et al. 2012) identified by our group. This gene buffers the impact of perturbations in *Drosophila* caused by environmental factors such as DNA damaging agents, extreme temperature, and by genetic injuries. We have argued that the mechanisms that maintain phenotypic stability involved sensing size (to detect mismatches) and systemic regulation to counterbalance size variations and ensure the correct size is attained. As such, I will first introduce in the next sections our current understanding of the genes and mechanisms involved in the organ-intrinsic growth control and the systemic signals (hormones) known to coordinate growth across the body.

3.1. Organ-intrinsic Control

The adult wings of *Drosophila* derive from the notum-wing imaginal disc (hereafter “wing disc”), arising from approximately 20-30 epithelial cells set aside in each lateral of the embryo (Garcia-Bellido & Merriam 1971; Mandaravally Madhavan & Schneiderman 1977). At the end of the first instar larvae, the wing imaginal disc cells resume cell proliferation, increasing the size of the imaginal disc by a 1000-fold by the end of the third instar stage. The growth of the imaginal discs is controlled by six main pathways that are highly evolutionarily conserved. These are the insulin/PI3 kinase pathway (Chen 1996; Leever et al. 1996), the Rheb/Tor pathway (Saucedo et al. 2003; Stocker et al. 2003), the receptor tyrosine kinase (RTK)/Ras pathway (Prober & Edgar 2000), the Myc pathway (L. A. Johnston et al. 1999), the JAK/STAT pathway (Bach et al. 2003), and the Hippo pathway (Justice et al. 1995; Xu et al. 1995). In addition, four pathways regulate patterning coupled to control of organ size and shape. These include the Notch (Dominguez 2014), the Wingless- β -catenin (Bejsovec & Martinez Arias 1991; Alexandre et al. 2014), the Hedgehog (Tabata & Kornberg 1994; Da Ros et al. 2013) and Dpp/BMP pathways (Lecuit et al. 1996; Barrio & Milán 2017).

How these diverse growth control pathways interact and coordinate growth is not fully understood. In both flies and mammals, the Hippo pathway consists of a cascade of protein kinases that inhibit the growth-promoting transcriptional co-activator, Yorkie (in mammals YAP and TAZ) (Huang et al. 2005). In *Drosophila*, recent studies showed that upstream of these kinases are the cell-atypical cadherin proteins Dachous and Fat (Bennett & Harvey 2006; Cho et al. 2006; Silva et al. 2006; Tyler & N. E. Baker 2007; Willecke et al. 2006), Crumbs (Chen et al. 2010; Grzeschik et al. 2010; Ling et al. 2010; Robinson et al. 2010), and Echinoid (Yue et al. 2012). The Hippo/Yorkie pathway acts cell autonomously, while the patterning pathways such as Notch, Dpp, Hedgehog and Wingless- β -catenin function largely as localized sources along ‘compartment’ boundaries. Wingless and Dpp, for example, are thought to act as diffusible, long-range morphogens (Simpson 1976). In addition, activated PI3K/Akt signalling and the Notch (Palomero et al. 2007) promote imaginal disc growth in part by regulating the Hippo pathway (Halder & Johnson 2011; Irvine 2012). The activity of PI3K/Akt also regulates cell growth, and links growth rate with nutritional state (Grewal 2009).

Myc activity regulates ribosome biogenesis and cell growth. Myc is also, among the known growth control genes, the strongest candidate for a cellular surveillance mechanism for robust size control. Myc is crucial for regulating growth homeostatically through a mechanism called cell competition (**Figure 2**) (la Cova et al. 2004; Moreno & Basler 2004). While overall Myc null mutants produce diminutive animals with less and smaller cells, genetic studies of null Myc mutants in genetic mosaics have demonstrated that developing organs monitor and compare fitness between neighbouring cells so that optimal cells outcompete their suboptimal neighbour cells, thereby

maintaining the integrity of tissues, indispensable for a correct development of the organism and to avoid tumorigenesis (Morata & Ripoll 1975; Simpson & Morata 1981) (**Figure 2**). Recently cell competition was also shown to occur in mammal embryos and during carcinogenesis (Clavería et al. 2013; Sancho et al. 2013). Myc and cell competition allows to act via a mechanism that maintains invariant size because dysregulation of Myc has been shown to generate animals with wings that are of variable size.

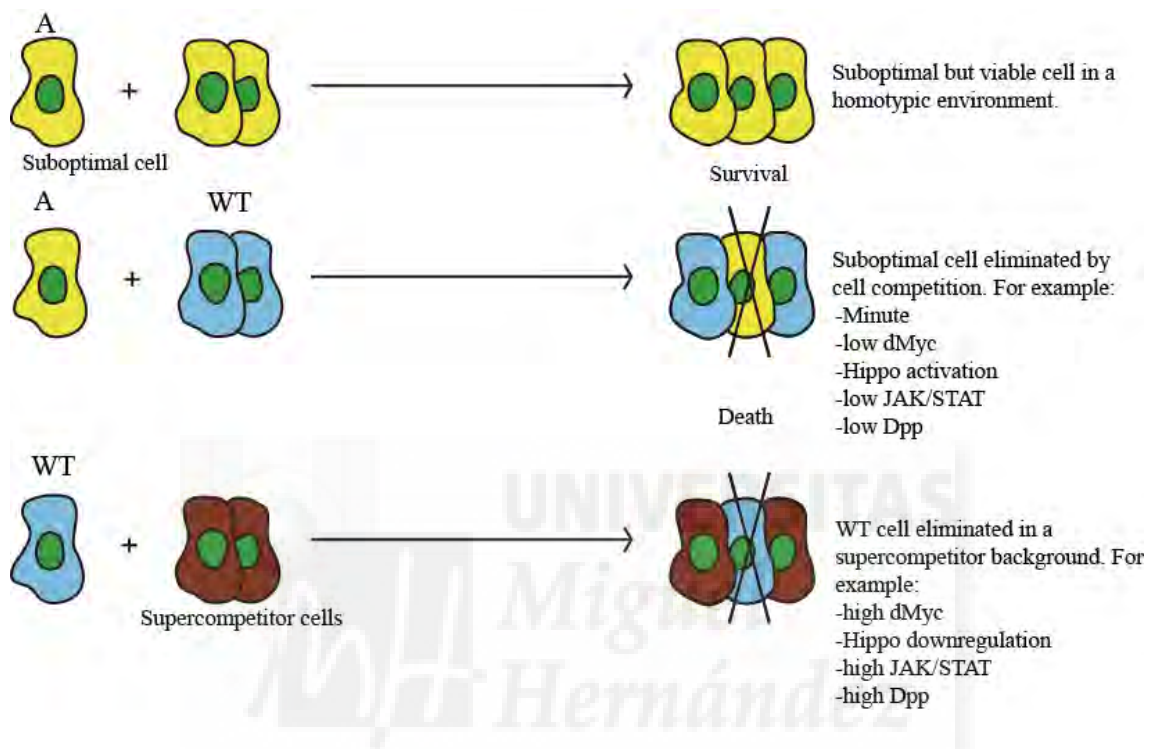


Figure 2: Organ size and homeostatic regulation relies on cell competition process. Schematic representation of cell competition, whereby a cell with a somatic mutation or damaged is out-competed by the surrounded fitter cells. This process ensures the fitter cells survive and reproduce. Overexpression of factors such as Myc converts cells into super-competitors and can eliminate the wild type cells as predicted to happen in pre- and neoplastic lesions. Adapted from Moreno 2008. It is yet unclear how through cell-competition, individual cells and the organ measure when the correct size is attained.

While it is clear that homeostatic mechanisms such as Myc and organ-intrinsic factors are essential for the control of organ size, it is also obvious that additional long-distance factors (e.g. hormones) are required for the coordination of growth among organs and synchronize growth across the left-right axis.

3.2. Hormonal control of growth

Animal growth is restricted to the juvenile stage before developmental timing program starts to induce sexual maturation. Thus, hormones that control the timing of metamorphosis also regulate

final animal size. Here, I will discuss the systemic control of both growth rate and the timing of metamorphosis.

While the characteristic growth rate of each imaginal disc and each disc part is regulated by the organ-intrinsic factors, the insulin/insulin-like growth factor signalling (IIS) regulates overall growth rate in response to nutrient availability (see below) and as such alterations in the systemic insulin signalling or response results in animals that are smaller or larger than normal but perfectly proportionated and bilaterally symmetrical (NIJHOUT 1981). Although there has been an on-going effort to understand the role of hormones in insect growth and the timing of metamorphosis, our understanding of these controls remains fragmentary and incomplete.

3.2.1. Insulin-like peptides (DILPs) and insulin receptor signalling

IIS and the Rheb/Tor signalling are highly conserved nutrient-sensing pathways in the animal kingdom. The peptides of the insulin/IGF hormone superfamily are characterized by an invariant six-cysteine residue motif (Shabanpoor et al. 2009) and in *Drosophila* the insulin genes are encoded by seven separated insulin/insulin-like peptide (Dilp1-7) genes (Ikeya et al. 2002; Rulifson et al. 2002). Recently, a new insulin-like peptide gene, called *dilp8*, was identified (Colombani et al. 2012; Garelli et al. 2012). *dilp8* gene has distinct roles to those reported for Dilp1-7 and in this Thesis work we have established it acts through a different receptor, and probably through a different signalling cascade, and hence the Dilp8 insulin-like peptide is discussed in a separate section.

Each DILP (1-7) is regulated independently in a different spatial and temporal manner. Dilp2, Dilp3, and Dilp5 are expressed in median neurosecretory cells of the protocerebrum, called insulin producing cells (IPCs) during the larval stages and adult (Broughton et al. 2005; Rulifson et al. 2002). Dilp1 is expressed in IPC as well, but during metamorphosis (Y. Liu et al. 2016). Dilp7 is expressed in a set of neurons of the abdominal ganglia that project to ovaries, indicating a possible role as a relaxin hormone (Miguel-Aliaga et al. 2008; Yang et al. 2008). Dilp6 is produced in the fat body cells to promote growth during non-feeding stages in wandering larva (Slaidina et al. 2009; Okamoto et al. 2009), and Dilp4 is presumed to be expressed in midgut (Brogiolo et al. 2001).

Dilp1-7 peptides are all well assumed to act through the single insulin receptor (InR) gene in *Drosophila*, although biochemical evidence for Dilp bindings to the InR has only been provided for the Dilp5 (Fernandez et al. 1995). The dInR like its mammalian homolog is a tyrosine kinase receptor that acts through a phosphorylation cascade that involves the insulin receptor substrate (IRS; called chico in flies, phosphoinositide-3 kinase (PI3K), and Akt/PKB (Oldham & Hafen 2003). When PI3K is phosphorylated, phosphatidylinositol 4,5-bisphosphate (PIP₂) is converted to phosphatidylinositol 3,4,5-triphosphate (PIP₃) in the cell (Auger et al. 1989). Conforming PIP₃ is increasing in the cell,

Phosphoinositide-dependent protein kinase 1 (PDK1) and Akt/PKB are phosphorylated and finally phospho-Akt (p-Akt) produces the phosphorylation of its targets such as the transcription factor FOXO (Mora et al. 2004; Arden 2008). The phosphorylated FOXO is translocated from the nucleus, thus impairing its transcriptional activity (**Figure 3**). Targets of dFOXO includes *the initiation factor 4e-binding protein (4e-bp)* and *InR* gene itself (Demontis & Perrimon 2010). The expression of *4e-bp* in the tissues, for example, provides a measurement of IIS activity and of growth rate, by dFOXO activity and reflecting negatively the rate of growth.

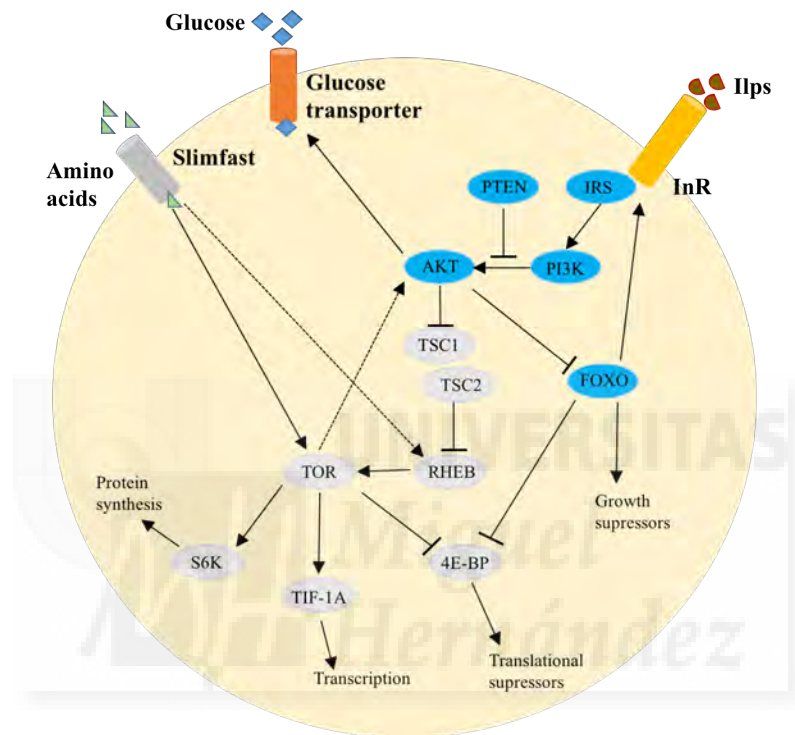


Figure 3: Representation of insulin signalling pathway in *Drosophila*. When circulating insulin hormones are bound to InR generate a cascade of phosphorylation of its effectors to promote growth in the tissues by inhibition of suppressor of growth FOXO by p-AKT. Furthermore, insulin pathway has a crosstalk with TOR pathway. TOR pathway is activated by intracellular amino acids levels and p-AKT to induces cell growth. Adapted from Danielsen et al. 2013.

The activation of target of rapamycin protein kinase (TOR) signalling in response to the amino acids levels and activation of IIS via Akt phosphorylation couples control growth to nutrition (Britton et al. 2002) and see also (Potter et al. 2002; Inoki et al. 2002) (**Figure 3**). TOR activation promotes cell growth by controlling protein synthesis through ribosomal protein S6 kinase (S6K) and the phosphorylation of 4E-BP (Hay & Sonenberg 2004).

The fat body of *Drosophila*, a homologous organ to the liver and adipose tissue in mammals, has the key role of sensing nutrients (amino acid levels) to control systemic growth and

developmental progression by regulation of insulin signalling and secretion of different DILPs from IPCs (Britton et al. 2002; Colombani et al. 2003; Géminard et al. 2009; Delanoue et al. 2016).

3.3. Hormonal control of metamorphosis: PTTH, 20-hydroxyecdysone and Juvenile

Hormone

Timing of metamorphosis is regulated by antagonistic action of two hormones, the steroid hormone 20-hydroxyecdysone (20E), and the sesquiterpenoid juvenile hormone (JH) (NIJHOUT 1981) (**Figure 4**). While 20E promotes metamorphosis, JH prevents it and ensures that metamorphosis only starts at the right body size or weight. In the next section, the regulation and action of these hormones are discussed separately.

The sesquiterpenoid JH is produced by the corpora allatum (CA), which is part of a larger endocrine gland called ring gland. JH levels maintain the juvenile stages and promote growth by mechanisms not fully understood. When the larva attains a weight (also called ‘critical weight’, Nijhout 2003) that will ensure that the animal will survive during metamorphosis, a non-feeding stage, the production of JH ceases by an unknown mechanism. The drop of JH is believed to provide competence to release the Prothoracicotropic hormone (PTTH) hormone by two pairs of PTTH-producing neurons in the central brain (Mirth & Riddiford 2007). PTTH then stimulates the production of ecdysone by the prothoracic gland, which is also part of the ring gland. The ecdysone released by prothoracic gland is proportional to the PTTH levels (Warren et al. 2006; McBrayer et al. 2007; Rewitz et al. 2010; Rewitz et al. 2013; Yamanaka, Rewitz, et al. 2013). PTTH stimulates first a small peak of ecdysone (in the absence of JH) that triggers behavioural and physiological changes that ultimately triggers the cessation of feeding. The larvae then leave the food to seek for a dry and dark place to start pupariation (Gong et al. 2010; Yamanaka, Romero, et al. 2013). This non-feeding stage is called wandering larval stage and can last 12-24 hours. A second and larger peak of ecdysone, followed by a high peak of PTTH, promotes metamorphic molt (**Figure 4**) (NIJHOUT 1981; S. F. Gilbert et al. 1996). The production of PTTH that ultimately triggers metamorphosis is assumed to be also regulated by a circadian clock mechanism based on indirect evidences that in many insects the circadian clock neurons are in proximity to the PTTH-producing neurons, and that wandering or metamorphosis time can be affected by some circadian clock mutations. Moreover, puberty in mammalian species is under circadian clock regulation (McBrayer et al. 2007).

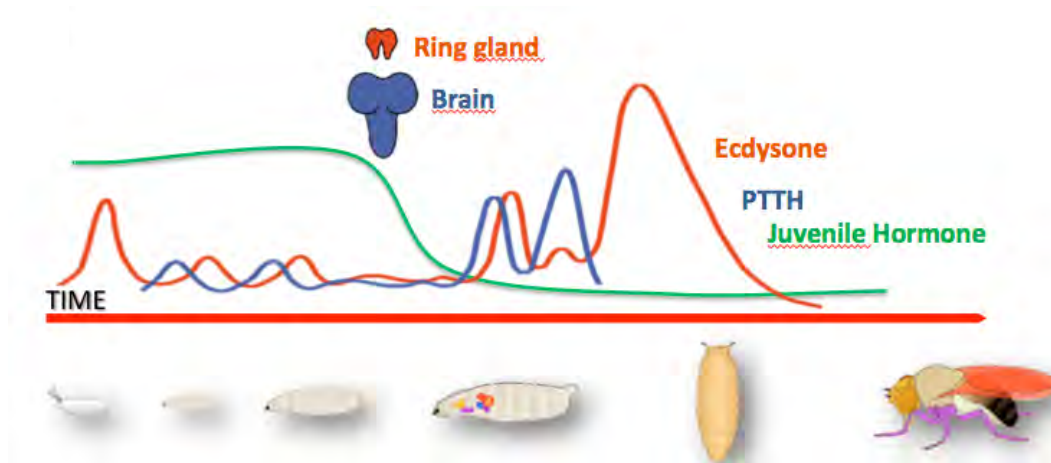


Figure 4: Representation of the hormones involved in the regulation of developmental timing in *Drosophila melanogaster*. The levels of JH (green) declines during the mid third instar stage after the attainment of critical weight. In the presence of JH, the egg-larva and each larval molt transition is controlled by pulses of ecdysone, which are preceded by a peak of expression of the PTTH neuropeptide. PTTH is produced in the brain and stimulates the synthesis of ecdysone in the endocrine gland called prothoracic gland. When the levels of JH declines, a high peak of PTTH and ecdysone trigger the larval-pupal transition and metamorphosis.

3.3.1. The Juvenile Hormone Receptors and Signalling

Although the JH has been intensely studied, the nature of its receptor has remained a mystery until recently. JH is a small lipophilic molecule capable of penetrating cell membranes to the nucleus, where it regulates transcription of specific genes. Recent work has established that JH can bind the Methoprene-tolerant (Met) receptor (Charles et al. 2011) and its paralog receptor called Germ-cell expressed (Gce) (Baumann et al. 2010). Met is a basic helix-loop-helix (bHLH)-PAS transcription factor (Ashok et al. 1998; Miura 2005). Met can form dimers and heterodimers with Gce in absence of JH (Met-Met or Met-Gce) (Goodman & Granger 2005), but when JH is present during the juvenile stages, the Met-Gce dimers are impaired by JH binding to Met's PAS-B domain. This binding of the hormone allows Met receptor to form a dimer with another protein called Taiman (Tai) (Charles et al. 2011; M. Li et al. 2011). This complex, Met-Tai, binds and recognizes JH-responsive elements (JHRE) in the promoter of genes that respond to JHs (**Figure 5**) (Kayukawa et al. 2012).

JH can also bind another nuclear protein, encoded by the *ultraspiracle (usp)* gene, which was the most favoured JH receptor candidate for many years (L. I. Gilbert et al. 2000; TRUMAN & RIDDIFORD 2002). There is also evidence that JH can signal by a non- genomic pathway via a plasma membrane receptor (Wheeler & Nijhout 2003). An outstanding open question is whether JH acts by modulating the ecdysteroid signalling or whether it acts through its own signal transduction pathway and target genes.

3.3.1.1. Role of Methoprene-tolerant (Met) in larval development and growth control

Met mutations render *Drosophila* resistant to the morphogenetic effects of JH (Wilson & Fabian 1986; Riddiford & Ashburner 1991; Wilson et al. 2003). Thus the JH analog Methoprene can be used to mimic effects of JH signalling or to rescue JH signalling in conditions of suppressed JH biosynthesis. *Met* is present in larval tissues and imaginal tissues and the abdominal histoblasts in pupae and reproductive organs, which are all tissues previously defined as JH target sites (Pursley et al. 2000). *Drosophila* paralog *Gce* (Godlewski et al. 2006; S. Wang et al. 2007) is expressed during early embryos and later in a subset of germ cells (Moore et al. 2000) and it is required together with *Met* to remodel the adult intestine of female in response to reproduction (Reiff et al. 2015). Although *Gce* is thought to be absent during larval stages, the weak effect of *Met* mutations compared to that of JH deficiency suggests that *Gce* can compensate for the loss of *Met* during these stages or in some larval tissues, although the *Drosophila gce* function or sites of its expression during postembryonic stages have been not characterized (Godlewski et al. 2006).

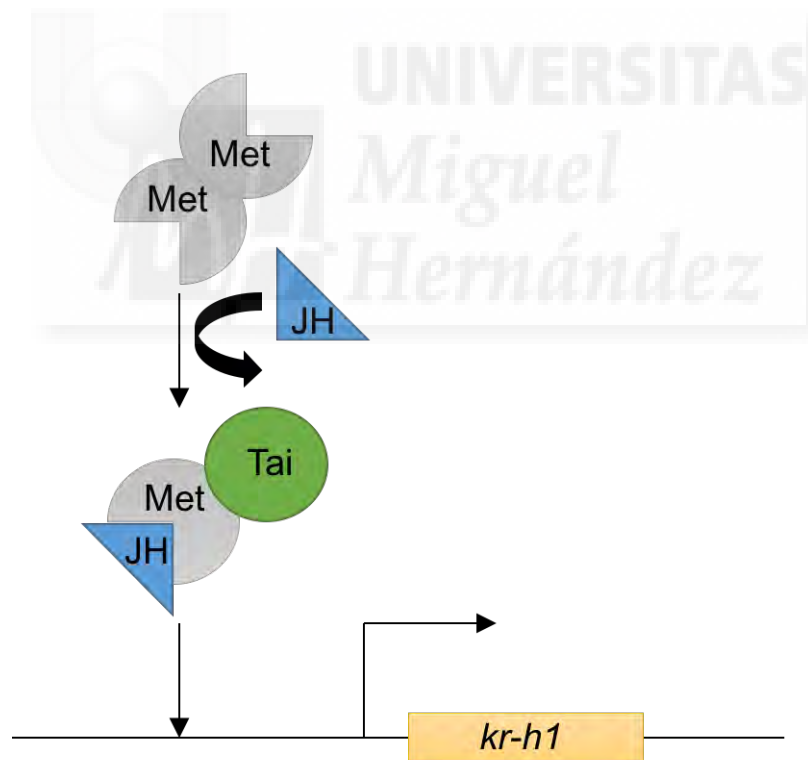


Figure 5: JH signalling pathway. In absence of JH, Met receptor forms homodimers with itself, but in the presence of the hormone, JH binding to its receptor Met generates a structural change that decreases the affinity for other Met partners. This low affinity of Met-JH complex enables to interact with high affinity with Taiman. The JH/Met/Taiman heterodimer induces a transcriptional response of target genes such as *Kr-h1*, which maintains growth and juvenile stages. Adapted from Jindra et al. 2013.

The potential compensatory function by *gce* may explain the absence of notable developmental defects in *Met* mutants. *Met* null animals develop normally to viable fertile adults (Ashok et al. 1998; Wilson et al. 2003) with only Slight anomalies including slower pupal development and some pupal mortality (Minkoff & Wilson 1992). However, although functional redundancy between *gce* and *Met* might account for the lack of more severe phenotypes that would reflect disrupted JH signalling (Wilson et al. 2003), it is unclear how the sole absence of *Met* causes resistance to JH and JH analog toxicity. The paucity of data on the functional significance of each *Drosophila* paralogs for JH signalling, the role of *Met/Gce* dimers, and the nature of the putative JH membrane receptor have hampered our understanding of JH signalling in growth regulation and the control of metamorphosis time.

In other insects (Berger & Dubrovsky 2005; Minakuchi, Zhou, et al. 2008; Jindra et al. 2013) *Met* is critically required for JH-regulated expression of the *BR-C*, a prototypical ecdysone target gene, and the *Krüppel-homolog 1 (Kr-h1)* genes. In the next section, I will discuss the regulation and known roles of *Kr-h1*, as the best JH receptor's regulated candidate gene to mediate JH signalling during the larval stage.

3.3.1.2. The Krüppel-homolog 1, a JH-dependent regulator of larval development

The *Krüppel-homolog 1 (Kr-h1)* is the best candidate JH's target to mediate the functions of JH during development as *Kr-h1* overexpression mimics the 'antimetamorphic' effect of JH (Minakuchi, Zhou, et al. 2008; Minakuchi et al. 2009). *Kr-h1* gene generates by alternative splicing two different isoforms, *Kr-h1 β* and *Kr-h1 α* . Both of them encode zinc-finger transcription factors. *Kr-h1 β* isoform is expressed in embryonic stages and nervous system (Beck et al. 2004) while *Kr-h1 α* is the main isoform expressed during the larval stages (Pecasse et al. 2000). Although the *Kr-h1* expression serves as a readout of JH signalling and activity during larval stages, some recent work has established that *Kr-h1* might be also required during the prepupae stages to modulate ecdysone-dependent gene expression at the onset of metamorphosis (Pecasse et al. 2000). This JH-independent role of *Kr-h1* complicates the genetic analysis of *Kr-h1* in the JH signalling in the larval stages.

In addition to *Kr-h1*, *BR-C* is also considered to be an essential mediator of the JH signal (Konopova & Jindra 2008). Loss and gain-of-function experiments with transgenic flies support a role of *BR-C* in JH signalling and it has been suggested that during metamorphic molt the low JH levels at the beginning of the pupal stage allow *BR-C* to bind the non-ligated *Met* to regulate expression of pro-metamorphic genes (Wilson 2005). *BR-C* is a major gene regulator of pupal development and a primary 20E-response gene whose expression sharply rises during larval to pupal transition. Loss of *BR-C* function in null mutants leads to death in the third (final) larval instar and

inability to initiate metamorphosis (Kiss et al. 1988).

3.3.1.3. How are JH levels regulated to facilitate metamorphic molt?

The essential role of JH in preventing precocious metamorphosis has been demonstrated in numerous hemimetabolous and holometabolous insects (WIGGLESWORTH 1934), but it remains under debate whether JH plays a similar role in *Drosophila melanogaster*. Experiments with ablated corpora allata glands (allatectomy) (WIGGLESWORTH 1954; Stall 1986) and genetic studies have confirmed the anti-metamorphic role of JH in the silkworms *Bombyx mori* and *Tribolium castaneum*, for example. However, such experiments in *Drosophila melanogaster* failed to prevent metamorphosis, perhaps in part because ablation of corpora allata (CA) cells was incomplete (Riddiford et al. 2010).

The biosynthesis of JHs by the CA involves a partially characterized enzymatic reaction that convert acetyl-CoA into JH (Hiruma K, et al. 2013; Belles X, et al. 2005). In particular, the *juvenile hormone acid O-methyltransferase (JHAMT)* gene (Minakuchi, Namiki, et al. 2008) encodes a key enzyme in the biosynthetic cascade that produce JH and the expression of *Jhamt* gene act as rate-limiting step in the cascade of JH production (Minakuchi, Zhou, et al. 2008; Daimon et al. 2012). Hence, the expression of *Jhamt* gene is used here as a proxy to measure synthesis of JH during larval stages and in our experimental conditions.

In some insects, precocious pupation is observed by depletion by RNA interference (RNAi) of the *Jhamt* gene (Minakuchi, Namiki, et al. 2008). However, unlike in *Tribolium* the presumed depletion of JH by RNAi silencing of *Jhamt* or the treatment of third instar larvae with JHA (Methoprene) did not result in precocious (Niwa et al. 2008) and delayed metamorphosis in *Drosophila* (our study; Vallejo et al. 2015). However, JH ectopic and deficiency does affect larval growth and its function is compared to that of the mammalian growth hormone (GH). For example, likewise in insects, mammalian GH is produced by an endocrine organ (the anterior part of the pituitary) and continual production of JH causes juveniles to grow continuously producing a condition called gigantism, which is analogous to the effect of ectopic JH signalling in many insects. The secretion of GH by the pituitary is modulated by neurosecretory signals from the hypothalamus. GH binds its receptor, GHR, which is expressed by liver, muscle and other peripheral tissues to promote growth in part by the stimulation of the production of IGF-1 (Morrison 2012). In insects, the production of insulin/insulin-like growth factors mostly relies on nutritional cues and is only partially dependent of JH.

Similar to mammalian GH, the JH production is abolished in response to unknown signals from the brain, imaginal discs and/or the fat body after the juvenile animal (larvae) attains a critical body mass or size.

3.3.2. 20-hydroxyecdysone (20E) and ecdysone

Larval ecdysteroids are synthesised in the prothoracic gland (L. I. Gilbert 2004) in response to PTHH (**Figure 4**). However, the prothoracic gland secretes ecdysone (Žitňan et al. 2007; McBrayer et al. 2007), which is a relatively inactive prohormone that is only converted into the active 20E in the fat body, midgut, epidermis, and malpighian tubules and epidermal cells by the enzyme Shade (Iga & Kataoka 2012; Luan et al. 2013).

20E signalling is essential for all molting transitions and metamorphosis (Thummel 1995; Thummel 1996; Thummel 2001; Riddiford 1993) and the morphological and behavioural changes associated with these transitions. During metamorphosis, 20E activate the ecdysone receptor (EcR) in the nucleus, and hormone-ligated EcR receptor binds its partner called Ultraspiracle (USP) (Thummel 1996; Thummel 1990; Thummel 1995; Koelle et al. 1991).

The *EcR* gene encodes three protein isoforms EcR-A, EcR-B1, EcR-B2 by alternative splicing (Koelle et al. 1991; Talbot et al. 1993). USP interacts with each of the EcR isoforms to form DNA-binding heterodimers (Yao et al. 1992; Bender et al. 1997). This heterodimer protein is stabilized by binding of 20E, which in turn activates the transcription of early genes, including the *E74*, *E75*, *E93* and *Broad-complex (BR-C)*, which I mentioned above. All these genes encode transcription factors than carry out the expression of ecdysone-dependent late genes to generate the different effects produced by ecdysone (**Figure 6A**) (Thummel 1996; Thummel 2001).

There are some evidences that ecdysone in larval imaginal tissues might induce proliferation negatively and positively (Hall & Thummel 1998; D'Avino & Thummel 2000; D'Avino & Thummel 1998; Zheng et al. 2003).

For example, it has been suggested that ecdysone bound to EcR/USP regulates imaginal disc cell proliferation and differentiation by repressing Wingless (*wg*) (L. A. Johnston & Edgar 1998; L. A. Johnston et al. 1999; L. A. Johnston & Sanders 2003; Duman-Scheel et al. 2004). Ecdysone bound to EcR/USP is also postulated to promote imaginal disc proliferation through stimulation of protein synthesis via stimulation of *myc* expression (Cranna & Quinn 2009) (**Figure 6B**).

3.3.2.1. PTTH Receptor and Signalling Cascade in the Prothoracic Gland

An important pathway in the control ecdysone production in prothoracic gland (PG) is the PTTH neuro peptide. As such, most of my studies include the analysis of the expression and function of PTTH. This hormone is produced by the PTTH gene, which is expressed only by two pairs of neurons, called the PTTH-producing neurons or PG neurons.

PTTH is released in the PG where it binds the tyrosine kinase receptor Torso (Rewitz et al. 2009). Torso activation generates a phosphorylation cascade via the mitogen-activated protein kinase (MAPK), Ras (Ras85D), Raf (Draf), MAPK kinase (MEK), and extracellular signal-regulated kinase (ERK) (D. W.-C. Li et al. 2005; Caldwell et al. 2005). The activation of PTTH-Torso pathway enhances the transcription of genes encoding key enzymes in the biosynthesis of ecdysone. These include the genes *disembodied (dib)*, *shadow (sad)*, *spook (spk)*, and *phantom (phm)*, which together with *shade (shd)* produced by fat body cells and imaginal disc cells are collectively known as Halloween genes (**Figure 7A**). All the Halloween genes encode cytochrome P450 enzymes involved in the hydrolysis of cholesterol, as a substrate, and *shade* expressed by the peripheral tissues catalyses the last step of the enzymatic reaction that produces the active ecdysone form, 20-HE (**Figure 7B**) (L. I. Gilbert 2004).

PTTH also regulates negatively Drosophila Hormone Receptor 4 (DHR4), which regulates negatively the expression of *Cyp6t3*, an uncharacterized cytochrome P450 required for ecdysone synthesis (Ou et al. 2011) in an as yet-uncharacterized step of this cascade. Additionally, other new members of the cholesterol metabolism have recently shown to generate ecdysone parallel pathways (Yoshiyama et al. 2006; Yoshiyama-Yanagawa et al. 2011; Niwa et al. 2010).

The release of ecdysone by PG is actively regulated by synaptotagmin-labelled vesicles in response to calcium signalling (Yamanaka et al. 2015) although passive, diffusible release of ecdysone is also possible to contribute to the maintenance of low levels of ecdysone in-between molting and to the high rise of ecdysone at the pupal transition.

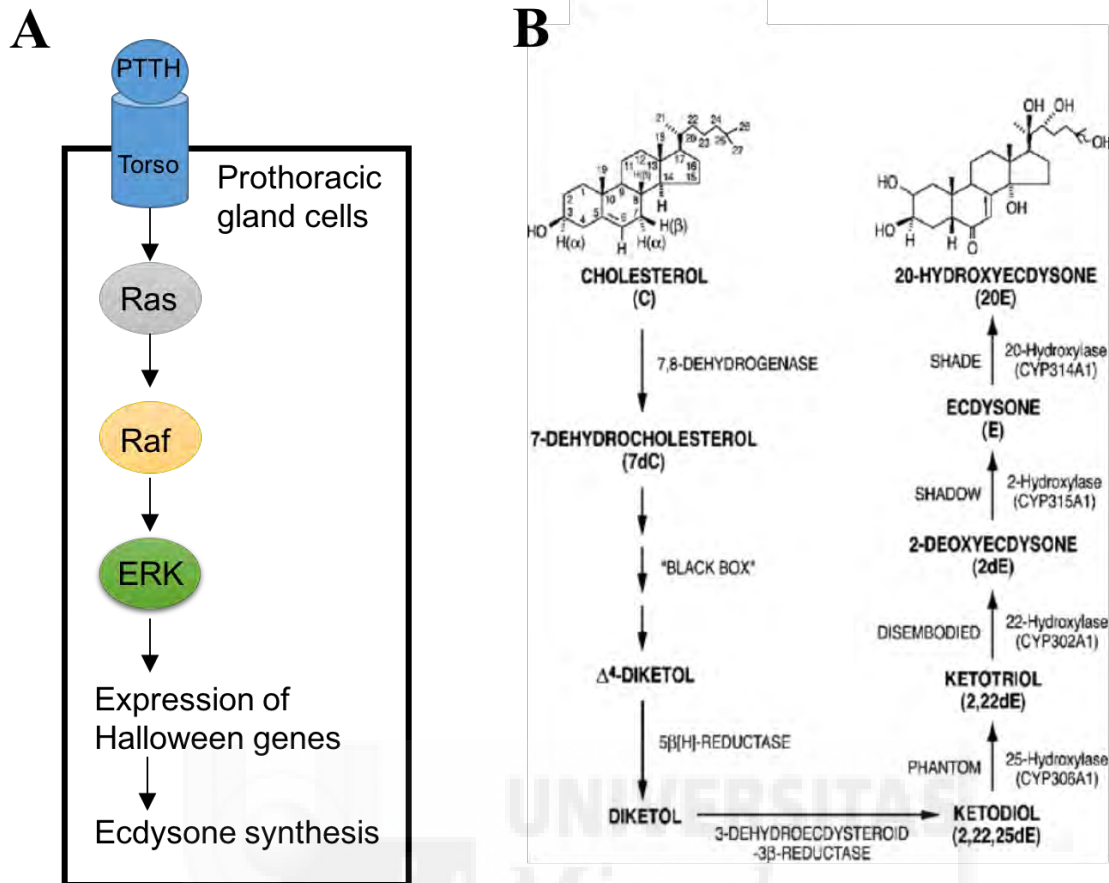


Figure 7: Canonical ecdysone biosynthetic pathway in the PG. (A) The brain-derived PTTH binds to its tyrosine receptor Torso in the PG and acts through a Ras/Raf/ERK phosphorylation cascade to promote the expression of Halloween genes for the synthesis of ecdysone. (B) Scheme of the known Halloween genes encoding the enzymatic reaction from cholesterol to ecdysone. PG cells to the hemolymph release the pro-hormone ecdysone. In the target tissues, ecdysone is converted to 20-hydroxyecdysone by Shade. Adapted from Scaraffia & Miesfeld 2013.

3.3.2.2. Nutritional control of metamorphosis and the biosynthesis of ecdysone

Several studies have advanced a role for the insulin/TOR signalling in the PG that could regulate the production of ecdysone production in response to nutritional cues. Although a role for the InR in the PG is unclear, several recent works have uncovered requirement for downstream components of the IIS and Rheb/TOR in the PG.

General stimulation of insulin pathway regulates positively growth, several authors found that activation of IIS in the PG by expressing the PI3K, p110 or by RNA interference of the negative regulator Pten causes the precocious stimulation of ecdysone by the PG and the formation of smaller than normal adults (Caldwell et al. 2005; Colombani et al. 2005; Mirth et al. 2005). In Colombani et al., 2005 also found that fat body-specific reduction of EcR increased systemic growth and larval size without affecting developmental timing by reduction of a direct target gene *myc* in the fat body,

although these observations also suggested additional factors are the target of ecdysone which might include the microRNA miR-8 (Jin et al. 2012). Moreover, the authors inferred that increased larval-pupal size reflected increased imaginal disc growth and thus increased final size. However, other authors reported that instead, the increased pupal size associated with reduced EcR in the fat body is associated with decreased imaginal disc cell proliferation (Mirth et al. 2009). Thus, although ecdysone via EcR autonomously suppress insulin signalling at the level of PI3K activity, dFOXO localization at the nuclei, and 4E-BP expression (Colombani et al. 2005; Delanoue et al. 2010; Grewal 2009) this does not impact imaginal disc growth via the IIS, and the effects are the opposite to that anticipated by a positive role of ecdysone-EcR in the imaginal disc proliferation.

There are discussions and controversies about this issue and one explanation about how IIS and Rheb/TOR in the PG can modulate ecdysone production. One hypothesis is IIS and Rheb/TOR act in the PG to sense when the larvae acquired the critical weight, generating the sensibility of PG to the PTTH release for ecdysone production (reviewed in Rewitz et al. 2013).

To complicate this issue further, two recent papers reported a role of EcR in the imaginal discs. The group of Barrio observed that loss of EcR decreased imaginal disc cells, used as a proxy to measure imaginal disc cell multiplication (Herboso et al. 2015). This led the authors to propose that EcR regulates positively imaginal disc growth. The group of Shingleton has recently reported that depleting EcR in the imaginal discs increases imaginal disc cell proliferation (Gokhale et al. 2016)— which is the opposite effect to that observed by Barrio's group. However, Shingleton inferred that this negative effect of depleting EcR mimics the effect of ecdysone binding to its receptor, and thus postulated that ecdysone-EcR normally promotes imaginal disc cell proliferation by antagonising non-ligated EcR negative control of cell proliferation.

A comprehensive summary of the postulated action of IIS and PTTH, and additional factors not investigated in this Thesis for the release of ecdysone, such as β FTZ-F1 (Parvy et al. 2005), *Drosophila* hormone receptor 3 (DHR3), the nitric oxide (NO) (Reinking et al. 2005; Cáceres et al. 2011) and the TGF β /Activin pathway (Gibbens et al. 2011) is outlined in **Figure 8**.

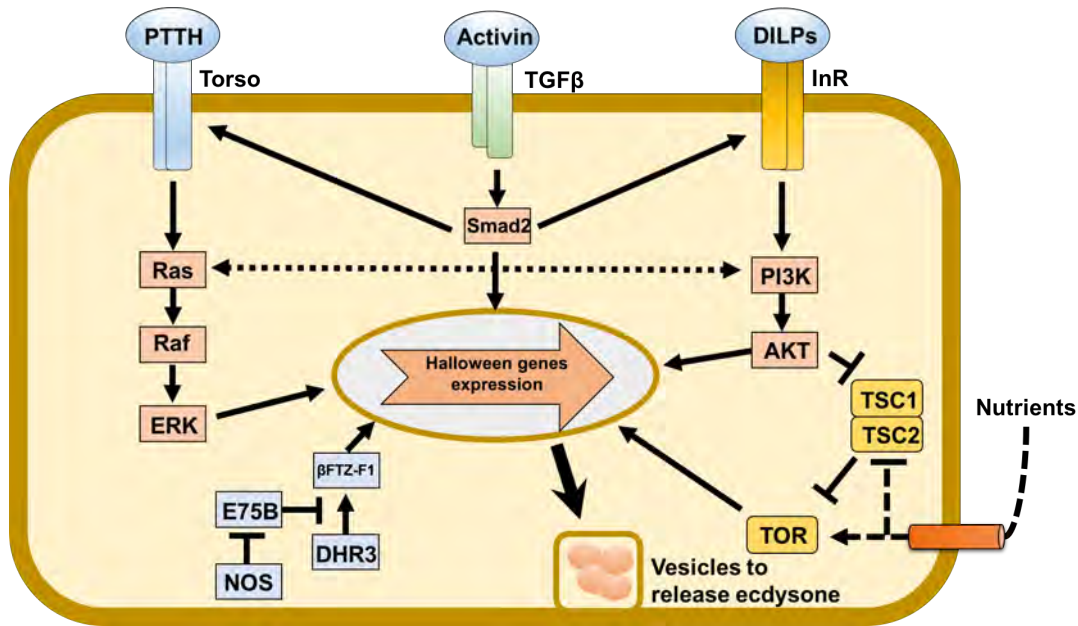


Figure 8: Canonical and non-canonical pathways that converge in the PG to regulated ecdysone production. PTTH/Torso signaling pathway activates the production of ecdysone. The non-canonical pathways controlling ecdysone synthesis involves the IIS, the activin/TGF β and their effectors, which control the expression of *torso* and *InR* to provide the competence of the PG cell to respond to the developmental and nutritional cues. The Nitric oxide pathway also controls growth and maturation by transcriptional regulation of Halloween genes. via an unknown mechanism. Adapted from Rewitz et al. 2013.

Presently, the model of ecdysone production postulates that larvae must surpass several check-points that includes first the attainment of a 'minimal viable weight' and 'critical weight' that would ensure to survive metamorphosis. 'Critical weight' which is defined as the body mass at which starvation does not produce delay and can induces puparium formation (Nijhout 2003). While starvation before the 'minimal viable weight' and the 'critical weight' delays puparation and slow growth the body size (McBrayer et al. 2007), starvation *after* 'critical weight' attainment actually accelerates metamorphosis and results in smaller than normal adults (Shingleton 2010). The second checkpoint 'tissue repair' is related to the size and damage of imaginal discs proposes a delay until repair and regrowth of the missing parts is completed. This checkpoint was postulated to act on PTTH release (NIJHOUT 1981) or the production of ecdysone itself. The release of PTTH after the acquirement of weight is considered the third checkpoint controlling by photoperiod so that competent larvae will not enter pupariation until in an open-gate window of 8 hours during the day (Truman & Riddiford 1974; McBrayer et al. 2007). This theoretical model has never been tested and it has been proposed that PDF-producing neurons via PDF peptides inhibits PTTH production or release (McBrayer et al. 2007).

PTTH is released only after JH levels in the hemolymph are cleared and in some insect also starvation maintains high levels of JH in hemolymph, which prevents PTTH production and also inhibits larval growth (Nijhout & Williams 1974; Cymborowski et al. 1982; Fain & Riddiford 1975). These observations suggest that critical weight is related to the clearance of JH to allow competence for PTTH production. PTTH is then released at the appropriate day-time via control of circadian clock through a mechanism not yet resolved. There is also evidence that ablation of CA increased ecdysone titers (Mirth et al. 2014), suggesting a link.





Chapter II

Dilp8 Signalling Coordinates Growth with Developmental Timing





1. Coordination of growth with developmental timing: The discovery of Dilp8.

An outstanding question of growth control is how the brain knows when the imaginal discs and the overall animal size has approached the correct size to stop producing the JH and to start producing PTTH and ecdysone to induce metamorphosis.

1.1. Classical regeneration studies suggested a negative feedback signal from imaginal discs

Classical regeneration studies in *Drosophila* revealed the existence of negative feedbacks so that the brain or PG does not trigger metamorphosis until all imaginal discs had completed their growth. Recent studies have expanded this notion by showing that damage to the imaginal disc extends the timing at which animals pupate (Halme et al. 2010; Parker & Shingleton 2011). Imaginal discs have remarkable capacity to regenerate physical damage such as those induced by injury, X-irradiation, or genetic ablation (Smith-Bolton et al. 2009; Sun & Irvine 2011). During regeneration, imaginal discs produce a signal that negatively regulates metamorphosis and also inhibits the growth of the undamaged imaginal discs (Parker & Shingleton 2011). Although damage to imaginal discs induces a delay in the developmental timing program, larvae without any imaginal disc can entry pupariation at a normal time indicating that damage-induced negative feedback is produced by the imaginal discs. Consistently, when damage is induced in a larva without imaginal discs, the larval development is not delayed (Simpson et al. 1980; Szabad & Bryant 1982; Poodry & Woods 1990). Moreover, when a damaged imaginal disc is transplanted to an undamaged larva, the damaged tissue is sufficient to induce a delay in developmental programme (Rahn 1972; Dewes 1975).

The retinoids were postulated to encode such a negative signal (Halme et al. 2010); however, this study failed to uncover where the retinoids are produced and whether endogenous retinoids are indeed the signal that damaged imaginal disc produce to delay pupariation. It was also unclear whether this signal also mediated delay in developmental timing by other growth perturbations.

1.2. Dilp8 is a universal signal produced by growth perturbed imaginal discs

Recently, two elegant works, one of them from my group, showed that this signal expressed and secreted from damage imaginal disc is *Drosophila insulin-like peptide 8 (dilp8)*. Dilp8 is secreted from damage imaginal discs (tumours, chemical or genetic damage) and delay the maturation time with the systemic inhibition of undamaged imaginal disc growth (**Figure 9**) (Colombani et al. 2012; Garelli et al. 2012).

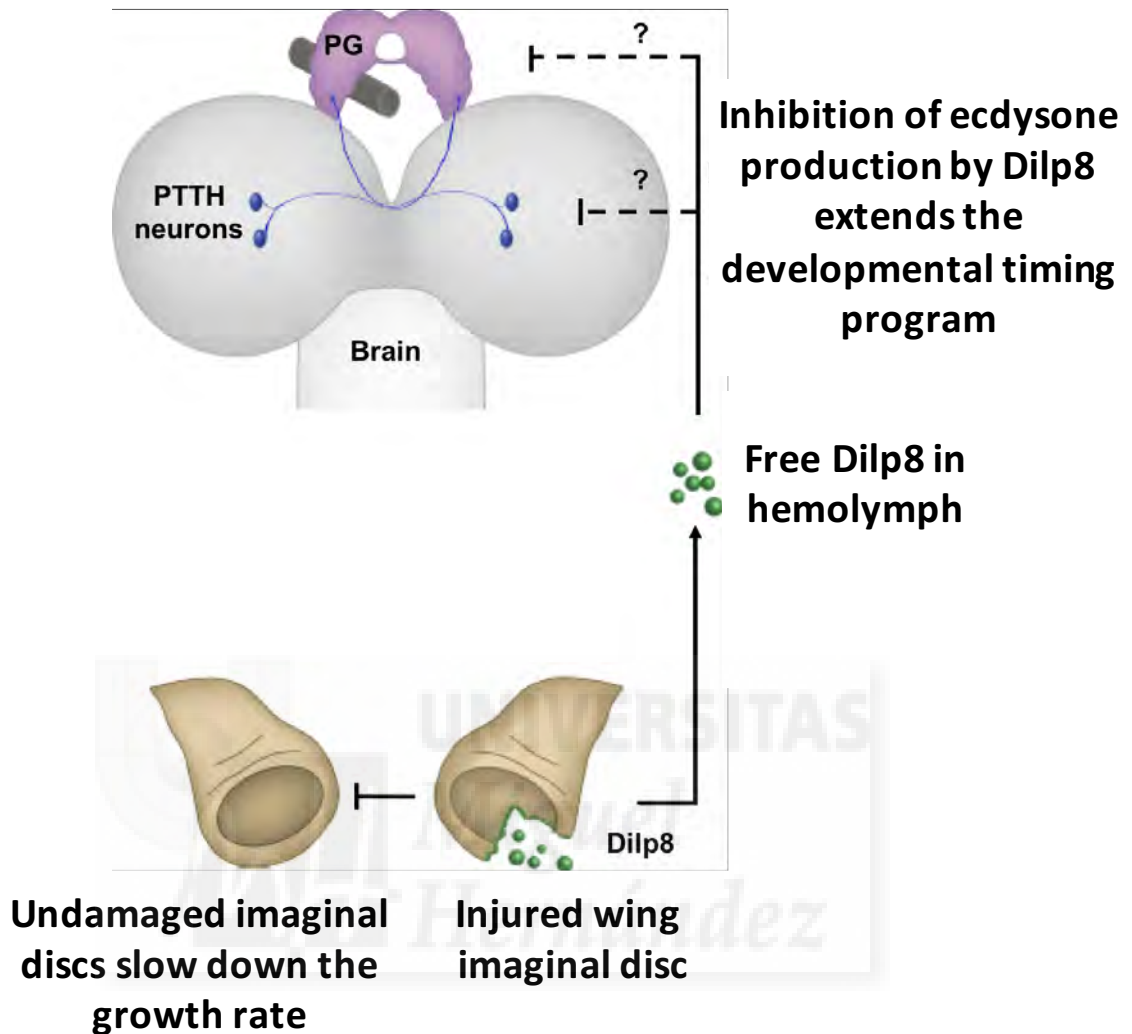


Figure 9: Inter-organ communication and homeostatic size control by the Dilp8 signalling. During third instar larva, the imaginal discs communicate their growth status to the brain via Dilp8, which inhibits developmental transition, providing a tissue repair checkpoint until proper disc size is attained. The *dilp8* gene is activated cell-autonomously in response to imaginal disc growth perturbation. Secreted Dilp8 signals growth status deficit and delays the metamorphosis program in the PG by inhibiting the synthesis of ecdysone so that the damaged or growth-delayed imaginal discs can catch-up growth. At same time Dilp8 reduces the growth rate of the undamaged imaginal discs to prevent they overgrowth during the extended larval period.

Dilp8 is a divergent insulin/relaxin peptide hormone that it has a conserved cysteine motif characteristic for this family. When Dilp8 is secreted by aberrant growth imaginal disc, it can act remotely to inhibit the ecdysone production in the PG and thus, to produce an extension of the pupation timing, generating an extra time for the damage tissue regeneration. This extra time is

generated only in L3 instar larva stage like *ptth* mutants. Furthermore, the non-damage discs slow down their growth to maintain their proportion and size in the adult body. Interestingly, Dilp8 has not effect in patterning of the imaginal disc indicating that Dilp8 acts after disc growth, as a damage sensing system, but upstream to the developmental timing program (Colombani et al. 2012; Garelli et al. 2012). The extension of the developmental timing program produced by *dilp8* up-regulation is directly proportional to the amount of Dilp8 release from the damage disc. Furthermore, the animals lacking *dilp8* showed high fluctuating asymmetry, indicating that Dilp8 controls developmental stability in *Drosophila* (**Figure 9**) (Garelli et al. 2012).

The homeostatic mechanism induced by Dilp8 could be induced by different ways: i) by controlling growth through the direct action in the imaginal disc and the timing program by acting in the PG or ii) regulating pathways of ecdysone production. One work showed how the induction of *dilp8* increased the activity of nitric oxide synthase (NOS) in the PG and thus, NOS limited the growth of undamaged imaginal tissues by reduction of ecdysone production (Jaszczak et al. 2015).

In another hand, expression of *dilp8* has been demonstrated to be regulated by signalling pathways that control the blastema formation. JAK/STAT pathway regulates the expression of *dilp8* in damage imaginal disc by regenerating cells (Katsuyama et al. 2015). Furthermore, JNK pathway is involved in the regulation of *dilp8* in blastemal cells during regeneration process (Colombani et al. 2012). Finally, it is known that Hippo pathway regulate *dilp8* expression in aberrant imaginal disc growth by the co-activator transcription factor York1 (Yki) and its partner Scalloped (sd) that it is bound to the *dilp8* promoter (Boone et al. 2016). Interestingly, *dilp8*-dependent expression by Yki/sd depends of Taiman, a co-activator of EcR indicating a functional loop between ecdysone and *dilp8* to regulate final growth of the maginal disc (Zhang et al. 2015).

About these works, it is supposed that the growth program of imaginal disc is a checkpoint for activation of the neuroendocrine system and general growth control of other tissues and it is an independent checkpoint to nutritional checkpoint related to acquired the 'critical weight'. At this moment the Dilp8 receptor is uncharacterized and the way of actions were not clarified.

1.3. Trade-Offs between Dilp8-mediated developmental homeostasis on late-life fitness or reproductive output?

Interestingly, Imperfection in size such body asymmetry has also been shown to impact performance, mate-choice and prospect to survive an attack from a predator and can even diminish

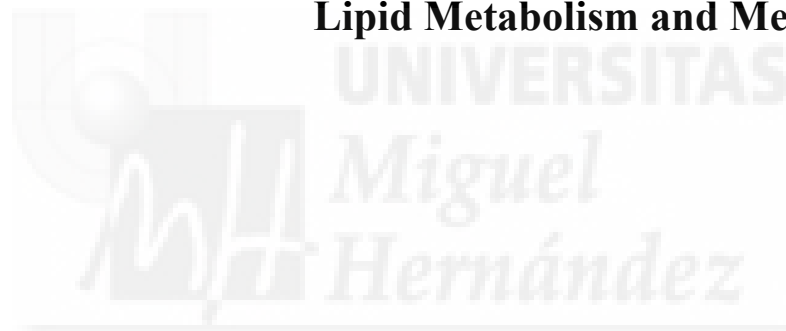
(Livshits & Kobylansky 1991). Smaller than normal body size also decreases fertility and reproductive success. Moreover, fatter adult females have been reported to be less fertile (Tissenbaum & Ruvkun 1998; Pettigrew & Hamilton-Fairley 1997; Tatar et al. 2003). Thus, homeostatic mechanisms that promote and ensure the correct size and body symmetry are likely to benefit animal fitness (Møller & Thornhill 1997). However, it has long been postulated that homeostatic mechanisms that increase some aspect of animal fitness have trade-offs and thus reduces other fitness parameters. For example, increases in fertility are often associated with decreased tolerance to stress and decreased lifespan (Le Bourg 2007; Blomquist 2009). Body weight at pre-puberty state can accelerate age of puberty and reduce fertility in humans (Pasquali 2006). However, the mechanisms underlying the connection between weight, metamorphosis and fitness are poorly understood. In this thesis we have studied the impact of body size and weight in adult fitness.



Chapter III

Circadian Clock: Linking Growth,

Lipid Metabolism and Metamorphosis





1. Circadian clock control of growth and metabolism. An overview

The transition from juvenile to adulthood is a one-on life process and yet this transition is believed to be under control of circadian clock in insects, birds, and mammals (Truman & Riddiford 1974; McBrayer et al. 2007). The circadian clock is a molecular system that sense the light::dark oscillator in the nature to adapt different aspects in the biological cycle of a organism, such as feeding, with sleep-wake cycles. This molecular system consists in the oscillation of transcriptional-translational feedback loops, where the activator promotes the transcription of the repressor genes, and their accumulation of feedback to inhibit their own transcription (Partch et al. 2014). The genetic basis of circadian clock regulation was first defined in *Drosophila* and this discovery has won the Nobel Prize this last year.

Drosophila circadian clock involves Clock (CLK) and Cycle (CYC) proteins, which generate a heterodimeric complex acting as the circadian activator. During light periods CLK-CYC induces the transcription of repressors genes, *period* (*per*) and *timeless* (*tim*). During dark periods, accumulated TIM and PER are translocated to the nucleus to inhibit the transcription of CLK-CYC. In the next cycle of light, PER and TIM are degraded by phosphorylation and a CLK-CYC induces a new positive feedback loop by transcriptional expression of *vri* (*vri*) that acts as a repressor of *Clk* and *Pdp1* (PAR domain protein 1) that then act as a positive regulator of *Clk* transcriptional expression (Zehring et al. 1984; Bargiello et al. 1984; Siwicki et al. 1988; Hardin et al. 1990; X. Liu et al. 1992; Vosshall et al. 1994; Price et al. 1998; Cyran et al. 2003).

The molecular circadian system is present in most tissues and the synchronisation of the peripheral clocks involves systemic signals from central pacemaker neurons in the brain. In *Drosophila* such signal includes the neuropeptide Pigment Dispersing Factor (PDF), which is required not only to synchronize circadian clock neurons within the brain but also to synchronize other peripheral clocks (Hardin 2005; Taghert & Shafer 2006; Yoshii et al. 2009; Myers et al. 2003).

1.1. PDF and Circadian regulation of developmental transition in insects

The coupling of developmental transition to the circadian clock is believed to enhance survival of the animals by restricting this vulnerable developmental transition to the safest time of the day. In insects, the feeding to wandering larvae transition, not the puparium transition, is under circadian clock control. It makes sense because the leaving of larvae from the food to seek an appropriate site

for metamorphosis is the most vulnerable time of the life-cycle of an insect and ensuring this process occurs at the time when there are less predators can increase the prospects of survival of the animals during the period. For example, in *Rhodnius*, the circadian clock gates the transition from feeding to wandering at the early hours of the day because most predators of this specie are nocturnal (Ampleford & Steel 1982). By contrast, the feeding to wandering transition in *Drosophila melanogaster* occurs at the dawn hours, because most *Drosophila*'s predators are diurnal (Markow & L. D. Smith 1979; Schnebel & Grossfield 1986). Eclosion and egg laying are also vulnerable stages and these processes are also gated by the circadian clock (Myers et al. 2003; Selcho et al. 2017).

1.2. Evidence of regulation of metamorphosis by Circadian Clock

Drosophila central pacemaker neurons (PDF neurons) in the larva brain are presumed to directly connect and synapse PTH-producing neurons. This is based on anatomical proximity and evidence in insects and mammals that circadian clock influences developmental timing and 'puberty' (Kyriacou et al. 1990). It is proposed that PDF neurons gate metamorphosis by inhibiting the release of PTH for ecdysone production (McBrayer et al. 2007) (**Figure 10**).

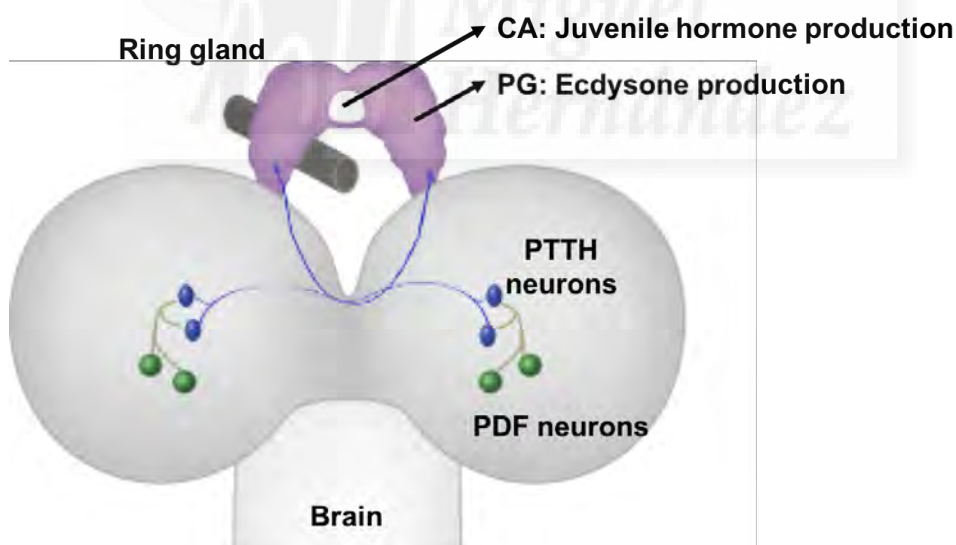
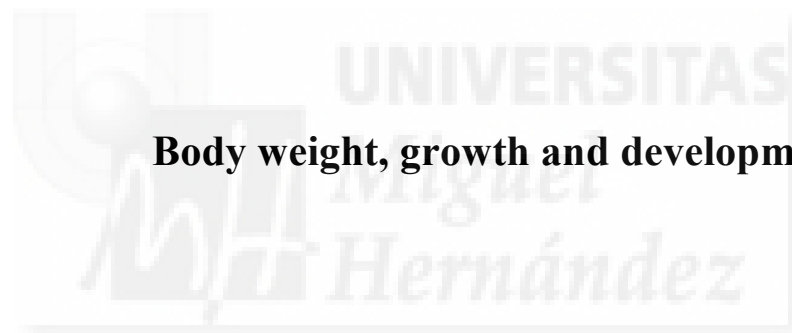


Figure 10: Representation of the hypothetical neuronal circuit controlling PTH release by PTH neurons (blue) by the PDF in pacemaker circadian neurons (green). PTH neurons project towards PG cells and PTH is directly released in the PG for ecdysone synthesis.

In addition, it has also been shown that a peripheral circadian clock in the PG regulates ecdysone production independent of PTH (Di Cara & King-Jones 2016). However, as mentioned above, in most insects including *Drosophila*, experimental evidence show that it is not the time of metamorphosis that is gated by the circadian clock, but the transition from feeding larvae to wandering stage is assume controlled by circadian clock. Moreover, in *Drosophila*, this transition occurs late in the afternoon and we observed that larvae overexpressing *dilp8* overexpression still maintain a circadian rhythm in spite of the dalays (Colombani et al. 2012; Garelli et al. 2012). Thus Dilp8 causes 24 or 48 hours dealys, suggesting that Dilp8-mediated developmental homeostasis is regulated by the circadian clock neurons.







Chapter IV

Body weight, growth and developmental timing



1. The critical weight Hypothesis of ‘Puberty’

It has long been postulated that the brain promotes developmental transition, puberty in humans and metamorphosis in insects, upon sensing the juvenile has surpassed a certain threshold of body mass or fatness (Frisch & Revelle 1970). This ‘critical weight’ hypothesis postulates that the neuroendocrine system could sense body mass or size by measuring fat stores, which it will ensure the adult can survive to generate offspring after puparium formation in holometabolous insect as *Drosophila melanogaster* (Bakker 1962; Bakker 1968; Robertson 2009; Royes & Robertson 1964) (**Figure 11 A**). Furthermore, reduction of nutrients availability before ‘critical weight’ attachment increase developmental timing program to ensure that this ‘critical weight’ is acquired to generate adult with normal body size (Bakker 1962; Robertson 2009; Royes & Robertson 1964; Gebhardt & Stearns 1993) (**Figure 11 B**).

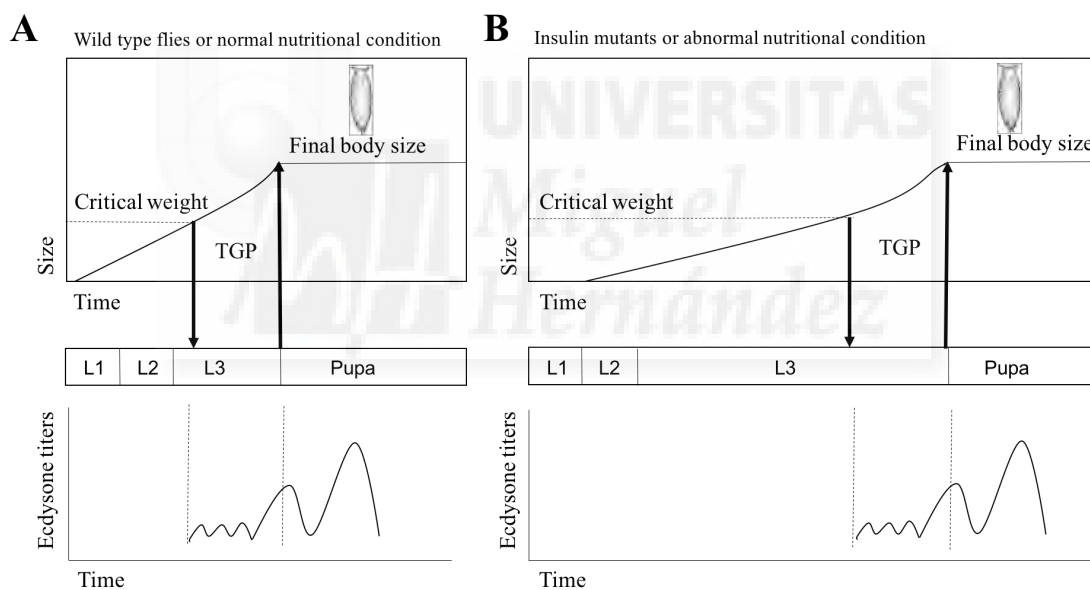


Figure 11: Critical weight control by nutrition and IIS. (A) The larvae grow exponentially until it reaches the minimal weight that would enable the animal to survive metamorphosis. Under normal conditions, after attainment of critical size or weight, the ecdysone titer increases and during this terminal growth period (TGP), the imaginal discs grow exponentially while larval growth decelerates. In the next high peak of ecdysone, metamorphosis ensues and the imaginal discs stop growing. (B) Mutants for IIS cause slow growth and delay attainment of the larval critical weight and size and larval development is extended. After a larva has attained the critical weight, reduced IIS and starvation accelerate pupariation and slow growth during TGP resulting in smaller adult flies. Adapted from Shingleton et al. 2005.

It has been proposed that the PG has capability to sense this ‘critical weight’ acquisition and induces the production of ecdysone to generate the metamorphosis molt in *Drosophila* (Caldwell et al. 2005; Colombani et al. 2005; Mirth et al. 2005). The ‘critical weight’ hypothesis does not inform which fat-signal or sensing pathway generate the PG competence to induce the bigger ecdysone pulse. It is

also unknown whether the neuroendocrine-brain axis monitors a particular form of energy stores or a relay signal that serves as a proxy of body mass.

1.1. Fat body-derived factors controls insulin secretion, body size and weight

Fat body is a sensor that monitors the energy status of the organisms and conveys this information to the IPCs in the brain, controlling the secretion of Dilps. For example, the fat body expresses the amino acid transporter *slimfast (slif)* and in the absence of this transporter the influx of amino acid through the intestine is inhibited and growth is suppressed via the suppression of systemic IIS (Colombani et al. 2003). In the same vein, a suppression of TOR pathway in fat body produces a non-autonomous inhibition of IIS and the suppression or reduction of systemic growth (**Figure 12**) (Britton & Edgar 1998; Géminard et al. 2009; Rideout et al. 2012; Storelli et al. 2011).

The influx of amino acid into the fat body cells activates TOR pathway and generates a released signal, Stunted (Sun), which acts through the G Protein Coupled Receptor (GPCR) Methuselah (Mth) in the IPCs, causing the release of Dilp2 and induction of systemic growth (**Figure 12**) (Delanoue et al. 2016).

Unpaired 2 (Upd2) is another signal released by the fat body that modulates the production of Dilps in the adult. Upd2 is postulated to acts a leptin-like factor in response to fat and sugar in the diet, but not in response to amino acid levels. Upd2 acts indirectly in the IPCs through a group of GABAergic neurons close to IPCs that express the Upd receptor Dome. Upd2 activates Dome which relies signalling through the JAK/STAT cascade within the GABAergic neurons, and indirectly activates the release of Dilps, and fat storage (Rajan & Perrimon 2012). Although Upd2 levels are not regulated by proteins in the diet, the lack of *slim* causes up-regulation of *upd2* indicating a compensatory mechanism to regulate growth in response to diet by remodelling the metabolic programs according to different sources of storage (**Figure 12**).

Protein synthesis also plays a fundamental role in growth control. In the fat body, when the synthesis of tRNA is increased, the protein production by ribosomes induces systemic growth by increased *dilp2* and *dilp5* transcript levels, inducing an acceleration of pupation (Rideout et al. 2012; Marshall et al. 2012).

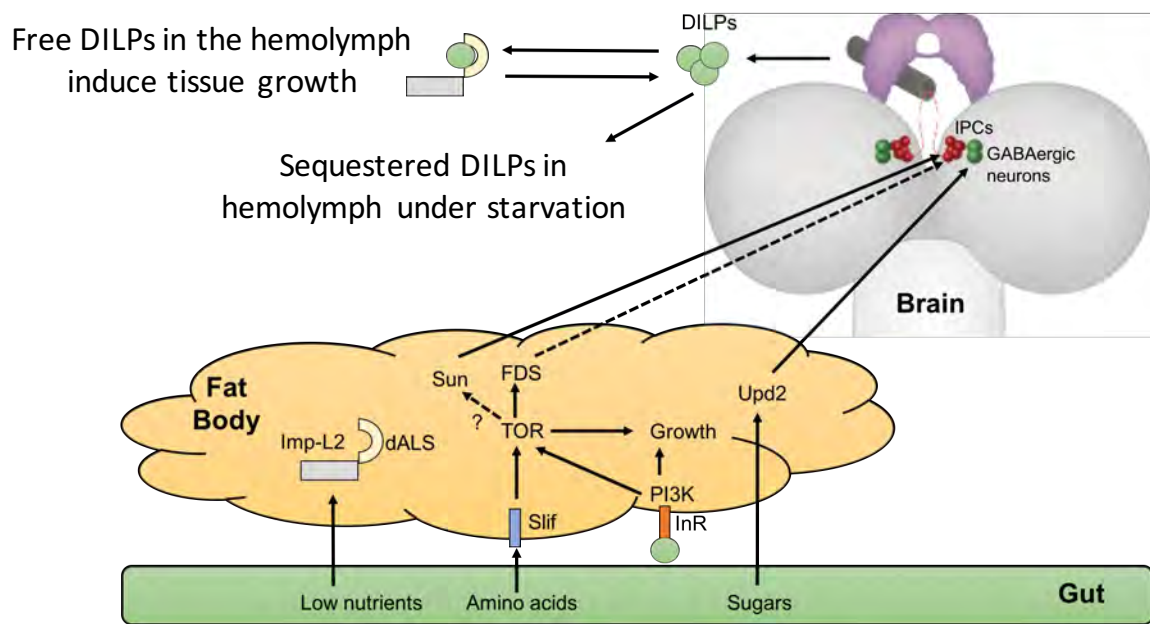


Figure 12: Inter-organ communication between IPCs and fat body to control growth by insulin release. During feeding stages nutrients are uptake from the gut. Amino acids sensing from the fat body produces a release of fat body secreted factors by TOR-dependent manner that induces Dilps release by IPCs in the brain. Furthermore, sugars sensing by fat body induce cytokine upd2 release and activate a IPCs-connecting-GABAergic neurons to induce the Dilps release. Nonetheless, the fat body when sense a lower nutrients uptake from the gut induces the release of Dilps-inhibitory factors such as Imp-L2 and dALS.

All these observations illustrate how nutrients uptake and the fat body influences systemic growth and the timing of metamorphosis but they do not explain how the brain or endocrine system monitor critical weight and triggers wandering behaviour and developmental timing at the correct body size.



2. OBJECTIVES





Specific Objectives:

1. Identification of the receptor(s) for Dilp8 and its/their role in homeostatic growth control and symmetry.
2. Characterization of the tissue(s) and specific cell-types receiving Dilp8 signal.
3. Defining the out-put pathways mediating developmental timing regulation and slow growth.
4. Defining the role of circadian clock in Dilp8-mediated homeostasis.
5. Role(s) of Dilp8 and its receptor in fitness and response to stress in adult stage
6. Identification of mechanism for ``critical weight`` checkpoint and fat sensing.

Objetivos específicos:

1. Identificación de el receptor o receptores para Dilp8 y su papel en el control del crecimiento homeostático y simetría del individuo.
2. Caracterización del tejido y células específicas que reciben la señal de Dilp8.
3. Definir las rutas por las cuales Dilp8 y su receptor (o receptores) regulan el control del tiempo de desarrollo y el crecimiento desde su tejido específico.
4. Definir el papel específico del ciclo circadiano en el control homeostático producido por Dilp8.
5. Estudiar el papel de Dilp8 y su receptor (o receptores) en la respuesta a estres y las consecuencias de su activacion durante el desarrollo en reproduccion y supervivencia.
6. Identificación de los mecanismos que controlan el peso crítico del organismo y la monitorización de grasa durante el desarrollo.





3. MATERIALS AND METHODS



***Drosophila* husbandry**

The five *lgr3* enhancer Gal4 lines (*R17G11-Gal4*, *R17H01-Gal4*, *R18A01-Gal4*, *R18C07-Gal4*, and *R19B09-Gal4*); the *R17G11-LexA*, *R19B09-LexA*, *13xLexAop2-IVS-myr::GFP* lines; and the *retnR9F04-Gal4* line are from the Janelia Farm Collection (Howard Hughes Medical Institute, Ashburn, VA). The *da-Gal4*, *dilp3-Gal4*, *dpp-Gal4*, *elav-Gal4*, *tub-Gal4*, *P0206-Gal4*, *NPF-Gal4*, *pdf-Gal4*, *per-Gal4*, *ptth-Gal4*, *tsh-Gal4*, *LexAop-CD4::spGFP11*, *UAS-CD4::spGFP1-10*, *UAS-dcr2*, *UAS-Denmark*, *UAS-DsRed*, *UAS-Flp*, *UAS-lgr3-TRiP.GL01056-RNAi*, *UAS-mCD8::GFP*, *UAS-mCD8::RFP*, *UASmKir2.1*, *UAS-NaChBac*, *UAS-Syt::GFP*, *pdf-Gal4*, *pdf01*, *hugS3-gal4*, and *hug-TRiP.JF03122-RNAi*, lines are from the Bloomington Stock Center at Indiana University (Bloomington, IN). *UAS-sema1a-IR (KK109430)* from Vienna Drosophila RNAi center. *UAS-dilp8* and *UAS-dilp8^{C150A}* are described in Garelli *et al*, Science. 2012. *CRE-F-luc* and *tor^{RL3}* were gifts from J. C. P. Yin and J. Casanova, respectively (Tanenhaus *et al*, 2012 and J. Casanova, G. Struhl. 1993, respectively). *phm-gal4* line was a gift of K.F. Rewitz.

Flies were reared in standard 'Iberian' fly food at 25°C (except when indicated) on a 14:10-hour light:dark cycle. The composition of Standard Iberian fly food is composed by 15 liters of water, 0,75 kg of wheat flour, 1kg of brown sugar, 0.5 kg of yeast, 0.17kg of agar, 130 ml of a 5% nipagin solution in ethanol, and 130 ml of propionic acid.

Generation of DNA constructs and transgenic lines

The *tub-dilp8::FLAG* construct, *dilp8* cDNA was C-terminally fused in frame to the 3xFLAG coding sequence (Garelli *et al*. 2012) and cloned into the pCaspertubulin promoter plasmid at the KpnI/NotI sites. The *lgr3*WT cDNA sequence was based on the WT amino acid sequence corresponding to GenBank accession number AAF56490, codon-optimized using GeneOptimizer (GENEART), and cloned into the pMK-RQ plasmid (SfiI/SfiI sites) (GENEART). The obtained construct was verified by sequencing and then cloned into the pUAS plasmid at the EcoRI/NotI sites. Constructs were injected in w1118 embryos following standard P-element-mediated transformation procedures (BestGene).

GRASP analysis

We built *R19B09-LexA*; *LexAop-CD4::spGFP11*, *UAS-CD4::spGFP1-10/TM6B* stocks and crossed them with *dilp3-Gal4/CyO-GFP*; *UAS-mCD8::RFP* (n = 14 larval brains were analyzed), *ptth-Gal4/CyO-GFP* (n = 43 larval brains were analyzed), *pdf-gal4* (n = 17 larval brains were analyzed), and *hugS3-gal4* (n = 9 larval brains were analyzed). Control experiments were performed by staining

larval brains of the following genotypes (n = 10 larval brains per genotype were analyzed): *R19B09-LexA*; *LexAop-CD4::spGFP11*, *UAS-CD4::spGFP1-10/TM6B*, *dilp3-Gal4/+*; *LexAop-CD4::spGFP11,UAS-CD4::spGFP1-10/+*; *ptth-Gal4/+*; *LexAop-CD4::spGFP11*, *UAS-CD4::spGFP1-10/+*; *pdf-Gal4/+*; *LexAop-CD4::spGFP11,UAS-CD4::spGFP1-10/+*; and *hugS3-Gal4/+*; *LexAop-CD4::spGFP11,UAS-CD4::spGFP1-10/+*. The following primary antibodies were used: rabbit anti-GFP (1/2000; Invitrogen) to detect GRASP signal between PTTH and Lgr3 neurons, guinea pig anti-PTTH [1/500], and rat anti-Drosophila E-Cadherin (anti-DE-Cad) [1/50, Developmental Studies Hybridoma Bank (DSHB)] to counterstain larval brains.

Confocal imaging and immunohistochemistry in brains and ovaries

Brains were dissected in cold phosphate-buffered saline (PBS), fixed in 4% paraformaldehyde (PFA) for 20 min (Morante & Desplan 2011), and stained with the following primary antibodies: guinea pig anti-PTTH [1/500 (Yamanaka, Romero, et al. 2013)], mouse anti-luciferase (1/200, Thermo Fisher Scientific), rabbit anti-Dilp2 [1/500 (Bader et al. 2013)], rabbit anti-Mira [1/2000 (Ikeshima-Kataoka et al. 1997)], rabbit anti-Pdp1 [1/1000 (Cyran et al. 2003)], anti-Pdf [(1/1000)] and rat anti-DE-Cad (1/50, DSHB). Secondary antibodies were purchased from Invitrogen and Jackson ImmunoResearch. The brains were mounted in Vectashield (Vector Labs), maintaining their three-dimensional (3D) configuration (Morante & Desplan 2011), and images were obtained on a Leica TCS SP2 confocal microscope. Z stacks were recorded at 1- μ m intervals. 3D reconstructions of individual WT Drosophila larval brains were created using Imaris software (Bitplane, Zurich, Switzerland). To assess changes in cAMP levels in the larval brain, we used the in vivo CRE-F-luc reporter system (Tanenhaus et al. 2012). Dissected brains were stained using mouse anti-luciferase (1/200, Thermo Fisher Scientific).

Ovaries were dissected in cold phosphate-buffered saline (PBS), fixed in 4% paraformaldehyde (PFA) for 20 min and stained with mouse anti-GFP (1/100). AlexaFluor secondary antibodies were purchased from Invitrogen and Jackson ImmunoResearch. The ovaries were mounted in Vectashield with DAPI (Vector Labs), maintaining their three-dimensional (3D) configuration, and images were obtained with inverted Zeiss LSM 780 laser scanning confocal microscope.

Maximum projection images of Z-stacks were recorded at 1- μ m intervals and generated in the ImageJ open source image-processing package.

Quantitative RT-PCR

To assess mRNA levels, total RNA was extracted from *Drosophila* larvae using RNAeasy-Mini Kit (Qiagen). To remove contaminating DNA, RNA was treated with Turbo DNA-free (Ambion, Life Technologies). cDNA was synthesized with SuperScript III First-Strand Synthesis System for RT-PCR (Life Technologies) using oligo-dT primers. Quantitative real time PCR was performed using SYBR Green PCR Master Mix (Applied Biosystems) using gene-specific primers, on an ABI7500 apparatus (Applied Biosystems). *Rp49* primers were used for mRNA normalization. Comparative qPCRs were performed in triplicates and the relative expression was calculated using the comparative Ct method.

Primer sequences:

E75B:

Forward 5'-CAACAGCAACAACACCCAGA-3'

Reverse 5'-CAGATCGGCACATGGCTTT-3'

Kr-h1:

Forward 5'-ACAATTTTATGATTCAGCCACAACC-3'

Reverse 5'-GTTAGTGGAGGCGGAACCTG-3'

dilp8:

Forward 5'-CGACAGAAGGTCCATCGAGT-3'

Reverse 5'-GATGCTTGTTGTGCGTTTTG-3'

dilp3:

Forward 5'-ATCCCGTGATTCCACACAAG-3'

Reverse 5'-GCGGTTCCGATATCGAGTTA-3'

dilp5:

Forward 5'-GCCTTGATGGACATGCTGA-3'

Reverse 5'-CATAATCGAATAGGCCCAAGG-3'

dilp2:

Forward 5'-ATCCCGTGATTCCACACAAG-3'

Reverse 5'-GCGGTTCCGATATCGAGTTA-3'

4e-bp:

Forward 5' - GAAGGTTGTCATCTCGGATCC- 3'

Reverse 5' - ATGAAAGCCCGCTCGTAG- 3'

SREBP:

Forward 5' - GCAAAGTGCGTTGACATTAACC- 3'

Reverse 5' - AGTGTCGTGTCCATTGCGAA- 3'

Ascl:

Forward 5' - CGGAGATCCGACAAAGCAGT- 3'

Reverse 5' - TGAGCACAGCTCCTCAAAGG- 3'

ACC:

Forward 5' - AATTCTCCAAGGCTCGTCCC- 3'

Reverse 5' - CATGCCGCAATTGTTTTTCGC- 3'

Bgm:

Forward 5' - GCAATCGATTTGCGTGACCA- 3'

Reverse 5' - GGCCCAGGACGATTGTAGAG- 3'

fas:

Forward 5' - GACATTCGATCGACGCCTCT- 3'

Reverse 5' - GCTTTGGCTTCTGCACTGAC- 3'

dib:

Forward 5' - GTGACCAAGGAGTTCATTAGATTTC- 3'

Reverse 5' - CCAAAGGTAAGCAAACAGGTTAAT- 3

phm:

Forward 5' - TAAAGGCCTTGGGCATGA- 3'

Reverse 5' - TTTGCCTCAGTATCGAAAAGC- 3

InR:

Forward 5' - GCTGTCAAGCAAGCAGCAGTGAA- 3'

Reverse 5' - TCTTTTTACCCGTCGTCGTCTCC- 3

Hex-C:

Forward 5' - CACTGGCACCTTGATGTCCT- 3'

Reverse 5' - GTCCAAGTACCACCCCTCAC- 3

PGM:

Forward 5' - AACTGGCTCCAATCACATCC- 3'

Reverse 5' - AGCGCACTCCTCATAATCGT- 3

bmm:

Forward 5' - TCCCGAGTTTCTGTCCAAGT- 3'

Reverse 5' - GCGTCCTTTCTGTGCTTCTT- 3

Lpin:

Forward 5' - CTCGGCGGCTATCAAAA- 3'

Reverse 5' - ACCTTGTCGTTGTGCTTCCA- 3

CG5966:

Forward 5' - CTCGCAGTGTCCCTTCCTTG- 3'

Reverse 5' - TGCTCCTGGTAATCCTCCTG- 3

pepck:

Forward 5' - CCTGAGCTATTGAACAAAGC- 3'

Reverse 5' - TGACAGACCGCAATTGTCC- 3

pdf:

Forward 5' - ACGATGCGGGCAAGTAAG- 3'

Reverse 5' - ATCTTTCAGTGGTGGGTCGT- 3

rp49:

Forward 5' -TGTCCTTCCAGCTTCAAGATGACCATC- 3'

Reverse 5' -CTTGGGCTTGCGCCATTTGTG- 3'

Measurement of the developmental timing of puparation

20-30 females and 20-30 males were crossed during 24-48 hours. After, the flies were transferred to grape juice agar plates with yeast paste and left 4 hours for egg deposition. Parental flies were removed and laid eggs were incubated 48 hours at 26,5°C. Second instar larvae were transferred onto

5 ml of *Drosophila* standard 'Iberian' food (20 larvae per tube) and reared at 26,5°C. A survey of the pupae was performed at 8 hours intervals, considering four hours after the initiation of egg laying as time "0".

Weight measurements

To measure weighing adult flies or larva, 20-30 females and 20-30 males were crossed during 24-48 hours for egg deposition. Parental flies were transferred every 24 hours to fresh tubes and laid eggs were reared at 26,5°C. Eclosed adult virgin males and virgin females or synchronizes larvae of each genotype were collected (5 groups of 5 individuals per males and 6 groups of 5 individuals per females) and weighed after 12-24 hours using a precision scale.

Larva and pupa size measurements

Pupae and larvae volume determination, 20-30 females and 20-30 males were crossed during 24-48 hours and left 24 hours for egg deposition. Parental flies were transferred every 24 hours to fresh tubes and laid eggs were reared at 26,5°C. Pupae were collected and photographed with their dorsal side up and length and width were measured using ImageJ. Volume was calculated according to the following formula $v = 4/3 \pi(L/2)*(l/2)^2$ (L: length, l: width).

Fluctuating asymmetry index

For adult wing measurements, 20 to 30 females and 20 to 30 males were crossed and left 24 hours for egg deposition. Parental flies were transferred every 24 hours to fresh tubes, and laid eggs were reared at 26.5°C. Adults were collected and left, and the right wings of each individual were excised and rinsed thoroughly with ethanol and mounted in a glycerol-ethanol solution. Wing areas were measured using ImageJ. Intraindividual variation of wing areas was calculated using fluctuating asymmetry index (FAi), employing the formula $FAi = \text{Var}(Ai)$, where Ai are the differences between left and right wing areas of each individual.

Juvenile hormone analog (methoprene) treatment

Males and females (20 to 30 of each) were crossed, and after 24 to 48 hours, flies were transferred to grape juice agar plates with yeast paste and left 4 hours for egg deposition. Parental flies were removed, and laid eggs were incubated 48 hours at 26.5°C. Second-instar larvae were transferred onto 5 ml of *Drosophila* standard Iberian food (20 larvae per tube) and incubated at 26.5°C. Larvae were transferred 24 hours later (72 hours AEL) to 3 ml of *Drosophila* standard Iberian food supplemented with a liquid solution of pure methoprene (Sigma, catalog no. 33375) at a Met:food ratio of 1 mm:1000 mm. An equivalent volume of water was added to the control.

20-Hydroxyecdysone (20E) treatment

20-30 females and 20-30 males were crossed during 24-48 hours. After, the flies were transferred to grape juice agar plates with yeast paste and left 4 hours for egg deposition at 26,5°C. Second instar larvae (48 hours after egg laying) were collected and transferred to plates covered with a thin layer of iberian food. Larvae were transferred 30 hours later approximately (80 hours AEL) to fresh food with 20E (Sigma) or ethanol as control. To supplement with 20E, fly food was melted and cooled, 1 mL dispensed in each tube, and 50 µL of ethanol or 20E stock solution added to reach 0.5 mg/mL final concentration. Developmental timing was measured as above.

Measurement of the starvation resistant experiments

Flies crosses for starvation resistant experiments were grown on iberian food at 26,5°C. The starvation assay start with synchronizes adult virgin flies (males and females) after eclosion from the pupa. The eclosed adult virgin flies were collected into tubes with agar 2% (4 groups of 15 individuals per males and females) and replace each tube every two days. Starvation resistant was measured each 8 hour intervals at 26,5°C.

Measurement of the triglycerides (TAG)

Collect 5 adult virgin flies. Transfer adult flies to a 2 ml microfuge tube and freeze animals in liquid nitrogen for later homogenization. To homogenization add 100 µl of cold PBS + 0.05% Tween 20 (PBST) with tissulaiser. After that, remove 10 µl of homogenized sample to measure protein content with a Bradford assay (Thermo scientific; 23227). Protein samples can be frozen and stored at -80 °C for later analysis. Heat supernatant for 10 min at 70 °C. Do not centrifuge the heat-treated lysate because lipids are partially insoluble in PBST. To measure the TAG first prepare standards: Dilute 40 µl of the glycerol standard solution (Sigma 2.5 mg/ml triolein equivalent glycerol standard; G7793) with 60 µl PBST (100 µl final volume) to generate a 1.0 mg/ml triolein equivalent standard. Do two 2-fold serial dilutions into PBST (50 µl 1 mg/ml + 50 µl PBST for 0.5 mg/ml standard, etc.) to generate 0.125, 0.25 and 0.5 mg/ml standards. Add 20 µl of the glycerol standards, fly samples, and a PBST blank to each 1.5 ml microfuge tubes. Add 20 µl of triglyceride reagent (Sigma; T2449) to each tube (the TAG in this sample will be digested by lipase to free the glycerol backbone). Incubate tubes at 37 °C for 30–60 min. Centrifuge for 3 min at full speed. Transfer 30 µl of each sample to a clear-bottom 96-well plate. Add 100 µl of free glycerol reagent (Sigma; F6428) to each sample and mix well. Seal the wells with parafilm to prevent evaporation and incubate the plate for 5 min at 37 °C. Use a plate reader to measure absorbance at 540 nm. Determine the TAG concentration for each sample by subtracting the absorbance for the free glycerol in the untreated

samples from the total glycerol concentration in samples that have been incubated with triglyceride reagent. The TAG content in each sample is calculated based on the triolein-equivalent standard curve. This assay is linear from 0–1.0 mg/ml TAG.

Behavioural mating and egg laying assays

All flies were raised on conventional cornmeal-agar-molasses medium at 25 °C in a 12 h:12 h dark:light cycle. Virgin males and females were collected after eclosion. Males were aged individually for five days and females were aged for five days in groups of 20. All assays were performed at circadian time 15:00–19:00, and on at least three independent occasions. For assays, single female and male virgins were paired in 10-mm-diameter chambers and were recorded for 1 h at 25°C and humidity control conditions. The time to copulation for each female was annotated to be used for the latency plot. The females that copulated were then transferred individually to food vials for 48 h, and the number of eggs laid by each female was counted manually. Females were then either re-tested for receptivity in the same manner in pairings with naive Canton-S males.





4. RESULTS

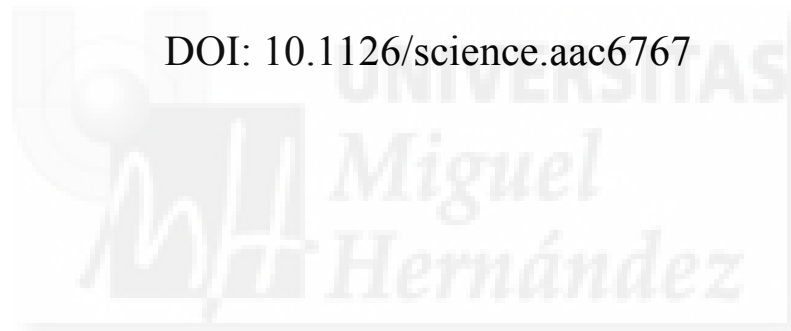


Part I:

A brain circuit that synchronizes growth and maturation revealed
through Dilp8 binding to Lgr3

Science, 13 November 2015, Vol. 350 Issue 6262

DOI: 10.1126/science.aac6767





RESEARCH ARTICLE SUMMARY

GROWTH CONTROL

A brain circuit that synchronizes growth and maturation revealed through Dilp8 binding to Lgr3

Diana M. Vallejo,* Sergio Juarez-Carreño,* Jorge Bolivar, Javier Morante,† Maria Dominguez†

INTRODUCTION: Animals have a remarkable capacity to maintain a constant size, even in the face of genetic and environmental perturbations. Size imperfections and asymmetries have an effect on fitness, potentially decreasing competitiveness, survival, and reproductive success. Therefore, immature animals must employ homeostatic mechanisms to counteract substantial size variations and withstand developmental growth perturbations caused by genetic errors, disease, environmental factors, or injury. Such mechanisms ensure that, despite inevitable variations, the appropriate final body size is attained. A better understanding of homeostatic size maintenance will afford insights into normal organ and organismal size control, as well as the developmental origin of anomalous random left-right asymmetries.

RATIONALE: The *Drosophila* insulin-like peptide Dilp8 has been shown to mediate homeostatic regulation. When growth is disturbed, Dilp8 is strongly activated and sexual maturation is postponed until the affected elements are reconstituted; simultaneously, the growth of other organs is retarded during this process. This compensatory mechanism allows the growth of the affected tissues to catch up. It maintains the synchrony between organs so that the animals achieve the correct size, preserving proportionality and bilateral symmetry. However, the Dilp8 receptor and its site of action remain uncharacterized.

RESULTS: We found that Dilp8 binds to and activates the relaxin leucine-rich repeat-containing G protein-coupled receptor Lgr3 to mediate homeostatic control through a

pathway dependent on adenosine 3',5'-monophosphate. Larvae that lack *Lgr3* in neurons alone do not respond to Dilp8, indicating that the homeostatic system is centered in the brain. Dilp8 delays reproductive maturation by suppressing the neurons releasing the prothoracicotrophic hormone (PTTH), which projects to the prothoracic gland and regulates ecdysone production for growth termination. However, this modulation alone is insufficient to adjust growth and stabilize body size. We show that Dilp8-Lgr3 balances growth against the extended growth period by dampening the production of *dilp3* and *dilp5* by insulin-producing cells (IPCs) in the brain and inhibiting synthesis of the juvenile hormone (JH).

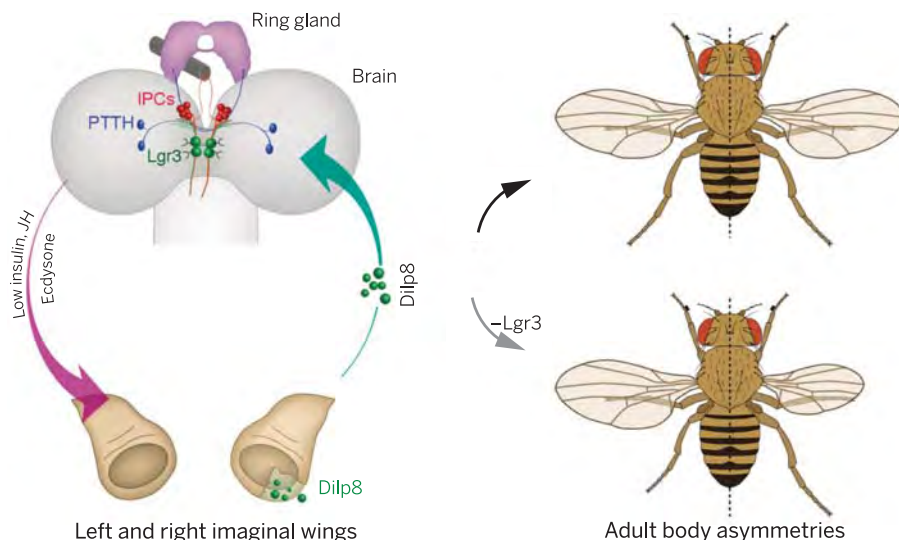
ON OUR WEB SITE

Read the full article at <http://dx.doi.org/10.1126/science.aac6767>

We also identify two pairs of dorsomedial neurons in the pars intercerebralis that are necessary and sufficient to mediate the effects of Dilp8. Simultaneous detection of pre- and postsynaptic markers revealed that the Lgr3 neurons mediating this homeostatic control have extensive axonal arborizations. Genetic and GRASP (GFP reconstitution across synaptic partners) analyses demonstrate that these neurons are connected to both the IPCs and PTTH neurons critical for adjusting growth and maturation rate, respectively. Thus, through their extensive axonal arborizations, Lgr3 neurons function like a "neuronal hub": They route peripheral information about growth status to other neuronal populations, thereby synchronizing damaged tissues and other (undamaged) ones and allocating additional development time so that each organ attains the correct size and maintains proportionality and symmetry.

CONCLUSION: We identified the relaxin receptor Lgr3 as a Dilp8 receptor and defined a brain circuit for homeostatic control of organismal and organ size in the face of perturbations. Lgr3 neurons that respond to Dilp8 signals directly input on the insulin-producing cells and the PTTH-producing neurons. As Lgr3 outputs, the modulation of these neuronal populations according to Dilp8 levels is critical to delay maturation and promote growth compensation in a manner that stabilizes body size. Without adequate Dilp8-Lgr3 signaling, the brain is incapable of stabilizing size between the distinct body parts, and we see left-right asymmetries and size variations that are greater than usual, reflecting developmental instability. ■

The list of author affiliations is available in the full article online.
*These authors contributed equally to this work.
†Corresponding author. E-mail: m.dominguez@umh.es (M.D.); j.morante@umh.es (J.M.)
Cite this article as D. M. Vallejo et al., *Science* 350, aac6767 (2015). DOI: 10.1126/science.aac6767



Dilp8-Lgr3 neural circuit and outputs for body-size homeostasis. The brain detects growth status and anomalies via Dilp8 activation of the Lgr3 receptor in two pairs of symmetric neurons. These neurons distribute this information to IPCs and PTTH neurons, which then trigger the hormonal responses that stabilize size. Without Dilp8-Lgr3 homeostasis, the brain cannot correct variation, and identical body parts can display imperfect symmetry and size.

RESEARCH ARTICLE

GROWTH CONTROL

A brain circuit that synchronizes growth and maturation revealed through Dilp8 binding to Lgr3

Diana M. Vallejo,^{1*} Sergio Juarez-Carreño,^{1*} Jorge Bolívar,² Javier Morante,^{1†} María Domínguez^{1†}

Body-size constancy and symmetry are signs of developmental stability. Yet, it is unclear exactly how developing animals buffer size variation. *Drosophila* insulin-like peptide Dilp8 is responsive to growth perturbations and controls homeostatic mechanisms that coordinately adjust growth and maturation to maintain size within the normal range. Here we show that Lgr3 is a Dilp8 receptor. Through the use of functional and adenosine 3',5'-monophosphate assays, we defined a pair of Lgr3 neurons that mediate homeostatic regulation. These neurons have extensive axonal arborizations, and genetic and green fluorescent protein reconstitution across synaptic partners show that these neurons connect with the insulin-producing cells and prothoracicotrophic hormone-producing neurons to attenuate growth and maturation. This previously unrecognized circuit suggests how growth and maturation rate are matched and co-regulated according to Dilp8 signals to stabilize organismal size.

The impressive consistency and fidelity in the size of developing organisms (1–3) reflect both the robustness of genetic programs and the developmental plasticity necessary to counteract the variations in size arising from genetic noise, erroneous morphogenesis, disease, or injury (4, 5). To counterbalance growth abnormalities, systemic homeostatic mechanisms are implemented that delay the onset of the reproductive stage of adulthood until the correct size of the individual and its body parts has been reached (6–9). Most animals initiate a pubertal transition only after the critical size and body mass have been achieved and, generally, in the absence of tissue damage or growth abnormalities (5, 8–11). However, the mechanisms underlying such homeostatic regulation have yet to be fully defined.

Recently, the secreted peptide Dilp8, a member of the insulin/relaxin-like family, has been identified as a factor that mediates homeostatic control in *Drosophila melanogaster*. During the larval (growth) stage, the expression of *dilp8* declines as maturation proceeds, whereas its expression is activated when growth is disturbed (12, 13). Hence, fluctuating Dilp8 levels provide a

reliable read-out of overall growth status (e.g., deficit) and the time needed to complete growth. In addition, Dilp8 orchestrates hormonal responses that stabilize body size. This includes (i) inhibiting the production of the steroid hormone ecdysone by the prothoracic gland (PG) until the elements or organs affected are re-composed and also (ii) slowing down growth rates of undamaged tissues to ensure that affected organs catch up with normal tissues so that the adult flies reach a normal body size and maintain body proportions and symmetry. Accordingly, in the absence of *dilp8*, mutant flies are incapable of maintaining such strict control over their size, as reflected by the exaggerated variation in terms of overall proportionality and imperfect bilateral symmetry (12). However, the receptor that transduces Dilp8 signals and its site of action remained unknown.

Two models can be envisioned to establish such homeostatic regulation: (i) a central mechanism that dictates coordinated adjustments in both the duration and rate of growth and (ii) an endocrine mechanism that involves sensing and processing Dilp8 signals directly by hormone-producing cells (Fig. 1A) (14). In *Drosophila*, several anatomically separate neural populations regulate growth and maturation time by impinging directly on the ring gland [which is made up of the PG and the juvenile hormone-producing corpus allatum (CA)] (1, 2, 4). Thus, the receptors that transduce the Dilp8 signals of growth status may act directly or may communicate with neurons that produce the prothoracicotrophic hormone (PTTH) (15) and/or the neurons of the pars intercerebralis, including the insulin-producing

cells (IPCs), which synthesize and release insulin-like peptides Dilp2, Dilp3, and Dilp5 (9, 16). Insect PTTH neurons, which are analogous to the gonadotropin-releasing hormone (GnRH) neurons in mammals (5, 10), signal the commitment to sexual reproduction by stimulating the production of ecdysone in the PG to terminate growth (14). The IPCs in the pars intercerebralis, a functional equivalent of the mammalian hypothalamus (10, 15), integrate nutritional signals and modulate tissue growth accordingly (16–20). Manipulation of IPCs by genetic ablation, starvation, or mutations in the single insulin receptor (17, 18, 20–22) leads to the generation of animals with smaller size. Similarly, manipulations of the PTTH neuropeptide and neurons result in adult fly size variations, leading to flies that are larger or smaller than normal due to an extension or acceleration of the larval period (15). The insulin receptor also directly activates synthesis of the juvenile hormone (JH) (a hormone that promotes growth and juvenile development) in the CA (23) and production of the steroid prohormone ecdysone in the PG (14), again augmenting the variation in normal adult size. These observations may explain how environmental and internal influences operate through individual IPCs or PTTH neurons to enable body-size variation and plasticity in developmental timing that can be vital for survival in changing environments. However, the origin of developmental stability and invariant body size may require different or more complex neural mechanisms from those involved in adaptive size regulation.

By employing a candidate approach and biochemical assays, we demonstrate that the orphan relaxin receptor Lgr3 acts as a Dilp8 receptor. We identify the neuronal population molecularly defined by the *Lgr3* enhancer fragment *R19B09* (24) and show that it is necessary and sufficient to mediate such homeostatic regulation. Using tools for circuit mapping and an adenosine 3',5'-monophosphate (cAMP) sensor as an indicator of Lgr3 receptor activation *in vivo*, we determined that a pair of these Lgr3 neurons is highly sensitive to Dilp8. These neurons display extensive axonal arborizations and appear to connect with IPCs and PTTH neurons to form a brain circuit for homeostatic body-size regulation. Our data identify the insulin genes, *dilp3* and *dilp5*, the JH, and the ecdysone hormone as central for developmental size stability. Collectively, these findings unveil a homeostatic circuit that forms a framework for studying how the brain stabilizes body size without constraining the adaptability of the system to reset body size in response to changing needs.

Results

The relaxin receptor Lgr3 mediates Dilp8-induced homeostatic control

Dilp8 bears homology to the human relaxin peptides (12, 25). Therefore, we investigated the role for the two fly relaxin receptors encoded by the orphan leucine-rich repeat-containing

¹Instituto de Neurociencias, Consejo Superior de Investigaciones Científicas and Universidad Miguel Hernández, Campus de Sant Joan, Apartado 18, 03550 Sant Joan, Alicante, Spain. ²Departamento de Biomedicina, Biotecnología y Salud Pública, Facultad de Ciencias, Universidad de Cadiz, Polígono Río San Pedro s/n, 11510 Puerto Real, Spain.

*These authors contributed equally to this work. †Corresponding author. E-mail: m.dominguez@umh.es (M.D.); j.morante@umh.es (J.M.)

lgr3-expressing peripheral tissues, such as the larval fat body (27), could also contribute.

Lgr3 is a Dilp8 receptor

Next, we used biochemical assays to investigate the interaction of Dilp8 and Lgr3. Human relaxin receptors largely activate cytosolic cAMP (25); thus, we tested whether the response of *Drosophila* Kc cells transiently expressing *lgr3* to synthetic *Drosophila* Dilp8 peptides (materials and methods) was coupled to cAMP. To control for specificity, we also transfected Kc cells with constructs encoding the structurally related Lgr4 (26, 27), as well as Lgr2, which is known to provoke a well-characterized cAMP-mediated response upon binding its respective cognate ligand (29). Only cells transfected with the *lgr3*-expressing plasmid responded to a 30-min exposure to Dilp8 (50 nM) with an increase in cAMP levels, from 213.8 ± 67.94 fmol/ 5×10^4 cells to $1.612.36 \pm 302.6$ fmol/ 5×10^4 cells (Fig. 2A and materials and methods). As a reference, the cAMP levels in Kc cells transfected with the empty vector alone were 132.69 ± 66.71 fmol/ 5×10^4 cells and 127.73 ± 77.19 fmol/ 5×10^4 cells in the presence and absence of synthetic Dilp8 (50 nM), respectively (Fig. 2A). This response to Dilp8 is highly specific, because we did not detect comparable changes in cAMP when cells expressing the Lgr4 and Lgr2 receptors were exposed to Dilp8 (Fig. 2A).

A dose-response curve indicated that Dilp8 peptides activate Lgr3 to produce a median effective concentration (EC_{50}) of 6.31 ± 0.12 nM, whereas Lgr4 and Lgr2 did not stimulate cAMP production in response to Dilp8 at any of the doses assayed (Fig. 2B). As the full receptor could not be solubilized, we used a strategy previously employed for the identification of LGR7 and LGR8 as receptors of human relaxin (30) and LGR4

and LGR5 of R-spondins (31). We cloned the ectodomain of Lgr3, fused it to the epitope 3x hemagglutinin (3xHA), and designated this as Lgr3-ECD::3xHA. On the basis of structural homology of LGRs to glycoprotein hormone receptors (25, 31), the extracellular domain of the Lgr3 is expected to be soluble and to bind cognate ligands. Indeed, we detected a strong colocalization of Dilp8 at the surface of Lgr3-expressing cells (Fig. 2C and fig. S2). Furthermore, we coimmunoprecipitated a Myc-tagged Dilp8 with the extracellular domain of Lgr3 (Lgr3-ECD::3xHA) (Fig. 2D, materials and methods, and fig. S2). Collectively, these data suggest that Lgr3 encodes a functionally relevant Dilp8 receptor that is coupled to cAMP signaling like the human relaxin receptors RXPF1-2 (25).

The Lgr3 receptor acts in a small set of central brain neurons

When the endogenous expression of the *lgr3* gene was quantified (fig. S1A) (27), it appeared to be expressed only very weakly. Not surprisingly, attempts to map *lgr3*-expressing neurons by conventional immunological approaches using antibodies against the Lgr3 protein (materials and methods) were unsuccessful. For example, the Lgr3⁷¹⁹⁻⁷³³ antiserum readily detected the Lgr3 protein ectopically expressed using the *GAL4/UAS* system (fig. S2, G to G''), confirming the specificity of our antisera, yet it could not detect endogenous *lgr3* expression, supporting the weak expression of the Lgr3 protein.

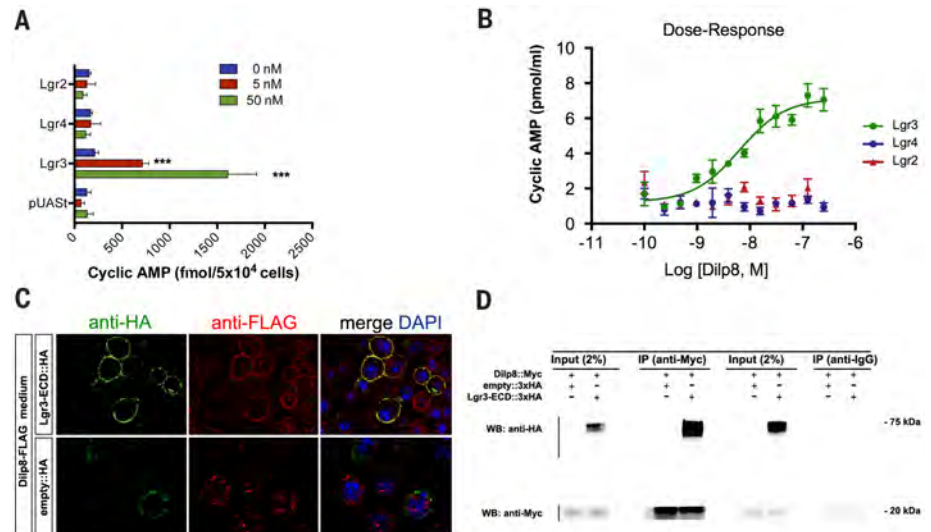
Using the *Gal4/UAS* system to coarsely map functionally relevant neurons, we found that Lgr3 is not required within the IPCs themselves (*dilp3-Gal4*), the neuropeptide F-expressing cells (*nprf-Gal4*), the circadian clock neurons (*pdf-Gal4* and *per-Gal4*), the PTTH neurons (*ptth-Gal4*), or

the ventral nerve cord (VNC) [*teashirt (tsh)-Gal4*], all of which have been previously established to regulate the larval-pupal transition and/or body size in response to nutrition, sensory inputs, and developmental cues (14, 15, 17, 20, 32, 33). When *UAS-lgr3-RNAi* was expressed in these specific brain regions using these *Gal4* lines in *tub-dilp8* animals, the animals entered pupation at times similar to those of *tub-dilp8* animals carrying *Gal4* or *UAS-lgr3-RNAi* alone (Fig. 3A).

We next took advantage of the available lines expressing *Gal4* under control of genomic fragments from the *lgr3* locus (24) (Fig. 3B). We found that using the *R19B09-Gal4* enhancer to deplete *lgr3* (Fig. 3B) fully suppressed the Dilp8-induced delay and did so with the same magnitude as when *lgr3* was ubiquitously depleted by *tub-Gal4* (Fig. 1B). No other *Gal4* enhancer lines prevented the Dilp8-induced delay (Fig. 3B). Depleting *lgr3* in neurons labeled by *R19B09-Gal4* also prevented the slow growth rate of imaginal discs induced by Dilp8, as reflected by the restoration of almost-normal transcript levels for the *Thor/4E-BP* gene, a direct target of the growth inhibitor FoxO, and a diagnosis for imaginal disc growth rates (12, 18) (Fig. 3C). Thus, Dilp8 influences growth and maturation through Lgr3 activation in neurons molecularly defined by the *R19B09* enhancer.

We also found that overexpression of the *UAS-lgr3* transgene in *R19B09*-labeled neurons was sufficient to evoke a ~12-hour delay in pupariation (Fig. 3D), but this process was not delayed when expressed under control of the other *lgr3* genomic fragments (fig. S3). Because most G protein-coupled receptors (GPCRs) display some level of constitutive activity [two-state model of GPCR function (34)] in the absence of agonist

Fig. 2. Lgr3 is a Dilp8 receptor. (A) cAMP measurement in untreated *Drosophila* Kc cells (5×10^4 cells per culture) transiently transfected with the indicated Lgr plasmids and the empty plasmid or treated with either 5 or 50 nM Dilp8 peptide for 30 min. Data are shown as mean \pm SD ($n = 3$ independent repeats), and the asterisks indicate that the cAMP level was statistically different from untreated controls, *** $P < 0.001$ (t test). (B) Dilp8-stimulated dose-dependent cAMP production by Kc cells expressing Lgr3. The concentration of Dilp8 ranged from 0 to 250 nM. Kc cells were transiently transfected with the *lgr3*, *lgr4*, or *lgr2* plasmids, and an EC_{50} value of 6.31 ± 0.1277 nM was obtained for Lgr3. Exposure of the Kc cells expressing the related receptors Lgr4 or Lgr2 to Dilp8 did not affect cAMP production. A sigmoid fit to the *lgr3* data is shown. Total cAMP production was measured in triplicate (materials and methods). Each data point is mean \pm SEM ($n = 3$ independent repeats). (C) Dilp8 and Lgr3 colocalization assessed by confocal immunofluorescence. Kc cells expressing the extracellular domain of Lgr3-ECD::3xHA were incubated with medium containing Dilp8-Flag (materials and methods). The cells were fixed without permeabilizing and were then stained with anti-FLAG (red) and anti-HA (green) antibodies. The nuclei were counterstained with 4',6-diamidino-2-phenylindole (DAPI). Images are also presented for Kc cells transiently transfected with the empty::3xHA vector and exposed to Dilp8-Flag. Representative images of three repeats are shown. (D) Binding of Dilp8 to Lgr3 assessed by coimmunoprecipitation. Rabbit anti-Myc or rabbit anti-IgG antibodies were used to pull down Lgr3-ECD::3xHA complexed to Dilp8-Myc. Input controls are also shown. IP, immunoprecipitation; WB, western blot.



ligands, delayed pupariation due to increased levels of endogenous *lgr3* via overexpression in *R19B09*-labeled neurons might reflect an increased response to a low concentration of endogenous Dilp8 or constitutive activity. However, Lgr3 displays high levels of constitutive activity only when expressed in a heterologous system [human embryonic kidney 293 cells (27)]; this high constitutive activity is not observed in *Drosophila* cells (Fig. 2A) or in vivo in neurons (see below). Moreover, Lgr3 activity is greatly increased in the presence of Dilp8 (Fig. 2, A and B, and below). Activation of *R19B09* neurons by expressing the *UAS-NaChBac* ion channel transgene (35) was sufficient to trigger a delay of ~18 hours (*R19B09>NaChBac*) (Fig. 3E), which suggests that Dilp8-stimulated Lgr3 activation excites these neurons electrically.

R19B09-Gal4 labels cells in the central brain (CB) and the VNC (Fig. 4A; see figs. S4 and S5A for expression of other *lgr3* enhancer fragments). Together with the observations made for the *tsh-Gal4* line (Fig. 3A), which typically labels all neurons in the VNC (33), we conclude that a

set of ~12 central neurons per hemisphere, molecularly defined by *R19B09-Gal4*, reflects the Lgr3 neurons that are necessary and sufficient to control size and developmental timing in response to Dilp8. These include neuronal clusters in the dorsomedial region and in the supraesophageal ganglion (SOG) region, as well as individual cells in the dorsal and ventral protocerebrum (Fig. 4, A and B).

A pair of dorsomedial neurons acutely responds to Dilp8

The Lgr3 receptor response to Dilp8 is strongly coupled to cAMP stimulation (Fig. 2, A and B), enabling us to precisely determine the Lgr3-responding neurons via a cAMP biosensor. We used the *CRE-F-luciferase (luc)* construct (CRE, cAMP response element) (Fig. 4B) that has already been characterized in vivo (36). Thus, by combining the *CRE-F-luc* construct with *UAS-Flp* and *R19B09-Gal4*, we could assay specific cAMP responses in a physiological context (*R19B09* neurons and *tub-dilp8* background) (Fig. 4, C and D). To test whether the depletion

of *lgr3* via *UAS-lgr3-RNAi* rendered the sensor insensitive to Dilp8, we used *elav-Gal4* on the X chromosome.

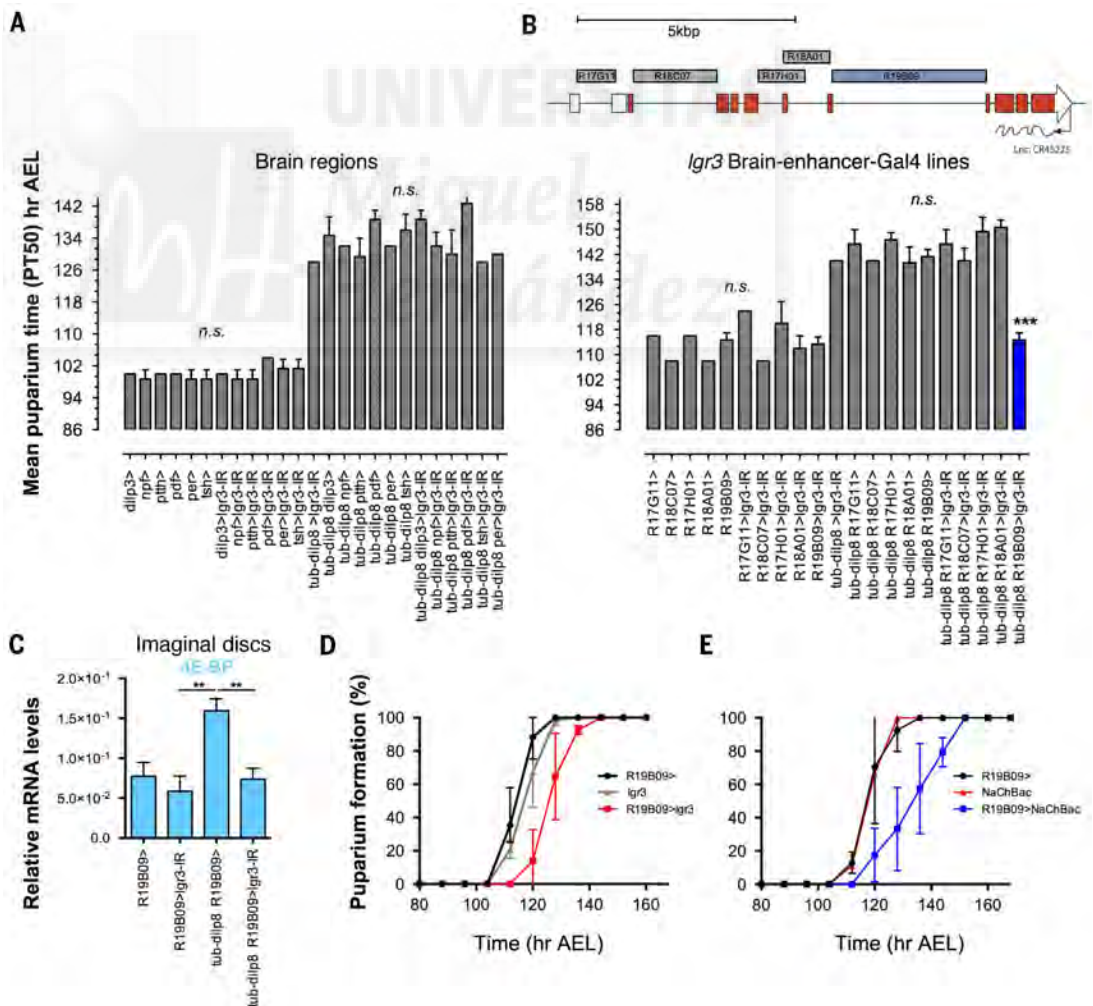
Typically, two neurons with their soma in the dorsomedial region of the pars intercerebralis were bilaterally and strongly labeled in all *tub-dilp8* brains (Fig. 4, C and C', cells designated as type 1) but not in wild-type (WT) brains (Fig. 4D) or in *tub-dilp8 elav-Gal4>lgr3-RNAi* brains (Fig. 4E). Two to three weakly labeled cells in the dorsolateral region of the CB (designated as type 2) (Fig. 4, B, C', and G) were also consistently labeled in *tub-dilp8* brains (Fig. 4, C, C', and F). Moreover, unilaterally labeled dorsal cells (type 3) were occasionally seen in the three genotypes, and these luciferase-positive cells were identified as neuroblasts and not neurons by simultaneously colabeling with the Miranda (Mira) protein (Fig. 4C).

Other *lgr3* genomic fragments (e.g., *R17G11-Gal4*) (fig. S5) that did not suppress the Dilp8-induced delay failed to produce levels of Dilp8-induced cAMP comparable to those found in *R19B09*-labeled neurons (fig. S5, A and B), in agreement with

Fig. 3. Lgr3 acts in a set of central neurons molecularly defined by *R19B09-Gal4*.

(A) Puparium time of animals with brain-region-specific knockdown of *lgr3*, using RNAi and the indicated *Gal4*. (B) Puparium time of animals with knockdown of *lgr3*, using *lgr3* brain-enhancer fragment-*Gal4* lines. Organization of the *lgr3* genomic region and the intervals of each of the Lgr3 enhancers (24) are presented in the top image. In (A) and (B), data are mean \pm SD and are pooled from three independent experiments; 60 pupae were scored per genotype. Error bars are invisible when the three replicates coincide.

*** $P < 0.001$ (two-tailed unpaired *t* test). (C) Imaginal disc growth rate in the indicated genotypes assayed by expression of the FoxO target gene, *Thor/4E-BP*, analyzed by qRT-PCR. mRNA was isolated from imaginal discs from 15 age-synchronized larvae (100 hours AEL) for each genotype ($n = 3$ biological repeats, mean \pm SD). ** $P < 0.01$ (two-tailed unpaired *t* test). (D and E) Cumulative puparium time of animals over-expressing *UAS-lgr3*, using *R19B09-Gal4* (D), or with electrical hyperexcitation of neurons labeled by *R19B09-Gal4*, using the *UAS-NaChBac* ion channel (E). Approximately 60 pupae were scored per genotype. Each data point is mean \pm SD ($n = 3$ independent repeats).



their inability to prevent Dilp8-induced delay (Fig. 3B). The number and position of cells that activated de novo luciferase in response to *tub-dilp8* in *CRE-F-luc* brains expressing the *UAS-Flp* pan-neuronally (Fig. 4F) matched the cells identified using the *R19B09-Gal4* line, which suggests that the neurons labeled by this intronic *lgr3* enhancer represent the majority of cells sensitive to Dilp8 signals. The intensity of luciferase in other *Lgr3*-independent cells in the *elav-Gal4* brains was not generally altered (fig. S5D), indicating that the loss of *CRE-F-luc* signal in the dorsomedial and dorsolateral neurons was not due to nonspecific effects of the *lgr3-RNAi*.

Lgr3 neurons are connected to PTTH neurons and IPCs

We used *R19B09-Gal4* and *-LexA* constructs (Fig. 5, A to G), presynaptic (*sytx::GFP*; GFP, green fluorescent protein) and postsynaptic

(DenMark, dendritic marker) markers (37) (Fig. 5, B and C), and brainbow tools (Fig. 5, D to D'') (38) to more precisely define the connectivity of possible synaptic interactions of the distinct *Lgr3* neuronal populations defined by *R19B09-Gal4*. *Lgr3* neurons with their soma in the dorsomedial region and with a prominent response to Dilp8 (Fig. 4C) display extensive axonal arborizations reminiscent of hub neurons (39). These axonal arborizations of the dorsomedial *Lgr3* neurons cover the dendritic fields and axons of PTTH neurons extensively [Fig. 5, A and B, blue denotes antibody to PTTH (anti-PTTH); and movie S1]. Note that the dendrites of PTTH neurons extend in the same direction as their axons (15). *Lgr3* axons and dendritic fields (revealed by *Syt::GFP* and DenMark) (Fig. 5C) are also in close apposition to the IPCs revealed by anti-Dilp2 (Fig. 5, A and C) and by *dilp3-Gal4* (movie S2).

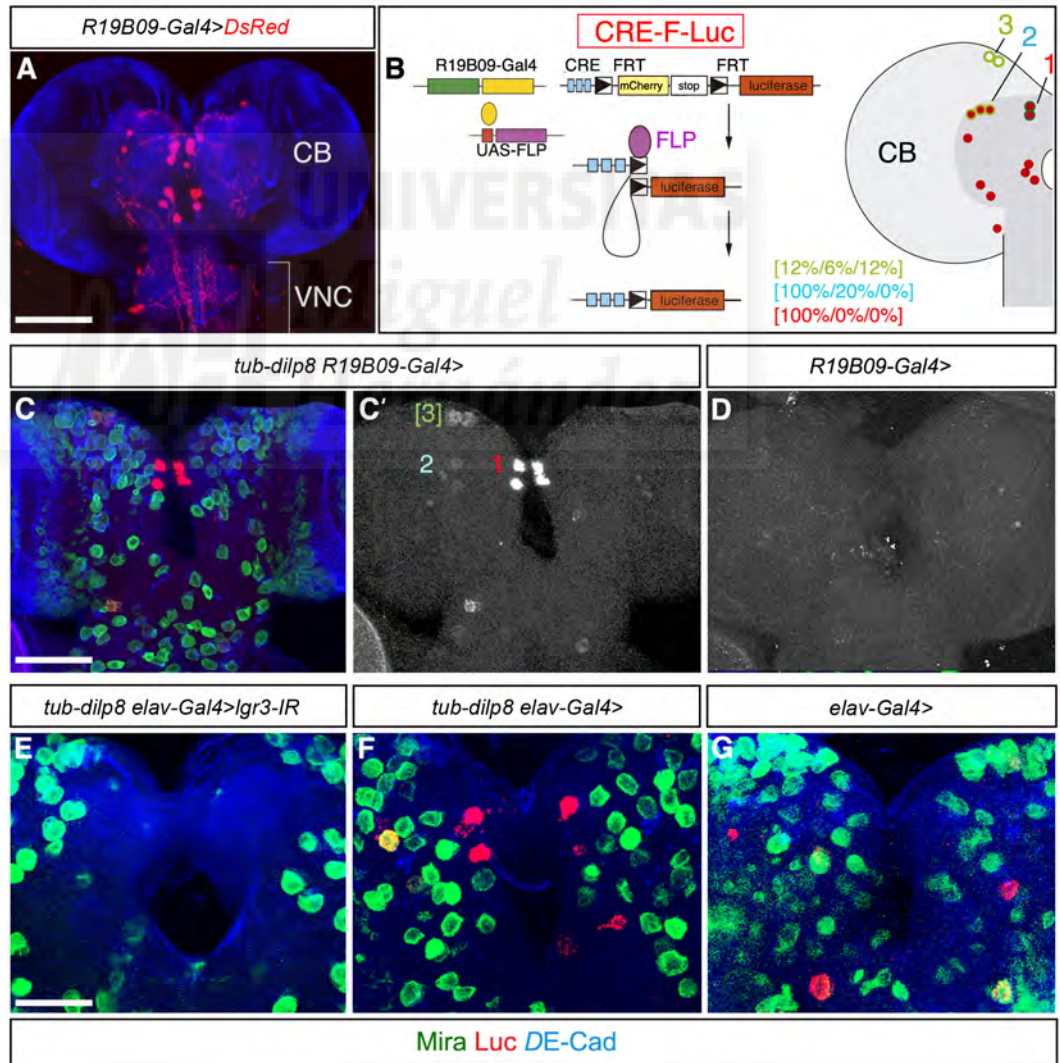
Brainbow-assisted analysis and the pre- and postsynaptic markers revealed that *Lgr3* neurons in the dorsomedial region extend both ipsilateral and contralateral axon projections (Fig. 5, D to D''), with thin dendrites descending into the VNC (Fig. 5, B and C, and movie S3). Brainbow analysis also suggests that a dialogue is maintained between the distinct cell subpopulations defined by *R19B09-Gal4* and that this converges on the synaptic sites of the *Lgr3* dorsomedial neurons (green neurons in brainbow image; Fig. 5, D and D'').

Spatial overlap between axonal and dendritic arborization is a prerequisite for potential connectivity between defined neurons and their potential targets. In this sense, the dense presynaptic sites of *Lgr3* neurons indicate strong connectivity between these neurons and the PTTH neurons and IPCs. Thus, to detect direct connections, we used GRASP (GFP reconstitution across synaptic partners) analysis, which

Fig. 4. A targeted cAMP biosensor reveals a pair of neurons responding acutely to Dilp8.

(A) Expression of *UAS-DsRed* in neurons defined by the *R19B09-Gal4* enhancer (see fig. S4 for the expression of the other *lgr3-Gal4*). (B) *CRE-F-luc* reporter activity is Flp-dependent. (Left) The transgene contains stop sequences flanked by a pair of FRTs (FRT-cassette) inserted between the CREs and the *luciferase* construct. *R19B09-Gal4* activates the *UAS-Flp* transgene, and the FLP protein (purple) excises the FRT cassette in the *CRE-F-luc* transgene, only in *R19B09* cells. (Right) Central neurons (red dots) labeled by *R19B09-Gal4* and cells that respond to Dilp8 signals (outlined in green). The color code denotes the intensity of the signal; the numbers indicate the quantification in *tub-dilp8/wt/tub-dilp8 lgr3-IR* brains ($n > 10$ brains scored for each genotype).

(C and C') Higher-magnification views of central neurons in the dorsomedial region stained with anti-Luc (red) and the neuroblast marker anti-Mira (green). The brain is counterstained with anti-DE-Cad (blue). The *luciferase* response in neuroblasts (Mira-positive cells) in the dorsal region (designated as [3]) is not reproducible and can occur unilaterally. (C') Single-channel confocal image of anti-Luc staining. Genotype: *UAS-Flp/+; tub-dilp8/+; CRE-F-luc/R19B09*. (D) Brain of WT control (*UAS-Flp/+; +/+; CRE-F-luc/R19B09*). (E) Knockdown of *lgr3* (*elav-Gal4/UAS-Flp; tub-dilp8/+; CRE-F-luc/UAS-lgr3-IR*) inhibits the Dilp8-induced cAMP response detected by luciferase driven by the *CRE-F-luc* construct, reflecting *Lgr3* activation and probing specificity of the *UAS-lgr3-IR* transgene. (F and G) Confocal sections of the control brains (F) *elav-Gal4/UAS-Flp; tub-dilp8/+; CRE-F-luc/+* and (G) *elav-Gal4/UAS-Flp; +/+; CRE-F-luc/+*. Scale bars, 75 μ m in (A) and (C) [also applies to (C') and (D)]; 40 μ m in (E) [also applies to (F) and (G)].



is based on the expression of two nonfluorescent split-GFP fragments (spGFP₁₋₁₀ and spGFP₁₁) tethered to the membrane in two neuronal populations (40). We used *R19B09-LexA* (24) to drive expression of *LexAop-spGFP₁₁* and *dilp3-Gal4* or *ptth-Gal4* to drive expression of *UAS-spGFP₁₋₁₀* in IPCs and PTTH neurons, respectively (Fig. 5, E and F). When paired with *R19B09-LexA*, strong, specific GRASP signals were observed for IPCs (Fig. 5E and fig. S6, A and B). GRASP signals also suggest possible connections between Lgr3 and PTTH neurons, as detected by immunofluorescence (anti-GFP, Invitrogen) (Fig. 5F) as in (40). This punctate staining was lacking in control brains (fig. S6C). We detected unreconstituted GFP, using immunofluorescence resulting from expression of the spGFP₁₋₁₀ fragment at the PTTH soma and axons (compare panels C and F in fig. S6). Immunofluorescence staining of PTTH neurons and signals of GRASP between IPCs and Lgr3 revealed probable synaptic contact sites in the circuit (Fig. 5G, asterisks, and fig. S6, D to H). These data suggest that Lgr3 neurons link Dilp8 input to IPCs and/or PTTH neurons to form a homeostatic circuit for synchronizing growth with maturation timing for body-size regulation.

Inhibition of PTTH neurons and mechanism for puparium delay

We reasoned that activation of Lgr3 neurons would delay pupariation by suppressing PTTH synaptic targets, so we used electrical silencing and genetic tools to investigate functional communication between Lgr3 and PTTH neurons. A PTTH receptor mutation (*torso^{RL3}*) that produces a constitutively active receptor has previously been shown to accelerate pupation formation in heterozygosity by 9.2 hours (41). Introducing the *tor^{RL3}* allelic mutation in *tub-dilp8* animals prevented pupariation delay (Fig. 5H) to the same extent as depleting *lgr3* (Fig. 1B) or feeding larvae with the active form of ecdysone, 20E ecdysone (12). These observations, coupled with the anatomical and genetic data, establish that the Dilp8-Lgr3 axis acts upstream of the PTTH-torso network, probably by suppressing PTTH neuron activity.

We wanted to probe the sufficiency of electrically silencing the PTTH neurons to delay the timing of the larval-pupal transition. Thus, we tested the effect of hyperpolarization of the membrane of PTTH neurons by expressing the potassium channel mKir2.1, which has proven to be a highly effective approach for shunting neuronal activity in excitable neurons (42). Expression of *UAS-mKir2.1* in the PTTH neurons using *ptth-Gal4* produced a larval-pupal transition delay of 12 hours compared with WT controls (Fig. 5I and see Fig. 5K for measurement of ecdysone signaling). This is similar to the effect of genetic ablation of PTTH neurons or genetic inactivation of the *Ptth* gene by RNAi reported previously (14). Hence, and as predicted (14), the release of PTTH that triggers the larval-pupal transition is related to PTTH neuron activity. However, electrical hyperexcitation by expressing the *UAS-NaChBac* ion channel by *ptth-Gal4*

could neither accelerate pupariation nor prevent Dilp8-induced delay (fig. S7). It is possible that the release of PTTH at the larval-pupal transition might additionally require disinhibition of inhibitory input(s), as proposed for the secretion of GnRH from hypothalamic neurons at the onset of puberty (5, 10). Electrical silencing of PTTH neurons did not trigger a compensatory growth response (Fig. 5J), and therefore, the animals bred after the extended larval period were larger than normal. Thus, the coupled control of the growth rate probably involves the other branch (the IPCs) of the Lgr3 neuronal circuit.

The IPCs as an Lgr3 output pathway and the role of JH in growth compensation

Our previous study showed that *dilp8* overexpression reduces the growth rate associated with a reduction in insulin-like peptide *dilp3* (12). Hence, we tested the possibility that this transcriptional modulation in the postsynaptic target (IPCs) may be a consequence of the inhibitory input to IPCs from the Lgr3 neurons. Ablation or electrical silencing of IPCs produces adults that are much smaller than normal (9, 16), suggesting that size compensation via Dilp8 is unlikely to affect insulin signaling globally or completely. IPCs modulate growth systemically via circulating insulin-like peptides (such as Dilp2, -3, and -5) and via endocrine mechanisms, such as direct regulation of JH synthesis in the CA (23, 43), which was also recently shown to instructively regulate larval growth in *Drosophila* (44, 45). We therefore examined the expression of candidate output pathways as a read-out of the physiological dialogue between Lgr3 neurons that directly contact the IPCs and the regulation of JH.

Because JH titer is normally determined by its rate of biosynthesis by the larval CA gland, as well as its rate of degradation, we used qRT-PCR to measure the expression of a gene encoding a key biosynthetic enzyme [*juvenile hormone acid methyltransferase (JHAMT)*] (43) and the direct target of JH that encodes a transcription factor that transduces the actions of JH [*kruppel-homolog-1 (kr-h1)*] (46, 47). Together, these elements should allow us to detect the effective JH signaling in *tub-dilp8* animals compared with age-synchronized and population-controlled WT animals, as well as *tub-dilp8* animals with depleted *lgr3* in the neurons labeled by *R19B09-Gal4*. We also measured the transcriptional levels of *Eip75B*, a direct target of the ecdysone receptor, as a read-out for ecdysone signaling (14).

Control larvae experience a steep increase in *Eip75B* level at 100 hours after egg laying (AEL), which reflects the surge of ecdysone levels at the time of pupariation in our experimental conditions. As expected, no such accumulation was observed in *tub-dilp8* larvae at 100 hours AEL, but expression of *Eip75B* was restored to almost normal levels in *tub-dilp8* in which the *lgr3* receptor was knocked down in neurons labeled by *R19B09-Gal4* (Fig. 6A). The levels of *dilp3* and *dilp5*, which are known to respond to nutrition and stress (16) (Fig. 6B), and of *JHAMT*

and *lcr-h1* in JH biosynthesis and signaling (Fig. 6C) were also significantly down-regulated in *tub-dilp8* larvae, and their expression was restored to almost-normal levels by specific knockdown of *lgr3* in *R19B09* neurons. This non-cell-autonomous effect was specific because the expression of *dilp2* was not altered (fig. S8).

Although the exact mechanism by which Lgr3 neurons influence JH synthesis and signaling is not known, we attempted to establish a causal role for the observed reduction in JH signaling by pharmacological means. To control for the genetic background, we used *UAS-dilp8* and *tub-Gal4 (tub>dilp8)* to treat animals overexpressing dilp8; the biologically inactive *UAS-dilp8^{CL50A}* peptide hormone served as a control (12). The *tub>dilp8* larvae reach the correct pupal size and adult size [as assessed by measuring pupal volume and adult wing size and shape (12)]. In contrast, *tub>dilp8* larvae fed with the JH analog (JHA) methoprene produced significantly larger pupae (~25%) than did control animals (Fig. 6D). The onset of pupariation was slightly delayed (~6 hours) and resulted in 100% lethality, which consequently prevented us from measuring adult size. Treatment of control *tub>dilp8^{CL50A}* animals that display normal pupation time (12) did not increase their size above that of their untreated siblings (Fig. 6D, right) (44). Thus, we conclude that reduced JH signaling diminishes larval growth, contributing to ensuing normal-sized *tub>dilp8* animals (Fig. 6E).

Discussion

Our data provide strong evidence that Dilp8 signals for organismal and organ homeostatic size regulation are transduced via the orphan relaxin receptor Lgr3 and that activation of Lgr3 in molecularly defined neurons mediates the necessary hormonal adjustments for such homeostasis. Human insulin/relaxin-like peptides are transduced through four GPCRs: RXFP1 to -4. RXFP1 and -2 are characterized by large extracellular domains containing leucine-rich repeats, similar to fly Lgr3 and Lgr4 receptors (25, 26). Additionally, as for Lgr3 (this study), activation of RXFP1 and -2 by their cognate ligand binding stimulates increased cAMP production (25). RXFP3 is distinctly different in structure from fly Lgr3 (25), and its biochemical properties are also distinct, but RXFP3 is analogous to fly Lgr3 in the sense that it is found in highest abundance in the brain, suggesting important central functions for relaxin 3/RXFP3 (48, 49). However, a function in pubertal development and/or growth control for vertebrate relaxin receptors is presently unknown.

The neuronal populations that regulate body size and, in particular, the mechanisms by which their regulation generates size variations (plasticity) in response to internal and environmental cues (such as nutrition) have been investigated thoroughly (4, 9, 14, 16, 45, 46). Less is known about how the brain stabilizes body size to ensure that developing organisms reach the correct, genetically determined size. We also do not know how limbs grow to precisely match the size of

their contralateral limbs, nor do we understand how limbs maintain proportion with other body parts, even when faced with perturbations (this statement is also applicable to other bilaterally symmetric traits). Paired organs are controlled

by an identical genetic program and grow in the same hormonal environment, yet small deviations in size can occur as a result of developmental stress, genetic noise, or injury. Imperfections in symmetry thus reflect the inability of an in-

dividual to counterbalance variations and growth abnormalities.

Our study shows that without *Lgr3*, the brain is unable to detect growth disturbances and, more importantly, cannot adjust the internal hormonal

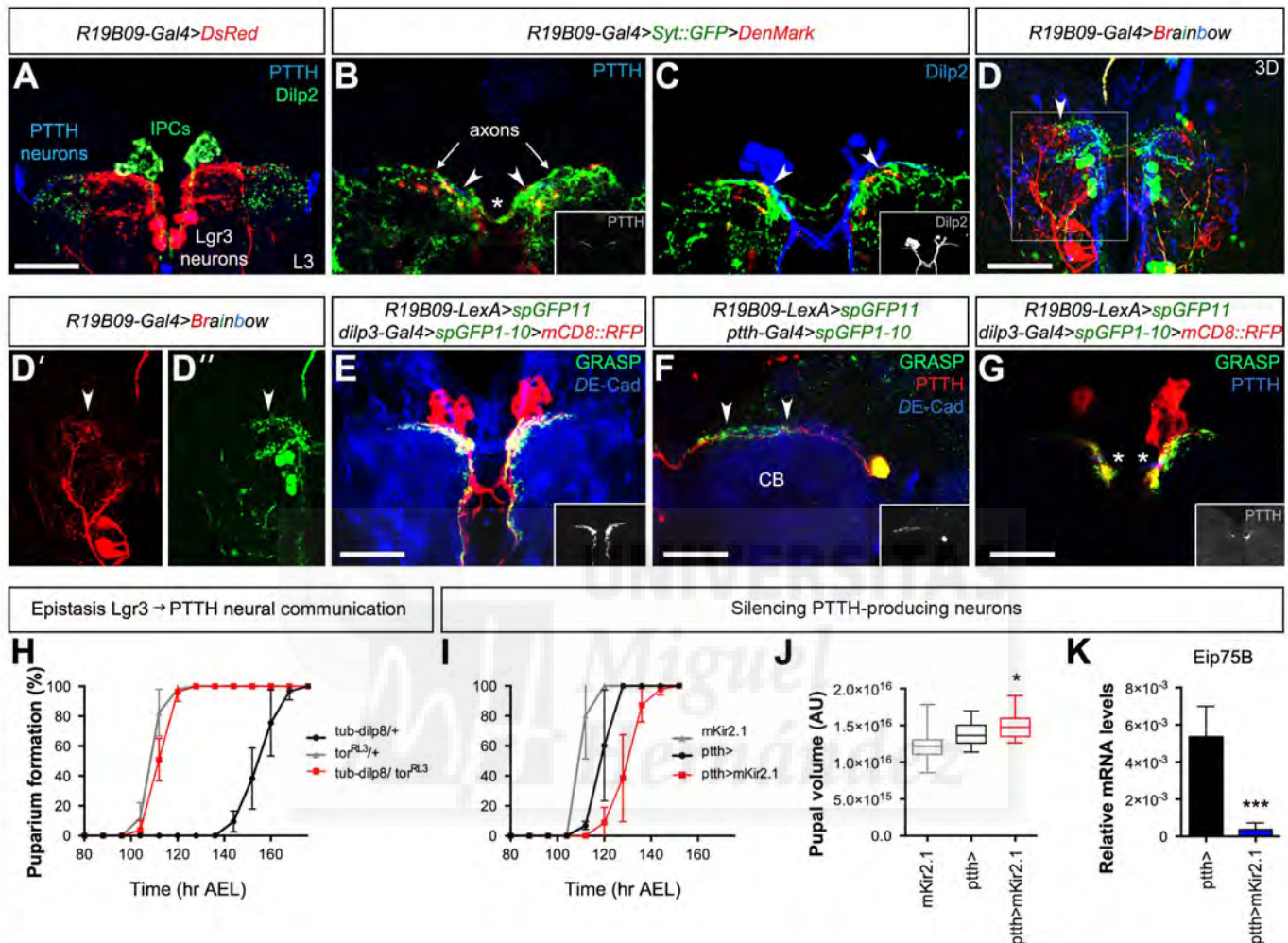


Fig. 5. Lgr3-responding neurons acts as hubs connecting distinct neuron subpopulations. (A) Lgr3 neurons with soma in the dorsomedial region and a prominent response to Dilp8 detected by *DsRed* (*R19B09-Gal4>DsRed*) ensheathed PTTH dendritic fields and axons (anti-PTTH, blue) and densely innervated IPCs (anti-Dilp2, green). Image represents a z-projection of confocal optical sections (29 μ m thick) from the brain of a larva in the late third-instar (L3) stage. (B and C) Single confocal optical sections of larval brains of *R19B09-Gal4* driven presynaptic (*UAS-syt::GFP*, green) and post-synaptic (*UAS-DenMark*, red) markers. PTTH-producing neurons are labeled by anti-PTTH [blue (B)] and IPCs by anti-Dilp2 [blue (C)]. Arrowheads point to Lgr3 axonal projections close to PTTH (B) and IPC neural projections (C). Lgr3 axons also project contralaterally (asterisk). Insets show single channels of PTTH (B) and Dilp2 (C). (D to D'') *UAS-dBrainbow* reveals that projections from distinct neural subpopulations labeled by *R19B09-Gal4* converge on the dorsomedial Lgr3 neurons (green neurons, arrowheads). Single-channel images of Lgr3 neurons in the SOG (red) and dorsomedial (green) regions are shown in (D') and (D''). Image is a 52- μ m-thickness reconstruction of confocal sections. (E) Positive, robust signals of GRASP revealed extensive connections between Lgr3 (*R19B09-LexA>spGFP11*) and IPCs (*dilp3-Gal4>spGFP1-10>mCD8::RFP*). Brains were counterstained with anti-DE-Cad (blue). A 21- μ m-thick reconstruction is shown. The inset shows GRASP signals (gray). (F) GRASP signals (arrowheads) between Lgr3 neurons (*R19B09-LexA>spGFP11*) and PTTH-producing neurons

(*ptth-Gal4>spGFP1-10*) are detected with immunofluorescence (green) (fig. S6, C and D). Brains were costained with anti-PTTH (red) and anti-DE-Cad (blue). The image represents a 26- μ m-thick reconstruction. The inset shows GRASP signals (gray). (G) Brains stained with anti-PTTH (blue) could detect potential contact sites (asterisks) of the circuit. GRASP signals (green) were contributed by connections between Lgr3 (*R19B09-LexA>spGFP11*) and IPCs (red) (*dilp3-Gal4>spGFP1-10>mCD8::RFP*). The inset shows single-channel staining (anti-PTTH, gray). The image is a single confocal section (1 μ m thick). (H) Dilp8-induced delay in pupariation is prevented by the constitutive active PTTH receptor *torso^{RL3}* mutation. (I) Electrical silencing of PTTH neurons (*ptth-Gal4 UAS-mKir2.1*) delays pupariation, as compared with controls. Data in (H) and (I) are pooled from three independent experiments, and each data point is mean \pm SD. Approximately 60 pupae were scored per genotype. (J) PTTH neuronal silencing does not evoke growth compensation and results in larger pupae, as compared with controls. Data are mean \pm SD ($n = 3$ independent repeats), and a total of 35 pupae were measured per genotype. * $P < 0.05$ (unpaired *t* test). AU, arbitrary units. (K) Expression of *Eip75B* at 100 hours AEL in control larvae (*ptth-Gal4*) and larvae with electrically silenced PTTH neurons (*ptth>mKir2.1*). *** $P < 0.001$ (unpaired *t* test). mRNA was obtained from seven larvae per genotype, and the experiment was repeated three times. Scale bars, 50 μ m in (A) [also applies to (C)]; 60 μ m in (D) [also applies to (D') and (D'')]; 40 μ m in (E) and (G); and 30 μ m in (F).

environment to allocate additional developmental time for restoring affected parts or catching up on growth. Without *Lgr3*, the brain is also not capable of retarding the growth rate to compensate for the extra time so that unaffected and affected tissues can develop with normal size, proportionality, and symmetry. Our study also identifies the *Lgr3*-expressing neurons necessary and sufficient to respond to Dilp8. Moreover, using a cAMP sensor, we have identified a pair of neurons that are highly sensitive to Dilp8.

Communication in neuronal networks is essential for synchronization and efficient performance. Notably, although most neurons have only one axon, *Lgr3*-responding neurons display extensive axonal arborizations reminiscent of hub neurons (39). GRASP analyses show that *Lgr3* neurons are broadly connected with the IPCs and, to a lesser extent, with PTTH neurons, linking (Dilp8) inputs to the neuronal populations that regulate the key hormonal outputs modulating larval and imaginal disc growth. Furthermore, the information flow from *Lgr3* neurons to IPCs and

PTTH may explain how the brain matches growth with maturation in response to Dilp8 (Fig. 6F). This brain circuit provides the basis for studying how the brain copes with genetic and environmental perturbations to stabilize body size, proportions, and symmetry, all of which are vital for survival.

Materials and methods Drosophila husbandry

The five *Lgr3* enhancer *Gal4* lines (*R17G11-Gal4*, *R17H01-Gal4*, *R18A01-Gal4*, *R18C07-Gal4*, and *R19B09-Gal4*); the *R17G11-LexA*, *R19B09-LexA*, and *13xLexAop2-IVS-myr::GFP* lines; and the *retn^{R9FO4}-Gal4* line are from the Janelia Farm Collection (Howard Hughes Medical Institute, Ashburn, VA). The *da-Gal4*, *dilp3-Gal4*, *dpp-Gal4*, *elav-Gal4*, *tub-Gal4*, *P0206-Gal4*, *NPF-Gal4*, *pdf-Gal4*, *per-Gal4*, *ptth-Gal4*, *tsh-Gal4*, *LexAop-CD4::spGFP_{II}*, *UAS-CD4::spGFP_{I-10}*, *UAS-*der2**, *UAS-Denmark*, *UAS-DsRed*, *UAS-Flp*, *UAS-lgr3-TRiP*, *GL01056-RNAi*, *UAS-mCD8::GFP*, *UAS-mCD8::RFP*, *UAS-mKir2.1*, *UAS-NaChBac*, and *UAS-Syt::GFP* lines

are from the Bloomington Stock Center at Indiana University (Bloomington, IN). *UAS-dilp8* and *UAS-dilp8^{C150A}* are described in (12). *CRE-F_{huc}* and *tor^{RL3}* were gifts from J. C. P. Yin and J. Casanova, respectively (36, 50).

Flies were reared in standard “Iberian” fly food at 25°C (except when indicated) on a 14:10-hour light:dark cycle (surrogate of laboratory summer time). Standard Iberian fly food consisted of 15 liters of water, 0.75 kg of wheat flour, 1 kg of brown sugar, 0.5 kg of yeast, 0.17 kg of agar, 130 ml of a 5% nipagin solution in ethanol, and 130 ml of propionic acid.

G-TRACE analysis

G-TRACE (Gal4 technique for real-time and clonal expression) analysis was performed by crossing *UAS-Flp*, *UAS-RedStinger*, and *ubip63-FRT-stop-FRT-StingerGFP* stocks (51) with *R19B09-Gal4*, *retn^{R9FO4}-Gal4*, and *P0206-Gal4* lines.

Brainbow clones

We built *hs-Cre; R19B09-Gal4* stocks and crossed them with *UAS-dBrainbow* (38) virgin females.

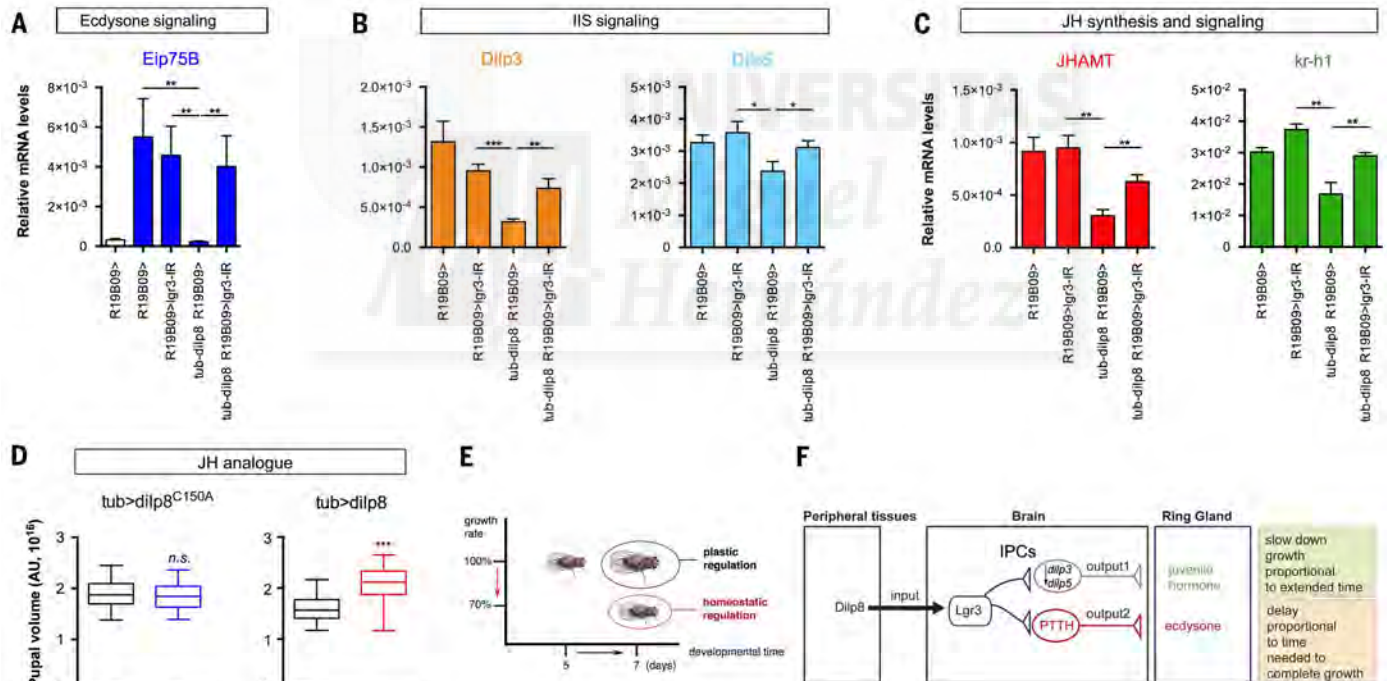


Fig. 6. Probing functional connection between *Lgr3* neurons and IPCs neurons. (A to C) Expression of *Eip75B* (A), *dilp3* and *dilp5* (B), *JHAMT* [(C), left] and *kr-h1* [(C), right] genes analyzed by qRT-PCR in mRNA isolated from ~10 larvae for each genotype and age [~90 hours AEL (white bar) and 100 hours AEL (all other bars)]. Overexpression of *dilp8* by the tubulin promoter (*tub-dilp8*) sustainably decreased *dilp3*, *dilp5*, *JHAMT*, and *kr-h1* transcripts in the extended third-instar larval period, and this regulation was abrogated by specific knockdown of *Lgr3* in *R19B09* neurons. Data are mean \pm SD ($n = 3$ repeats). * $P < 0.05$; ** $P < 0.01$; *** $P < 0.001$ (two-tailed unpaired t test). IIS, insulin/IGF-like signaling. (D) Treatment of JHA abrogates the compensatory growth response of *tub-dilp8* animals. Box-and-whisker plots of the pupal volume of control animals (*tub>dilp8^{C150A}*) (left) and animals overexpressing *dilp8* (*tub>dilp8*) (right). Any differences between *tub>dilp8^{C150A}* animals fed with methoprene [Met] or without (control) are not significant. Met-fed *tub>dilp8* animals produced noticeably larger pupae. Plotted data are pooled from three biological repeats (50 pupae per genotype and treatment). *** $P < 0.001$ (two-tailed unpaired t test). (E) Model for plastic and homeostatic regulation of body size. If the growth rate is fixed, an extension of the developmental time results in larger adults (plastic regulation). If developmentally delayed animals also experience a proportional decrease in growth rate, they will reach a normal adult size (homeostatic regulation). Developmental time (days) represents age at the larval-pupal transition. (F) Model of *Lgr3* circuit and output pathways. Dilp8 produced by peripheral tissues conveys information about overall growth status. Circulating Dilp8 enters the brain through the blood-brain barrier, in an unknown manner, and binds and activates *Lgr3* in a dose-dependent manner. With their high connectivity, *Lgr3*-responding neurons distribute this growth-status information to IPCs (gray) and PTTH neurons (red), which ensures that rates of growth and maturation are matched and co-regulated according to the intensity of the Dilp8 signals.

We reared fly crosses at 25°C and did not heat-shock them. The following primary antibodies were used: rabbit anti-HA (1/500; Abcam) and mouse anti-V5 (1/500, Invitrogen).

GRASP analysis

We built *R19B09-LexA*; *LexAop-CD4::spGFP₁₁*, *UAS-CD4::spGFP₁₋₁₀*/TM6B stocks and crossed them with *dilp3-Gal4/CyO-GFP*; *UAS-mCD8::RFP* ($n = 14$ larval brains were analyzed) or *ptth-Gal4/CyO-GFP* ($n = 43$ larval brains were analyzed). Control experiments were performed by staining larval brains of the following genotypes ($n = 10$ larval brains per genotype were analyzed): *R19B09-LexA*; *LexAop-CD4::spGFP₁₁*, *UAS-CD4::spGFP₁₋₁₀*/TM6B, *dilp3-Gal4/+*; *LexAop-CD4::spGFP₁₁*, *UAS-CD4::spGFP₁₋₁₀*+, or *ptth-Gal4/+*; *LexAop-CD4::spGFP₁₁*, *UAS-CD4::spGFP₁₋₁₀*+. The following primary antibodies were used: rabbit anti-GFP (1/2000; Invitrogen) to detect GRASP signal between PTTH and Lgr3 neurons, guinea pig anti-PTTH [1/500 (52)], and rat anti-*Drosophila* E-Cadherin (anti-DE-Cad) [1/50, Developmental Studies Hybridoma Bank (DSHB)] to counterstain larval brains.

Confocal imaging and immunohistochemistry in brains

Brains were dissected in cold phosphate-buffered saline (PBS), fixed in 4% paraformaldehyde (PFA) for 20 min (53), and stained with the following primary antibodies: guinea pig anti-PTTH [1/500 (52)], mouse anti-luciferase (1/200, Thermo Fisher Scientific), rabbit anti-Dilp2 [1/500 (54)], rabbit anti-Mira [1/2000 (55)], rabbit anti-Pdp1 [1/1000 (56)], and rat anti-DE-Cad (1/50, DSHB). Secondary antibodies were purchased from Invitrogen and Jackson ImmunoResearch. The brains were mounted in Vectashield (Vector Labs), maintaining their three-dimensional (3D) configuration (53), and images were obtained on a Leica TCS SP2 confocal microscope. Z stacks were recorded at 1- μ m intervals. 3D reconstructions of individual WT *Drosophila* larval brains were created using Imaris software (Bitplane, Zurich, Switzerland). To assess changes in cAMP levels in the larval brain, we used the in vivo CRE-F-luc reporter system (36). Dissected brains were stained using mouse anti-luciferase (1/200, Thermo Fisher Scientific).

Generation of DNA constructs and transgenic lines

For the *tub-dilp8::FLAG* construct, *dilp8* cDNA was C-terminally fused in frame to the 3xFLAG coding sequence (12) and cloned into the pCasper-tubulin promoter plasmid at the KpnI/NotI sites.

The *lgr3* WT cDNA sequence was based on the WT amino acid sequence corresponding to GenBank accession number AAF56490, codon-optimized using GeneOptimizer (GENEART), and cloned into the pMK-RQ plasmid (SfiI/SfiI sites) (GENEART). The obtained construct was verified by sequencing and then cloned into the pUAS plasmid at the EcoRI/NotI sites.

Constructs were injected in *w¹¹¹⁸* embryos following standard P-element-mediated transformation procedures (BestGene).

The entire open reading frame (ORF) sequence of *lgr4* was PCR-amplified from total mRNA obtained from *w¹¹¹⁸* larvae using primers containing attB1 and attB2 Gateway recombination sites whose sequences were as follows:

lgr4 forward primer: 5'-ATGTGTATAGCTCAC-CTGCCTATCAC-3'

lgr4 reverse primer: 5'-CTACAGATAGCTCAT-CTGCCGGTGTG-3'

The amplified product was cloned into a pDON/Zeo entry vector (Life Technologies), according to the Gateway technology manual (Life Technologies), and verified by sequencing. Verified entry clones were used to introduce full-length ORFs into the pUAS Gateway plasmid [Drosophila Genomics Resource Center (DGRC), stock no. 1129] by LR recombination (Gateway technology, Life Technologies).

The Lgr3 extracellular domain (hereafter Lrg3-ECD) (amino acid residues 1 to 433) was PCR amplified from the pUAS-*lgr3* full-length plasmid described above using primers containing attB1 and attB2 Gateway recombination sites with the following sequences:

lgr3-ECD forward primer: 5'-ATGGTGTACG-GCCGAGTATCGCCGTG-3'

lgr3-ECD reverse primer: 5'-CAGCACGGG-CTTGTCTCAGCAGGTC-3'

The PCR product was cloned into pDON/Zeo entry vector (Life Technologies) following the Gateway technology manual instructions (Life Technologies) and verified by sequencing. Entry *Lrg3-ECD* construct was used to introduce the insert into the pUAS-C-terminal 3xHA Gateway plasmid (DGRC, stock no. 1100) by LR recombination (Gateway technology, Life Technologies).

Cell culture

Drosophila S2 and Kc cells (Invitrogen) were cultured in Schneider's *Drosophila* medium (Invitrogen) supplemented with 10% fetal bovine serum (Gibco, Thermo Fisher Scientific) at 25°C in a nonhumidified, ambient-air-regulated incubator.

cAMP measurement

Concentrations of cAMP were measured using the cAMP Enzymeimmunoassay (EIA) System (Amersham, catalog no. RPN2251). *Drosophila* Kc cells (Invitrogen) were seeded (50,000 per well) in a 96-well plate and transfected with the plasmid DNA indicated, using Fugene-HD (Promega). After 36 hours of transfection, cells were exposed for 30 min to the Dilp8 peptide (at 0, 5, or 50 nM; Phoenix Pharmaceuticals, catalog no. 035-79) and 3-isobutyl-1-methylxanthine (IBMX) (100 μ M; Sigma, catalog no. 15879). After treatment, the cells were processed according to the manufacturer's protocol, and the cAMP concentrations are presented as femtomoles per well.

EC₅₀ determination

The cAMP concentrations were determined using the Direct cAMP ELISA Kit (Enzo Lifescience, catalog no. ADI-900-066) according to the manufacturer's protocol. 50,000 *Drosophila* Kc cells (Invitrogen) were seeded per well in a 96-well plate and transfected with the indicated plasmid DNA, using Fugene-HD (Promega). After 36 hours

of transfection, cells were exposed for 30 min to IBMX (100 μ M) and Dilp8 peptide (12 serial dilutions of Dilp8 starting from 250 nM to 0 nM). Total intracellular cAMP concentration was determined using the nonacetylation cAMP enzyme immunoassay from 100 μ l of 0.1 M HCl in all experiments. cAMP levels were calculated using the 4 Parameter Logistic Curve (4PL) online data analysis tool (MyAssays). Results are expressed in picomoles per milliliter of cAMP. The EC₅₀ analysis was calculated with GraphPad Prism software (version 6, for Mac), using a sigmoidal dose-response (variable slope) equation.

Coimmunoprecipitation assays

Drosophila S2 cells (3×10^6 cells per 10-cm dish) were transiently cotransfected with *pActin-Gal4* and either *UAS-lgr3-ECD::3XHA* or empty vector *UAS::3XHA*, using Fugene-HD (Promega). To obtain secreted tagged Dilp8, 6×10^6 S2 cells per 10-cm dish were transiently transfected using the *pActin-Gal4* and *UAS-dilp8::Myc* plasmid. Thirty-six hours after transfection, supernatant containing Dilp8::Myc was collected, filtered, and used to replace the medium of *UAS-lgr3-ECD::3XHA* and *UAS::3XHA* dishes. After 2 hours of incubation, cells were PBS-washed and cross-linked for 30 min using DTSSP [3,3'-dithiobis(sulfosuccinimidyl propionate)] (Thermo Fisher Scientific). Cells were PBS-washed and then lysed using modified RIPA buffer containing proteinase inhibitors. Pre-cleared extracts were incubated at 4°C with 1 μ g of rabbit anti-Myc (Abcam, ab9606) or rabbit anti-immunoglobulin G (anti-IgG) (Sigma, I8140). After 2 hours, 25 μ l of equilibrated protein A magnetic beads (Millipore, catalog no. 16-661) was added to each extract and incubated overnight at 4°C. After three washes using the modified RIPA buffer containing proteinase inhibitors, proteins bound to beads were recovered by boiling for 10 min in 25 μ l of 3x sample buffer and were separated by SDS-polyacrylamide gel electrophoresis. After blotting, membranes were incubated in rat anti-HA-horseradish peroxidase (clone 3F10, Roche) and analyzed.

Immunostaining of *Drosophila* cultured cells

Drosophila Kc cells (8×10^5 cells per well) were cotransfected in six-well plates with *pActin-Gal4* and either *UAS-lgr3-ECD::3XHA* or empty vector *UAS::3XHA* and, in parallel, were cotransfected with *tub-dilp8::FLAG* using Fugene-HD (Promega). Thirty-six hours after transfection, supernatant containing Dilp8:FLAG was collected, filtered, and used to replace medium from *UAS-lgr3-ECD::3XHA* and *UAS::3XHA*. After a 2-hour incubation period, cells were washed twice with PBS, fixed using 4% PFA, and immunostained (cells were not permeabilized). Antibodies used: rabbit anti-HA (1/200, Abcam ab9110) and mouse anti-FLAG-M2 (1/200, Sigma).

Lgr3 antibody

To generate specific antiserum for Lgr3, two peptides corresponding to amino acids 719 to 733 (C+ GWKKITSRKRAEAGN) and 487 to 501

(C+ GVQDYRYRNEYKVV) (57) were synthesized by Eurogentec (Seraing, Belgium) and used to immunize rabbits according to an 87-day polyclonal antibody program.

Quantitative RT-PCR

To assess mRNA levels, total RNA was extracted from *Drosophila* larvae using the RNeasy-Mini Kit (Qiagen). To remove contaminating DNA, RNA was treated with Turbo DNA-free (Ambion, Life Technologies). cDNA was synthesized with SuperScript III First-Strand Synthesis System for RT-PCR (Life Technologies) using oligo-dT primers. qRT-PCR was performed using SYBR Green PCR Master Mix (Applied Biosystems), with gene-specific primers, on an ABI7500 apparatus (Applied Biosystems). *Rp49* primers were used for mRNA normalization. Comparative qRT-PCRs were performed in triplicates, and relative expression was calculated using the comparative Ct method.

Primer sequences:

lgr3:

Forward 5'-GGCAAAGGAGCATACATTTGA-3'

Reverse 5'-TTAAGTCCAGGATTACACAGC-3'

Thor/4E-BP:

Forward 5'-GAAGGTTGTTCATCTCGGATCC-3'

Reverse 5'-ATGAAAGCCCGCTCGTAG-3'

E75B:

Forward 5'-CAACAGCAACAACACCCAGA-3'

Reverse 5'-CAGATCGGCACATGGCTTT-3'

JHAMT:

Forward 5'-ATTTCGCATCGACCATGCACT-3'

Reverse 5'-GAAGTCCATGAGCACGTTACC-3'

Kr-h1:

Forward 5'-ACAATTTTATGATTCAGCCACAACC-3'

Reverse 5'-GTTAGTGGAGGCGGAACCTG-3'

dilp2:

Forward 5'-ATCCCGTGATTCCACACAAG-3'

Reverse 5'-GCGGTTCCGATATCGAGTTA-3'

dilp3:

Forward 5'-ATCCCGTGATTCCACACAAG-3'

Reverse 5'-GCGGTTCCGATATCGAGTTA-3'

dilp5:

Forward 5'-GCCTTGATGGACATGCTGA-3'

Reverse 5'-CATAATCGAATAGGCCCAAGG-3'

rp49:

Forward 5'-TGTCCTTCCAGCTTCAAGATGAC-CATC-3'

Reverse 5'-CTTGGGCTTGCCTATTGTG-3'

Measurement of the developmental timing of pupariation

Females and males (20 to 30 of each) were crossed and, after 24 to 48 hours, flies were transferred to grape juice agar plates with yeast paste and left 4 hours for egg deposition. Parental flies were removed, and laid eggs were incubated 48 hours at 26.5°C. Second-instar larvae were transferred onto 5 ml of *Drosophila* standard Iberian food (20 larvae per tube) and reared at 26.5°C. A survey of the pupae was performed at 8-hour intervals, with "time 0" designated as 4 hours after the initiation of egg laying.

Weight and size measurements

For weighing adult flies, 20 to 30 females and 20 to 30 males were crossed and left 24 hours for

egg deposition. Parental flies were transferred every 24 hours to fresh tubes, and laid eggs were reared at 26.5°C. Eclosed adult males of each genotype were collected (five groups of five individuals) and weighed after 12 to 24 hours, using a precision scale.

For pupae volume determination, 20 to 30 females and 20 to 30 males were crossed and left 24 hours for egg deposition. Parental flies were transferred every 24 hours to fresh tubes, and laid eggs were reared at 26.5°C. Pupae were collected and photographed with their dorsal side up. Length and width were measured using ImageJ; volume was calculated according to the following formula: $v = 4/3\pi(L/2)(l/2)^2$ (L , length; l , width).

For adult wing measurements, 20 to 30 females and 20 to 30 males were crossed and left 24 hours for egg deposition. Parental flies were transferred every 24 hours to fresh tubes, and laid eggs were reared at 26.5°C. Adults were collected and left, and the right wings of each individual were excised and rinsed thoroughly with ethanol and mounted in a glycerol-ethanol solution. Wing areas were measured using ImageJ. Intra-individual variation of wing areas was calculated using fluctuating asymmetry index (FAi) as in (12), employing the formula $FAi = Var(Ai)$, where Ai are the differences between left and right wing areas of each individual.

Juvenile hormone analog (methoprene) treatment

Males and females (20 to 30 of each) were crossed, and after 24 to 48 hours, flies were transferred to grape juice agar plates with yeast paste and left 4 hours for egg deposition. Parental flies were removed, and laid eggs were incubated 48 hours at 26.5°C. Second-instar larvae were transferred onto 5 ml of *Drosophila* standard Iberian food (20 larvae per tube) and incubated at 26.5°C. Larvae were transferred 24 hours later (72 hours AEL) to 3 ml of *Drosophila* standard Iberian food supplemented with a liquid solution of pure methoprene (Sigma, catalog no. 33375) at a Met:food ratio of 1 μ m:1000 μ m. An equivalent volume of water was added to the control.

REFERENCES AND NOTES

- B. A. Edgar, How flies get their size: Genetics meets physiology. *Nat. Rev. Genet.* **7**, 907–916 (2006). doi: [10.1038/nrg1989](https://doi.org/10.1038/nrg1989); pmid: [17139322](https://pubmed.ncbi.nlm.nih.gov/17139322/)
- A. W. Shingleton, The regulation of organ size in *Drosophila*: Physiology, plasticity, patterning and physical force. *Organogenesis* **6**, 76–87 (2010). doi: [10.4161/org.6.2.10375](https://doi.org/10.4161/org.6.2.10375); pmid: [20885854](https://pubmed.ncbi.nlm.nih.gov/20885854/)
- L. Wolpert, Arms and the man: The problem of symmetric growth. *PLoS Biol.* **8**, e1000477 (2010). doi: [10.1371/journal.pbio.1000477](https://doi.org/10.1371/journal.pbio.1000477); pmid: [20838659](https://pubmed.ncbi.nlm.nih.gov/20838659/)
- J. M. Tennesen, C. S. Thummel, Coordinating growth and maturation - insights from *Drosophila*. *Curr. Biol.* **21**, R750–R757 (2011). doi: [10.1016/j.cub.2011.06.033](https://doi.org/10.1016/j.cub.2011.06.033); pmid: [21959165](https://pubmed.ncbi.nlm.nih.gov/21959165/)
- K. P. Tolson, P. E. Chappell, The changes they are a-timed: Metabolism, endogenous clocks, and the timing of puberty. *Front. Endocrinol.* **3**, 45 (2012). doi: [10.3389/fendo.2012.00045](https://doi.org/10.3389/fendo.2012.00045); pmid: [22645521](https://pubmed.ncbi.nlm.nih.gov/22645521/)
- N. F. Parker, A. W. Shingleton, The coordination of growth among *Drosophila* organs in response to localized growth-perturbation. *Dev. Biol.* **357**, 318–325 (2011). doi: [10.1016/j.ydbio.2011.07.002](https://doi.org/10.1016/j.ydbio.2011.07.002); pmid: [21775756](https://pubmed.ncbi.nlm.nih.gov/21775756/)

- J. F. Hackney, O. Zolali-Meybodi, P. Cherbas, Tissue damage disrupts developmental progression and ecysteroid biosynthesis in *Drosophila*. *PLoS ONE* **7**, e49105 (2012). doi: [10.1371/journal.pone.0049105](https://doi.org/10.1371/journal.pone.0049105); pmid: [23166607](https://pubmed.ncbi.nlm.nih.gov/23166607/)
- I. K. Hariharan, How growth abnormalities delay "puberty" in *Drosophila*. *Sci. Signal.* **5**, pe27 (2012). doi: [10.1126/scisignal.2003238](https://doi.org/10.1126/scisignal.2003238); pmid: [22715466](https://pubmed.ncbi.nlm.nih.gov/22715466/)
- D. S. Andersen, J. Colombani, P. Léopold, Coordination of organ growth: Principles and outstanding questions from the world of insects. *Trends Cell Biol.* **23**, 336–344 (2013). doi: [10.1016/j.tcb.2013.03.005](https://doi.org/10.1016/j.tcb.2013.03.005); pmid: [23587490](https://pubmed.ncbi.nlm.nih.gov/23587490/)
- C. L. Sisk, D. L. Foster, The neural basis of puberty and adolescence. *Nat. Neurosci.* **7**, 1040–1047 (2004). doi: [10.1038/nrn1326](https://doi.org/10.1038/nrn1326); pmid: [20920296](https://pubmed.ncbi.nlm.nih.gov/20920296/)
- O. Karapanou, A. Papadimitriou, Determinants of menarche. *Reprod. Biol. Endocrinol.* **8**, 115 (2010). doi: [10.1186/1477-7827-8-115](https://doi.org/10.1186/1477-7827-8-115); pmid: [20920296](https://pubmed.ncbi.nlm.nih.gov/20920296/)
- A. Garelli, A. M. Gontijo, V. Miguéla, E. Caparros, M. Dominguez, Imaginal discs secrete insulin-like peptide 8 to mediate plasticity of growth and maturation. *Science* **336**, 579–582 (2012). doi: [10.1126/science.1216735](https://doi.org/10.1126/science.1216735); pmid: [22556250](https://pubmed.ncbi.nlm.nih.gov/22556250/)
- J. Colombani, D. S. Andersen, P. Léopold, Secreted peptide Dilp8 coordinates *Drosophila* tissue growth with developmental timing. *Science* **336**, 582–585 (2012). doi: [10.1126/science.1216689](https://doi.org/10.1126/science.1216689); pmid: [22556251](https://pubmed.ncbi.nlm.nih.gov/22556251/)
- K. F. Rewitz, N. Yamanaka, M. B. O'Connor, Developmental checkpoints and feedback circuits time insect maturation. *Curr. Top. Dev. Biol.* **103**, 1–33 (2013). doi: [10.1016/B978-0-12-385979-2.00001-0](https://doi.org/10.1016/B978-0-12-385979-2.00001-0); pmid: [23347514](https://pubmed.ncbi.nlm.nih.gov/23347514/)
- Z. McBrayer et al., Prothoracicotropic hormone regulates developmental timing and body size in *Drosophila*. *Dev. Cell* **13**, 857–871 (2007). doi: [10.1016/j.devcel.2007.11.003](https://doi.org/10.1016/j.devcel.2007.11.003); pmid: [18061567](https://pubmed.ncbi.nlm.nih.gov/18061567/)
- D. R. Nässel, O. I. Kubrak, Y. Liu, J. Luo, O. V. Lushchak, Factors that regulate insulin producing cells and their output in *Drosophila*. *Front. Physiol.* **4**, 252 (2013). doi: [10.3389/fphys.2013.00252](https://doi.org/10.3389/fphys.2013.00252); pmid: [24062693](https://pubmed.ncbi.nlm.nih.gov/24062693/)
- W. Brogiolo et al., An evolutionarily conserved function of the *Drosophila* insulin receptor and insulin-like peptides in growth control. *Curr. Biol.* **11**, 213–221 (2001). doi: [10.1016/S0960-9822\(01\)00068-9](https://doi.org/10.1016/S0960-9822(01)00068-9); pmid: [11250149](https://pubmed.ncbi.nlm.nih.gov/11250149/)
- T. Ikeya, M. Galic, P. Belawat, K. Nairz, E. Hafen, Nutrient-dependent expression of insulin-like peptides from neuroendocrine cells in the CNS contributes to growth regulation in *Drosophila*. *Curr. Biol.* **12**, 1293–1300 (2002). doi: [10.1016/S0960-9822\(02\)01043-6](https://doi.org/10.1016/S0960-9822(02)01043-6); pmid: [12176357](https://pubmed.ncbi.nlm.nih.gov/12176357/)
- S. Grönke, D. F. Clarke, S. Broughton, T. D. Andrews, L. Partridge, Molecular evolution and functional characterization of *Drosophila* insulin-like peptides. *PLoS Genet.* **6**, e1000857 (2010). doi: [10.1371/journal.pgen.1000857](https://doi.org/10.1371/journal.pgen.1000857); pmid: [20195512](https://pubmed.ncbi.nlm.nih.gov/20195512/)
- J. S. Britton, W. K. Lockwood, L. Li, S. M. Cohen, B. A. Edgar, *Drosophila*'s insulin/P13-kinase pathway coordinates cellular metabolism with nutritional conditions. *Dev. Cell* **2**, 239–249 (2002). doi: [10.1016/S1534-5807\(02\)00117-X](https://doi.org/10.1016/S1534-5807(02)00117-X); pmid: [11832249](https://pubmed.ncbi.nlm.nih.gov/11832249/)
- H. Zhang et al., Deletion of *Drosophila* insulin-like peptides causes growth defects and metabolic abnormalities. *Proc. Natl. Acad. Sci. U.S.A.* **106**, 19617–19622 (2009). doi: [10.1073/pnas.0905083106](https://doi.org/10.1073/pnas.0905083106); pmid: [19887630](https://pubmed.ncbi.nlm.nih.gov/19887630/)
- C. Chen, J. Jack, R. S. Garofalo, The *Drosophila* insulin receptor is required for normal growth. *Endocrinology* **137**, 846–856 (1996). pmid: [8603594](https://pubmed.ncbi.nlm.nih.gov/8603594/)
- Y. H. Belgacem, J. R. Martin, Hmgcr in the corpus allatum controls sexual dimorphism of locomotor activity and body size via the insulin pathway in *Drosophila*. *PLoS ONE* **2**, e187 (2007). doi: [10.1371/journal.pone.0000187](https://doi.org/10.1371/journal.pone.0000187); pmid: [17264888](https://pubmed.ncbi.nlm.nih.gov/17264888/)
- A. Jenett et al., A GAL4-driver line resource for *Drosophila* neurobiology. *Cell Reports* **2**, 991–1001 (2012). doi: [10.1016/j.celrep.2012.09.011](https://doi.org/10.1016/j.celrep.2012.09.011); pmid: [23063364](https://pubmed.ncbi.nlm.nih.gov/23063364/)
- R. A. Bathgate et al., Relaxin family peptides and their receptors. *Physiol. Rev.* **93**, 405–480 (2013). doi: [10.1152/physrev.0001.2012](https://doi.org/10.1152/physrev.0001.2012); pmid: [23303914](https://pubmed.ncbi.nlm.nih.gov/23303914/)
- M. B. Van Hiel, H. P. Vandersmissen, T. Van Loy, J. Vanden Broeck, An evolutionary comparison of leucine-rich repeat containing G protein-coupled receptors reveals a novel LGR subtype. *Peptides* **34**, 193–200 (2012). doi: [10.1016/j.peptides.2011.11.004](https://doi.org/10.1016/j.peptides.2011.11.004); pmid: [22100731](https://pubmed.ncbi.nlm.nih.gov/22100731/)
- M. B. Van Hiel, H. P. Vandersmissen, P. Proost, J. Vanden Broeck, Cloning, constitutive activity and expression profiling of two receptors related to relaxin receptors in *Drosophila melanogaster*. *Peptides* **68**, 83–90 (2015). doi: [10.1016/j.peptides.2014.07.014](https://doi.org/10.1016/j.peptides.2014.07.014); pmid: [25064813](https://pubmed.ncbi.nlm.nih.gov/25064813/)

28. J. Q. Ni *et al.*, A *Drosophila* resource of transgenic RNAi lines for neurogenetics. *Genetics* **182**, 1089–1100 (2009). doi: [10.1534/genetics.109.103630](https://doi.org/10.1534/genetics.109.103630); pmid: [19487563](https://pubmed.ncbi.nlm.nih.gov/19487563/)
29. A. Scopelliti *et al.*, Local control of intestinal stem cell homeostasis by enteroendocrine cells in the adult *Drosophila* midgut. *Curr. Biol.* **24**, 1199–1211 (2014). doi: [10.1016/j.cub.2014.04.007](https://doi.org/10.1016/j.cub.2014.04.007); pmid: [24814146](https://pubmed.ncbi.nlm.nih.gov/24814146/)
30. S. Y. Hsu *et al.*, Activation of orphan receptors by the hormone relaxin. *Science* **295**, 671–674 (2002). doi: [10.1126/science.1065654](https://doi.org/10.1126/science.1065654); pmid: [11809971](https://pubmed.ncbi.nlm.nih.gov/11809971/)
31. K. S. Carmon, X. Gong, Q. Lin, A. Thomas, Q. Liu, R-spondins function as ligands of the orphan receptors LGR4 and LGR5 to regulate Wnt/ β -catenin signaling. *Proc. Natl. Acad. Sci. U.S.A.* **108**, 11452–11457 (2011). doi: [10.1073/pnas.1106083108](https://doi.org/10.1073/pnas.1106083108); pmid: [21693646](https://pubmed.ncbi.nlm.nih.gov/21693646/)
32. Q. Wu *et al.*, Developmental control of foraging and social behavior by the *Drosophila* neuropeptide Y-like system. *Neuron* **39**, 147–161 (2003). doi: [10.1016/S0896-6273\(03\)00396-9](https://doi.org/10.1016/S0896-6273(03)00396-9); pmid: [12848939](https://pubmed.ncbi.nlm.nih.gov/12848939/)
33. J. Berni, S. R. Pulver, L. C. Griffith, M. Bate. Autonomous circuitry for substrate exploration in freely moving *Drosophila* larvae. *Curr. Biol.* **22**, 1861–1870 (2012). doi: [10.1016/j.cub.2012.07.048](https://doi.org/10.1016/j.cub.2012.07.048); pmid: [22940472](https://pubmed.ncbi.nlm.nih.gov/22940472/)
34. G. Milligan, Constitutive activity and inverse agonists of G protein-coupled receptors: A current perspective. *Mol. Pharmacol.* **64**, 1271–1276 (2003). doi: [10.1124/mol.64.6.1271](https://doi.org/10.1124/mol.64.6.1271); pmid: [14645655](https://pubmed.ncbi.nlm.nih.gov/14645655/)
35. M. N. Nitabach *et al.*, Electrical hyperexcitation of lateral ventral pacemaker neurons desynchronizes downstream circadian oscillators in the fly circadian circuit and induces multiple behavioral periods. *J. Neurosci.* **26**, 479–489 (2006). doi: [10.1523/JNEUROSCI.3915-05.2006](https://doi.org/10.1523/JNEUROSCI.3915-05.2006); pmid: [16407545](https://pubmed.ncbi.nlm.nih.gov/16407545/)
36. A. K. Tanenhaus, J. Zhang, J. C. P. Yin. In vivo circadian oscillation of dCREB2 and NF- κ B activity in the *Drosophila* nervous system. *PLOS ONE* **7**, e45130 (2012). doi: [10.1371/journal.pone.0045130](https://doi.org/10.1371/journal.pone.0045130); pmid: [23077489](https://pubmed.ncbi.nlm.nih.gov/23077489/)
37. L. J. Nicolai *et al.*, Genetically encoded dendritic marker sheds light on neuronal connectivity in *Drosophila*. *Proc. Natl. Acad. Sci. U.S.A.* **107**, 20553–20558 (2010). doi: [10.1073/pnas.1010198107](https://doi.org/10.1073/pnas.1010198107); pmid: [21059961](https://pubmed.ncbi.nlm.nih.gov/21059961/)
38. S. Hampel *et al.*, *Drosophila* Brainbow: A recombinase-based fluorescence labeling technique to subdivide neural expression patterns. *Nat. Methods* **8**, 253–259 (2011). doi: [10.1038/nmeth.1566](https://doi.org/10.1038/nmeth.1566); pmid: [21297621](https://pubmed.ncbi.nlm.nih.gov/21297621/)
39. P. Bonifazi *et al.*, GABAergic hub neurons orchestrate synchrony in developing hippocampal networks. *Science* **326**, 1419–1424 (2009). doi: [10.1126/science.1175509](https://doi.org/10.1126/science.1175509); pmid: [19965761](https://pubmed.ncbi.nlm.nih.gov/19965761/)
40. M. D. Gordon, K. Scott, Motor control in a *Drosophila* taste circuit. *Neuron* **61**, 373–384 (2009). doi: [10.1016/j.neuron.2008.12.033](https://doi.org/10.1016/j.neuron.2008.12.033); pmid: [19217375](https://pubmed.ncbi.nlm.nih.gov/19217375/)
41. K. F. Rewitz, N. Yamanaka, L. I. Gilbert, M. B. O'Connor, The insect neuropeptide PTTH activates receptor tyrosine kinase torso to initiate metamorphosis. *Science* **326**, 1403–1405 (2009). doi: [10.1126/science.1176450](https://doi.org/10.1126/science.1176450); pmid: [19965758](https://pubmed.ncbi.nlm.nih.gov/19965758/)
42. J. J. Hodge, Ion channels to inactivate neurons in *Drosophila*. *Front. Mol. Neurosci.* **2**, 13 (2009). doi: [10.3389/fnro.2010.013.2009](https://doi.org/10.3389/fnro.2010.013.2009); pmid: [19750193](https://pubmed.ncbi.nlm.nih.gov/19750193/)
43. T. Flatt, M. P. Tu, M. Tatar. Hormonal pleiotropy and the juvenile hormone regulation of *Drosophila* development and life history. *BioEssays* **27**, 999–1010 (2005). doi: [10.1002/bies.20290](https://doi.org/10.1002/bies.20290); pmid: [16163709](https://pubmed.ncbi.nlm.nih.gov/16163709/)
44. C. K. Mirth *et al.*, Juvenile hormone regulates body size and perturbs insulin signaling in *Drosophila*. *Proc. Natl. Acad. Sci. U.S.A.* **111**, 7018–7023 (2014). doi: [10.1073/pnas.1313058111](https://doi.org/10.1073/pnas.1313058111); pmid: [24778227](https://pubmed.ncbi.nlm.nih.gov/24778227/)
45. L. M. Riddiford, J. W. Truman, C. K. Mirth, Y. C. Shen, A role for juvenile hormone in the prepupal development of *Drosophila melanogaster*. *Development* **137**, 1117–1126 (2010). doi: [10.1242/dev.037218](https://doi.org/10.1242/dev.037218); pmid: [20181742](https://pubmed.ncbi.nlm.nih.gov/20181742/)
46. M. Jindra, S. R. Palli, L. M. Riddiford, The juvenile hormone signaling pathway in insect development. *Annu. Rev. Entomol.* **58**, 181–204 (2013). doi: [10.1146/annurev-ento-120811-153700](https://doi.org/10.1146/annurev-ento-120811-153700); pmid: [22994547](https://pubmed.ncbi.nlm.nih.gov/22994547/)
47. C. Minakuchi, X. Zhou, L. M. Riddiford, *Krüppel homolog 1 (Kr-h1)* mediates juvenile hormone action during metamorphosis of *Drosophila melanogaster*. *Mech. Dev.* **125**, 91–105 (2008). doi: [10.1016/j.mod.2007.10.002](https://doi.org/10.1016/j.mod.2007.10.002); pmid: [18036785](https://pubmed.ncbi.nlm.nih.gov/18036785/)
48. R. J. Summers, R. A. Bathgate, J. D. Wade, E. T. van der Westhuizen, M. L. Halls, Roles of the receptor, the ligand, and the cell in the signal transduction pathways utilized by the relaxin family peptide receptors 1–3. *Ann. N. Y. Acad. Sci.* **1160**, 99–104 (2009). doi: [10.1111/j.1749-6632.2009.03828.x](https://doi.org/10.1111/j.1749-6632.2009.03828.x); pmid: [19416167](https://pubmed.ncbi.nlm.nih.gov/19416167/)
49. C. M. Smith, I. T. Hosken, S. W. Sutton, A. J. Lawrence, A. L. Gundlach, Relaxin-3 null mutation mice display a circadian hypoactivity phenotype. *Genes Brain Behav.* **11**, 94–104 (2012). doi: [10.1111/j.1601-183X.2011.00730.x](https://doi.org/10.1111/j.1601-183X.2011.00730.x); pmid: [21899720](https://pubmed.ncbi.nlm.nih.gov/21899720/)
50. J. Casanova, G. Struhl, The torso receptor localizes as well as transduces the spatial signal specifying terminal body pattern in *Drosophila*. *Nature* **362**, 152–155 (1993). doi: [10.1038/362152a0](https://doi.org/10.1038/362152a0); pmid: [8450886](https://pubmed.ncbi.nlm.nih.gov/8450886/)
51. C. J. Evans *et al.*, G-TRACE: Rapid Gal4-based cell lineage analysis in *Drosophila*. *Nat. Methods* **6**, 603–605 (2009). pmid: [19633663](https://pubmed.ncbi.nlm.nih.gov/19633663/)
52. N. Yamanaka *et al.*, Neuroendocrine control of *Drosophila* larval light preference. *Science* **341**, 1113–1116 (2013). doi: [10.1126/science.1241210](https://doi.org/10.1126/science.1241210); pmid: [24009394](https://pubmed.ncbi.nlm.nih.gov/24009394/)
53. J. Morante, C. Desplan, Dissection and staining of *Drosophila* optic lobes at different stages of development. *Cold Spring Harbor Protoc.* **2011**, 652–656 (2011). doi: [10.1101/pdb.prot5629](https://doi.org/10.1101/pdb.prot5629); pmid: [21632779](https://pubmed.ncbi.nlm.nih.gov/21632779/)
54. R. Bader *et al.*, The IGFBP7 homolog Imp-L2 promotes insulin signaling in distinct neurons of the *Drosophila* brain. *J. Cell Sci.* **126**, 2571–2576 (2013). doi: [10.1242/jcs.120261](https://doi.org/10.1242/jcs.120261); pmid: [23591813](https://pubmed.ncbi.nlm.nih.gov/23591813/)
55. H. Ikeshima-Kataoka, J. B. Skeath, Y. Nabeshima, C. Q. Doe, F. Matsuzaki, Miranda directs Prospero to a daughter cell during *Drosophila* asymmetric divisions. *Nature* **390**, 625–629 (1997). doi: [10.1038/37641](https://doi.org/10.1038/37641); pmid: [9403694](https://pubmed.ncbi.nlm.nih.gov/9403694/)
56. S. A. Cyran *et al.*, *vriple*, *Pdp1*, and *dClock* form a second feedback loop in the *Drosophila* circadian clock. *Cell* **112**, 329–341 (2003). doi: [10.1016/S0092-8674\(03\)00074-6](https://doi.org/10.1016/S0092-8674(03)00074-6); pmid: [12581523](https://pubmed.ncbi.nlm.nih.gov/12581523/)
57. Single-letter abbreviations for the amino acid residues are as follows: A, Ala; C, Cys; D, Asp; E, Glu; F, Phe; G, Gly; H, His; I, Ile; K, Lys; L, Leu; M, Met; N, Asn; P, Pro; Q, Gln; R, Arg; S, Ser; T, Thr; V, Val; W, Trp; and Y, Tyr.

ACKNOWLEDGMENTS

We thank P. Leopold for reagents and the PTTH antibody; M. Vidal for the *Igr2* plasmid; E. Hafen and H. Stocker for Dilp antibodies; A. Garelli for stock construct and initial work on this project; A. Gontijo for plasmid design; and J. Casanova, J. C. P. Yin, B. J. Dickson, J. Blau, B. Hassan, and F. Matsuzaki for fly stocks or antibodies. We also thank the Bloomington Stock Center (NIH grant P400D018537), the DGRC (NIH grant OD010949-10), and the Transgenic RNAi Project at Harvard Medical School (NIH National Institute of General Medical Sciences grant R01-GM084947) for providing the fly stocks and plasmids used in this study and the Developmental Studies Hybridoma Bank at the University of Iowa for antibodies. This work was supported by a Ramon y Cajal grant (RyC-2010-07155) and a Ministerio de Economía y Competitividad grant (SAF2012-31467) to J.M.; a Junta de Andalucía PAIDI group CTS-569 to J.B.; and Spanish national grants (SAF2012-35181 and SEV-2013-0317) and a Generalitat Valenciana grant (PROMETEO II/2013/001) to M.D. M.D. was also supported by the Botin Foundation. S.J.-C. is a fellow from Formación del Personal Investigador (grant BES-2013-064947) from the Spanish Ministerio de Economía y Competitividad.

SUPPLEMENTARY MATERIALS

www.sciencemag.org/content/350/6262/aac6767/suppl/DC1
Figs. S1 to S8
Movies S1 to S3

29 May 2015; accepted 24 September 2015
Published online 1 October 2015
[10.1126/science.aac6767](https://doi.org/10.1126/science.aac6767)



A brain circuit that synchronizes growth and maturation revealed through Dilp8 binding to Lgr3

Diana M. Vallejo, Sergio Juarez-Carreño, Jorge Bolivar, Javier Morante and Maria Dominguez (October 1, 2015)

Science **350** (6262), . [doi: 10.1126/science.aac6767] originally published online October 1, 2015

Editor's Summary

Brain keeps body size and shape in check

Animal systems show amazing left-right symmetry—think of how our legs or arms, or the legs or wings of an insect, are matched in size and shape. Environmental insults and growth defects can challenge these developmental programs. In order to limit the resultant variation, juvenile organisms buffer variability through homeostatic mechanisms, so that the correct final size is attained. Vallejo *et al.* report that the *Drosophila* brain mediates such homeostatic control via an insulin-like peptide Dilp8 binding to the relaxin hormone receptor Lgr3. Lgr3 neurons distribute this information to other neuronal populations to adjust the hormones ecdysone, insulin, and juvenile hormone in a manner that stabilizes body and organ size.

Science, this issue p. 10.1126/science.aac6767

This copy is for your personal, non-commercial use only.

Article Tools Visit the online version of this article to access the personalization and article tools:
<http://science.sciencemag.org/content/350/6262/aac6767>

Permissions Obtain information about reproducing this article:
<http://www.sciencemag.org/about/permissions.dtl>

Science (print ISSN 0036-8075; online ISSN 1095-9203) is published weekly, except the last week in December, by the American Association for the Advancement of Science, 1200 New York Avenue NW, Washington, DC 20005. Copyright 2016 by the American Association for the Advancement of Science; all rights reserved. The title *Science* is a registered trademark of AAAS.



Supplementary Materials for

A brain circuit that synchronizes growth and maturation revealed through Dilp8 binding to Lgr3

Diana M. Vallejo, Sergio Juarez-Carreño, Jorge Bolivar, Javier Morante,* Maria Dominguez*

*Corresponding author. E-mail: m.dominguez@umh.es (M.D.); j.morante@umh.es (J.M.)

Published 1 October 2015 on *Science Express*
DOI: 10.1126/science.aac6767

This PDF file includes:

Figs. S1 to S8
Captions for Movies S1 to S3

Other Supplementary Material for this manuscript includes the following:
(available at www.sciencemag.org/cgi/content/full/science.aac6767/DC1)

Movies S1 to S3

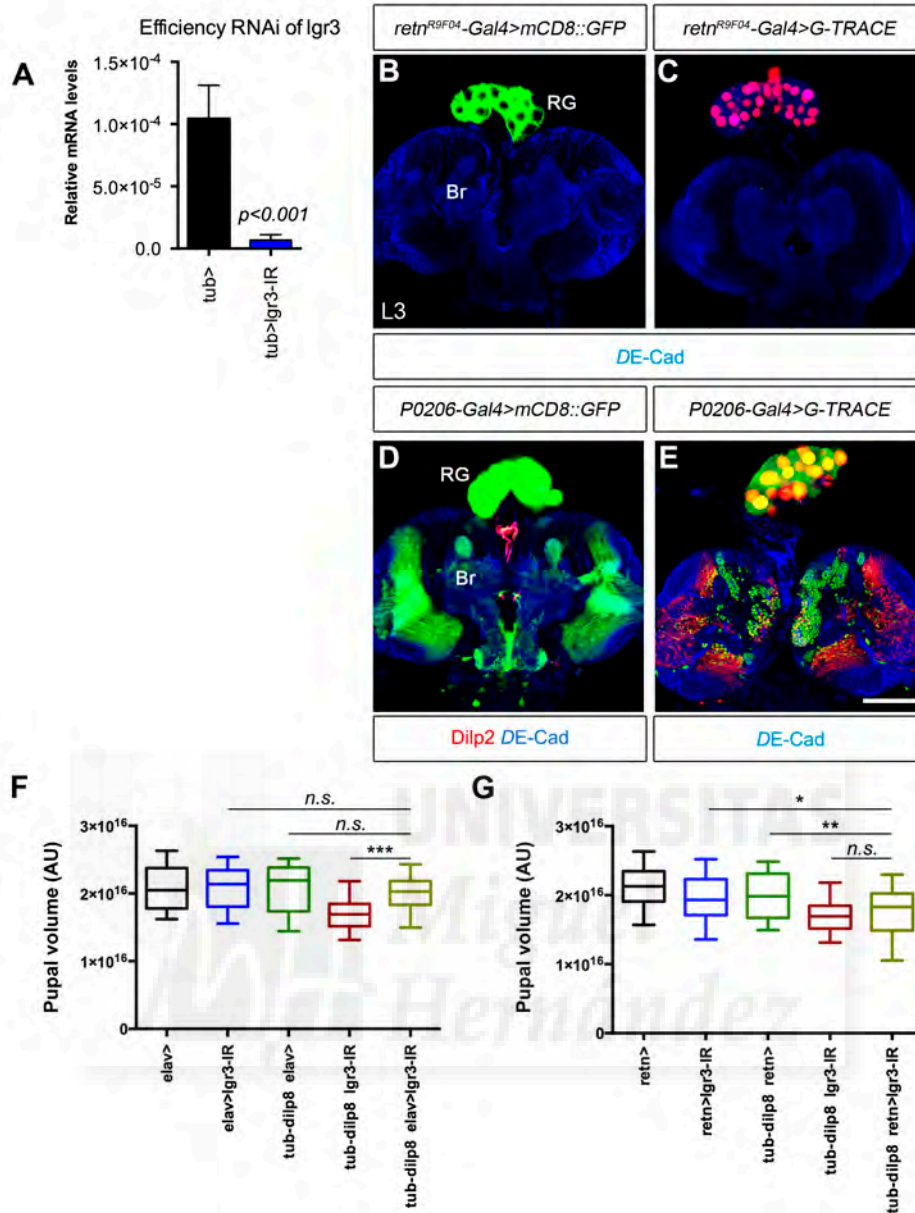


Fig. S1. Control of *lgr3* RNAi and pupal volume of animals with neural or ring gland specific knockdown of *lgr3*. (A) *lgr3* mRNA levels normalized to *rp49* in age-synchronized larvae expressing *lgr3^{GL01056}* [*UAS-lgr3-IR*, *P{TRiP.GL01056}*] described in (28)]. Shown are mRNA levels of *lgr3* in animals expressing the RNAi transgene (*tub>lgr3-IR*) or not (*tub>*) analysed by qRT-PCR. Data were analyzed by a two-tailed unpaired *t*-test and values represent the mean \pm SD of three independent repeats. (B-C) Confocal images of late third instar larval brain (Br)/ring gland (RG) complexes showing *retn-Gal4* driven expression of *UAS-mCD8::GFP* (B) and *G-TRACE* (51) (C). *G-TRACE* differentially marks cells that currently express a *Gal4* driver in red and cells that expressed the driver in the past in green. Note that *retn^{R9F04}-Gal4* is highly specific for the endocrine ring gland, particularly the prothoracic gland cells. (D-E) In contrast, *P0206-Gal4* line drives expression of the *UAS-mCD8::GFP* (D) and *G-TRACE* (E) in the ring gland and also broad, strong expression in the brain, including the optic lobes, neuroblasts, etc. Brains were counterstained using anti-*DE-Cad* (blue). Scale bar, 75 μ m. (F) Shown is pupal

volume of *tub-dilp8* animals with neural-specific depletion of *lgr3* using *elav-Gal4* and controls of genetic background. If neural specific depletion of *lgr3* would not rescue Dilp8-induced reduction of growth, one would expect that larvae of the *tub-dilp8 elav>lgr3-IR* to reach pupation at a smaller size than controls *elav>lgr3-IR*. However, note that animals reach a correct size (unpaired *t*-test, $n > 30$ pupae analysed per genotype, shown is mean \pm SD). This indicates that depletion of *lgr3* in neurons also rescues the Dilp8-induced reduction of growth rate. (G) Graph shows pupal volume measurements of animals with depleted *lgr3* in ring gland using *retn^{R9F04}-Gal4*. $n > 30$ pupae analysed per genotype. Given the variability introduced by the genetic background of the *retn^{R9F04}-Gal4* and the $P\{TRiP.GL01056\}$ (*UAS-lgr3-IR*) donor animals, variations in size between experimental animals and controls likely reflect a major contribution of the genetic background of the transgenes rather than specific effect of *lgr3* knockdown.



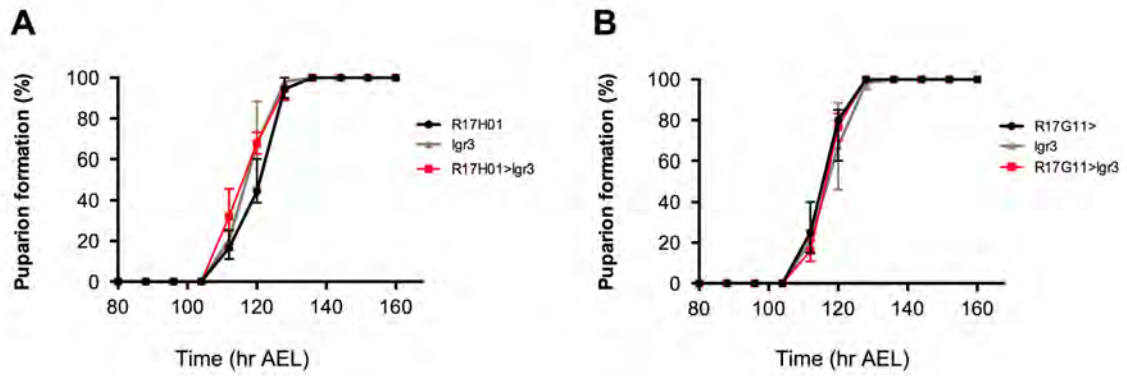


Fig. S3. Overexpression of *lgr3* using other *lgr3* enhancer DNA fragments does not delay pupation formation. Accumulative pupation time of larvae with overexpression of *lgr3* using *lgr3* brain enhancer fragments (*R17H01-Gal4>lgr3*, **A**) and (*R17G11-Gal4>lgr3*, **B**) and control larvae. Approximately 60 pupae scored per genotype. Data plotted is pooled from three independent repeats. Each data point is mean \pm SD ($n = 3$).



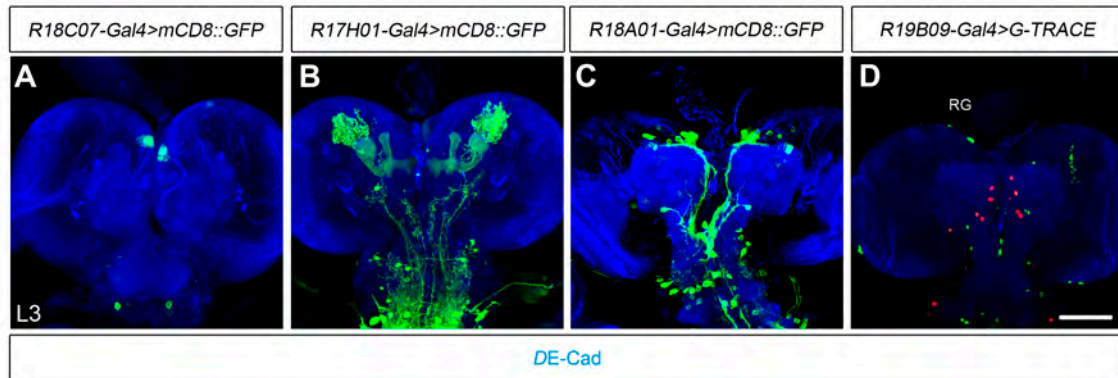


Fig. S4. Expression pattern of the *lgr3* enhancer fragments that do not rescue *Dilp8* actions and *G-TRACE* analysis of the *R19B09* enhancer. (A-C) Expression of *UAS-mCD8::GFP* driven by the *lgr3* brain enhancers *R18C07* (A), *R17H01* (B) and *R18A01* (C). (D) *G-TRACE* analysis (51) using the *lgr3* enhancer *R19B09-Gal4*. *G-TRACE* in red marks cells that currently express the *R19B09-Gal4* and in green, cells that expressed the driver in earlier stages. No red or green expression is detected in the endocrine ring gland (RG) cells. Brains were counterstained using anti-*DE-Cad* (blue) antibody. Scale bar, 75 μ m.



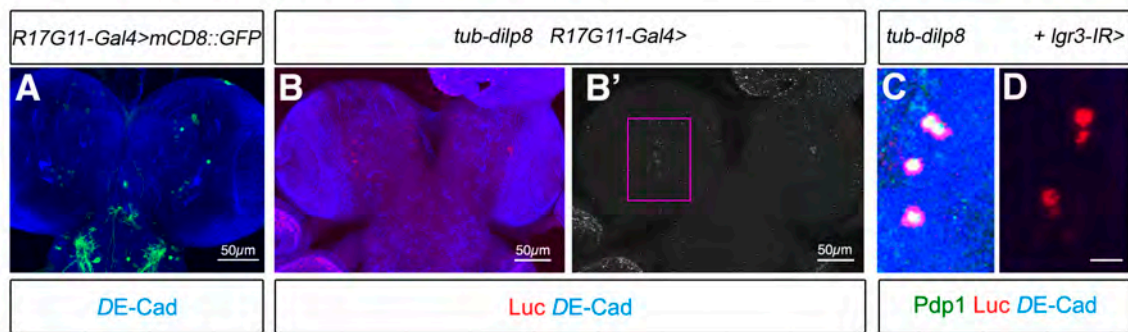


Fig. S5. Targeted cAMP sensor in the *R17G11* pattern. (A) Expression of *UAS-mCD8::GFP* in the pattern of *R17G11-Gal4*. (B and B') The *R17G11-Gal4* labelled cells do not show cAMP response to Dilp8 signals. The four neurons (box) that show weak luciferase staining are pacemaker cells [as defined by co-labelling with the clock marker anti-Pdp1 (56), green in C]. cAMP response in pacemaker cells may reflect another GPCR as luciferase-positive labelling is still seen in larval brains with depleted *lgr3* by *UAS-lgr3-IR* (D). Genotype: *UAS-Flp/elav-Gal4, tub-dilp8/CRE-F-luc, UAS-lgr3-IR*. Scale bar in D represents 20 μ m.



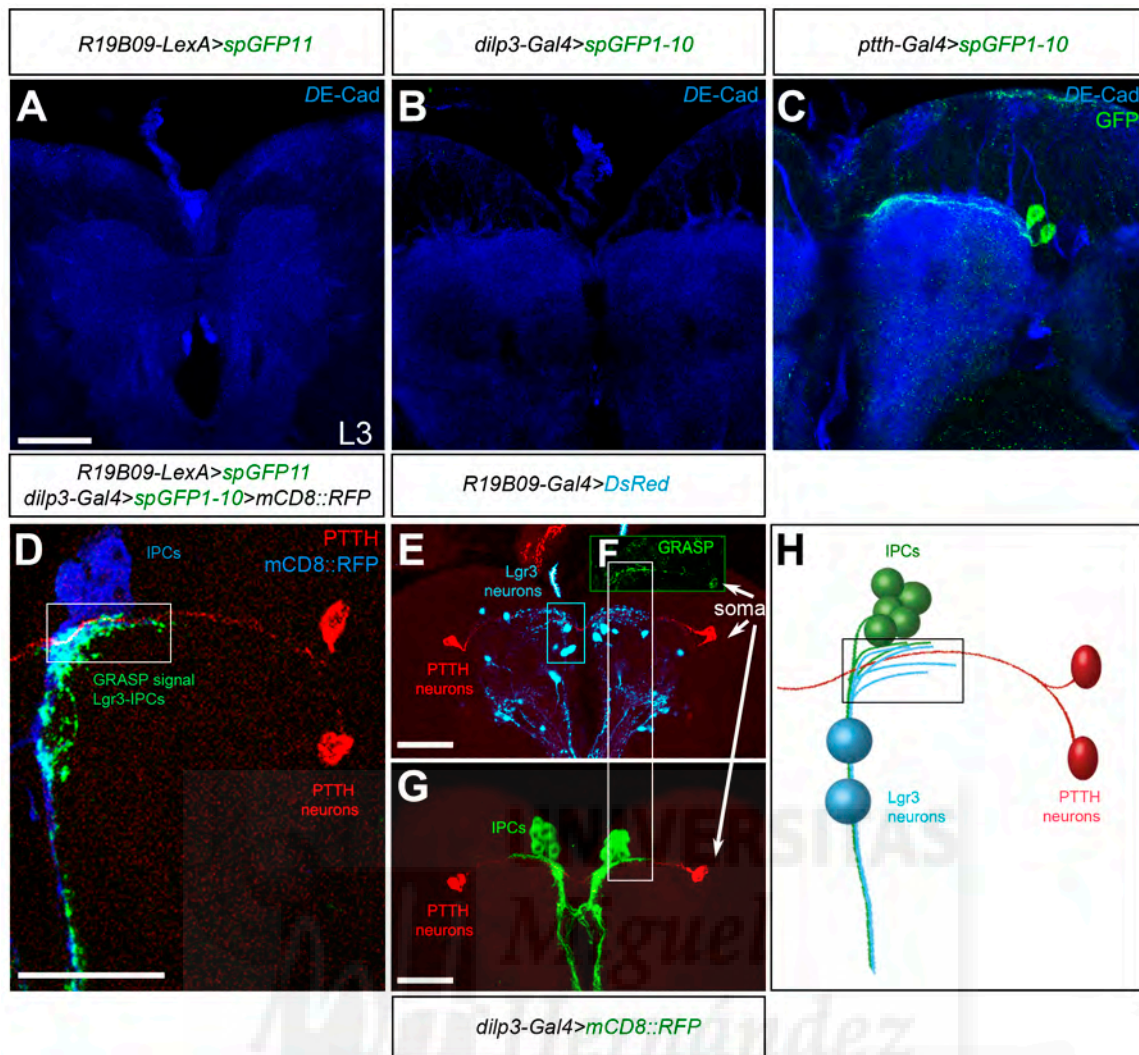


Fig. S6. Single GRASP component control brains and mapping of potential connectivity among the *Lgr3*, IPCs and PTTH-producing neurons. (A) No fluorescent signal was observed in *R19B09-LexA>spGFP₁₁* brains ($n = 10$). (B) No fluorescence was detected in *dilp3-Gal4>spGFP₁₋₁₀* control brains ($n = 10$). In A and B, control brains were imaged as in brains containing the two GRASP components in Fig. 5, E and F. (C) Single GRASP component control brain *ptth-Gal4>spGFP₁₋₁₀* stained with anti-GFP (green, Invitrogene) detect signal in soma and axons of PTTH neurons resulting from the *spGFP₁₋₁₀* fragment, but not the punctuate staining of reconstituted GFP ($n = 10$). Brains were counterstained using anti-DE-Cad (blue). (D) Brain *R19B09-LexA>spGFP₁₁ dilp3-Gal4>spGFP₁₋₁₀>mCD8::RFP* (GRASP signals, in green) stained for anti-PTTH (red). (E) *R19B09>DsRed* brain stained for anti-PTTH (red). Inset (F) shows reconstituted GFP punctuate signal, likely dendrites, of *R19B09-LexA>spGFP₁₁ ptth-Gal4>spGFP₁₋₁₀*. (G) IPCs (green) also project towards the PTTH neuron projections (red). (H) Scheme view of the circuit. Region depicted in white boxes in D and E-G and the black box in H represents potential membrane contacts of IPCs, PTTH, and *Lgr3* responding neurons. Scale bars, 40 μ m.

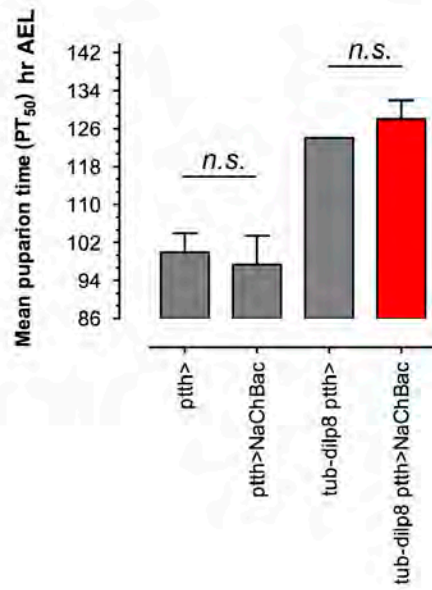


Fig. S7. Activation of PTH neurons by expressing NaChBach ion channel is not sufficient to evoke a precocious pupariation transition. Graph shows the mean pupation time of animals expressing the *UAS-NaChBac* transgene driven by *pth-Gal4* in the presence or absence of *tub-dilp8* transgene and controls of genetic background. Approximately 60 pupae per genotype were scored and graph shows data pooled from three independent experiments. (*n.s.*, $p > 0,05$, two-tailed unpaired *t*-test, mean \pm SD). Error bars (SD) are invisible when the three replicates coincide.

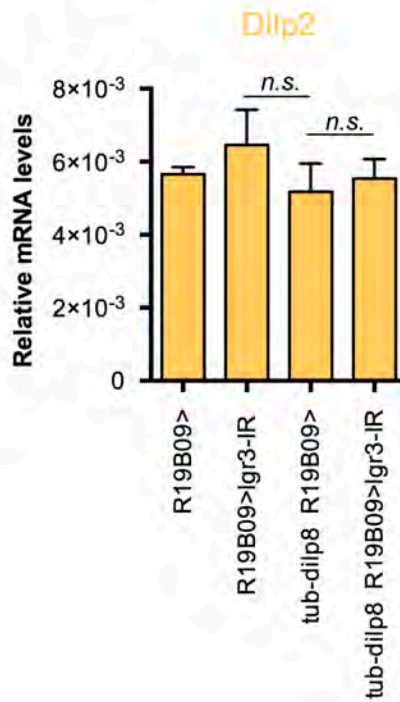
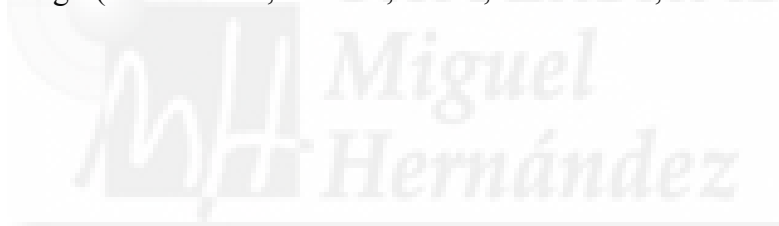


Fig. S8 Analysis of transcription of the *dilp2* gene. Expression of *dilp2* gene analysed by quantitative RT-PCR in mRNA isolated from ~10 larvae for each genotype and age (100 hr AEL, animals, $n = 3$, mean \pm SD, two-tailed unpaired t -test).



Supplementary movie captions

Movie S1. Three-dimensional reconstruction of wild type *Drosophila* larval brain stained for Lgr3 neurons using the *R19B09-LexA* and *LexAop2-IVS-myr::GFP* (green) and PTTH neurons using anti-PTTH antiserum (red). 3D reconstruction was obtained from about 43 optical sections (thickness about 1 μm) using Imaris software (Bitplane AG, Zurich, Switzerland).

Movie S2. Three-dimensional reconstruction of wild type *Drosophila* larval brain stained for Lgr3 neurons using the *R19B09-LexA* driven *LexAop2-IVS-myr::GFP* (green) and insulin-producing cells using *dilp3-Gal4 UAS-DsRed* (red) obtained from about 34 optical sections (thickness about 1 μm) using Imaris software (Bitplane AG, Zurich, Switzerland).

Movie S3. Three-dimensional reconstruction of wild type *Drosophila* larval brain labelling Lgr3 neuron subpopulations in different colours using *UAS-dBrainbow* via the *R19B09-Gal4* line. 3D reconstruction was obtained from about 53 optical sections (thickness about 1 μm) using Imaris software (Bitplane AG, Zurich, Switzerland).

Summary

In this Part 1, I described a new buffering mechanism in *Drosophila* that involves communication between the growing imaginal discs and the brain mediated by a thus far orphan receptor, namely the relaxin family GPCR Lgr3. Using a candidate approach and functional genomic analysis, immunohistochemical and neural tools, I have identified that the receptor encoded by the *lgr3* gene is a receptor for the hormone Dilp8, and I have defined a small set of central brain neurons as the site of action of this receptor. Here, I named these Dilp8 responding Lgr3 neurons (``sync`` neurons) because they mediate synchronization between growth control and developmental timing that enables buffering variations and the homeostatic control of size, proportion and bilateral symmetry. I also defined two populations of neurons that mediate the Lgr3-dependent homeostatic control of growth and developmental timing. Dr. Javier Morante using GRASP (GFP reconstitution across synaptic partners) tools demonstrated that the ``sync`` Lgr3 neurons form synapses and are directly connected to both PTH neurons and the insulin producing cells (IPCs). Using genetic tools, I further showed that electrical silencing or activation each of these neurons provoke the expected phenotypes, indicating that these three neuronal populations form a circuit for co-regulation of maturation and growth rate in response to perturbation. Finally, I have shown that Dilp8-Lgr3 balances growth against the extended growth period by dampening the production of two insulin genes, *dilp3* and *dilp5*, in the insulin producing cells (IPCs) in the brain. Dilp8-Lgr3 system also modulates growth by regulating the juvenile hormone. Further, I have shown that without Dilp8-Lgr3 signalling, the brain is incapable of stabilizing size between the distinct body parts, resulting in the developmental instability and imperfect bilateral symmetry.



Part II.

Trade-Off between Dilp8-Lgr3-mediated homeostatic growth control and Fitness response to Stress and modulation by circadian clock





Dilp8 enhances tolerance to starvation in virgin flies

Systemic expression of *dilp8* by the ubiquitous promoter α -tubulin (referred to as *tub-dilp8*) causes an extension of the feeding stage without a corresponding increment in body size (Colombani et al. 2012; Garelli et al. 2012). Generally, energy storage and utilization is homeostatically controlled so that an increase in energy stores increases growth and animal size. However, Dilp8-Lgr3 system suppresses systemically imaginal disc growth during the extended larval period to ensure that the animal attains the correct size. Previous work in the laboratory showed that the extended larval stage produced normal sized adults that nevertheless were 20-30% heavier than control siblings. It is known that stored resources during the pre-reproductive stages have two main functions: (1) is to ensure reproductive capacity for the adult individual and (2) is to increase tolerance to starvations during periods of famine (Tissenbaum & Ruvkun 1998; Pettigrew & Hamilton-Fairley 1997; Tatar et al. 2003; Le Bourg 2007; Blomquist 2009). It is also known that the mechanisms that increase mobilization of energy stores for reproduction generally increase fertility and reproductive output, but as trade-off, these mechanisms are associated with reduced resistance to starvation. Conversely, mutations that increase resistance to starvation by increasing mobilization of energy stores towards somatic maintenance typically reduce fertility and increase life-span (Broughton et al. 2005; Tatar et al. 2001; Clancy et al. 2001; Giannakou et al. 2004; Hwangbo et al. 2004). Thus, given that *tub-dilp8* flies have the correct size but are overweighted, an open question was whether such pre-reproductive 'obesity' could impact on starvation resistance or the reproductive output of *tub-dilp8* animals or both.

To this end, I tested the impact of overweight resulting from the extended larval period by systemically overexpressed *dilp8* might have on survival to starvation.

Adult flies (females and males) of the genotype *tub-dilp8*, and controls, were collected and transferred to vials with 2% of agar ('wet starvation'). This food restriction generates a food-stress condition, including an increase in expenditure of metabolic resources, to maintain the survival of the flies (Flier 2004). Flies that are defective in mobilizing these energetic resources have typically reduced starvation resistance. However, mating increases food intake in female flies, therefore nullifying the effect of energy stores accumulated in the pre-reproductive stage (Carvalho et al. 2006). All experiments were carried out using age-synchronized virgin animals. The *tub-dilp8* flies showed a marked increase in tolerance to starvation compared to sibling control of background controls (**Figure 13. A and B**).

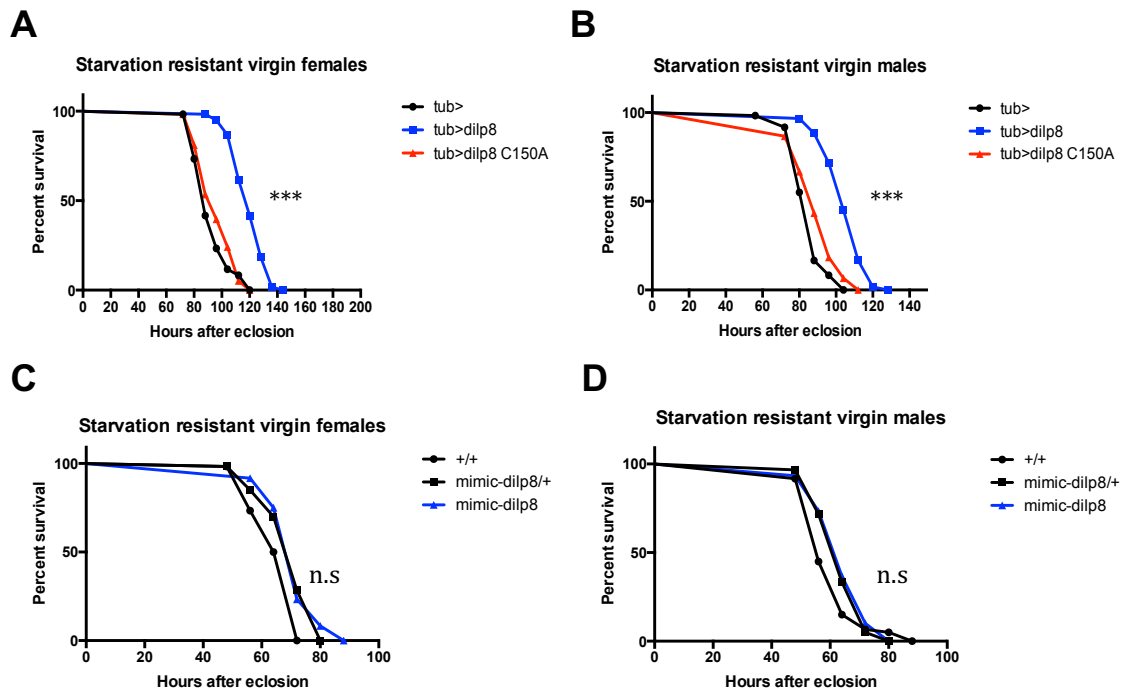


Figure 13: *dilp8* overexpression under *tub* promoter control extends larval feeding period and generates adult flies more resistant to starvation. (A) Adult virgin females emerging from larvae-pupae overexpressing *dilp8* systemically (*tub>dilp8*) more starvation resistance than control flies. Flies overexpressing an inactive form of *dilp8* (*dilp8^{C150A}*) transgene by *tubulin-Gal4* (*tub>*) served as control of genetic background. (B) Starvation resistant of *tub>dilp8* adult virgin males. (C) Adult *dilp8*⁻ mutant virgin females and (D) males are not starvation sensitive or resistant. The graphs show data pooled from four independent experiments, and each data point represent the flies that died at the indicated time point after eclosion from the pupa. A total of 60 flies were scored *per* genotype. *P* values: ****P*<0.001; *P*>0.05 (long-rank test), n.s., not significant.

Flies deficient for *dilp8* are of varied body size and often present imperfect bilateral symmetry. As a population, virgin females defective for *dilp8* did not show any difference in the starvation resistance as compared to control flies. *dilp8* deficient flies showed normal body weight and generally display normal developmental timing, or slightly accelerated metamorphosis (Figure 13. C and D; (Colombani et al. 2012; Garelli et al. 2012)). I concluded that the increase in body weight in *tub-dilp8* flies may be responsible for the increase in starvation resistance observed.

Starvation resistant is controlled by Dilp8 acting on Lgr3 in the ``sync`` neurons

In a previous work (Vallejo et al. 2015), I found that the overweight associated with *tub-dilp8* extended feeding period during development is fully rescued by *lgr3* knocked-down systematically. Here, I tested whether this overweight is controlled by ``sync`` neurons, which also control developmental timing and compensate growth rate through Dilp8 signalling. To this end, I silenced *lgr3* receptor in ``sync`` neurons using the *R19B09-Gal4* (Vallejo et al. 2015). I found that the flies that overexpressed *dilp8* with silenced *lgr3* in ``sync`` neurons did not increase their weight in the same way the sibling flies of the indicated genotypes, both males and females (Figures 14. A and C).

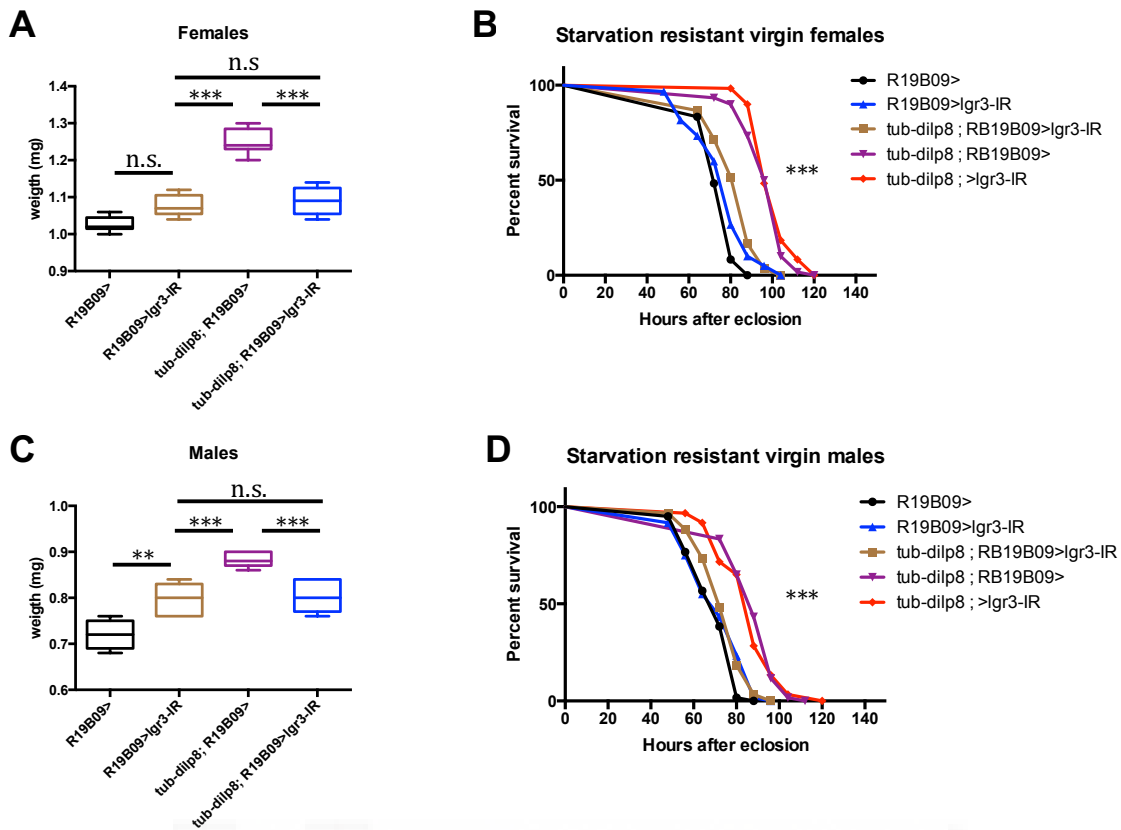


Figure 14: Dilp8 signaling through Lgr3 receptor in the ‘sync’ neurons mediates Dilp8-induced body overweight and for starvation resistant. In all cases RNAi-silencing of *lgr3* in the ‘sync’ neurons is done using the *R19B09-Gal4* line (*R19B09>*) and *dilp8* overexpression is under direct control of *tub* promoter (*tub-dilp8*). (A) Graph represents body weight of adult virgin females of the indicated genotypes. Mean \pm SD, *** $P < 0.001$ (two-tailed unpaired *t* test), and $n = 30$ age-synchronizes adult virgin females *per* genotype. (B) Starvation resistance in virgin females of the indicated genotypes. The graph shows data pooled from four independent experiments, and each data point is the flies died at this hour after eclosion from the pupa. A total of 60 flies per each genotype were scored *per* genotype. *** $P < 0.001$ (long-rank test). (C-D) Body weight in adult virgin males of the indicated genotypes. Mean \pm SD, *** $P < 0.001$; ** $P < 0.01$ (two-tailed unpaired *t* test), and data $n = 25$ age-synchronizes adult virgin females in each genotype for weight experiment for C. The graphs show data pooled from four independent experiments, and each data point represent number of flies that died at the indicated timepoint after eclosion from the pupa. A total of 60 flies were scored *per* genotype. *** $P < 0.001$ (long-rank test) for D.

Furthermore, this extra body weight had a positive correlation with the starvation resistance observed in the flies overexpressing *dilp8*. The *tub-dilp8* flies lacking *lgr3* in ‘sync’ neurons were starvation sensitive as compared to the *tub-dilp8* flies (Figure 14. B and D). Thus, the overweight acquired as a ‘side-effect’ of Dilp8-Lgr3 buffering mechanism seems to produce benefits not only by enhancing size robustness but also by enhancing later-life fitness by increasing starvation resistance to potential famine periods.

Dilp8-Lgr3 signalling increases lipogenesis reflected as high triglycerides levels

Lipids are the most important energy storages correlated with starvation resistant (Service 1987; Chippindale et al. 1996; M.-H. Wang et al. 2004; Ballard et al. 2008). For this reason, I explored whether the increased body weight of *tub-dilp8* animals is merely a passive effect of extended feeding behavior with a normal rate of lipogenesis. Alternatively, Dilp8-Lgr3 could influence more directly lipid metabolism. To discern between both options, I analyzed the expression level of key genes involved in the synthesis of lipids by quantitative RT-PCR. In particular, I studied the expression of *ACC*, *Ascl*, *bgm*, *FAS*, and *SREBP* (Xie et al. 2015; Reiff et al. 2015). I found that *ACC*, *Ascl*, and *bgm* genes are up-regulated in the *tub-dilp8* larvae. The increased levels of lipogenic genes were dependent on the interaction between Dilp8-Lgr3 (Figures 15. A, B, C, D, and E).

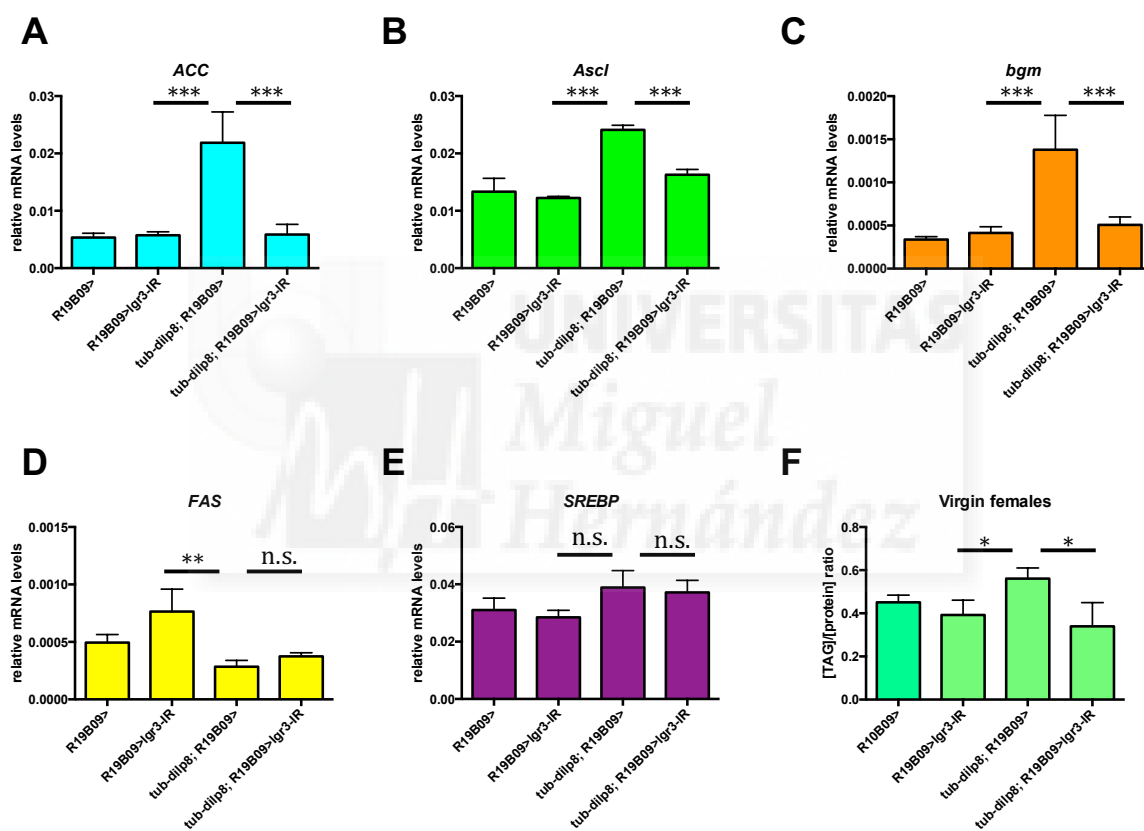


Figure 15: Dilp8-Lgr3 increased the lipogenesis during developmental delay to increased TAG in adult virgin flies. (A to E) Transcriptional expression levels of five lipogenesis genes, *ACC*, *Ascl*, *bgm*, *FAS*, and *SREBP* analyzed by qRT-PCR in mRNA isolated from 10 larvae for each genotype 100 hours AEL. Data are mean \pm SD (n = 3 repeats). *** $p < 0.001$; ** $p < 0.01$; n.s. $p > 0.05$ (Two-tailed unpaired *t* test). (D) Quantification of total triglycerides normalized to protein in adult virgin females. Data are mean \pm SD (n = 3 repeats). * $p < 0.05$ (Two-tailed unpaired *t* test).

This up-regulation of key enzymes in lipogenesis in *tub-dilp8* larvae indicates a pro-active role of Dilp8-Lgr3 in the formation of fat storage and the suppression of mobilization of these stores for animal growth, which may account for the significant increase of body weight of adult *tub-dilp8* flies. Furthermore, most of the overweight of these flies is reflected in an increase in the levels of triglycerides (TAGs) (Figure 15. F).

PTTH neurons respond to Dilp8-Lgr3 signalling and regulate the timing of steroid hormone biosynthesis and lipogenesis

The temporal transition from feeding to wandering larvae, and pupal development is coordinated by surges of the PTTH hormone, which in turn stimulate the surges of the steroid hormone ecdysone in the prothoracic gland (**Figure 7**). Previous work has established that flies lacking the PTTH neuropeptide showed an extended larval stage that results in increased adult body size and overweight (McBrayer et al. 2007). In those flies the increased body size was produced by the absence of a homeostatic growth mechanism that would slow down the growth rate, which might be mediated by the activation of Dilp8 in the imaginal discs and the binding of Dilp8 to its receptor Lgr3 in “sync” neurons. Indeed, I found that Dilp8 activation of Lgr3 neurons inhibited PTTH neurons, and concomitantly also downregulated *dilp3* and *dilp5* in the IPCs and also reduced the levels of JH titers (Vallejo et al. 2015).

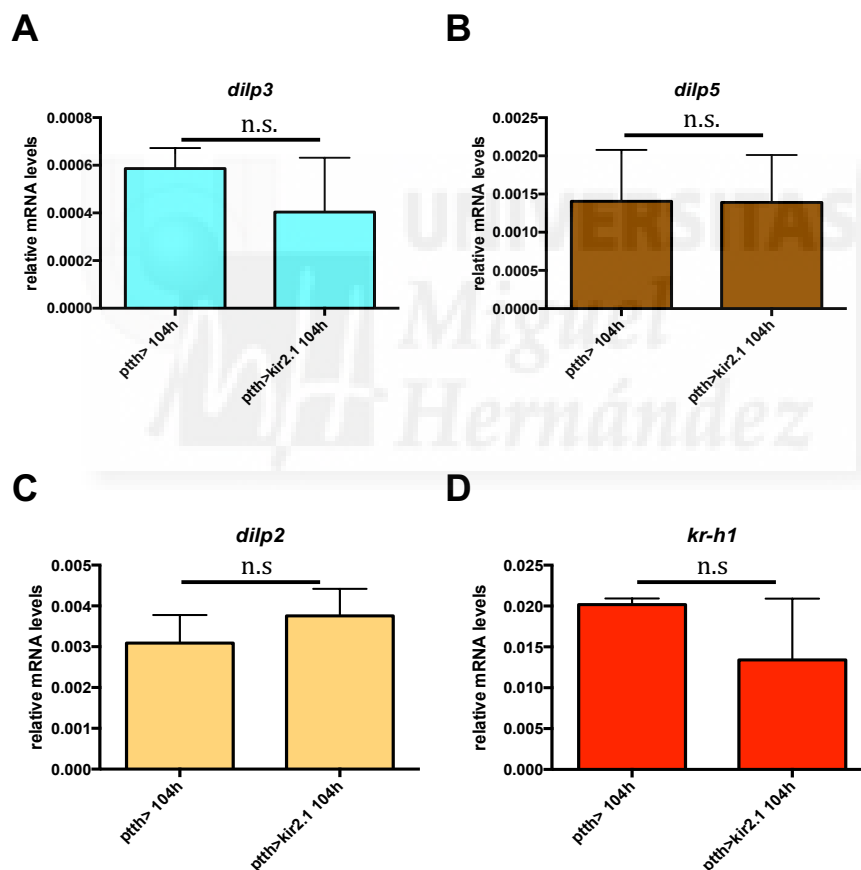


Figure 16: Activation of plastic growth mechanism does not change insulin signaling and juvenile hormone signaling. (A to C) Expression levels of the three insulin-like peptides expressed in the IPCs, *dilp2*, *dilp5* and *dilp3* analyzed by qRT-PCR in mRNA isolated from 10 larvae for each genotype 104 hours AEL. Data are mean \pm SD (n = 3 repeats). n.s. $p > 0.05$ (Two-tailed unpaired *t* test). (D) Expression levels of the main juvenile hormone signaling target gene *krüppel-homolog 1* analyzed by qRT-PCR in mRNA isolated from 10 larvae for each genotype 104 hours AEL. Data are mean \pm SD (n = 3 repeats). n.s. $p > 0.05$ (Two-tailed unpaired *t* test).

To investigate the role of PTTH-producing neurons in the *tub-dilp8*-dependent overweight and starvation resistance behavior, I first measured the expression of *dilp3* and *dilp5* and of the JH-

responsive gene *krüppel-homolog 1* in larvae with silenced PTTH neurons. This was accomplished by expressing the ion channel *mKir2.1* (Hodge 2009), which mimics the inhibition of PTTH neurons produced by Dilp8-mediated activation of Lgr3 neurons (Vallejo et al. 2015). The *dilps* genes and JH signalling was not affected by PTTH neuronal silencing (**Figures 16. A, B, C, D**).

The main target of PTTH is the production of the steroid hormone ecdysone (McBrayer et al. 2007; Rewitz et al. 2009). Steroid ecdysone is a key player of the juvenile-to-adult transition, which is often modulated in a nutrient-dependent manner (Caldwell et al. 2005; Colombani et al. 2005; Mirth et al. 2005). However, the underlying genetic mechanisms of this regulation generally evoke mechanisms involving the IIS. Thus, to investigate the potential contribution of PTTH-Ecdysone to the increased lipogenesis and overweight phenotype of *tub-dilp8* animals, we measured the expression of the lipogenic enzymes in larvae with electrically silenced PTTH neurons, which again mimics the effect of Dilp8-mediated activation of Lgr3 neurons and its effects of post-synaptic PTTH neurons.

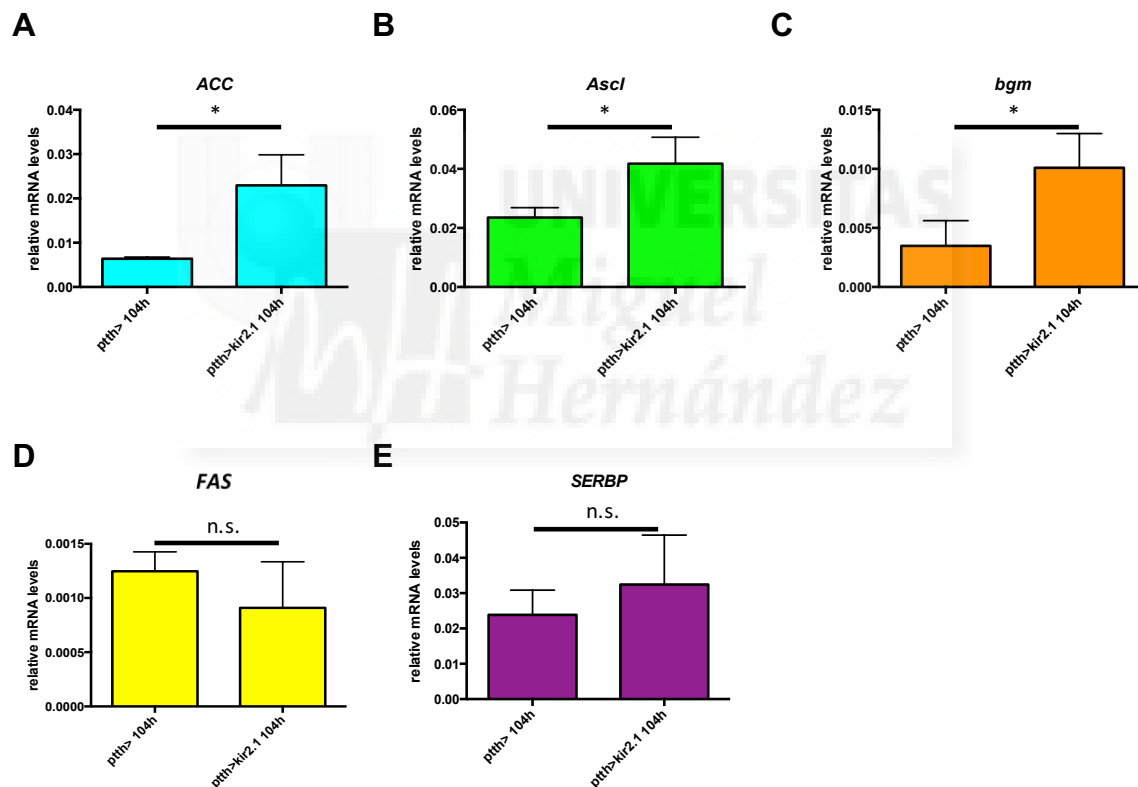


Figure 17: Activation of a plastic growth mechanism increased lipogenesis-related genes. (A to E) Expression levels of five lipogenesis genes, *ACC*, *Ascl*, *bgm*, *FAS*, and *SREBP* analyzed by qRT-PCR in mRNA isolated from 10 larvae for each genotype 100 hours AEL. Data are mean \pm SD (n = 3 repeats). * $p < 0.05$; n.s. $p > 0.05$ (Two-tailed unpaired *t* test).

Neural silencing of the two pairs of PTTH neurons resulted in an increased expression of the lipogenic enzymes *Acc*, *Ascl* and *Bgm* (**Figures 17. A, B, C, D, E**). These results indicate the contribution of ecdysone in lipogenesis regulation.

Lgr3 ``sync`` neurons synaptically interact with circadian pacemaker neurons (PDF⁺ neurons)

In the course of studying the neuronal populations that responded and were directly connected to the Lgr3 ``sync`` neurons, Javier Morante and myself have found that Lgr3 ``sync`` neurons directly synapse with the circadian master clock neurons that are labeled by the PDF neuropeptide. Subsequently, we have found that PDF neurons also form synapses with the PTTH neurons, thereby forming an unexpected circuit with GRASP (GFP reconstitution across synaptic partners) analysis, that is based on the expression of two nonfluorescent split-GFP fragments (spGFP1-10 and spGFP11) tethered to the membrane in two neuronal populations. We demonstrate the synaptic interaction between PDF neurons and Lgr3 ``sync`` neurons (**Figure 18. A**). The transition from feeding to non-feeding (wandering) larvae is gated by the circadian clock in many insects (Ampleford & Steel 1982; Markow & L. D. Smith 1979; Schnebel & Grossfield 1986). The circadian master clock neurons (PDF⁺ neurons) receive inputs from the photoreceptors and form neural connections with PTTH neurons in different insects including *Drosophila* (Helfrich-Förster et al. 2002; Helfrich-Förster et al. 2007; Malpel et al. 2002; Yasuyama et al. 2006). Both PDF⁺ and PTTH neurons are involved in controlling light avoidance behavior during metamorphosis. Moreover, it has been postulated that PDF neuropeptide negatively regulates the temporal expression pattern of PTTH, and that PDF mutations would be expected to accelerate the developmental timing program (McBrayer et al. 2007; Yamanaka, Rewitz, et al. 2013).

In this context, as Lgr3 neurons are connected to PTTH and PDF neurons, I wondered whether PDF neurons exert the control of developmental timing by Lgr3 and PTTH neurons. I postulated that as a consequence of this interaction Dilp8-Lgr3 and PDF neuropeptide work together in the coupling developmental timing and growth mediated by Dilp8-Lgr3 signalling. To address this hypothesis, I crossed flies overexpressing *dilp8* (to activate Lgr3 ``sync`` neurons) in a *pdf* null mutant background. *pdf* null mutant does not show any impact in developmental timing compared to wild type control, but interestingly when *pdf* null mutant is in a *dilp8*-overexpression context the delay of developmental timing program produces by Dilp8 is enhanced (**Figure 18. B**).

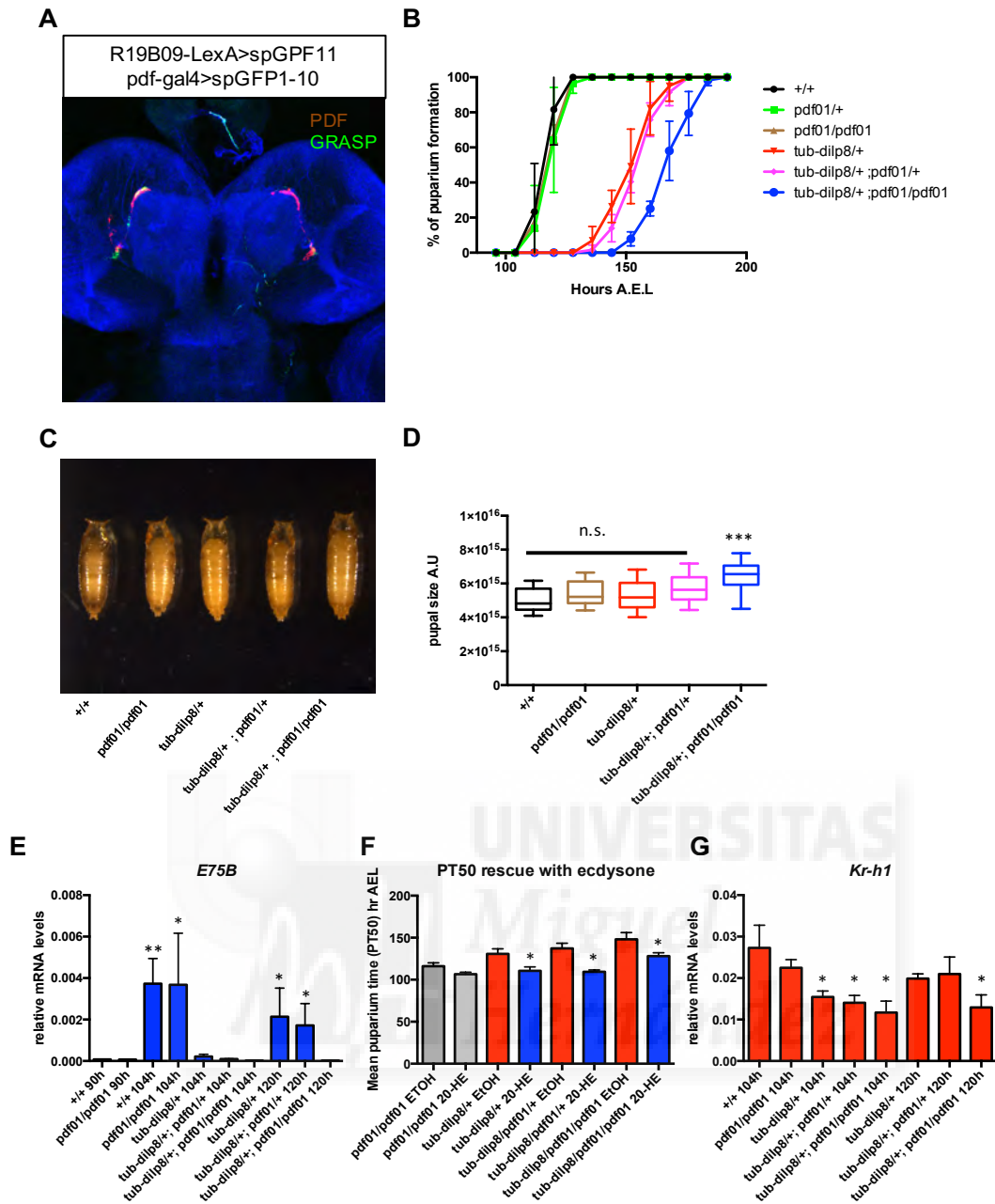


Figure 18: PDF neurons contact synaptically with Lgr3 "sync" neurons to mediated developmental delay of Dilp8-Lgr3 interaction. (A) Positive signals of GRASP in green revealed connections between Lgr3 "sync" neurons (*R19B09-LexA>spGFP11*) and PDF neurons (*pdf-Gal4>spGFP1-10*). Brains were counterstained with anti-DE-Cad (Blue). PDF neurons were stained with anti-pdf show in red. (B) Dilp8-induced developmental delay in puparium formation is enhances in the presences of *pdf* null mutant background (*tub-dilp8/+; pdf01/pdf01*). Data are pooled from three independent experiments, and each data point is mean \pm SD. (C-D) The increment in developmental delay induces by Dilp8 in *pdf* null mutant background increased the final body size. ≥ 30 larvae per genotype were scored. *** $p < 0.001$ (Two-tailed unpaired *t* test). (E) Transcriptional levels of *Eip75B* an ecdysone signaling target gen. (F) Rescue of developmental delay produces by Dilp8 with ecdysone treatment (20-hydroxyecdysone). The graph shows data pooled from three independent experiments, and each data point is mean \pm SD. A total of 60 pupae were scored per genotype in B and F. * $p < 0.05$ (Two-tailed unpaired *t* test). (G) Transcriptional levels of *Kr-h1* a target gene of juvenile hormone signaling. Data are mean \pm SD (n = 3 repeats). * $p < 0.05$ (Two-tailed unpaired *t* test). For quantitative RT-PCR, mRNA was isolated from 10 larvae for each genotype at the different hours AEL indicating in the plot for E and G.

It has been shown that Dilp8-Lgr3 interaction mediates a homeostatic growth control, coupling developmental timing with slow growth rate of the undamaged parts of the body and thus, maintaining the correct final body size (Vallejo et al. 2015). In this new paradigm, where *dilp8* is overexpressed in a *pdf* null mutant background, the body size is increased and uncouple from the growth control program. Interestingly, this phenotype is shared with *ptth* null mutants and in animals with inactivated PTH neurons (*ptth>kir2.1*) (McBrayer et al. 2007; Vallejo et al. 2015). Moreover, this extra-developmental timing delay produced by overexpression of *tub-dilp8* in a *pdf* null mutant background is prolonged by increased repression of ecdysone production (**Figure 18. E**). Consistently with these results, feeding larvae with the active form of ecdysone, 20E ecdysone, rescues the developmental timing produced by *dilp8* overexpression, as reported in Garelli et al. 2012, as well as the extra-delay produces by *dilp8* overexpression in a *pdf* null mutant background (**Figure 18. F**). Moreover, the levels of juvenile hormone reflected by the *krüppel-homolog 1* (*kr-h1*) target gene are decreased in the presence of Dilp8, as we reported in (Vallejo et al. 2015), and continued being low in a *pdf* mutant background (**Figure 18. G**).

Overweight and starvation resistance produces by Dilp8-Lgr3 signalling is enhances in the *pdf* mutant background

I have shown that the overweight and starvation resistance phenotypes produced by Dilp8 are Lgr3 ``sync`` neuron-dependent. Moreover, these overweight and starvation resistance phenotypes are reflected in an increase in the levels of triglycerides during development where ecdysone levels are low. As a consequence, after pupal eclosion these major resources might increase the survival of the adult fly under starvation conditions. I attributed these features to low levels of ecdysone during the extended feeding period and delayed of developmental timing. I measured the adult body weight and starvation resistant in *dilp8*-overexpressing flies with the *pdf* mutant background where ecdysone titters are more delayed.

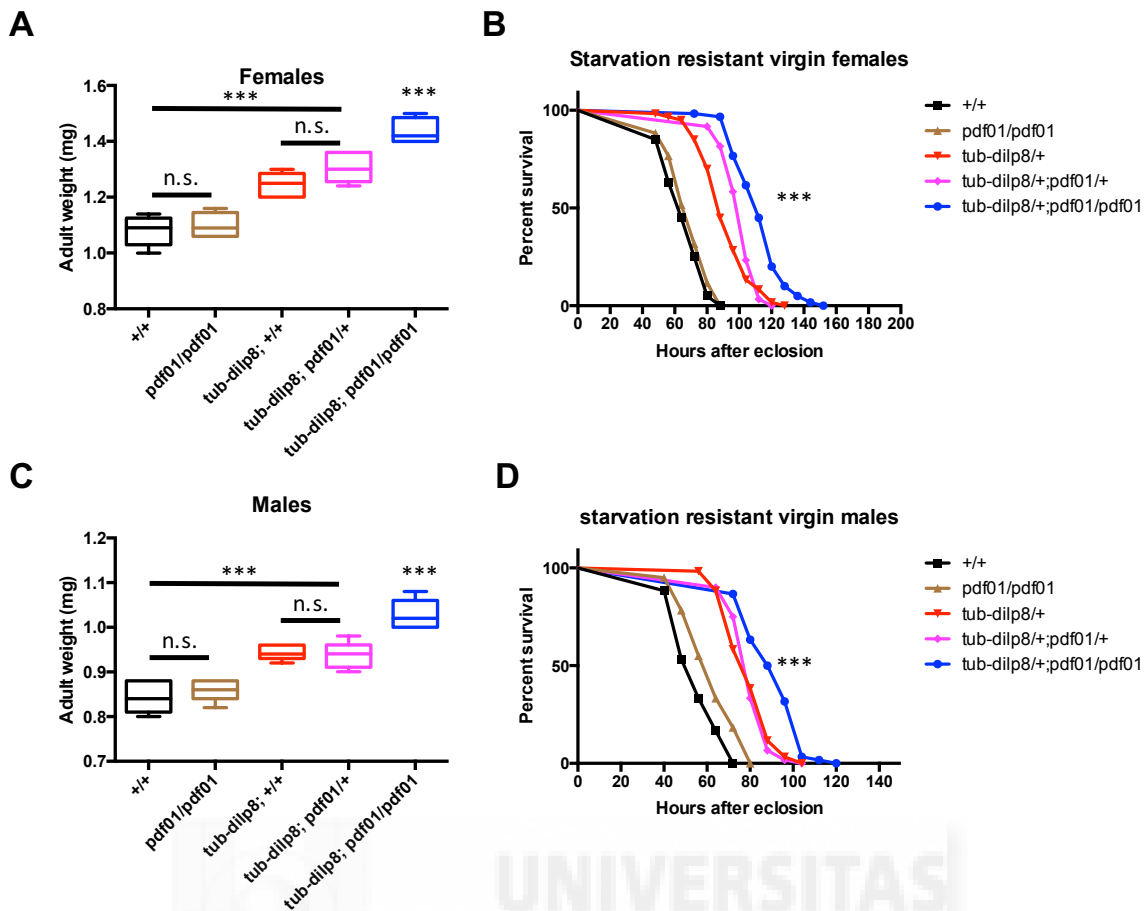


Figure 19: Enhance developmental delay of Dilp8 by *pdf* mutant increased the body weight impacting in starvation resistance. (A) Lack of *pdf* increase the body overweight produces by Dilp8 as a consequence for the extra developmental timing (*tub-dilp8; pdf01/pdf01*). *** $p < 0.001$; *n.s.* $p > 0.05$ (Two-tailed unpaired *t* test). Data are mean \pm SD. *n* = 30 age-synchronizes adult virgin females in each genotype. (B) Flies overexpressing *dilp8* in the lack of *pdf* neuropeptide (*tub-dilp8; pdf01/pdf01*) have more weight are more starvation resistant. A total of 60 flies per each genotype were scored per genotype. *** $p < 0.001$ (long-rank test). (C-D) The same phenotype (more overweight and more starvation resistance) is recapitulated in flies that overexpress *dilp8* in the absent of *pdf* in adult virgin males. *** $p < 0.001$; ** $p < 0.01$; *n.s.* $p > 0.05$ (Two-tailed unpaired *t* test) and data are mean \pm SD. *n* = 25 age-synchronizes adult virgin females in each genotype for weight experiment for C. The graph shows data pooled from four independent experiments, and each data point represents the flies that died at the specified hour after eclosion from the pupa. A total of 60 flies per each genotype were scored per genotype. *** $p < 0.001$ (long-rank test) for D.

pdf null mutant female and male flies overexpressing *dilp8* are heavier compare to flies that overexpress *dilp8* alone (Figure 19. A and C). As I expected, these female and male flies that overexpress *dilp8* in a *pdf* mutant background are more starvation resistance compare to flies that only overexpress *dilp8* (Figure 19. B and D).

The extra developmental timing delay produces by *pdf* mutant with Dilp8-Lgr3 signaling during development systemically increased lipogenesis.

As I have previously demonstrated, Dilp8-Lgr3 interaction extended the developmental timing program with an extension of the feeding period, increasing the levels of *Acc*, *Ascl*, and *bgm* lipogenic genes (Figure 15). In the context of *dilp8* overexpressing flies in *pdf* null mutant background I measured the transcriptional levels of lipogenic genes, because they are more time in feeding period and possibly maintain lipogenesis actively.

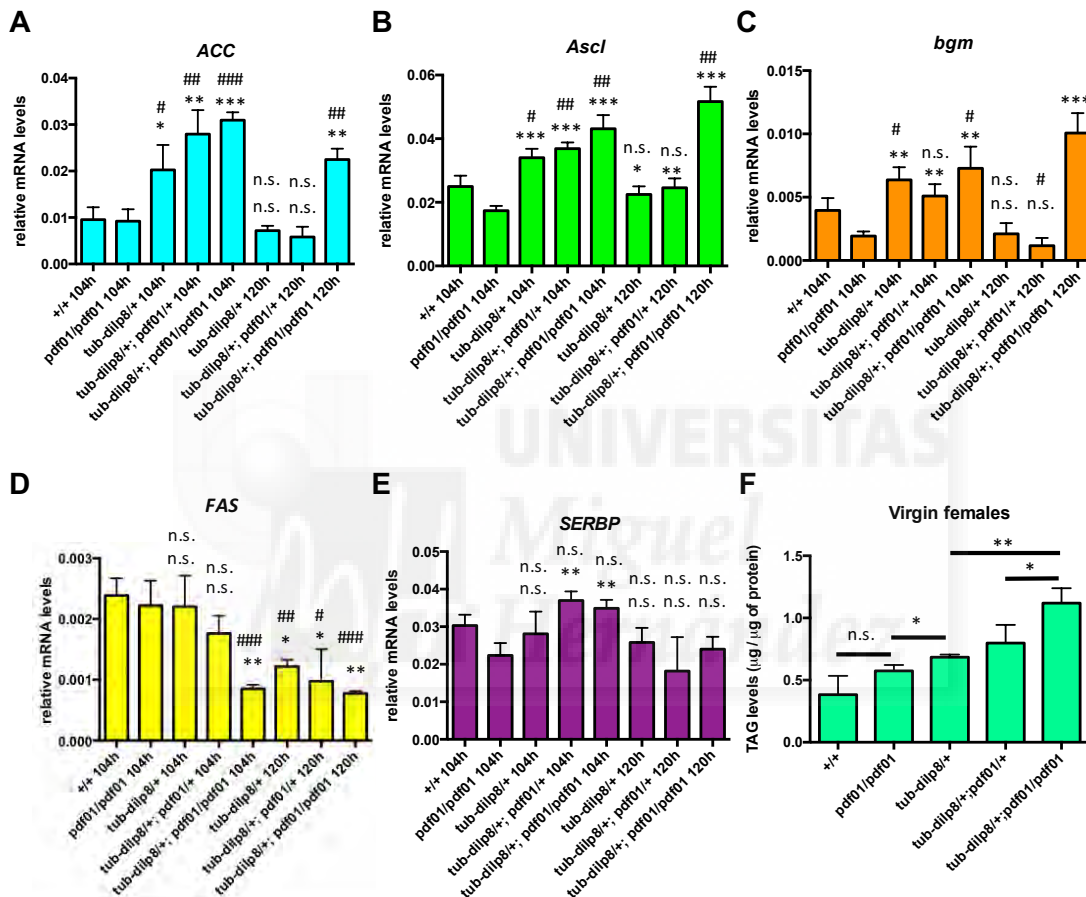


Figure 20: The interaction of Lgr3 `sync` and PDF neurons increased the lipogenesis during developmental delay to increased triglycerides in adult virgin flies. (A to E) Expression levels of five lipogenic genes, *ACC*, *Ascl*, *bgm*, *FAS*, and *SREBP* analyzed by qRT-PCR in mRNA isolated from 10 larvae for each genotype at 104 and 120 hours AEL. Overexpression of *dilp8* systemically synergizes with PDF neurons to maintain the increment in the transcript of *ACC*, *Ascl*, and *bgm*, but not for *FAS* and *SREBP* during the feeding period in the extra developmental delay. Data are mean \pm SD (n = 3 repeats). ### $p < 0.001$; ## $p < 0.01$; # $p < 0.05$; n.s. $p > 0.05$ (Two-tailed unpaired *t* test) for analysis with +/+ as a control. *** $p < 0.001$; ** $p < 0.01$; * $p < 0.05$; n.s. $p > 0.05$ (Two-tailed unpaired *t* test) for analysis with *pdf01/pdf01* as a control. (D) Quantification of total triglycerides acids (TAGs) normalize to protein show that overexpression of *dilp8* systemically in the absent of *pdf* (*tub-dilp8/+; pdf01/pdf01*) enhances the total levels of TAGs in adult virgin females compared to flies that only overexpress *dilp8* during development (*tub-dilp8/+*). Data are mean \pm SD (n = 3 repeats). ** $p < 0.01$; * $p < 0.05$ (Two-tailed unpaired *t* test).

Acc, *Ascl*, and *bgm* lipogenic genes (Figure 20 A-C) are up-regulated in the larva flies at 120 hours A.E.L. (*tub-dilp8/+; pdf01/pdf01*), where the controls have pupa. These results are a

consequences of the maintenance of foreging stages, where the larvae eating continuously and they present low ecdysone levels, promoting accumulation of stores (*tub-dilp8/+; pdf01/pdf01*) (**Figure 18**). Not-surprisingly, *FAS*, and *SREBP* do not change accordingly with previous results (**Figures 20. D-E**). Furthermore, this up-regulation of lipogenic genes led to an increase of TAGs levels in virgin adult flies eclosed from those pupa (*tub-dilp8/+; pdf01/pdf01*) (**Figure 20. F**) compare to wild type flies and flies that overexpress *dilp8*. ted at this time, and this lipogenic levels are showed at 104 hours A.E.L.

PDF neurons are regulated by neuronal activity to regulated developmental timing as PTTH neurons.

To molecularly define the role of PDF neurons and the neuropeptide PDF in the homeostatic growth control mediated by Dilp8-Lgr3 signalling, I measured by quantitative RT-qPCR the mRNA levels of *pdf* in i) the *dilp8*-overexpressing flies and ii) in the absence of *lgr3* in "sync" neurons (**Figure 21. A**). I did not find any significant change on the *pdf* mRNA levels, indicating that most likely the effect on the PDF neuropeptide produced by Dilp8-lgr3 is through neuronal activity, as in the case for PTTH neurons (Vallejo et al. 2015). To demonstrate that, we hyperpolarized PDF neurons by over-expressing a potassium ion channel *mKir2.1* that inhibited the electrical activation of those neurons. The electrical inactivation by hyperpolarization of PDF neurons demonstrated the intrinsic capability to induce developmental delay of the pacemaker neurons (**Figure 21. B**) by reducing the ecdysone synthesis in the PG (**Figure 21. C**). This phenotype was followed by an increase in the final body size (**Figure 21. D**) and an increase of the adult body weight in females and males (**Figure 21. E and F**). These phenotypes are commonly attributed to the PTTH neuropeptide and PDF has been postulated to be a negative regulator of PTTH (McBrayer et al. 2007). In this scenario we can postulate that PDF neurons regulate positively PTTH neurons to regulate developmental timing.

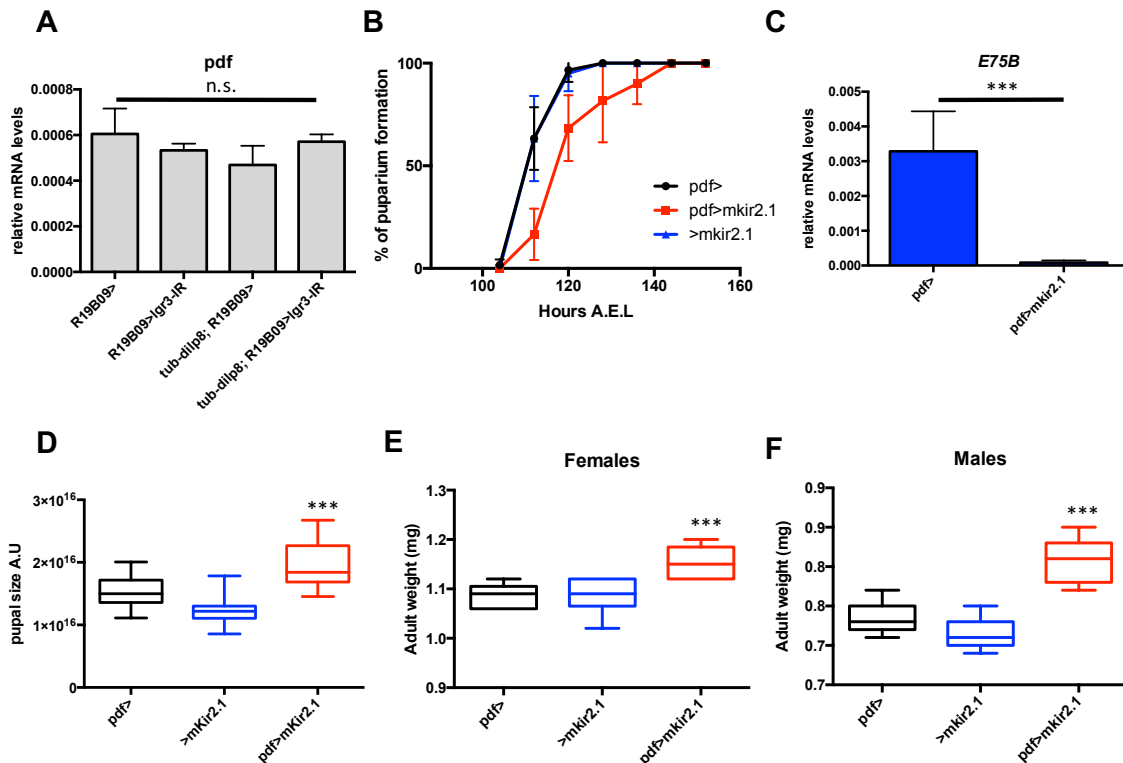


Figure 21: Inhibition of PDF neurons generate developmental timing delay. (A) Expression levels of *pdf* in a *dilp8*-overexpression context do not show any change in the transcriptional level. Analyzed by qRT-PCR in mRNA isolated from 10 larvae for each genotype at 100 hours AEL. n.s. $p > 0.05$ (Two-tailed unpaired *t* test). (B) Inhibition of PDF neurons excitation by overexpression of *mKir2.1* ion channel generates a developmental delay similar to overexpression of *dilp8* or absent of PTH neuropeptide. Data are pooled from three independent experiments, and each data point is mean \pm SD. Approximately 60 pupae were scored per genotype. (C) Transcriptional levels of *Eip75B* in the developmental delay induces by neuronal inhibition of PDF neurons inhibit ecdysone titers. *** $p < 0.001$ (Two-tailed unpaired *t* test). The qRT-PCR in mRNA isolated from 10 larvae for each genotype at 96 hours AEL. (D) The increment in developmental delay of PDF neuronal inactivation generates bigger body size such as *pth* mutant. ≥ 35 larvae per genotype were scored. *** $p < 0.001$ (Two-tailed unpaired *t* test). (E-F) PDF inhibition increases body weight in virgin adult females and males. *** $p < 0.001$ (Two-tailed unpaired *t* test). Data are mean \pm SD. $n = 30$ age-synchronizes adult virgin females in each genotype and 25 age-synchronizes adult virgin males.

PTTH are regulated by PDF neuropeptide in the presence of Dilp8-Lgr3 interaction.

Previous works have indirectly shown the functional interaction between PDF and PTH neurons (Gong et al. 2010; Yamanaka, Romero, et al. 2013). Now, to detect direct connections between PDF- and PTH neurons, we used GRASP (GFP reconstitution across synaptic partners) analysis, that is based on the expression of two nonfluorescent split-GFP fragments (spGFP1-10 and spGFP11) tethered to the membrane in two neuronal populations (Feinberg et al. 2008) (**Figure 22. A**)

Although it has been genetically demonstrated that PDF is a ligand for the PDF receptor (PDFR), the specific expression pattern for PDFR in larval brains still remains controversial (Hyun et al. 2005). Furthermore, the expression of PDFR has not been shown in PTTH neurons, although a recent work has shown a functional role for PDFR in PTTH neurons (Selcho et al. 2017). Meanwhile, the direct interaction between PDF neurons and PTTH neurons is better established.

Thus, I wondered if the role of PDF in the context of *dilp8*-overexpression is mediated by PDFR in the PTTH neurons. To address this question, I overexpressed *dilp8* in PTTH neurons in a *pdfr* mutant background. I mimicked the same phenotype as in *pdf* mutant background. The developmental delay induced by Dilp8 is enhanced by the lack of *pdfr* in PTTH neurons (*tub-dilp8; ptth > pdfrIR*) (**Figure 22. B**). As I expected, the increase in developmental timing delay results in an increase in the final body size (**Figure 22. C and D**) due to the low levels of ecdysone production, and the extended developmental timing program and feeding behavior (**Figure 22. E**). Feeding larvae with ecdysone rescues the developmental timing phenotype (*tub-dilp8; ptth > pdfrIR*) (**Figure 22. F**). Non-surprisingly, the levels of juvenile hormone are downregulated, reflected by the *krüppel-homolog 1* target gene, like in the *pdf* null mutant (**Figure 22. G**)



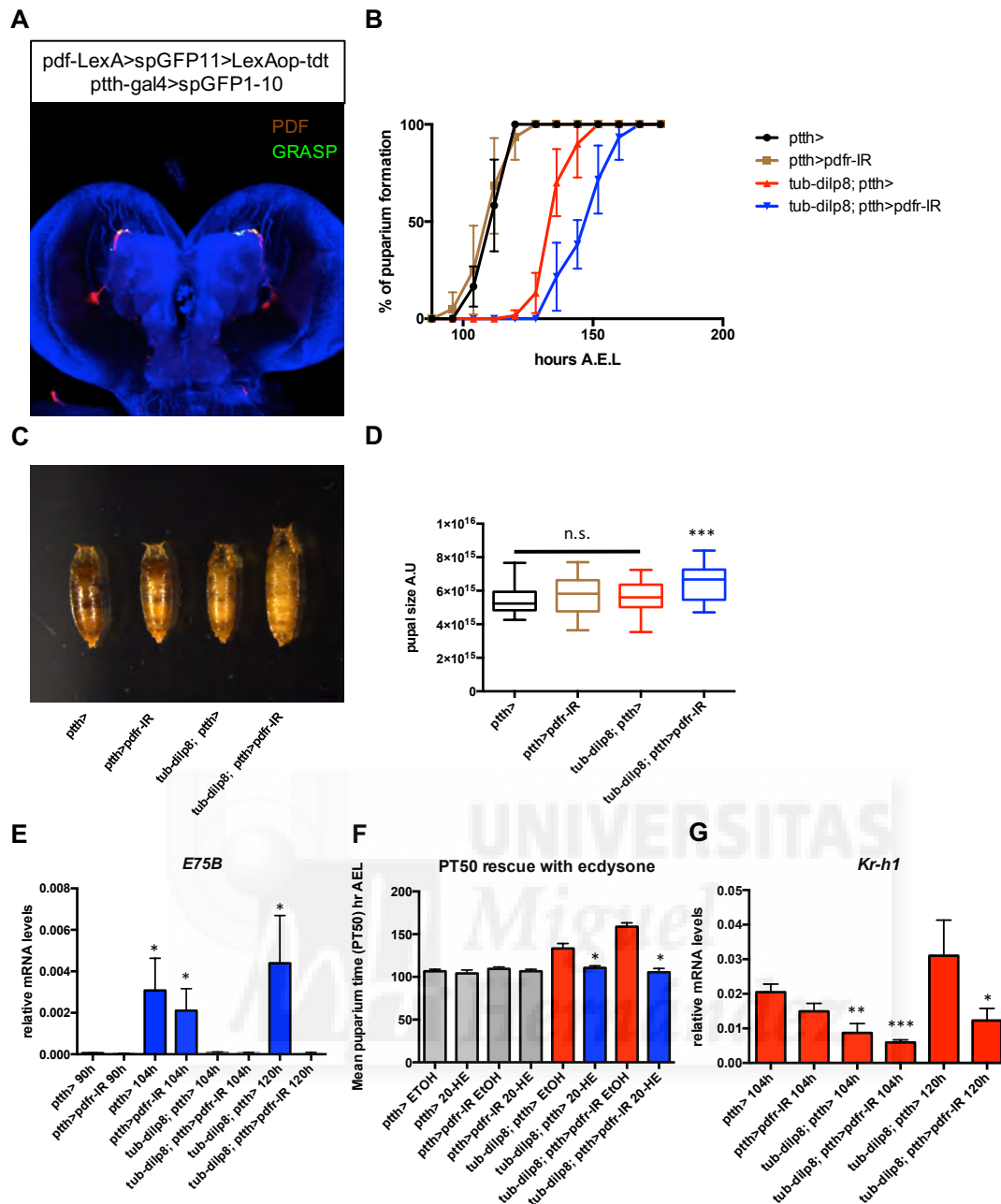


Figure 22: PTH mediates through PDFR the action of PDF neuropeptide in the presence of Dilp8. (A) Positive signals of GRASP in green revealed connections between PDF neurons (*pdf-LexA>spGFP₁₁*) and PTTH neurons (*ptth-Gal4>spGFP₁₋₁₀*). Brains were counterstained with anti-DE-Cad (Blue). PDF neurons is show in red (*>LexAop-tdt*). (B) Dilp8-induced developmental delay in puparium formation is enhances in the absent of *pdfr* in the PTTH neurons (*tub-dilp8; ptth> pdfr-IR*). Data are pooled from three independent experiments, and each data point is mean \pm SD. Approximately 60 pupae were scored per genotype. (C-D) The increment in developmental delay of Dilp8 by absent of *pdfr* in PTTH neurons increased the final body size (*tub-dilp8; ptth> pdfr-IR*). ≥ 30 larvae per genotype were scored. $***p < 0.001$ (Two-tailed unpaired *t* test). (E) Transcriptional levels of *Eip75B*, a target gen of ecdysone production. (F) Rescue of developmental delay by ecdysone treatment (20-hydroxyecdysone). The graph shows data pooled from three independent experiments, and each data point is mean \pm SD. A total of 60 pupae were scored per genotype. $*p < 0.05$ (Two-tailed unpaired *t* test). (G) Transcriptional levels of *Kr-h1*, a target gen of juvenile hormone production. Data are mean \pm SD (n = 3 repeats). $***p < 0.001$; $**p < 0.01$; $*p < 0.05$ (Two-tailed unpaired *t* test). The qRT-PCR in mRNA isolated from 10 larvae for each genotype at the different hours AEL indicating in the plot for D and G.

Lacking *pdf* in the PTTH neurons in the presence of Dilp8 enhances the overweight and starvation resistance produces by Dilp8.

Up to this point, I have shown that *pdf* mutant flies are heavier and have an increased starvation resistance response compared to *dilp8*-overexpressing flies and wild type controls (**Figure 19**). To measure the impact of the extra-time induced by Dilp8 and the control by PDFR in the PTTH neurons during development, I weighted adult virgin flies and I measured the starvation resistance.

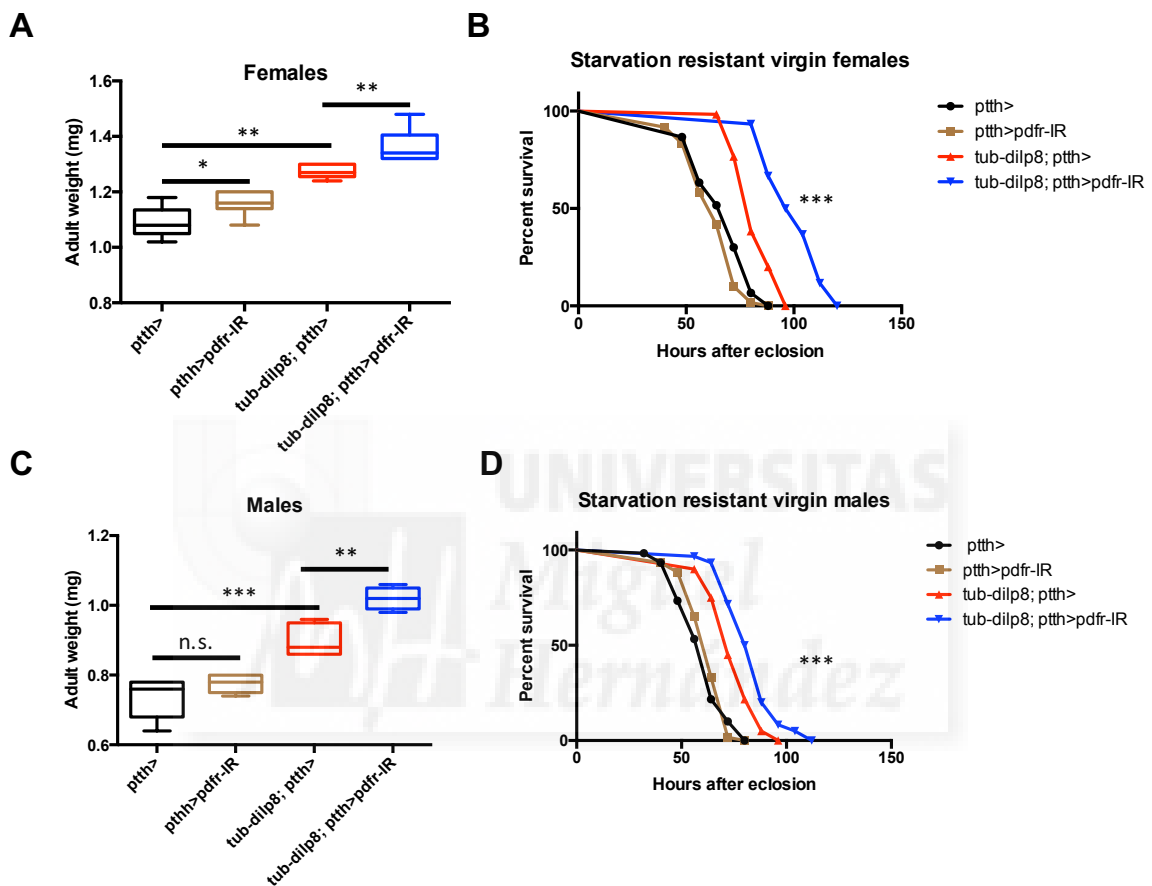


Figure 23: Enhanced developmental delay of Dilp8 by *pdf* depletion in PTTH neurons increased the body weight with impact in starvation resistance. (A) Lack of *pdf* increase the body overweight produces by Dilp8 as a consequence for the extra developmental timing (*tub-dilp8; ptth>pdfr-IR*). *** $p < 0.001$; ** $p < 0.01$; * $p < 0.05$ (Two-tailed unpaired *t* test). Data are mean \pm SD. $n = 30$ age-synchronizes adult virgin females in each genotype. (B) The flies overexpressing *dilp8* in the lack of *pdf* (*tub-dilp8; ptth>pdfr-IR*) have more weight and more starvation resistant in comparison with flies that only express *dilp8* (*tub-dilp8; ptth>*). A total of 60 flies per each genotype were scored per genotype. *** $p < 0.001$ (long-rank test). (C-D) The same phenotype (more overweight and more starvation resistance) is recapitulated in flies that overexpress *dilp8* in the absence of *pdf* in adult virgin males. *** $p < 0.001$; ** $p < 0.01$; n.s. $p > 0.05$ (Two-tailed unpaired *t* test) and data are mean \pm SD. $n = 25$ age-synchronizes adult virgin females in each genotype for weight experiment for C. The graph shows data pooled from four independent experiments, and each data point is the number of dead flies at that hour after eclosion from the pupa. A total of 60 flies were scored per genotype. *** $p < 0.001$ (long-rank test) for D.

These virgin flies that overexpress *dilp8* in the lack of *pdf* in PTTH neurons during development show an increment of the adult weight (**Figure 23. A and C**), as a consequence of the

extended feeding period. This extra-weight is accompanied by a stronger starvation resistant response in virgin female and male flies (*tub-dilp8; ptth>pdfr-IR*) compared to the controls (**Figure 23. B and D**).

The extra developmental timing delay produce by the lack of PDFR in combination with Dilp8-Lgr3 signaling during development increased systemically lipogénesis.

As I demonstrated, the extended feeding period generated an up-regulation of lipogenic genes followed by a higher accumulation of triglycerides in virgin flies (**Figure 15**). I wondered if the extra-timing of the feeding period induced by overexpression of *dilp8* and the lack of *pdfr* in the PTTH neurons mimicked the phenotype induced by the lack of *pdf* using a *pdf* null mutant and the overexpression of *dilp8*, maintaining up-regulation of lipogenic genes and accumulation of TAGs to generate heavier flies and bigger sizes (**Figure 20**).

To measure the impact of the extra-time induced by Dilp8 and the control by PDFR in the PTTH neurons during development in lipogénesis, I quantify by qRT-PCR the lipogenic genes in foreaging stages larvae. *Acc*, *Ascl*, and *bgm* lipogenic genes (**Figure 24 A-C**) are up-regulated in the larva flies at 120 hours A.E.L. (*tub-dilp8; ptth>pdfr-IR*), where the controls have pupated at this time, and this lipogenic levels are showed at 104 hours A.E.L., as in the *tub-dilp8/+; pdf01/pdf01* context. Not-surprisingly, as in the *tub-dilp8/+; pdf01/pdf01* condition, *FAS* and *SREBP* do not change accordingly with previous results (**Figures 24. D-E**). Furthermore, this up-regulation of lipogenic genes led to an increase of TAGs levels in virgin adult flies eclosed from those pupa (*tub-dilp8; ptth>pdfr-IR*) (**Figure 24. F**) compare to wild type flies and flies that overexpress *dilp8*.

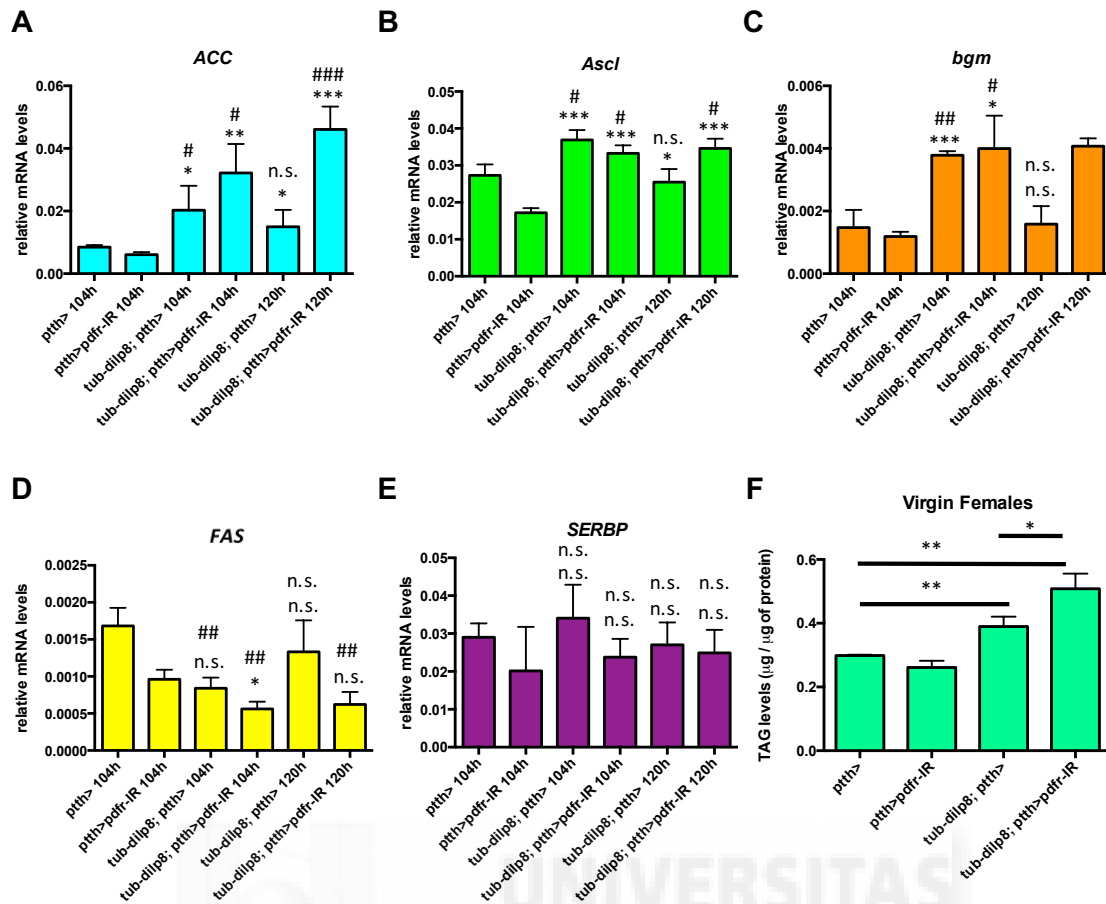


Figure 24: The loss of function of *pdfr* in PTTH neurons increased the lipogenesis during developmental delay and increased TAG in adult virgin flies in a *dilp8*-overexpression background. (A to E) Expression levels of five lipogenesis genes, *ACC*, *Ascl*, *bgm*, *fas*, and *SREBP* analyzed by qRT-PCR in mRNA isolated from 10 larvae for each genotype at 104 hours AEL and 120 hours AEL. Overexpression of *dilp8* systemically synergizes with the absence of *pdfr* in PTTH neurons to maintain the increment in the transcript levels of *ACC*, *Ascl*, and *bgm*, but not for *FAS* and *SREBP* during the feeding period in the extra developmental delay. Data are mean \pm SD (n = 3 repeats). ### $p < 0.001$; ## $p < 0.01$; # $p < 0.05$; n.s. $p > 0.05$ (Two-tailed unpaired *t* test) for analysis with *ptth>* as a control. *** $p < 0.001$; ** $p < 0.01$; * $p < 0.05$; n.s. $p > 0.05$ (Two-tailed unpaired *t* test) for analysis with *ptth>pdfr-IR* as a control. (D) Quantification of total triglycerides (TAGs) normalized to protein show that overexpression of *dilp8* combined with lack of *pdfr* in the PTTH neurons (*tub-dilp8; ptth>pdfr-IR*) enhances the total levels of TAGs in adult virgin females compared to flies that only overexpress *dilp8* during development (*tub-dilp8; ptth>*). Data are mean \pm SD (n = 3 repeats). ** $p < 0.01$; * $p < 0.05$ (Two-tailed unpaired *t* test).

Insulin signalling is decreased in *pdfr* depletion in PTTH neurons in the context of *dilp8*-overexpression.

Dilp8 induces a homeostatic growth control regulating the developmental timing program, by inhibition of PTTH release and slow growth of the undamaged organs by reduction of insulin signaling in the IPCs (Vallejo et al. 2015). As a follow up question, I wondered if the loss of growth compensation induced by the *dilp8*-overexpression in a *pdf* null mutant background (or by knocking-down *pdfr* in the PTTH neurons) was caused by uncoupling the insulin signaling and the developmental timing program.

The transcriptional levels of the three *Drosophila* insulin-like peptides expressed in IPCs showed that *dilp3* is reduced in the context of a *dilp8*-overexpression and lack of *pdfr* in PTTH neurons during the extra feeding period (**Figure 25. A**), but *dilp5* and *dilp2* did not show any significant decrease in a *dilp8* overexpression context (**Figure 25. B-C**).

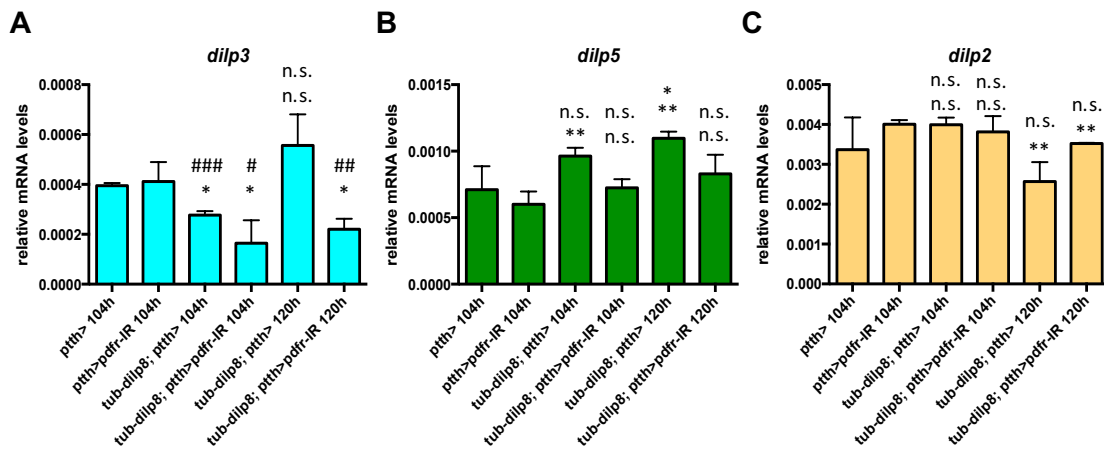
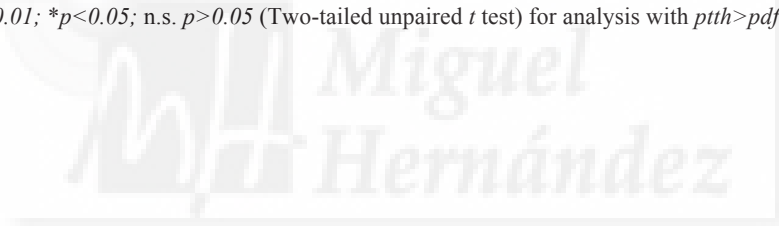
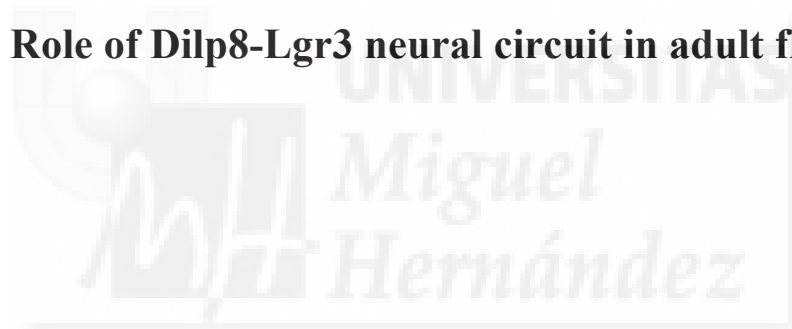


Figure 25: Loss of function of PDFR in PTTH neurons decreased insulin signaling in a *dilp8*-overexpression background. (A to E) Expression levels of the three insulin like-peptides in *Drosophila* expressed in IPCs, *dilp3*, *dilp5*, and *dilp2* analyzed by qRT-PCR in mRNA isolated from 10 larvae for each genotype at 104 hours AEL and 120 hours AEL. Overexpression of *dilp8* systemically synergizes with the absence of *pdfr* in PTTH neurons to decreased the transcriptional levels of *dilp3*, but not *dilp5* and *dilp2* during the feeding period in the extra developmental delay. Data are mean \pm SD (n = 3 repeats). ### $p < 0.001$; ## $p < 0.01$; # $p < 0.05$; n.s. $p > 0.05$ (Two-tailed unpaired *t* test) for analysis with *ptth>* as a control. ** $p < 0.01$; * $p < 0.05$; n.s. $p > 0.05$ (Two-tailed unpaired *t* test) for analysis with *ptth>pdfr-IR* as a control.



Part. III

Role of Dilp8-Lgr3 neural circuit in adult flies





dilp8 is expressed in mature oocytes in virgin females

dilp8 is expressed in the female reproductive tissues but not in males (Garelli et al. 2012). Using quantitative RT-PCR I measured the mRNA levels of *dilp8* in oocytes of virgin female flies to describe the temporal expression pattern of *dilp8* in adult female flies. mRNA levels of *dilp8* start to increase in virgin females two days after eclosion from the pupa, reaching the maximum level in the fourth day (Figure 26. A).

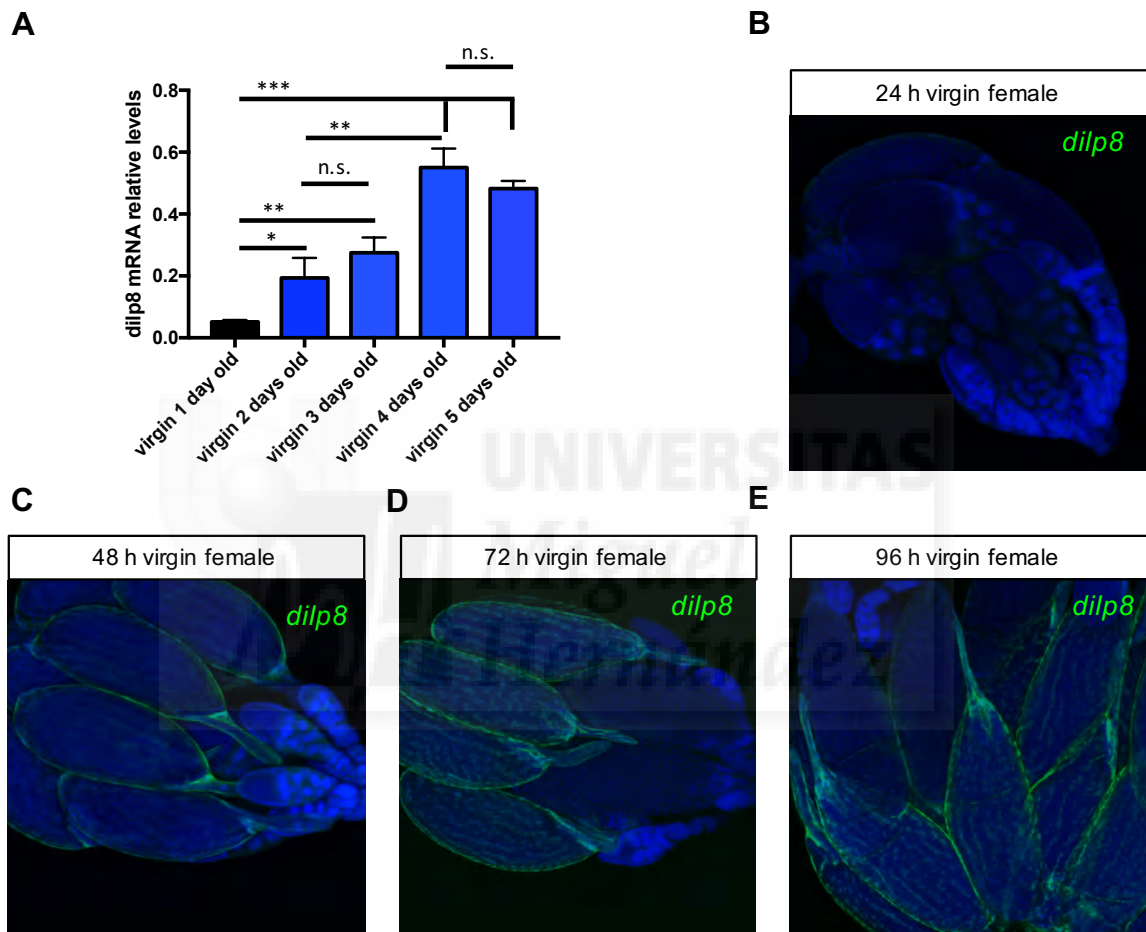


Figure 26: Temporal expression pattern of *dilp8* in oocytes in virgin females. (A) Transcriptional expression levels of *dilp8* in oocytes at different days measured by real time q-PCR in w^{1118} background. mRNA isolated from 7 virgin female flies. *** $p < 0.001$; ** $p < 0.01$; * $p < 0.05$; n.s. $p > 0.05$ (Two-tailed unpaired t test). (B-E) Immunostaining of oocytes in $dilp8^{M100727}$ virgin female flies that express GFP under *dilp8* promoter. Oocytes were counterstained with DAPI (Blue).

To corroborate these RT-qPCR results, I carried out immunostaining in the $dilp8^{M100727}$ mutant (Garelli et al. 2012) that expresses a GFP reporter gene under the *dilp8* promoter. I show how within the first 24 hours *dilp8* is not expressed in oocytes (Figure 26. B), but at 48 hours the mature oocytes appear and expression of *dilp8* starts (Figure 26. C). Interestingly, after 48 hours the levels of *dilp8* increase (Figure 26. A), due to an increase in the number of mature oocytes (Figure 26. D and E).

Insulin signaling in adult female flies is controlled by Dilp8-Lgr3 interaction.

As we have shown previously, Dilp8 binds to Lgr3 receptor in the "sync" neurons in the brain during development to mediate the homeostatic growth control and maturation during development upon damage conditions of imaginal discs (Vallejo et al. 2015). These Lgr3 "sync" neurons have as outputs the control of PTH release as an output to control developmental timing, and insulins and juvenile hormone to control growth during the repaired period of injured organs (Vallejo et al. 2015). Like Dilp8, Lgr3 relaxin receptor has a sexual dimorphism regarding the expression pattern in adult flies mediated by Fruitless and Doublesex transcription factors at their promoter genes in the *lgr3* locus (Meissner et al. 2016).

During development *R19B09-Gal4* line defines molecularly the neurons that respond to Dilp8 via Lgr3. They are two pair of neurons in the *par intercerebralis* of the larval brain of *Drosophila melanogaster* (Vallejo et al. 2015; Garelli et al. 2015; Colombani et al. 2015). Moreover, in the *R19B09-Gal4* line has a Doublesex binding sites to control the transcriptional expression of *lgr3* receptor in adult females, but not in males. In the *par intercerebralis* the axons of Lgr3 cells project to the dorsal part of the adult female brain where the IPCs are positioned in adult brains of *Drosophila* (Meissner et al. 2016).

Moreover, *dilp8* is not expressed in adult male flies, but the different *Gal4* lines for *lgr3* locus have expression in neurons in adult females and males regulated by Fruitless in the abdominal ganglia, and also by Doublesex in female flies (Meissner et al. 2016). That indicates the possibility about of other molecules working as a ligand for Lgr3 receptor.

Following Dilp8-Lgr3 interaction during development and the transcriptional control of *dilp3* and *dilp5* in the IPCs, and the location of Lgr3 neurons defined by *R19B09-Gal4* line in the adult females in close proximity to the IPCs, I wondered whether Dilp8 from the female oocytes can interact with its Lgr3 receptor and can control insulin signalling in the adult female. To address this hypothesis, Javier Morante and myself first carried out GRASP analysis in adult female flies. We used *R19B09-LexA* to drive expression of *LexAop-spGFP11* and *dilp3-Gal4* to drive expression of *UASspGFP1-10* in IPCs neurons, respectively. GRASP signals suggested possible connections between Lgr3 neurons and IPCs (**Figure 27. A**). Second, as *dilp8* is expressed in mature oocytes, *lgr3* was knocked-down temporally using *R19B09-Gal4* line and *tub-Gal80^{ts}* in 4 days old adult flies. I analyzed transcriptional expression levels of the different insulin-like peptides by RTq-PCR in this previous condition described to study the Dilp8-Lgr3 interaction in adult females. *dilp5* and *dilp2* genes are upregulated but *dilp3* remain unchanged in adult females, pointing to the relevant control of insulin signalling by Dilp8/Lgr3 axis in adult females (**Figure 27. B**). The changes in the

transcriptional levels of *dilp2* and *dilp5* are female-specific, because males in the same genetic condition do not change the *insulin like-peptides* transcript levels (**Figure 27. C**).

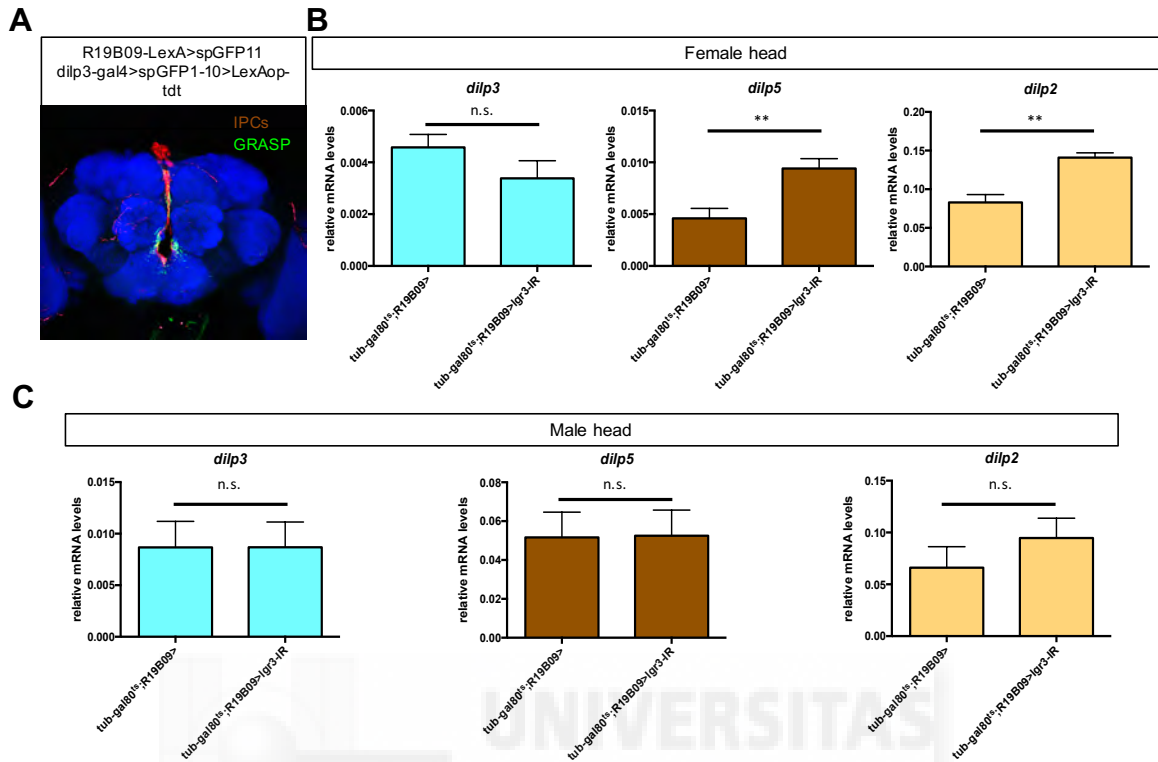


Figure 27: Insulin signalling control in the adult *Drosophila* female by Dilp8-Lgr3 interaction. (A) Positive signals of GRASP in green revealed connections between Lgr3 neurons (*R19B09-LexA>spGFP₁₁*) and IPCs (*dilp3-Gal4>spGFP₁₁*). Brains were counterstained with anti-DE-Cad (Blue). IPCs are shown in red (*>LexAop-tdt*). Expression levels of the three insulin like-peptides in *Drosophila* expressed in IPCs, *dilp3*, *dilp5*, and *dilp2* analyzed by qRT-PCR in mRNA isolated from 7 female heads (B), or 7 male heads (C), for each genotype at 4 days after mating. Data are mean \pm SD ($n = 3$ repeats). ** $p < 0.01$; n.s. $p > 0.05$ (Two-tailed unpaired t test).

Dilp8 does not control the receptivity behavior in female virgin flies.

Lgr3 neurons in adult flies have a sexual dimorphism in terms of expression pattern. Furthermore, *lgr3* expressing neurons in the abdominal ganglia in adult female flies were postulated to regulate receptivity behavior and egg laying in female flies (Meissner et al. 2016). Due to *dilp8* expression in mature oocytes and the binding of Dilp8 to the Lgr3 receptor, I wondered if *lgr3* played a role in mating behavior controlling female receptivity. I carried out these behavioral experiments in my intership at the Neurogenetics and Behavior lab of Leslie B. Vosshall at Rockefeller University (New York, USA) with Nilay Yapici, a postdoctoral researcher as a mentor.

First, if the Lgr3 activation in abdominal ganglia reduces female receptivity and decreases the number of egg laid, I expected to have the opposite phenotypes in the *dilp8* mutants. Courtship behavioral experiments were carried out with *dilp8*^{M100727} mutant female flies without detecting any phenotype in mating or receptivity response (**Figure 28. A**). Moreover, *dilp8* overexpression do not

show any problem in receptivity behavior contrary to previous results (Meissner et al. 2016) (**Figure 28. A**). Following the previous results, I expected to see high latency in *dilp8*^{M100727} mutants and low latency in flies that overexpressed *dilp8*. Interestingly, the latency remains unchanged in *dilp8*^{M100727} mutants and in *dilp8* gain of function female flies (**Figure 28. B**).

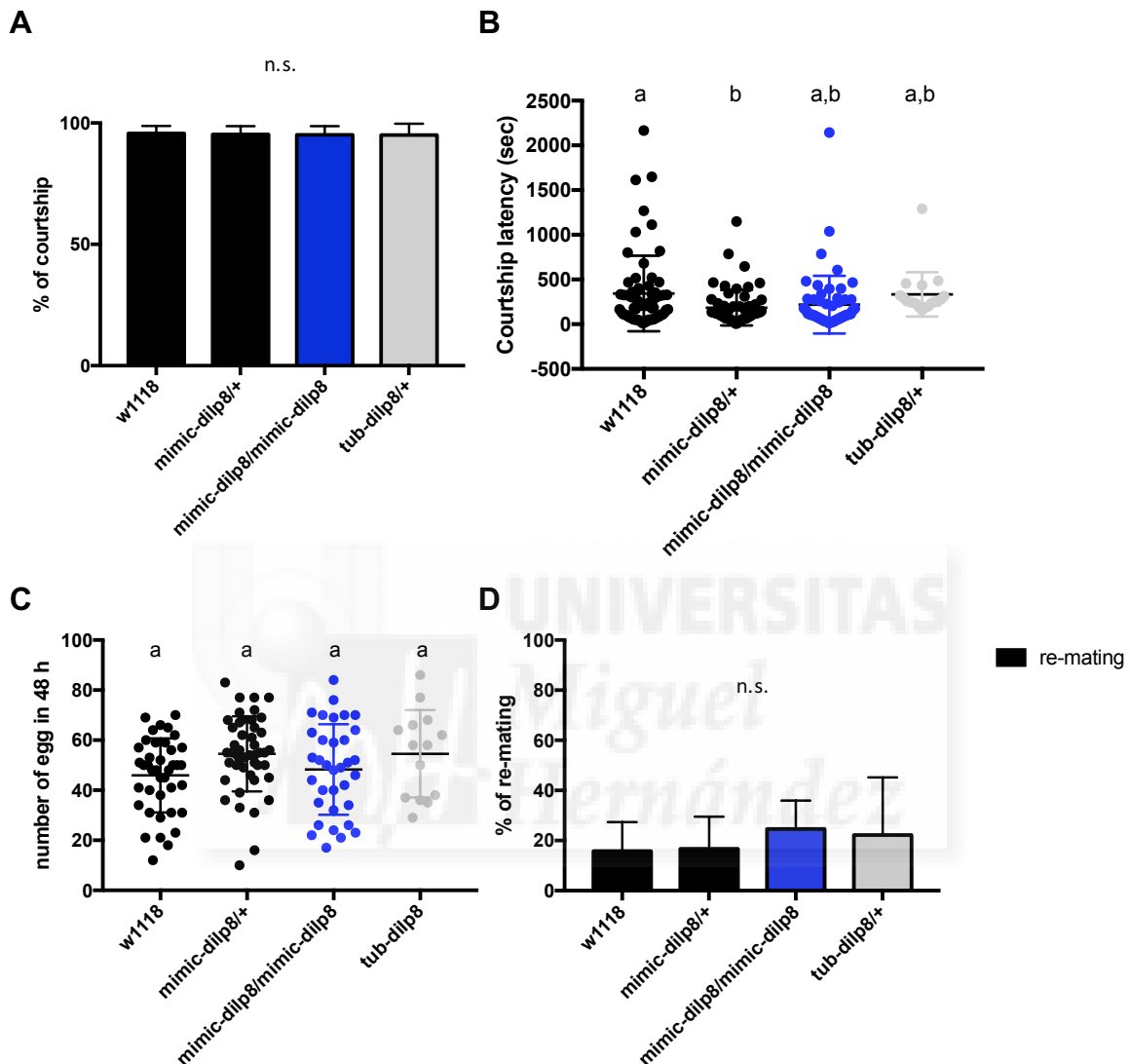


Figure 28: Dilp8 does not regulate female receptivity and remating. (A) Courtship behavior in *dilp8* loss of function and gain of function. Chi-square test, pairwise post hoc comparisons with Fisher's exact test with Bonferroni correction; population percentage and 95% confidence interval. *N.S* $p > 0,05$. (B) courtship latency (the time when the females are courted by the male) in *dilp8* loss of function and gain of function. One-way ANOVA, Tukey's multiple comparisons test. $p > 0,05$. Approximately 60 virgin flies 5 days old were scored per genotype. (C) Egg laying of females 48 hours after mating in *dilp8* loss of function and gain of function backgrounds. One-way ANOVA, Tukey's multiple comparisons test. $p > 0,05$. (D) Remating behavior of the flies that were mating in *dilp8* loss of function and gain of function after 48 hours of mating. Chi-square test, pairwise post hoc comparisons with Fisher's exact test with Bonferroni correction; population percentage and 95% confidence interval. *n.s* $P > 0,05$.

Furthermore, egg laying number remain unchanged in *dilp8*^{M100727} loss of function and *dilp8* gain of function conditions (**Figure 28. C**). Finally, Dilp8 could be involved in the remating female

behavior by the regulation of different Dilps. Indeed, *dilp2*, *dilp3*, and *dilp5* have been postulated to regulate remating behavior (Wigby et al. 2010). Taking in account my previous results showing that Dilp8-Lgr3 interaction regulates *dilp2* and *dilp5* expression in adult females (**Figure 28**), I show here that *dilp8* has not effect in remating behavior in mated female flies (**Figure 28. D**).

The receptivity behavior in female virgin flies is not controlled by Lgr3 receptor.

lgr3 expressing neurons in the abdominal ganglia in adult female flies were postulated to regulated receptivity behavior and egg laying in female flies (Meissner et al. 2016). Now, I have demonstrated that Dilp8 is not the ligand responsible for receptivity behavior regulation through Lgr3 receptor. Thus, I wondered if Lgr3 has a relevant role regulating receptivity behavior through other ligands. To address this question I have carried out courtship behavioral experiments in *lgr3* mutants (Colombani et al. 2015). I found normal courtship behavior in *lgr3* null mutants (**Figure 29. A**). Surprisingly, we did not see any reduced latency in *lgr3* null mutants as I expected given the results from Meissner et al. 2016 (**Figure 29. B**).

After that, I measured the number of egg layed by *lgr3* mutants. As *dilp8* loss of function, *lgr3* null mutant do not show any different in egg laying number (**Figure 29. C**). Moreover, I showed that Lgr3 neurons synaptically interact with IPCs (**Figure 27. A**), and they regulate *dilp2* and *dilp5* expression in adult females through Dilp8 (**Figure 27. B and C**). I show here that *lgr3* do not affect remating behavior in mated female flies (**Figure 29. D**).

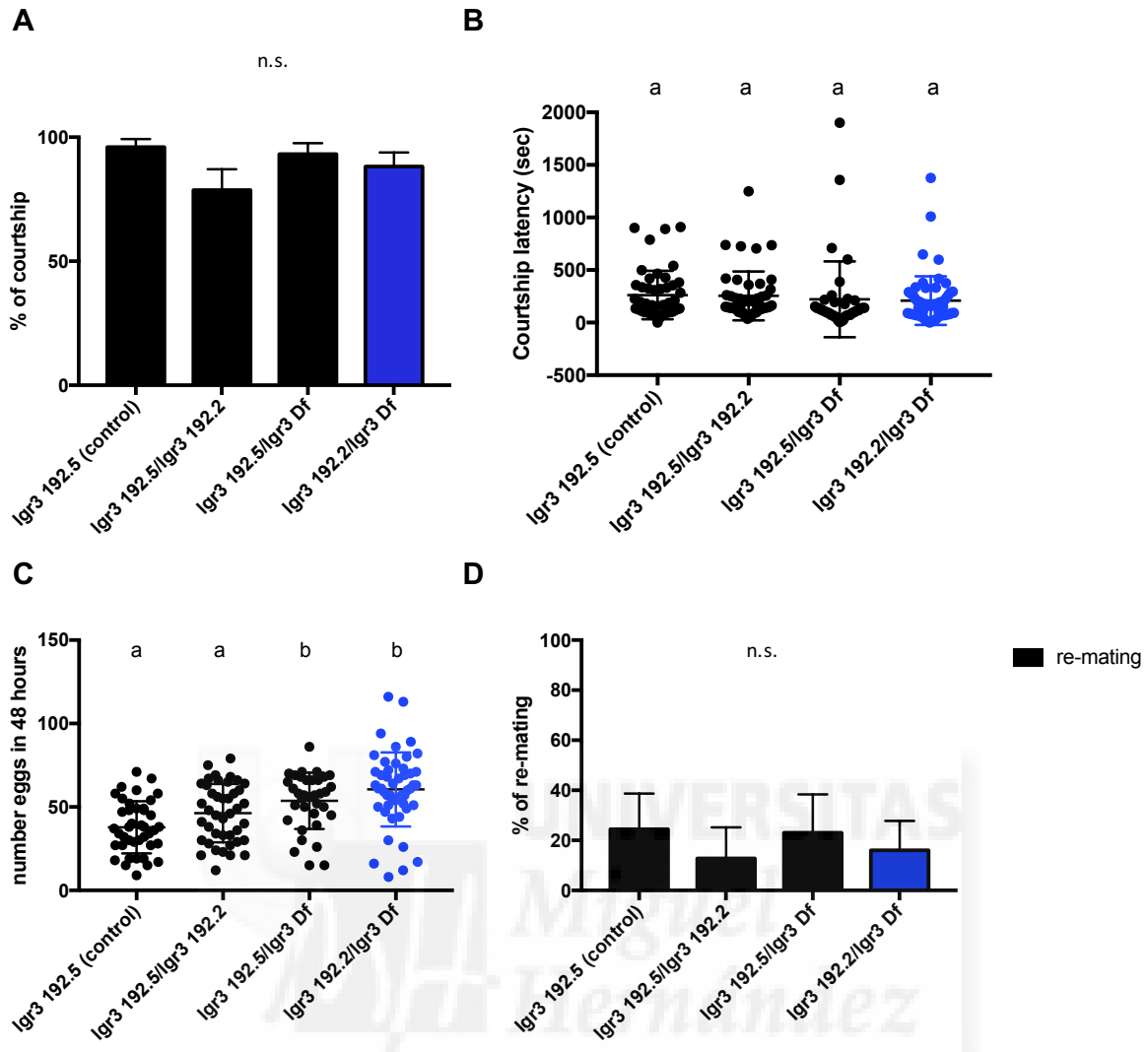
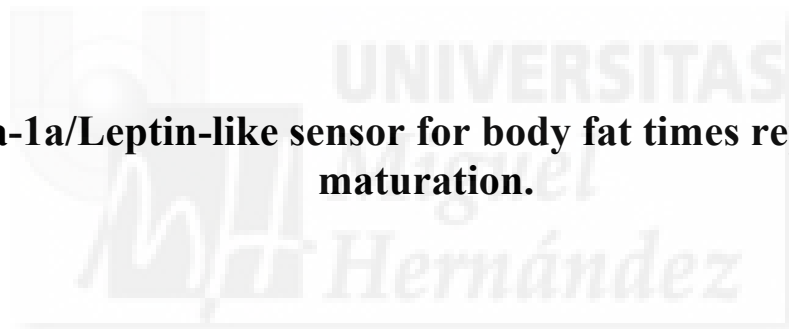


Figure 29: Female receptivity and remating is not regulated by *Lgr3*. (A) Courtship behavior in *lgr3* loss of function. Chi-square test, pairwise post hoc comparisons with Fisher's exact test with Bonferroni correction; population percentage and 95% confidence interval. *N.S* $p > 0,05$ (B) courtship latency (the time when the females are courted by the male) in *lgr3* loss of function. One-way ANOVA, Tukey's multiple comparisons test. $p > 0,05$. Approximately 60 virgin flies 5 days old were scored per genotype. (C) egg laying of females 48 hours after mating in *lgr3* loss of function. One-way ANOVA, Tukey's multiple comparisons test. $p > 0,05$. (D) Remating behavior of the flies that were mating in *lgr3* loss of function after 48 hours of mating. Chi-square test, pairwise post hoc comparisons with Fisher's exact test with Bonferroni correction; population percentage and 95% confidence interval. *n.s* $p > 0,05$.

Part. IV

A Sema-1a/Leptin-like sensor for body fat times reproductive maturation.





Prothoracic gland screen identifies *sema1a* as a new component in the developmental transition from larva to pupa

It is known that the onset and progression of puberty and sexual maturation is controlled by multiple permissive factors in all animals (Sisk & Foster 2004). It has been shown that the body weight and fat content in the juvenile body play a fundamental role to control the onset of puberty. Without this critical weight, animals cannot progress to the adult stages to become sexually mature and generate offspring. On the contrary, if a critical weight has been surpassed this can accelerate the onset of. This “critical weight” hypothesis was postulated by Frisch-Revelle (Frisch & Revelle 1970; F. E. Johnston et al. 1971; Crawford & Osler 1975; E. R. Baker 1985).

In humans, when the critical weight is achieved, the hypothalamic sensitivity to estrogens decreases and release of hormones controlled the hypothalamic (gonadotropin-releasing hormone: GnRH) and pituitary gland cells (Luteinizing hormone: LH ; follicle-stimulating hormone: FSH) promote the developmental transition to pubertal stages and production of steroids (E. R. Baker 1985). In *Drosophila*, the steroid hormone ecdysone is produced by the prothoracic gland (PG). PG in *Drosophila* has been postulated to sense the critical weight and to generate the decline of JH and switches the sensitivity of PG to other signals to promote ecdysone titers. The IIS pathway modulated, by nutritional cues, plays an important role in the switch and detection of the critical weight (Caldwell et al. 2005; Colombani et al. 2005; Mirth et al. 2005).

Although it is known that PG plays a crucial role in sensing when the critical weight is achieved, a sensor of fatness or fat signals needs to be identified to explain how this switch is controlled. For this reason, the Morante’s lab performed a screen using the *phm-Gal4* line, specifically expressed in the PG, to knock-down a RNAi library to find genes involved in critical weight sensing (**Figure 30. A**). The predicted genes to be found should be lethal and cause developmental arrest in larval stages followed by an extended feeding period, indicating that these mutants have surpassed the critical weight to induce the larval-to-pupal transition. However, they never do because they are unable to sense their fat contents in the body and therefore they are maintained in juvenile stages.

One of the genes identified in the screen was *sema-1a*, a secretable protein with an C-terminal immunoglobulin and a transmembrane domain. When *sema-1a* is knocked-down specifically in the PG, the larva develops until L3 instar larva, but when it is supposed to induce the sexual maturation by the onset of the metamorphic process, the *sema-1a* mutants prolong their feeding behavior and continue in a juvenile stage for more than 10 days (240 hours A.E.L) (**Figure 30. B**). This extended period generates bigger body sizes (**Figure 30. C**) and heavier larvae compare

with their control siblings (**Figure 30. D**). These results indicate that *sema-1a* in the PG is required to sense the critical weight and induce the onset of the maturation process that follows the feeding and growth period.

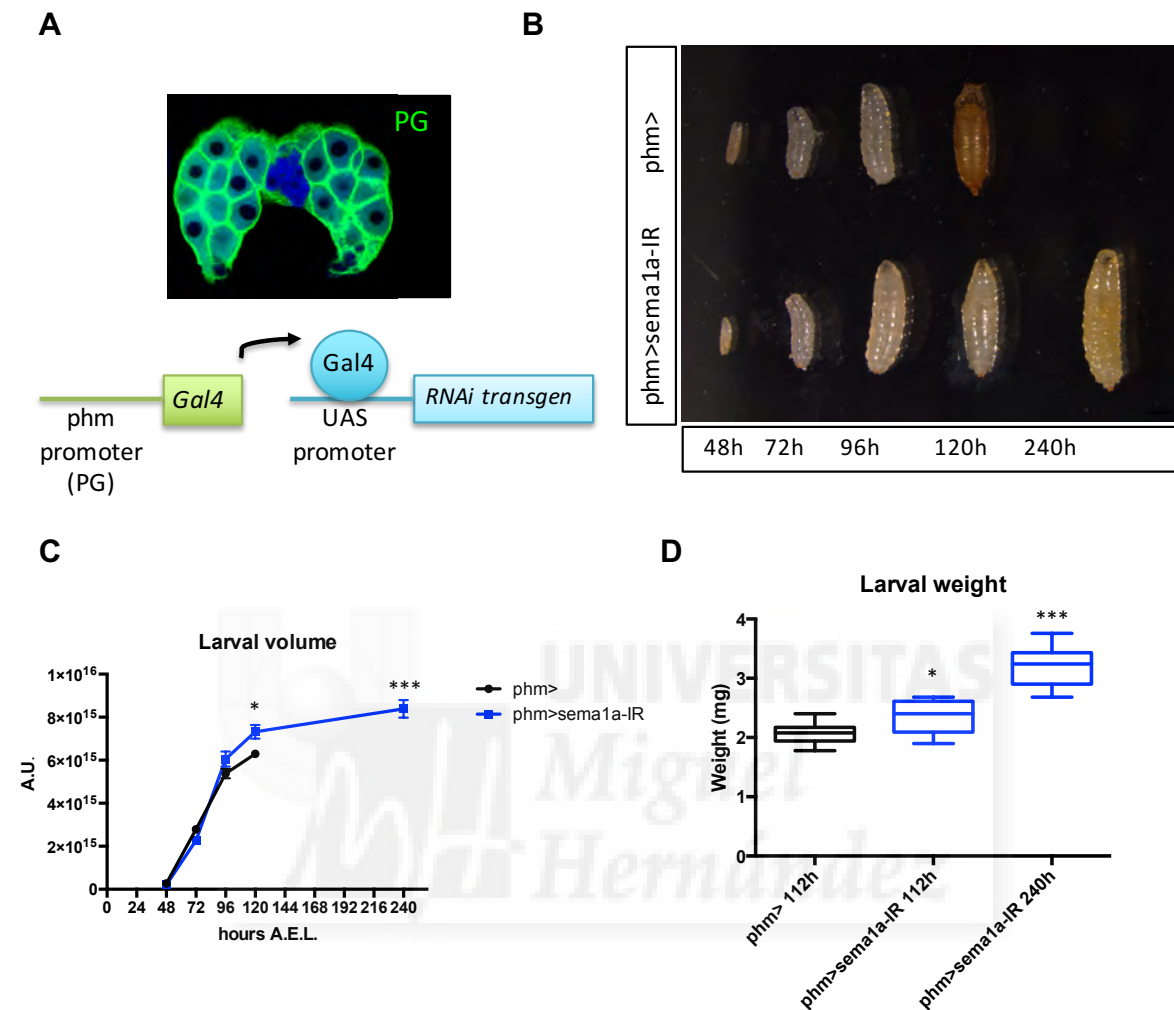


Figure 30: Characterization of *sema1a* mutant in the prothoracic gland by *phm-gal4* line. (A) Scheme of the RNAi transgenic flies screening carried out by the specific *phm-gal4* line expressed in the PG cells shown in green. (B) Representation of the different stages of the *sema1a* mutant in the PG by *phm-gal4* line. 48h A.E.L represent second instar larva. 72h A.E.L represent third instar larva before critical weight. 96 hours A.E.L. represent third instar larva after critical weight. 120 hours A.E.L. represent a time when the wild type larva pass the metamorphosis process generating a pupa, indicating that the *sema1a* mutant in the PG does not induces this transition and remain in feeding period until 240 hours A.E.L. (C) Measurement of the larval size in the *sema1a* mutant in PG by *phm-gal4* line and the *phm-gal4* line control. The final point of the *phm-gal4* line control corresponds to the pupa body size and is the control data for the statistical analysis. At least 10 larvae or pupa were scored per genotype and time point. *** $p < 0.001$; * $p < 0.05$ (Two-tailed unpaired t test). (D) Measurement of the larval weight in the *sema1a* mutant in PG by *phm-gal4* line and the *phm-gal4* line control. 45 larvae were scored per genotype and condition. *** $p < 0.001$; * $p < 0.05$ (Two-tailed unpaired t test).

***sema1a* depletion in the PG impaired the ecdysone titters.**

The most important role of PG is the generation of ecdysone hormone. This hormone promotes molting during larval stages and generates a bigger peak when the JH declines and thus, promoting metamorphosis +(Rewitz et al. 2010; McBrayer et al. 2007). To demonstrate that *sema1a* depletion in the PG generates a larval arrest of development and maintains larvae in a feeding and growth period, impairing ecdysone production, I carried out measurements by quantitative RT-PCR of *phm* and *dib*, two key Halloween genes involved in ecdysone biosynthesis cascade, and *E75B*, a target gene of ecdysone signalling activation. In the three cases, the transcriptional expression levels of *phm* (Figure 31. A), *dib* (Figure 31. B), and *E75B* (Figure 31. C) are increased at 112 hours A.E.L in the case of the control *phm-Gal4* line, when the larvae start the metamorphosis process.

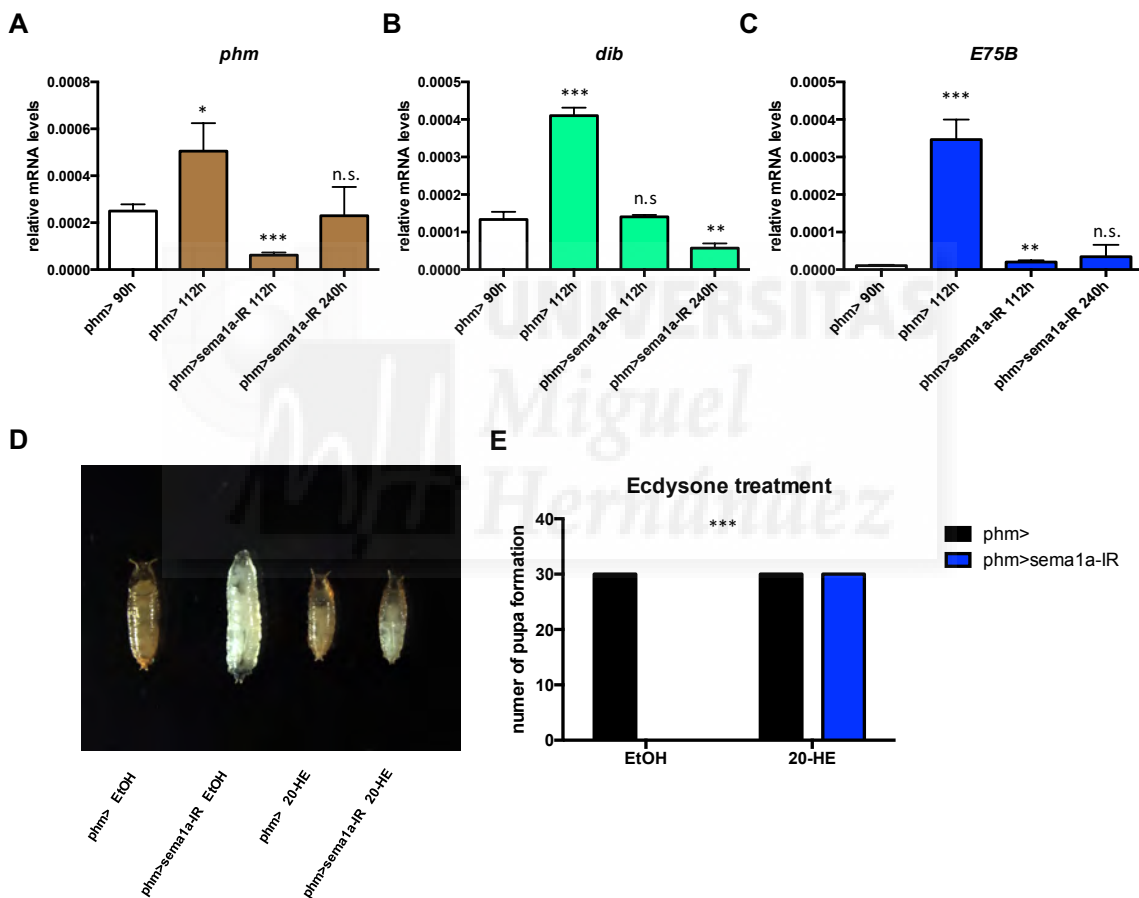


Figure 31: *sema1a* depletion in the PG impair the ecdysone titters to inhibit the sexual maturation of the larvae. (A-C) Transcriptional expression levels of *phm* (A) and *dib* (B), and *E75B* (C) measurement by real time q-PCR. mRNA isolated from 10 larvae. White columns indicate stages before wandering (90 hours A.E.L.) and the other colors indicate when wandering stages should be adquired, but are in feeding stage (112 hours A.E.L.) and the feeding period at 240 hours A.E.L. where the *sema1a* mutant in the PG remained in feeding stage. *** $p < 0.001$; ** $p < 0.01$; * $p < 0.05$; n.s $p > 0.05$ (Two-tailed unpaired *t* test). (D) 20-Hydroxyecdysone (an active form of ecdysone) treatment of the food at 72 hours A.E.L. rescued the developmental transition of the larvae *sema1a* mutant in the PG. The controls are treated with ethanol, as vehicule for 20-hydroxyecdysone. (E) Quantification of the rescue larva treated by 20-hydroxyecdysone. Three replicates were done with 10 larvae per genotype each one. Chi-square test, pairwise post hoc comparisons with Fisher's exact test with Bonferroni correction; population percentage and 95% confidence interval. *** $p < 0,001$.

sema-1a depletion in the PG inhibit the ecdysone synthesis cascade, showed by the lower transcriptional expression levels of *phm*, *dib*, and *E75B* at 112 hours A.E.L., and very similar to the levels shown by the control *phm-Gal4* line at 90 hours A.E.L. (Figure 31. A-C).

The arrested and extended developmental timing program shown by depletion of *sema-1a* in PG cells is rescued by addition of 20-hydroxyecdysone (active form of ecdysone) in the food, indicating that *sema-1a* is required for promoting the synthesis of ecdysone (Figure 31. D and F).

***sema1a* depletion in PG increases body size and maintained juvenile stage by increased insulin signaling pathway.**

Uptake of nutrients during the feeding behavior promotes release of signals from the fat body (the sensing organ of nutrients availability) to the IPCs to release insulin-like peptides; and thus promoting growth of the different body parts (Colombani et al. 2003; Géminard et al. 2009; Delanoue et al. 2016).

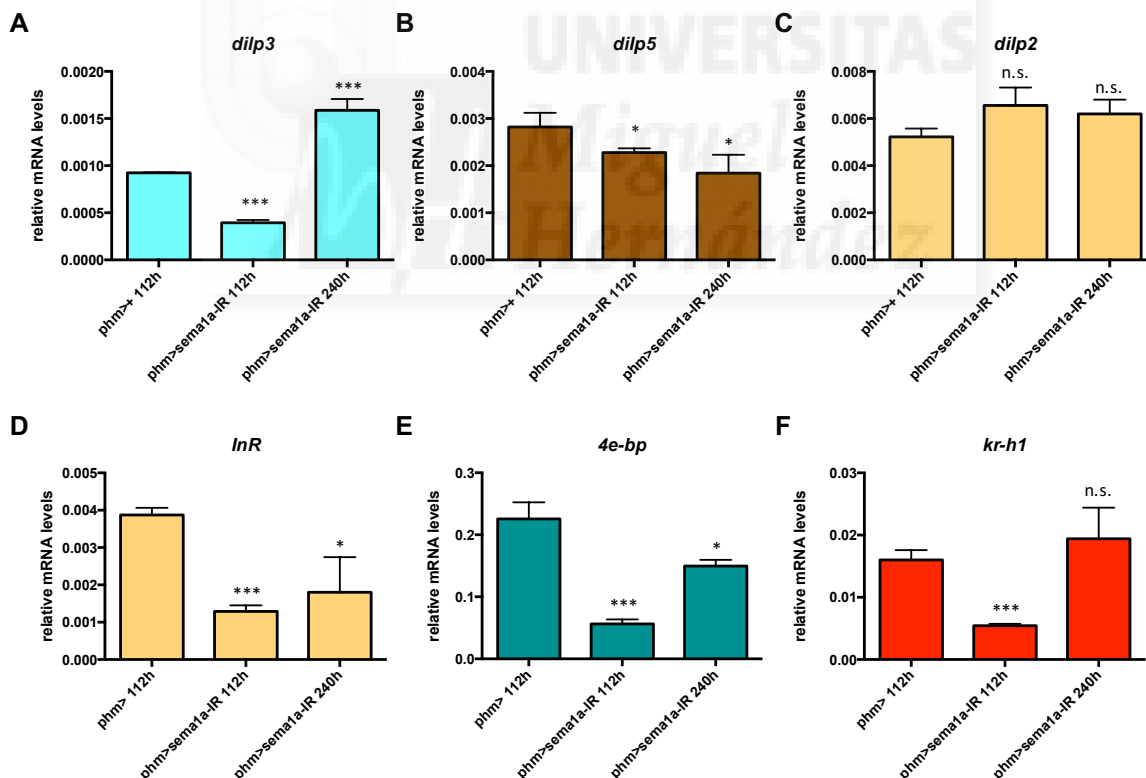


Figure 32: Insulin signaling pathway sustains growth in the *sema1a* mutant in the PG. (A-C) Transcriptional expression levels of the three *Drosophila* insulin-like peptides *dilp3* (A), *dilp5* (B), and *dilp2* (C). (D-E) Transcriptional expression levels of *InR* (D), and *4e-bp* (E), as reporter genes of insulin signaling pathway. (F) Transcriptional expression levels of *kr-h1* as a target gen of juvenile hormone pathway controlled directly by insulin signaling pathway. Measurements are done by real time q-PCR. mRNA isolated from 10 larvae per genotype and time (112 hours A.E.L. and 240 hours A.E.L.) where the *sema1a* mutant in the PG remain in feeding stage at both time points, while the control *phm-gal4* line progress to the wandering stage. *** $p < 0.001$; * $p < 0.05$; n.s. $p > 0.05$ (Two-tailed unpaired *t* test).

sema-1a depletion in the PG maintained larvae in juvenile stages and kept the feeding behavior; increasing the final body size. For this reason, only an active IIS to promote growth during the extended feeding behavior could explain the increased body size. I measured by quantitative RT-PCR the transcriptional expression levels of the three insulin-like peptides expressed in IPCs: *dilp3*, *dilp5*, and *dilp2*. Only *dilp3* is up-regulated in those mutant animals at 240 hours A.E.L., respect to the *phm-Gal4* control animals at 112 hours A.E.L. (**Figure 32. A**). *dilp5* show lower levels at 112 hours A.E.L and 240 hours A.E.L in mutant animals compared with control animals, although were not statistically significant (less than 0.001 in relative data) (**Figure 32. B**). *dilp2* do not show any change in its transcriptional levels (**Figure 32. C**). Consistent with a hyperphagic phenotype, general expression of *InR* and *4e-bp* are markedly down-regulated in mutant animals (**Figure 32. D and E**). These genes are direct targets of dFoxO, a transcription factor inhibited by IIS. Therefore, a decrease in *InR* or *4e-bp* expression is a sign of insulin signalling activation by *dilp3*. Not surprisingly, *kr-h1* expression levels, a readout of JH signaling, are maintained upregulated in mutant animals at 240 hours A.E.L similar to control animal at 112 hours A.E.L. (**Figure 32. F**). These results indicate the important role of insulin signalling and juvenile hormone signalling, promoting growth in *sema1a* mutant in the PG.

***sema1a* depletion in PG results in weight gain due to increased lipogenesis induced by an extended feeding period.**

The obese phenotype promoted by depletion of *sema-1a* in PG cells is produced by an extension of the larval feeding period and an increased insulin signalling. An increased insulin signalling and reduced ecdysone signalling are postulated to regulate the lipogenic genes during development (DiAngelo & Birnbaum 2009; Kamoshida et al. 2012; Xie et al. 2015), and could explain the accumulation of fat in the fat body and the increased body weight. To test this hypothesis, the levels of the five key lipogenic genes (*ACC*, *Ascl*, *bgm*, *fas*, and *SREBP*) are measured by quantitative RT-PCR. At 112 hours A.E.L *ACC* (**Figure 33. A**), *Ascl* (**Figure 33. B**), and *bgm* (**Figure 33. C**) were up-regulated in mutant animals compared with controls, but not *fas* (**Figure 33. D**), and *SREBP* (**Figure 33. E**). Interestingly, at 240 hours A.E.L. the levels of *ACC* were maintained (**Figure 33. A**), *Ascl* and *bgm* increased respect to 112h A.E.L (**Figure 33. B and C**), and now *fas* and *SREBP* also showed a statistically significant increase at 240 hours A.E.L. (**Figure 33. D and E**). Taking together this data, the lipogenesis activation in *sema1a* mutants promote the accumulation of stores, generating havier larvae with resources for growth.

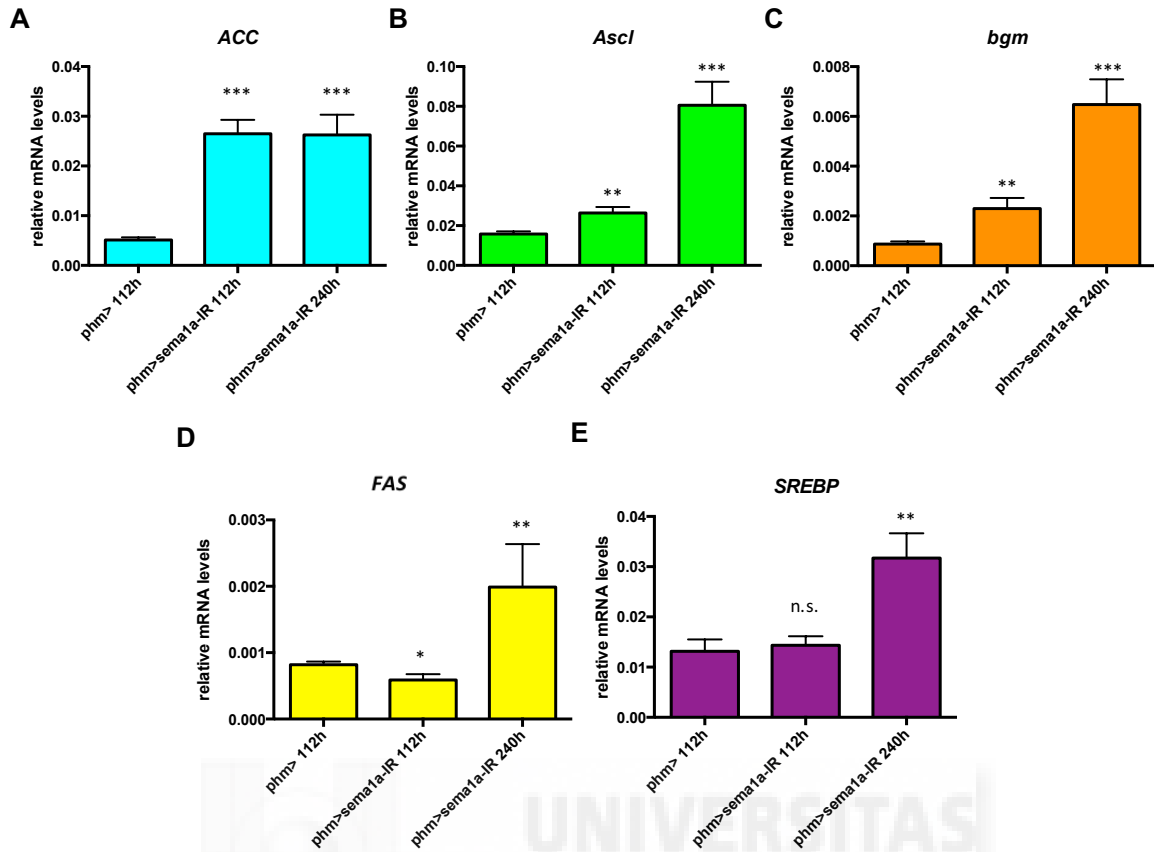


Figure 33: Weight gain in the *sema1a* mutant in the PG is produced by up-regulation of lipogenesis genes. (A to E) Expression levels of five lipogenesis genes, *ACC*, *Ascl*, *bgm*, *FAS*, and *SREBP* analyzed by qRT-PCR in mRNA isolated from 10 larvae for each genotype and time point. Data are mean \pm SD ($n = 3$ repeats). *** $p < 0.001$; ** $p < 0.01$; * $p < 0.05$; n.s. $p > 0.05$ (Two-tailed unpaired t test).

***sema1a* depletion in PG induces an unusual starvation response during feeding extended period.**

It is known that before the critical weight is achieved, if the larva is under low levels of nutrients or in starvation conditions the fat body mobilizes its resources to obtain energy for growth such as glycogen and lipids. *sema-1a* mutant animals cannot entry in puparation due to an extended feeding period and growth, a similar phenotype observed in starved larva before critical weight is achieved.

To clarify whether depletion of *sema-1a* in the PG induces a starvation response I measured by quantitative RT-PCR mRNA levels of different genes that codify enzymes involved in catalysis of glycogen and triglycerides. For glycolysis I measured *hexokinase C* (*Hex-C*) and *phosphoglucose mutase* (*PGM*) were measured, while for lipolysis *brummer* (*bmm*), that it has a phospholipase domain, *Lipin* (*Lpin*), and *CG5966* that it codifies for a lipase were monitored. *Hex-C* and *PGM* are up-regulated at 240 hours A.E.L in mutant animals respect to the control line (**Figure 34. A and B**) (Barrio et al. 2014). Moreover, at 112 hours A.E.L mutant animals also has up-regulated *PGM*

(**Figure 34. B**), indicating that the starvation response occurs before the extended feeding period. For lipolysis, only *bmm* is up-regulated at 240 hours A.E.L (**Figure 34. C**), indicating that lipids were also mobilized to generate more energy for growth (**Figure 34. D and E**). Furthermore, *pepck*, a gene commonly used as a marker of starvation (Pasco & Léopold 2012), was upregulated in mutant animals at 240 hours A.E.L. (**Figure 34. F**).

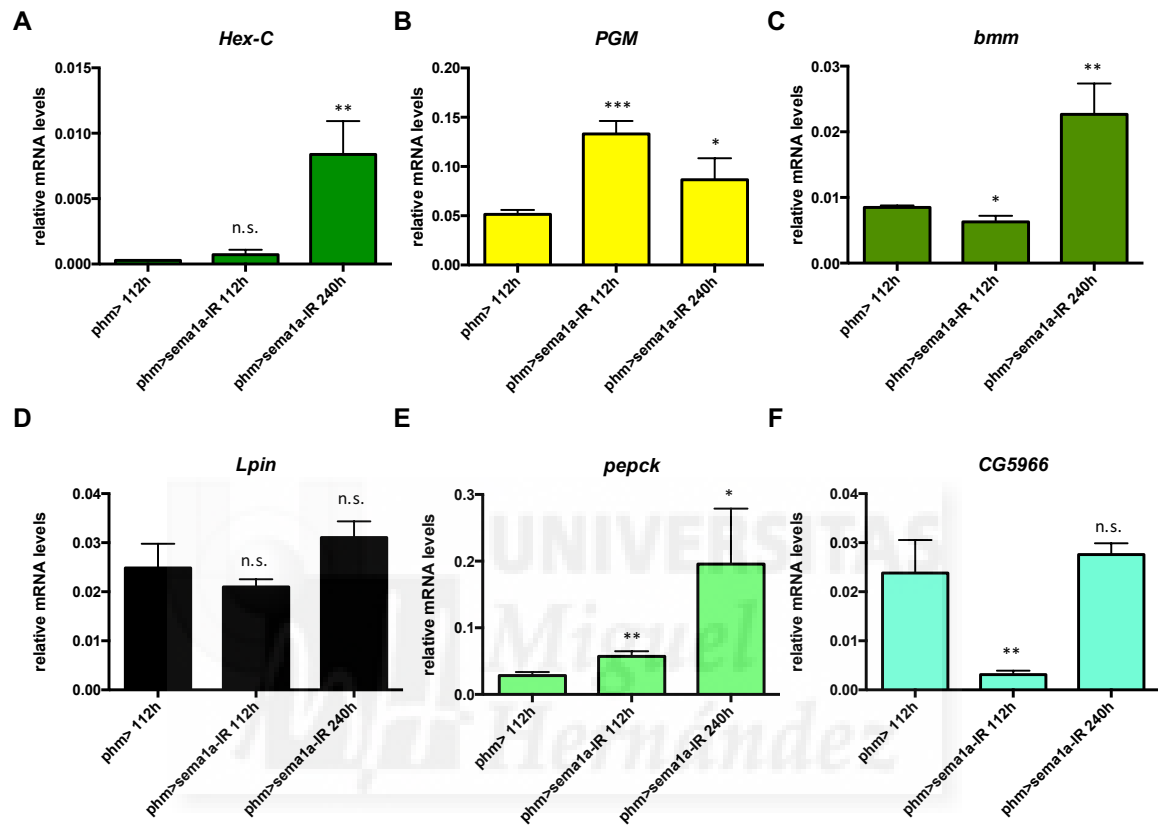


Figure 34: starvation response is induced by up-regulation of lipolysis and glycolysis genes in *sema1a* mutants. (A-B) Transcriptional expression levels of two glycolysis genes *Hex-C* and *PGM*. (C-E) Transcriptional expression levels of three lipolysis genes involve in starvation response *bmm*, *Lpin*, and *CG5966*. (F) Transcriptional expression levels of *pepck*, a gene up-regulated in starvation response. Data were obtained by qRT-PCR in mRNA isolated from 10 larvae for each genotype and time point. Data are mean \pm SD (n = 3 repeats). *** $p < 0.001$; ** $p < 0.01$; * $p < 0.05$; n.s. $p > 0.05$ (Two-tailed unpaired *t* test).



5. DISCUSSION





1. A brain circuit that synchronizes growth and maturation revealed by Dilp8 binding to Lgr3

Previously, my lab and Pierre Leopold labs described that *Drosophila* insulin-like peptide 8 (Dilp8) is a new hormone belonging to the insulin/relaxin family and that it mediates a homeostatic growth control to maintain body proportions and symmetry. Dilp8 is up-regulated upon injury or during abnormal imaginal growth tissue to induce the extension of the developmental timing program (mediated by inhibition of ecdysone production) and to slow growth of the other undamaged imaginal tissues of the body, and thus, maintaining the proper final body size (Garelli et al. 2012; Colombani et al. 2012).

In the present thesis project, I employed a candidate approach to demonstrate that the relaxin receptor Lgr3 (and not Lgr4) acts as a receptor for Dilp8. I found that the relaxin receptor *lgr3* is necessary in the brain to induce all the phenotypes produced by *dilp8*-overexpression. Unexpectedly, *lgr3* was not required in the prothoracic gland, where ecdysone is produced to control developmental timing program (McBrayer et al. 2007). Moreover, depletion of *lgr3* in the brain alone, like in *dilp8* mutants (Garelli et al. 2012), produced asymmetries in the adult body; further supporting its role in developmental stability (Vallejo et al. 2015).

To elucidate where *lgr3* is required in the brain for Dilp8 action, *lgr3* was knocked-down in various subset of neurons involved in growth and developmental timing control (e.g ventral cord, IPCs, PDF clock neurons, NPF neurons and PTHH neurons) without any positive result, indicating that Lgr3 receptor was required to mediate Dilp8 action in a different population of neurons. I took advantage of the available lines expressing *Gal4* under control of genomic fragments from the *lgr3* locus generated by Jannelia Farm-HHMI (Jenett et al. 2012). I found that only depleting *lgr3* using the *R19B09-Gal4* enhancer fully suppressed the Dilp8-induced delay and did so with the same magnitude as when *lgr3* was ubiquitously depleted by *tub-Gal4*. No other *lgr3-Gal4* enhancer lines prevented the Dilp8-induced delay.

Dilp8 is incapable to produce developmental delay and slow growth rate of undamaged imaginal tissues when *lgr3* is depleted using the *R19B09-Gal4* line, indicating that these neurons regulate growth rate and developmental timing program at the same time by *dilp8* and *lgr3* genetic interaction. Furthermore, I demonstrated that the neurons molecularly defined by *R19B09-Gal4* line can produce delay in developmental timing program only by neuronal depolarization using NaChBac (Nitabach et al. 2006), indicating that the Dilp8-Lgr3 interaction produces neuronal activation (Vallejo et al. 2015).

In collaboration with Diana M. Vallejo from my lab, we showed that the activation of Lgr3 by nanomolar concentrations of Dilp8 produced a robust activation of cyclic AMP. Moreover, through colocalization and immunoprecipitation experiments *in vitro* we demonstrated that Dilp8 binds to Lgr3 directly. Furthermore, using a biochemical readout of cAMP *in vivo*, we identified using the *R19B09-Gal4* line a pair of neurons per brain lobe that acutely responded to Dilp8-Lgr3 physical interaction, increasing cAMP signal (Vallejo et al. 2015).

We characterized that these pair of neurons defined by *R19B09-Gal4* line that responded to Dilp8-Lgr3 interaction, have extensive axonal arborizations (hub-like structure) and by GRASP experiments, with the help of Javier Morante, we demonstrated their synaptic connection with PTTH neurons and insulin-producing cells (Vallejo et al. 2015). We called these neurons ``sync`` neurons.

Functional connectivity between Lgr3 ``sync`` neurons and PTTH neurons, and Lgr3 and IPCs was evaluated using genetics, perturbing neural activity, and/or assessing changes in transcription of candidate output pathways; as read-outs for ecdysone and insulin signaling. Thus, I identified that *dilp3* and *dilp5*, and the Juvenile hormone signalling were output pathways of this circuit for growth compensation (Vallejo et al. 2015). In summary, Lgr3 identification and the novel circuit defined form a framework for future investigations into plastic and homeostatic size regulation, and may provide novel insights into asymmetric and disproportional growth syndromes in humans (such as Silver Russell).

Mutations in relaxin receptors have not been related with any mammalian developmental disorder, but interestingly *drosophila* Lgr3 shows structural similarities to mammalian RXFP1 and RXFP2 receptors, with large extracellular domains containing leucine-rich repeats. Relaxin receptor family is well characterized, with relevant functions in reproduction in mammals. Insulin/relaxin peptides are the natural ligands of mammalian relaxin receptors RXFP1, RXFP2, RXFP3, and RXFP4. When insulin or relaxin peptides bind to RXFP1 or RXFP2 induce the generation of cAMP (Bathgate et al. 2013), like the interaction of Dilp8 through Lgr3 receptor. Moreover, RXFP3 is highly expressed in the hypothalamic-pituitary axis in the mammalian brain, suggesting a potential role for Relaxin3/RXFP3 in developmental stability in mammals (C. M. Smith et al. 2012).

Trade-Off between Dilp8-Lgr3-mediated homeostatic growth control and Fitness response to Stress and modulation by circadian clock

It was previously shown by Garelli et al. 2012; Colombani et al. 2012, that *dilp8*-overexpressing flies accumulate more weight as a consequence of developmental timing program delay and extension of the feeding period. Now I have shown that systemic knocked-down of *lgr3* in the presence of Dilp8 rescues this overweight acquired during larval development, due to rescue of the developmental timing delay and reduction of the feeding period (Vallejo et al. 2015).

Moreover, we have now shown in Vallejo et al. 2015 that the *lgr3* receptor is only required to mediate Dilp8 function in two pair of neurons in the brain by *in vivo* cAMP increment, as a biochemical readout of Dilp8 action through Lgr3. No expression was found in the fat body or in imaginal discs using five *Gal4* lines generated for the *lgr3* locus, indicating that all activity mediated by Dilp8 binding through Lgr3 is required in the brain. According with previous results (Garelli et al. 2012), I found that the overweight accumulated by Dilp8 during development is mediated by Lgr3 receptor in the two pair of neurons molecularly defined by *R19B09-Gal4* line, called ``sync'' neurons. Knocked-down of *lgr3* rescued the developmental timing delay and extension of feeding period, and generated adult flies with the same weight as wild type in virgin females and males.

The overweight acquired in *dilp8*-overexpressing flies, mediated by the Lgr3 receptor, should generate acquisition of an evolutionary improved fitness feature for reproduction and survival of the specie. Accordingly, the best-fit organism is the most resistant one under stress conditions. Stress is any environmental factor that can reduce the survival of an organism (KOEHN & BAYNE 2009). Nutrient deprivation is one of the most relevant stresses that an organism can face in the environment, inducing an energy storage mobilization and a rapid response in locomotor activity to look for better and nutritional enriched environments (Rion & Kawecki 2007). Thus, I wondered whether this overweight flies have more capability to survive in starved nutritional conditions. I observed that these heavier flies were more starvation resistance respect to wild type flies in virgin females and males. Accordingly, *dilp8* mutants or animals overexpressing an inactive form of *dilp8* did not show any difference in their starvation response; indicating that this starvation resistance response is mediated by Dilp8 during development. Moreover, this starvation resistance phenotype induced by overexpression of *dilp8* during development was rescued when *lgr3* was knocked-down using *R19B09-Gal4* in virgin adult female and male flies. Thus, I can conclude that Dilp8-Lgr3 signalling modulated developmental timing program and feeding period generating havier flies with higher starvation resistance.

Typically, the starvation resistance response is correlated with an accumulation of lipids or triglycerides accumulation in the body (Chippindale et al. 1996; Häder et al. 2003; Harbison et al.

2004). Differentially, other metabolic resources such as glycogen and carbohydrates have been correlated with other stresses like desiccation (Djawdan et al. 1998; Graves et al. 1992). For these reasons, I measured the transcriptional levels of key lipogenic genes *Ascl*, *ACC*, *bgm*, *FAS*, and *SREBP* (Reiff et al. 2015; Lodhi et al. 2012) in *dilp8*-overexpressing larva and in animals that lacked the *lgr3* receptor in the ``sync`` neurons defined by *R19B09-Gal4* line in a *dilp8*-overexpressing context. As I expected, *Ascl*, *ACC*, and *bgm* were transcriptionally up-regulated in a *dilp8*-overexpressing animals, but their transcriptional levels were rescued in the absence of *lgr3* in the brain, indicating that the extended developmental timing program and feeding period was under the lipogenic control mediated by Dilp8-Lgr3 signalling. Furthermore, this transcriptional up-regulation of lipogenic genes during development were reflected in higher triglyceride levels in adult virgin females and males, and a major resistance capability to starvation in the adult pre-reproductive stage. I can speculate that this increased starvation resistance response in those developing animals that suffered a damage, in a period where they are very vulnerable to predators, would provide more opportunities to survive and to generate off-spring in comparison with undamaged flies.

Several developmental check-points should be exceed before metamorphosis initiation. Firstly, a nutritional check-point (critical weight) must be surpassed to induce the clearance of juvenile hormone and to allow PTTH expression and ecdysone titter production (Shingleton et al. 2005; Mirth & Riddiford 2007; Mirth et al. 2014; Rewitz et al. 2013). Secondly, a tissue repair check-point controlled by Dilp8-Lgr3 monitors that all tissues are growing proportionally in the different parts of the body, and decline Dilp8 levels in the hemolymph to allow PTTH release and ecdysone synthesis (Garelli et al. 2012; Colombani et al. 2012; Vallejo et al. 2015; Colombani et al. 2015; Garelli et al. 2015; Boone et al. 2016). Finally, it is supposed that the circadian clock modulates developmental timing program. When the previous check-points have been surpassed, the photoperiod check-point controlled by the circadian clock master neurons or PDF⁺ neurons (Gong et al. 2010; Yamanaka, Romero, et al. 2013) indicates when the larva can switch their behavior from foraging to wandering and induce puparium formation. The regulation of this switch is poorly understood. For example, in *Manduca sexta* was demonstrated that the secretion of PTTH can only happen in a open photoperiodic gate (Truman & Riddiford 1974). Experiments in *Drosophila* suggested that the activation of PTTH neurons is by their presynaptic PDF⁺ neurons, controlling light avoidance in *Drosophila* larva (Gong et al. 2010; Yamanaka, Romero, et al. 2013). Other studies have shown asynchronical transcriptional levels of *ptth* in a *pdf* null mutant background; postulating a negative control of PTTH neuropeptide by PDF neuropeptide (McBrayer et al. 2007). A study performed in *Bombyx mori* showed that PDF neuropeptide can positive regulate ecdysone titter during development in the PG directly (Iga et al. 2014).

Taking in consideration the close apposition of PDF+ neurons with Lgr3 ``sync`` neurons and the description of the Dilp8-Lgr3 check point axis, next I wondered whether Lgr3 ``sync`` neurons could participate in the photo-period check-point regulated by the circadian clock master neurons to control the release of PTTH, and thus, controlling the transition between foraging behavior and wandering behavior. Following this idea, I demonstrated that the circadian clock is modulated by Dilp8-Lgr3 interaction. Firstly, using GRASP experiment Javier Morante and myself showed that Lgr3 ``sync`` neurons are synaptically connected to PDF⁺ neurons in L3 instar larval brains. Secondly, I showed that the interaction of Dilp8-Lgr3 that extends the developmental timing program can be extended even further in a null *pdf* mutant background; indicating the relevant role of PDF neuropeptide in the metamorphic process. These results were unexpected, because McBrayer et al. 2007 postulated that PDF neuropeptide was a negative signal for PTTH release. However, the developmental timing program did not show any change in *pdf* null animals. Surprisingly, in a *dilp8*-overexpressing context, the loss of *pdf* can extend the developmental timing by regulation of the Dilp8-Lgr3 interaction.

The genetic interaction of Dilp8-Lgr3 with *pdf* also showed how the extra developmental timing program is uncoupled with growth. Lacking *pdf* in a *dilp8*-overexpressing context generated animals with bigger final body size, indicating the disruption of the homeostatic growth mechanism that involves Dilp8-Lgr3. This phenotype has been previously reported for all the genes involved in the ecdysone signalling pathway (McBrayer et al. 2007; Rewitz et al. 2010); indicating the positive regulation of PTTH by PDF neuropeptide. Moreover, I have demonstrated the direct regulation of PTTH by PDF neuropeptide by the low levels of ecdysone signalling induced by Dilp8-Lgr3 interaction. This positive regulation is reinforced by the lack of *pdf* in a *dilp8*-overexpressing context. All together, plus the ecdysone treatment rescue indicates that the extra timing generated by the lack of *pdf* in a Dilp8-Lgr3 context is mediated by ecdysone signalling.

Next I analyzed the epistatic relationship between *pdf* and *dilp8*. As I expected, the lack of *pdf* in a *dilp8*-overexpressing context generated animals with bigger final body size, allowing an extra capability of the starvation resistance response in virgin male and female adults. This effect was a consequence of a major lipid accumulation in the body of these flies, revealed by an up-regulation of *ACC*, *Ascl*, and *bgm* during the extended feeding period and followed by a major accumulation of triglycerides in adult virgin flies. I now propose that all these effects are mediated by inhibition of PDF release by Lgr3 ``sync`` neurons, when they are activated by Dilp8-Lgr3 interaction. Thus, when I hyperpolarized PDF neurons using *mKir2.1* ion channel generates a developmental timing delay as hyperpolarization of PTTH neurons does, followed by ecdysone titter inhibition and bigger final body size with more weight. These effects are mimicked in *ptth* mutant animals (McBrayer et al. 2007). Indicating the positive relationship between PDF neurons and PTTH

neurons, and their neuropeptides (PDF and PTTH) in the ecdysone production syntesis.

It is known that PDF⁺ neurons are connected to PTTH neurons (Gong et al. 2010; Yamanaka, Romero, et al. 2013), but it is not clear whether PDF acts in PTTH neurons through its receptor PDFR (Hyun et al. 2005). For this reason, I knocked-down *pdfr* in PTTH neurons in the presence of Dilp8. Those mutant animals mimicked the same phenotypes shown in a *pdf* null mutant overexpressing *dilp8* background, with an increment in the developmental timing program delay, an uncoupled growth control that lead to bigger and heavier adult animals and a more starvation resistant response, and reduction of ecdysone titters in larval stages. Those experiments assigned the first functional mechanism to PDF/PDFR axis and Lgr3 `sync` neurons and PTTH neurons in developmental timing program. Moreover, these experiments are the first demonstration of a molecular relationship between two previously separated check-points (photoperiod and tissue repair) that now I can show are working together to maintain the homeostatic control during development and thus, to generate fitness of adult organism. Accordingly, *relaxin 3* have been postulated to act on mammalian circadian clock neurons and control diary rhythmicity (C. M. Smith et al. 2012); further supporting the important role of relaxin signaling in the mammalian hypothalamic-pituitary axis and their interaction with the circadian clock.



Dilp8-Lgr3 signalling in adult virgin female.

In a previous study, Garelli et al. 2012 showed that *dilp8* is only expressed in the female ovary, indicating a potential sexual dimorphism and function for *dilp8*. Furthermore, Meissner et al. 2016 showed that different *lgr-3 Gal4* lines were differentially expressed in adult females and males. As *dilp8* is only produced in adult female flies and not in males, this result suggested that Lgr3 receptor could have other ligands different to Dilp8. Moreover, I have previously shown that only 2 pair of neurons (called ``sync`` neurons) defined by *R19B09-Gal4* line are required to mediate Dilp8 action in larval brains, with many other not been activated by Dilp8. Meissner et al. 2016 showed that *lgr3* was expressed in *par intercerebralis* neurons that projected dorsally and also in some neurons in the abdominal ganglia of female flies. Furthermore, they showed that depolarization of these *lgr3*⁺ abdominal ganglia neurons with a TRPA channel induced a reduction in courtship behavior of virgin female flies, with less number of egg and offspring of these female flies, as it was reported by others using alternative *Gal4* lines (Feng et al. 2014; Bussell et al. 2014).

I have now shown that Lgr3 neurons defined molecularly by *R19B09-Gal4* line uniquely in adult females are synaptically connect with adult IPCs and that this Dilp8-Lgr3 interaction controls expression levels of *dilp2* and *dilp5*. Moreover, I showed that *dilp8* is expressed in mature oocytes starting on the second day in virgin female flies and reached its maximum levels of expression on the fourth day. Unexpectedly, *dilp8* and *lgr3* mutants did not reveal any phenotype in courtship and egg laying behaviors. Accordingly, to Meissner et al. 2016 I was expecting to observe less latency in courtship behavior and more eggs number deposition in those mutants. However, I failed to recapitulate those phenotypes described. Furthermore, I failed to recapitulate any effect in courtship behavior inhibition and egg laying impairment in animals overexpressing *dilp8*, indicating that Dilp8-Lgr3 interaction is not involved in courtship behavior.

On the other hand, Wigby et al. 2010 showed that insulin signaling can control remating behavior in adult females. Thus, I wondered whether Dilp8-Lgr3 interaction in the adult female could control remating behavior by inhibition of *dilp2* and *dilp5*. Unexpectedly, I did not see any difference in remating behavior in adult female mutant flies for *dilp8* or *lgr3*, or overexpressing *dilp8*. These experiments suggest a potential role for Dilp8-Lgr3 interaction in the adult female to control insulin signaling in adult females and thus, to control metabolism and egg growth (Das & Arur 2017).



A *Sema-1a*/Leptin-like sensor for body fat times reproductive maturation

Nutrient up-take is indispensable for body growth. Developing animals need to sense their weight increment as a readout of body growth. Only when a critical weight has been surpassed they can become sexually mature, in order to ensure survival through puberty/metamorphosis and allow their reproductive success (critical weight hypothesis: (Frisch & Revelle 1970; Nijhout 2003)) The fly fat body, the mammal liver homolog tissue, is known to sense the nutritional status and availability. In a rich nutrient environment, the larval fat body promotes body growth by remote control of insulin signalling, and thus controls the growth rates and ecdysone titters in PG (Caldwell et al. 2005; Colombani et al. 2005; Mirth et al. 2005). But how do developing organisms (and their brain) know when it is time to enter puberty? And exactly how are the internal and external cues reflecting size and body fat integrated and regulated to dictate when an animal can become sexually mature?

In a RNAi based screen *sema-1a* was found as a gene required to sense the critical weight in the PG. Larva with depleted *sema-1a* function in the PG arrested in their third instar stage and showed an overgrown phenotype due to an extended larval feeding period. During this extended larval period (10-12 days), those mutant animals continued growing and become obese. This phenotype is commonly observed for edysone-deficient animals (Rewitz et al. 2009; McBrayer et al. 2007). Indeed, this overgrown phenotype was consequence of a sustained insulin (by up-regulation of *dilp3* and down regulation of *4e-bp* and *InR*), and juvenile hormone signaling (by both up-regulation of *juvenile hormone acid methyltransferase* and *krüppel-homolog 1*, a direct target of JH that encodes a transcription factor that transduces the actions of JH). Concomitantly, I observed the lack of induction of *halloween* genes (e.g *phm* and *dib*) and low systemic ecdysone signaling, inhibiting metamorphosis.

Obesity is reflected by the accumulation of fat. Indeed, I observed an accumulation of lipids in those mutant animals in all tissues analyzed (e.g brain, imaginal discs, fat body). Analysis of lipogenic enzymes in wholly larva and in dissected tissues (fat body, brain and hemolymph) revealed an up-regulation of key enzymes involved in the lipogenesis *de novo* (*SREBP*, *ACC*, *Ascl*, *Fas* and *Bgm*) during the extended feeding period. Surprisingly, analysis of genes involved in lipolysis and glycolysis, required for nutrient mobilization in starved conditions, such as *pepck*, *bmm*, *Hex-C*, and *PGM* were significantly upregulated. Thus, *sema-1a* is required to sense the critical weight that promotes the larval-to-pupal transition. In its absence, I can conclude that this exarcebated starvation-like response promotes tissue and larval growth.



6. CONCLUSIONS / CONCLUSIÓN





A brain circuit that synchronizes growth and maturation revealed by Dilp8 binding to Lgr3:

1. The relaxin receptor Lgr3 mediates Dilp8-induced homeostatic control.
2. Lgr3 is a Dilp8 receptor confirmed by biochemical direct interaction.
3. The Lgr3 receptor acts in a small set of new central brain neurons to mediate Dilp8 functions.
4. A pair of dorsomedial neurons in the *par intercerebralis* ('sync neurons') acutely responds to Dilp8.
5. Lgr3 'sync' neurons are connected to PTTH neurons and IPCs.
6. Inhibition of PTTH neurons regulates the developmental timing delay mediated by Dilp8-Lgr3 interaction.
7. The IPCs act as an Lgr3 output pathway to mediate the slow growth rate of undamaged imaginal tissues and to regulate the levels of JH in juvenile stages.

Trade-Off between Dilp8-Lgr3-mediated homeostatic growth control and Fitness response to Stress and modulation by circadian clock

1. The weight gain in *dilp8*-overexpressing flies is mediated by Lgr3 receptor in the two pair of neurons in the *par intercerebralis*, called 'sync' neurons.
2. The weight gain generated by Dilp8-Lgr3 interaction produces more starvation resistance animals as a consequence of an increased lipogenesis during development.
3. Inhibition of PDF neurons controls developmental timing program as positive signal of ecdysone production.
4. PDF neurons are connected with Lgr3 neurons to mediate the developmental timing program induced by Dilp8-Lgr3 interaction and to control the open-gate window.
5. The lack of *pdf* in a *dilp8*-overexpressing context generates animals with bigger final body size.
6. The extra weight acquired by the synergic interaction between *pdf* and *dilp8* generates more starvation resistance flies by prolongation of the feeding period and accumulation of TAGs.
7. PDF neurons are connected with PTTH neurons to regulate the open-gate window for puparium formation.
8. All the phenotypes generated by the lack of *pdf* in a *dilp8*-overexpressing context are transduced by *pdfr* in the PTTH neurons.

Dilp8-Lgr3 signalling in adult virgin female:

1. Dilp8 is expressed in mature oocytes in *Drosophila* virgin females.
2. Dilp8 starts to be expressed at 48 hours after eclosion from the pupa and achieves its maximum level of expression at 72 hours after eclosion from the pupa.
3. Lgr3 neurons are synaptically connected to IPCs in the adult female brain.
4. Dilp8-Lgr3 interaction control *dilp2* and *dilp5* expression exclusively in adult virgin females.
5. *dilp8*-overexpression or *dilp8* loss of function do not control mating, egg laying or remating behavior in *Drosophila* females.
6. *lgr3* loss of function do not control mating, egg laying or remating behavior in *Drosophila* females.

A Sema-1a/Leptin-like sensor for body fat times reproductive maturation:

1. Depletion of *sema-1a* in the PG prevents the larval-to-pupal transition.
2. Depletion of *sema-1a* in the PG inhibits ecdysone synthesis.
3. Depletion of *sema-1a* in the PG leads to heavier larva and increased body size as a consequence of an extended larval lifespan.
4. Depletion of *sema-1a* in the PG extends the larval feeding period and induces accumulation of lipids in all tissues.
5. Depletion of *sema-1a* in the PG leads to aberrant larval growth due to sustained insulin and juvenile hormone signalling.
6. This aberrant growth is due to an exarcebated starvation-like response.
7. *sema-1a* is required in the PG to sense the critical weight.

Un circuito cerebral que sincroniza crecimiento y maduración revelado por la interacción de Dilp8 y Lgr3:

1. El receptor relaxina Lgr3 media el control homeostático inducido por Dilp8.
2. Lgr3 es el receptor de Dilp8 confirmado por interacción directa usando técnicas de bioquímica.
3. El receptor Lgr3 actúa en una pequeña fracción neuronal en el cerebro central para mediar las funciones de Dilp8.
4. Un par de neuronas dorsomediales en el *par intercerebralis* (neuronas ``sync``) responden altamente a la señal de Dilp8.
5. Las neuronas Lgr3 ``sync`` están conectadas a las neuronas PTTH e IPCs
6. La inhibición de las neuronas PTTH regula el retraso del tiempo de desarrollo mediado por la interacción Dilp8-Lgr3.
7. Las IPCs actúan postsinápticamente de las neuronas Lgr3 ``sync`` para mediar la reducción del crecimiento de los discos imaginales no dañados y a su vez controlar los niveles de la hormona juvenil en estadios larvarios.

Compensaciones entre el mecanismo homeostático del crecimiento mediado por Dilp8-Lgr3 y respuesta al estrés modulada por el ciclo circadiano

1. La ganancia de peso en las moscas que sobreexpresan *dilp8* es mediado por el receptor Lgr3 en las neuronas denominadas ``sync`` en el *par intercerebralis*.
2. La ganancia de peso generada por la interacción de Dilp8-Lgr3 produce mayor resistencia a inanición en las moscas vírgenes adultas, como consecuencia del incremento de lipogénesis durante el desarrollo.
3. La inhibición de las neuronas PDF controlan el tiempo de desarrollo como señal positiva en la regulación de la producción de ecdisona.
4. Las neuronas PDF están conectadas con las neuronas Lgr3 ``sync`` para mediar el tiempo de desarrollo inducido por la interacción de Dilp8-Lgr3 y controlan la fase permisiva para la puparación.
5. La falta del neuropéptido PDF en el contexto de sobreexpresión de *dilp8* genera animales de mayor tamaño del cuerpo en moscas adultas.
6. El mayor peso adquirido en la interacción sinérgica entre el mutante *pdf* y la sobreexpresión de *dilp8* genera mayor resistencia a inanición en las moscas vírgenes adultas por la prolongación del periodo de alimentación y mayor acumulación de triglicéridos.
7. Las neuronas PDF están conectadas a las neuronas PTTH regulando la fase abierta para la puparación de las larvas.
8. Todos los fenotipos generados por la falta de *pdf* en el contexto de sobreexpresión de *dilp8*

son recapitulados cuando se elimina *pdfr* de las neuronas PTTH.

Papel de la interacción de Dilp8-Lgr3 en hembras vírgenes adultas

1. Dilp8 es expresado en oocitos maduros en hembras vírgenes de *Drosophila*.
2. Dilp8 comienza a expresarse a las 48 horas después de eclosionar de la pupa y adquiere el máximo nivel de expresión a las 72 horas después de la eclosión de la pupa.
3. Las neuronas Lgr3 están sinápticamente conectadas con las IPCs en el cerebro adulto de las hembras.
4. La interacción de Dilp8-Lgr3 controla la expresión de *dilp2* y *dilp5* exclusivamente en hembras vírgenes adultas.
5. La sobreexpresión de *dilp8* o la falta de función de *dilp8* no controla el apareamiento, deposición de huevos y el reapareamiento en las hembras de *Drosophila*.
8. La falta de función de *lgr3* no controla el apareamiento, deposición de huevos y el reapareamiento en las hembras de *Drosophila*.

Sema-1a/Leptina como sensor de grasa para controlar la maduración del 146juvenile

1. Eliminación de *sema-1a* en la PG previene la transición de larva a pupa.
2. Eliminación de *sema-1a* en la PG inhibe la síntesis de ecdisona.
3. Eliminación de *sema-1a* en la PG genera larvas de mayor tamaño y peso como consecuencia de la 146juvenile146 de la fase juvenil de la larva.
4. Eliminación de *sema-1a* en la PG extiende el tiempo de alimentación de la larva generando mayor acumulación de lípidos en todos los tejidos.
5. Eliminación de *sema-1a* en la PG genera un crecimiento aberrante de la larva como consecuencia de la activación continuada en la producción de insulina y la hormona juvenil.
6. Este crecimiento aberrante produce una respuesta común a la inanición de las larvas.
7. *sema-1a* es requerida en la PG para sensor el peso crítico de la larva.



BIBLIOGRAPHY



- Adams, M.S. & Niswander, J.D., 1967. Developmental “noise” and a congenital malformation. *Genetical research*, 10(3), pp.313–317.
- Alexandre, C., Baena-Lopez, A. & Vincent, J.-P., 2014. Patterning and growth control by membrane-tethered Wingless. *Nature*, 505(7482), pp.180–185.
- Ampleford, E.J. & Steel, C.G.H., 1982. The behaviour of *Rhodnius prolixus*(Stål) during the imaginal ecdysis. *Canadian Journal of Zoology*, 60(2), pp.168–174.
- Arden, K.C., 2008. FOXO animal models reveal a variety of diverse roles for FOXO transcription factors. *Oncogene*, 27(16), pp.2345–2350.
- Ashok, M., Turner, C. & Wilson, T.G., 1998. Insect juvenile hormone resistance gene homology with the bHLH-PAS family of transcriptional regulators. *Proceedings of the National Academy of Sciences*, 95(6), pp.2761–2766.
- Auger, K.R. et al., 1989. PDGF-dependent tyrosine phosphorylation stimulates production of novel polyphosphoinositides in intact cells. *Cell*, 57(1), pp.167–175.
- Averof, M. & Cohen, S.M., 1997. Evolutionary origin of insect wings from ancestral gills. *Nature*, 385(6617), pp.627–630.
- Bach, E.A. et al., 2003. A sensitized genetic screen to identify novel regulators and components of the *Drosophila* janus kinase/signal transducer and activator of transcription pathway. *Genetics*, 165(3), pp.1149–1166.
- Bader, R. et al., 2013. The IGFBP7 homolog Imp-L2 promotes insulin signaling in distinct neurons of the *Drosophila* brain. *Journal of cell science*, 126(Pt 12), pp.2571–2576.
- Baker, E.R., 1985. Body weight and the initiation of puberty. *Clinical obstetrics and gynecology*, 28(3), pp.573–579.
- Bakker, K., 1962. An Analysis of Factors Which Determine Success in Competition for Food Among Larvae of *Drosophila Melanogaster*. *Archives Néerlandaises de Zoologie*, 14(2), pp.200–281.
- Bakker, K., 1968. Selection for Rate of Growth and Its Influence On Competitive Ability

- of Larvae of *Drosophila Melanogaster*. *Netherlands Journal of Zoology*, 19(4), pp.541–595.
- Balázsi, G., van Oudenaarden, A. & Collins, J.J., 2011. Cellular decision making and biological noise: from microbes to mammals. *Cell*, 144(6), pp.910–925.
- Ballard, J.W.O., Melvin, R.G. & Simpson, S.J., 2008. Starvation resistance is positively correlated with body lipid proportion in five wild caught *Drosophila simulans* populations. *Journal of insect physiology*, 54(9), pp.1371–1376.
- Bar-Even, A. et al., 2006. Noise in protein expression scales with natural protein abundance. *Nature genetics*, 38(6), pp.636–643.
- Bargiello, T.A., Jackson, F.R. & Young, M.W., 1984. Restoration of circadian behavioural rhythms by gene transfer in *Drosophila*. *Nature*, 312(5996), pp.752–754.
- Barrio, L. & Milán, M., 2017. Boundary Dpp promotes growth of medial and lateral regions of the *Drosophila* wing. *eLife*, 6, p.663.
- Barrio, L., Dekanty, A. & Milán, M., 2014. MicroRNA-mediated regulation of Dp53 in the *Drosophila* fat body contributes to metabolic adaptation to nutrient deprivation. *Cell reports*, 8(2), pp.528–541.
- Bate, M. & Arias, A.M., 1991. The embryonic origin of imaginal discs in *Drosophila*. *Development (Cambridge, England)*, 112(3), pp.755–761.
- Bathgate, R.A.D. et al., 2013. Relaxin family peptides and their receptors. *Physiological reviews*, 93(1), pp.405–480.
- Baumann, A., Fujiwara, Y. & Wilson, T.G., 2010. Evolutionary divergence of the paralogs Methoprene tolerant (Met) and germ cell expressed (gce) within the genus *Drosophila*. *Journal of insect physiology*, 56(10), pp.1445–1455.
- Beck, Y., Pecasse, F. & Richards, G., 2004. Krüppel-homolog is essential for the coordination of regulatory gene hierarchies in early *Drosophila* development. *Developmental Biology*, 268(1), pp.64–75.
- Bejsovec, A. & Martinez Arias, A., 1991. Roles of wingless in patterning the larval

- epidermis of *Drosophila*. *Development (Cambridge, England)*, 113(2), pp.471–485.
- Bender, M. et al., 1997. *Drosophila* ecdysone receptor mutations reveal functional differences among receptor isoforms. *Cell*, 91(6), pp.777–788.
- Bennett, F.C. & Harvey, K.F., 2006. Fat Cadherin Modulates Organ Size in *Drosophila* via the Salvador/Warts/Hippo Signaling Pathway. *Current Biology*, 16(21), pp.2101–2110.
- Bergantiños, C., Corominas, M. & Serras, F., 2010. Cell death-induced regeneration in wing imaginal discs requires JNK signalling. *Development (Cambridge, England)*, 137(7), pp.1169–1179.
- Berger, E.M. & Dubrovsky, E.B., 2005. Juvenile Hormone Molecular Actions and Interactions During Development of *Drosophila melanogaster*. In *Insect Hormones. Vitamins & Hormones*. Elsevier, pp. 175–215.
- Bergman, A. & Siegal, M.L., 2003. Evolutionary capacitance as a general feature of complex gene networks. *Nature*, 424(6948), pp.549–552.
- Blomquist, G.E., 2009. Trade-off between age of first reproduction and survival in a female primate. *Biology letters*, 5(3), pp.339–342.
- Boone, E. et al., 2016. The Hippo signalling pathway coordinates organ growth and limits developmental variability by controlling *dilp8* expression. *Nature communications*, 7, p.13505.
- Brand, A.H. & Perrimon, N., 1993. Targeted gene expression as a means of altering cell fates and generating dominant phenotypes. *Development (Cambridge, England)*, 118(2), pp.401–415.
- Britton, J.S. & Edgar, B.A., 1998. Environmental control of the cell cycle in *Drosophila*: nutrition activates mitotic and endoreplicative cells by distinct mechanisms. *Development (Cambridge, England)*, 125(11), pp.2149–2158.
- Britton, J.S. et al., 2002. *Drosophila*'s insulin/PI3-kinase pathway coordinates cellular metabolism with nutritional conditions. *Developmental cell*, 2(2), pp.239–249.
- Broggiolo, W. et al., 2001. An evolutionarily conserved function of the *Drosophila* insulin

- receptor and insulin-like peptides in growth control. *Current biology : CB*, 11(4), pp.213–221.
- Broughton, S.J. et al., 2005. Longer lifespan, altered metabolism, and stress resistance in *Drosophila* from ablation of cells making insulin-like ligands. *Proceedings of the National Academy of Sciences*, 102(8), pp.3105–3110.
- Bryant, P.J., 1971. Regeneration and duplication following operations in situ on the imaginal discs of *Drosophila melanogaster*. *Developmental Biology*, 26(4), pp.637–651.
- Bussell, J.J. et al., 2014. Abdominal-B neurons control *Drosophila* virgin female receptivity. *Current biology : CB*, 24(14), pp.1584–1595.
- Caldwell, P.E., Walkiewicz, M. & Stern, M., 2005. Ras activity in the *Drosophila* prothoracic gland regulates body size and developmental rate via ecdysone release. *Current biology : CB*, 15(20), pp.1785–1795.
- Carvalho, G.B. et al., 2006. Allochrine modulation of feeding behavior by the Sex Peptide of *Drosophila*. *Current biology : CB*, 16(7), pp.692–696.
- Cáceres, L. et al., 2011. Nitric oxide coordinates metabolism, growth, and development via the nuclear receptor E75. *Genes & development*, 25(14), pp.1476–1485.
- Charles, J.-P. et al., 2011. Ligand-binding properties of a juvenile hormone receptor, Methoprene-tolerant. *Proceedings of the National Academy of Sciences of the United States of America*, 108(52), pp.21128–21133.
- Chen, C., 1996. The *Drosophila* insulin receptor is required for normal growth. *Endocrinology*, 137(3), pp.846–856.
- Chen, C.-L. et al., 2010. The apical-basal cell polarity determinant Crumbs regulates Hippo signaling in *Drosophila*. *Proceedings of the National Academy of Sciences of the United States of America*, 107(36), pp.15810–15815.
- Chippindale, A.K., Chu, T.J.F. & Rose, M.R., 1996. COMPLEX TRADE-OFFS AND THE EVOLUTION OF STARVATION RESISTANCE IN *DROSOPHILA MELANOGASTER*. *Evolution*, 50(2), pp.753–766.

- Cho, E. et al., 2006. Delineation of a Fat tumor suppressor pathway. *Nature genetics*, 38(10), pp.1142–1150.
- Clancy, D.J. et al., 2001. Extension of life-span by loss of CHICO, a Drosophila insulin receptor substrate protein. *Science (New York, N.Y.)*, 292(5514), pp.104–106.
- Clavería, C. et al., 2013. Myc-driven endogenous cell competition in the early mammalian embryo. *Nature*, 500(7460), pp.39–44.
- Cohen, B., Simcox, A.A. & Cohen, S.M., 1993. Allocation of the thoracic imaginal primordia in the Drosophila embryo. *Development (Cambridge, England)*, 117(2), pp.597–608.
- Cohen, B., Wimmer, E.A. & Cohen, S.M., 1991. Early development of leg and wing primordia in the Drosophila embryo. *Mechanisms of development*, 33(3), pp.229–240.
- Colombani, J. et al., 2003. A nutrient sensor mechanism controls Drosophila growth. *Cell*, 114(6), pp.739–749.
- Colombani, J. et al., 2005. Antagonistic actions of ecdysone and insulins determine final size in Drosophila. *Science (New York, N.Y.)*, 310(5748), pp.667–670.
- Colombani, J. et al., 2015. Drosophila Lgr3 Couples Organ Growth with Maturation and Ensures Developmental Stability. *Current biology : CB*, 25(20), pp.2723–2729.
- Colombani, J., Andersen, D.S. & Léopold, P., 2012. Secreted peptide Dilp8 coordinates Drosophila tissue growth with developmental timing. *Science (New York, N.Y.)*, 336(6081), pp.582–585.
- Cranna, N. & Quinn, L., 2009. Impact of steroid hormone signals on Drosophila cell cycle during development. *Cell Division*, 4(1), p.3.
- Crawford, J.D. & Osler, D.C., 1975. Body composition at menarche: The Frisch-Revelle hypothesis revisited. *Pediatrics*, 56(3), pp.449–458.
- Cymborowski, B. et al., 1982. Juvenile hormone titres and metabolism during starvation-induced supernumerary larval moulting of the tobacco hornworm, *Manduca sexta* L. *Journal of insect physiology*, 28(2), pp.129–135.

- Cyran, S.A. et al., 2003. vrille, Pdp1, and dClock form a second feedback loop in the *Drosophila* circadian clock. *Cell*, 112(3), pp.329–341.
- D'Avino, P.P. & Thummel, C.S., 1998. crooked legs encodes a family of zinc finger proteins required for leg morphogenesis and ecdysone-regulated gene expression during *Drosophila* metamorphosis. *Development (Cambridge, England)*, 125(9), pp.1733–1745.
- D'Avino, P.P. & Thummel, C.S., 2000. The ecdysone regulatory pathway controls wing morphogenesis and integrin expression during *Drosophila* metamorphosis. *Developmental Biology*, 220(2), pp.211–224.
- Da Ros, V.G. et al., 2013. Dampening the signals transduced through hedgehog via microRNA miR-7 facilitates notch-induced tumorigenesis. M. P. Scott, ed. *PLoS biology*, 11(5), p.e1001554.
- Daimon, T. et al., 2012. Precocious metamorphosis in the juvenile hormone-deficient mutant of the silkworm, *Bombyx mori*. D. L. Stern, ed. *PLoS genetics*, 8(3), p.e1002486.
- Danielsen, E.T., Moeller, M.E. & Rewitz, K.F., 2013. Nutrient signaling and developmental timing of maturation. *Current topics in developmental biology*, 105, pp.37–67.
- Das, D. & Arur, S., 2017. Conserved insulin signaling in the regulation of oocyte growth, development, and maturation. *Molecular reproduction and development*, 84(6), pp.444–459.
- Debat, V. & Peronnet, F., 2013. Asymmetric flies: the control of developmental noise in *Drosophila*. *Fly*, 7(2), pp.70–77.
- Debat, V. et al., 2011. Developmental stability: a major role for cyclin G in *Drosophila melanogaster*. G. Gibson, ed. *PLoS genetics*, 7(10), p.e1002314.
- Delanoue, R. et al., 2016. *Drosophila* insulin release is triggered by adipose Stunted ligand to brain Methuselah receptor. *Science (New York, N.Y.)*, 353(6307), pp.1553–1556.
- Delanoue, R., Slaidina, M. & Léopold, P., 2010. The steroid hormone ecdysone controls

- systemic growth by repressing dMyc function in *Drosophila* fat cells. *Developmental cell*, 18(6), pp.1012–1021.
- Demontis, F. & Perrimon, N., 2010. FOXO/4E-BP signaling in *Drosophila* muscles regulates organism-wide proteostasis during aging. *Cell*, 143(5), pp.813–825.
- Dewes, E., 1975. [Development of complete and bisected male genital disks after transplantation, and duration of host development in *Ephesia kuehniella* Z.]. *Wilhelm Roux's Archives of Developmental Biology*, 178(2), pp.167–183.
- Di Cara, F. & King-Jones, K., 2016. The Circadian Clock Is a Key Driver of Steroid Hormone Production in *Drosophila*. *Current Biology*, 26(18), pp.2469–2477.
- DiAngelo, J.R. & Birnbaum, M.J., 2009. Regulation of fat cell mass by insulin in *Drosophila melanogaster*. *Molecular and cellular biology*, 29(24), pp.6341–6352.
- Djawdan, M. et al., 1998. Metabolic reserves and evolved stress resistance in *Drosophila melanogaster*. *Physiological Zoology*, 71(5), pp.584–594.
- Dominguez, M., 2014. Oncogenic programmes and Notch activity: An “organized crime?” *Seminars in Cell & Developmental Biology*, 28, pp.78–85.
- Dominguez, M. & de Celis, J.F., 1998. A dorsal/ventral boundary established by Notch controls growth and polarity in the *Drosophila* eye. *Nature*, 396(6708), pp.276–278.
- Duman-Scheel, M., Johnston, L.A. & Du, W., 2004. Repression of dMyc expression by Wingless promotes Rbf-induced G1 arrest in the presumptive *Drosophila* wing margin. *Proceedings of the National Academy of Sciences*, 101(11), pp.3857–3862.
- Fain, M.J. & Riddiford, L.M., 1975. Juvenile hormone titers in the hemolymph during late larval development of the tobacco hornworm, *Manduca sexta* (L.). *The Biological bulletin*, 149(3), pp.506–521.
- Feinberg, E.H. et al., 2008. GFP Reconstitution Across Synaptic Partners (GRASP) defines cell contacts and synapses in living nervous systems. *Neuron*, 57(3), pp.353–363.
- Feng, K. et al., 2014. Ascending SAG neurons control sexual receptivity of *Drosophila* females. *Neuron*, 83(1), pp.135–148.

- Fernandez, R. et al., 1995. The *Drosophila* insulin receptor homolog: a gene essential for embryonic development encodes two receptor isoforms with different signaling potential. *The EMBO journal*, 14(14), pp.3373–3384.
- Ferres-Marco, D. et al., 2006. Epigenetic silencers and Notch collaborate to promote malignant tumours by Rb silencing. *Nature*, 439(7075), pp.430–436.
- Flier, J.S., 2004. Obesity wars: molecular progress confronts an expanding epidemic. *Cell*, 116(2), pp.337–350.
- Frisch, R.E. & Reville, R., 1970. Height and weight at menarche and a hypothesis of critical body weights and adolescent events. *Science (New York, N.Y.)*, 169(3943), pp.397–399.
- GangestadThornhill, 1999. Individual differences in developmental precision and fluctuating asymmetry: a model and its implications. *Journal of Evolutionary Biology*, 12(2), pp.402–416.
- Garcia-Bellido, A. & Merriam, J.R., 1971. Parameters of the wing imaginal disc development of *Drosophila melanogaster*. *Developmental Biology*, 24(1), pp.61–87.
- Garelli, A. et al., 2015. Dilp8 requires the neuronal relaxin receptor Lgr3 to couple growth to developmental timing. *Nature communications*, 6(1), p.8732.
- Garelli, A. et al., 2012. Imaginal discs secrete insulin-like peptide 8 to mediate plasticity of growth and maturation. *Science (New York, N.Y.)*, 336(6081), pp.579–582.
- Gebhardt, M.D. & Stearns, S.C., 1993. Phenotypic plasticity for life history traits in *Drosophila melanogaster*. I. Effect on phenotypic and environmental correlations. *Journal of Evolutionary Biology*, 6(1), pp.1–16.
- Géminard, C., Rulifson, E.J. & Léopold, P., 2009. Remote control of insulin secretion by fat cells in *Drosophila*. *Cell metabolism*, 10(3), pp.199–207.
- Giannakou, M.E. et al., 2004. Long-lived *Drosophila* with overexpressed dFOXO in adult fat body. *Science (New York, N.Y.)*, 305(5682), pp.361–361.
- Gibbens, Y.Y. et al., 2011. Neuroendocrine regulation of *Drosophila* metamorphosis

- requires TGFbeta/Activin signaling. *Development (Cambridge, England)*, 138(13), pp.2693–2703.
- Gilbert, L.I., 2004. Halloween genes encode P450 enzymes that mediate steroid hormone biosynthesis in *Drosophila melanogaster*. *Molecular and Cellular Endocrinology*, 215(1-2), pp.1–10.
- Gilbert, L.I., A Granger, N. & Roe, R.M., 2000. The juvenile hormones: historical facts and speculations on future research directions. *Insect Biochemistry and Molecular Biology*, 30(8-9), pp.617–644.
- Gilbert, S.F., Opitz, J.M. & Raff, R.A., 1996. Resynthesizing Evolutionary and Developmental Biology. *Developmental Biology*, 173(2), pp.357–372.
- Godlewski, J., Wang, S. & Wilson, T.G., 2006. Interaction of bHLH-PAS proteins involved in juvenile hormone reception in *Drosophila*. *Biochemical and biophysical research communications*, 342(4), pp.1305–1311.
- Gokhale, R.H. et al., 2016. Intra-organ growth coordination in *Drosophila* is mediated by systemic ecdysone signaling. *Developmental Biology*, 418(1), pp.135–145.
- Gong, Z. et al., 2010. Two pairs of neurons in the central brain control *Drosophila* innate light preference. *Science (New York, N.Y.)*, 330(6003), pp.499–502.
- Goodman, W.G. & Granger, N.A., 2005. The Juvenile Hormones. In *Comprehensive Molecular Insect Science*. Elsevier, pp. 319–408.
- Graves, J.L. et al., 1992. Desiccation, Flight, Glycogen, and Postponed Senescence in *Drosophila melanogaster*. *Physiological Zoology*, 65(2), pp.268–286.
- Grewal, S.S., 2009. Insulin/TOR signaling in growth and homeostasis: a view from the fly world. *The international journal of biochemistry & cell biology*, 41(5), pp.1006–1010.
- Grzeschik, N.A. et al., 2010. Lgl, aPKC, and Crumbs regulate the Salvador/Warts/Hippo pathway through two distinct mechanisms. *Current biology : CB*, 20(7), pp.573–581.
- Hadorn, E., 1963. Differenzierungsleistungen wiederholt fragmentierter Teilstücke männlicher Genitalscheiben von *Drosophila melanogaster* nach Kultur in vivo.

- Developmental Biology*, 7, pp.617–629.
- Halder, G. & Johnson, R.L., 2011. Hippo signaling: growth control and beyond. *Development (Cambridge, England)*, 138(1), pp.9–22.
- Hall, B.L. & Thummel, C.S., 1998. The RXR homolog ultraspiracle is an essential component of the *Drosophila* ecdysone receptor. *Development (Cambridge, England)*, 125(23), pp.4709–4717.
- Halme, A., Cheng, M. & Hariharan, I.K., 2010. Retinoids regulate a developmental checkpoint for tissue regeneration in *Drosophila*. *Current biology : CB*, 20(5), pp.458–463.
- Harbison, S.T. et al., 2004. Quantitative trait loci affecting starvation resistance in *Drosophila melanogaster*. *Genetics*, 166(4), pp.1807–1823.
- Hardin, P.E., 2005. The circadian timekeeping system of *Drosophila*. *Current biology : CB*, 15(17), pp.R714–22.
- Hardin, P.E., Hall, J.C. & Rosbash, M., 1990. Feedback of the *Drosophila* period gene product on circadian cycling of its messenger RNA levels. *Nature*, 343(6258), pp.536–540.
- Hay, N. & Sonenberg, N., 2004. Upstream and downstream of mTOR. *Genes & development*, 18(16), pp.1926–1945.
- Häder, T. et al., 2003. Control of triglyceride storage by a WD40/TPR-domain protein. *EMBO reports*, 4(5), pp.511–516.
- Helfrich-Förster, C. et al., 2007. Development and morphology of the clock-gene-expressing lateral neurons of *Drosophila melanogaster*. *The Journal of comparative neurology*, 500(1), pp.47–70.
- Helfrich-Förster, C. et al., 2002. The extraretinal eyelet of *Drosophila*: development, ultrastructure, and putative circadian function. *The Journal of neuroscience : the official journal of the Society for Neuroscience*, 22(21), pp.9255–9266.
- Hendrickx, F., Maelfait, J.P. & Lens, L., 2003. Relationship between fluctuating

- asymmetry and fitness within and between stressed and unstressed populations of the wolf spider *Pirata piraticus*. *Journal of Evolutionary Biology*, 16(6), pp.1270–1279.
- Herboso, L. et al., 2015. Ecdysone promotes growth of imaginal discs through the regulation of Thor in *D. melanogaster*. *Scientific Reports*, 5(1), p.344.
- Hodge, J.J.L., 2009. Ion channels to inactivate neurons in *Drosophila*. *Frontiers in molecular neuroscience*, 2, p.13.
- Hood, C.S., 1999. Asymmetry, Developmental Stability, and Evolution. Anders Pape Moller , John P. Swaddle. *The Quarterly Review of Biology*, 74(3), pp.346–347.
- Huang, J. et al., 2005. The Hippo signaling pathway coordinately regulates cell proliferation and apoptosis by inactivating Yorkie, the *Drosophila* Homolog of YAP. *Cell*, 122(3), pp.421–434.
- Hwangbo, D.S. et al., 2004. *Drosophila* dFOXO controls lifespan and regulates insulin signalling in brain and fat body. *Nature*, 429(6991), pp.562–566.
- Hyun, S. et al., 2005. *Drosophila* GPCR Han is a receptor for the circadian clock neuropeptide PDF. *Neuron*, 48(2), pp.267–278.
- Iga, M. & Kataoka, H., 2012. Recent Studies on Insect Hormone Metabolic Pathways Mediated by Cytochrome P450 Enzymes. *Biological and Pharmaceutical Bulletin*, 35(6), pp.838–843.
- Iga, M. et al., 2014. Pigment dispersing factor regulates ecdysone biosynthesis via bombyx neuropeptide G protein coupled receptor-B2 in the prothoracic glands of *Bombyx mori*. S. R. Palli, ed. *PloS one*, 9(7), p.e103239.
- Ikeshima-Kataoka, H. et al., 1997. Miranda directs Prospero to a daughter cell during *Drosophila* asymmetric divisions. *Nature*, 390(6660), pp.625–629.
- Ikeya, T. et al., 2002. Nutrient-dependent expression of insulin-like peptides from neuroendocrine cells in the CNS contributes to growth regulation in *Drosophila*. *Current biology : CB*, 12(15), pp.1293–1300.
- Inoki, K. et al., 2002. TSC2 is phosphorylated and inhibited by Akt and suppresses mTOR

- signalling. *Nature cell biology*, 4(9), pp.648–657.
- Irvine, K.D., 2012. Integration of intercellular signaling through the Hippo pathway. *Seminars in Cell & Developmental Biology*, 23(7), pp.812–817.
- Jaszczak, J.S. et al., 2015. Nitric Oxide Synthase Regulates Growth Coordination During *Drosophila melanogaster* Imaginal Disc Regeneration. *Genetics*, 200(4), pp.1219–1228.
- Jenett, A. et al., 2012. A GAL4-driver line resource for *Drosophila* neurobiology. *Cell reports*, 2(4), pp.991–1001.
- Jin, H., Kim, V.N. & Hyun, S., 2012. Conserved microRNA miR-8 controls body size in response to steroid signaling in *Drosophila*. *Genes & development*, 26(13), pp.1427–1432.
- Jindra, M., Palli, S.R. & Riddiford, L.M., 2013. The Juvenile Hormone Signaling Pathway in Insect Development. *Annual review of entomology*, 58(1), pp.181–204.
- Johnston, F.E. et al., 1971. Height, Weight and Age at Menarche and the “Critical Weight” Hypothesis. *Science (New York, N.Y.)*, 174(4014), pp.1148–1149.
- Johnston, L.A. & Edgar, B.A., 1998. Wingless and Notch regulate cell-cycle arrest in the developing *Drosophila* wing. *Nature*, 394(6688), pp.82–84.
- Johnston, L.A. & Sanders, A.L., 2003. Wingless promotes cell survival but constrains growth during *Drosophila* wing development. *Nature cell biology*, 5(9), pp.827–833.
- Johnston, L.A. et al., 1999. *Drosophila* myc regulates cellular growth during development. *Cell*, 98(6), pp.779–790.
- Justice, R.W. et al., 1995. The *Drosophila* tumor suppressor gene warts encodes a homolog of human myotonic dystrophy kinase and is required for the control of cell shape and proliferation. *Genes & development*, 9(5), pp.534–546.
- Kamoshida, Y. et al., 2012. Ecdysone receptor (EcR) suppresses lipid accumulation in the *Drosophila* fat body via transcription control. *Biochemical and biophysical research communications*, 421(2), pp.203–207.

- Katsuyama, T. et al., 2015. During *Drosophila* disc regeneration, JAK/STAT coordinates cell proliferation with Dilp8-mediated developmental delay. *Proceedings of the National Academy of Sciences of the United States of America*, 112(18), pp.E2327–36.
- Kayukawa, T. et al., 2012. Transcriptional regulation of juvenile hormone-mediated induction of Krüppel homolog 1, a repressor of insect metamorphosis. *Proceedings of the National Academy of Sciences of the United States of America*, 109(29), pp.11729–11734.
- Kiss, I. et al., 1988. Interactions and developmental effects of mutations in the Broad-Complex of *Drosophila melanogaster*. *Genetics*, 118(2), pp.247–259.
- KOEHN, R.K. & BAYNE, B.L., 2009. Towards a physiological and genetical understanding of the energetics of the stress response. *Biological Journal of the Linnean Society*, 37(1-2), pp.157–171.
- Koelle, M.R. et al., 1991. The *Drosophila* EcR gene encodes an ecdysone receptor, a new member of the steroid receptor superfamily. *Cell*, 67(1), pp.59–77.
- Konopova, B. & Jindra, M., 2008. Broad-Complex acts downstream of Met in juvenile hormone signaling to coordinate primitive holometabolite metamorphosis. *Development (Cambridge, England)*, 135(3), pp.559–568.
- Kumar, S. & Cakouros, D., 2004. Transcriptional control of the core cell-death machinery. *Trends in Biochemical Sciences*, 29(4), pp.193–199.
- Kyriacou, C.P. et al., 1990. Clock mutations alter developmental timing in *Drosophila*. *Heredity*, 64 (Pt 3), pp.395–401.
- la Cova, de, C. et al., 2004. *Drosophila* myc regulates organ size by inducing cell competition. *Cell*, 117(1), pp.107–116.
- Le Bourg, E., 2007. Does reproduction decrease longevity in human beings? *Ageing research reviews*, 6(2), pp.141–149.
- Lecuit, T. et al., 1996. Two distinct mechanisms for long-range patterning by Decapentaplegic in the *Drosophila* wing. *Nature*, 381(6581), pp.387–393.

- Leevers, S.J. et al., 1996. The Drosophila phosphoinositide 3-kinase Dp110 promotes cell growth. *The EMBO journal*, 15(23), pp.6584–6594.
- Leung, K.-C. et al., 2004. Estrogen Regulation of Growth Hormone Action. *Endocrine Reviews*, 25(5), pp.693–721.
- Li, D.W.-C. et al., 2005. Calcium-activated RAF/MEK/ERK signaling pathway mediates p53-dependent apoptosis and is abrogated by alpha B-crystallin through inhibition of RAS activation. *Molecular biology of the cell*, 16(9), pp.4437–4453.
- Li, M., Mead, E.A. & Zhu, J., 2011. Heterodimer of two bHLH-PAS proteins mediates juvenile hormone-induced gene expression. *Proceedings of the National Academy of Sciences of the United States of America*, 108(2), pp.638–643.
- Ling, C. et al., 2010. The apical transmembrane protein Crumbs functions as a tumor suppressor that regulates Hippo signaling by binding to Expanded. *Proceedings of the National Academy of Sciences of the United States of America*, 107(23), pp.10532–10537.
- Liu, X. et al., 1992. The period gene encodes a predominantly nuclear protein in adult Drosophila. *The Journal of neuroscience : the official journal of the Society for Neuroscience*, 12(7), pp.2735–2744.
- Liu, Y. et al., 2016. Drosophila insulin-like peptide 1 (DILP1) is transiently expressed during non-feeding stages and reproductive dormancy. *Scientific Reports*, 6(1), p.213.
- Livshits, G. & Kobylansky, E., 1991. Fluctuating asymmetry as a possible measure of developmental homeostasis in humans: a review. *Human biology*, 63(4), pp.441–466.
- Lodhi, I.J. et al., 2012. Inhibiting adipose tissue lipogenesis reprograms thermogenesis and PPAR γ activation to decrease diet-induced obesity. *Cell metabolism*, 16(2), pp.189–201.
- Luan, J.-B. et al., 2013. Silencing the ecdysone synthesis and signaling pathway genes disrupts nymphal development in the whitefly. *Insect Biochemistry and Molecular Biology*, 43(8), pp.740–746.
- Malpel, S., Klarsfeld, A. & Rouyer, F., 2002. Larval optic nerve and adult extra-retinal

- photoreceptors sequentially associate with clock neurons during *Drosophila* brain development. *Development (Cambridge, England)*, 129(6), pp.1443–1453.
- Mandaravally Madhavan, M. & Schneiderman, H.A., 1977. Histological analysis of the dynamics of growth of imaginal discs and histoblast nests during the larval development of *Drosophila melanogaster*. *Wilhelm Roux's Archives of Developmental Biology*, 183(4), pp.269–305.
- Marin, G. et al., 1994. The effects of estrogen priming and puberty on the growth hormone response to standardized treadmill exercise and arginine-insulin in normal girls and boys. *The Journal of clinical endocrinology and metabolism*, 79(2), pp.537–541.
- Markow, T.A. & Smith, L.D., 1979. Genetics of phototactic behavior in *Drosophila ananassae*, a member of the *melanogaster* species group. *Behavior genetics*, 9(1), pp.61–67.
- Marshall, L., Rideout, E.J. & Grewal, S.S., 2012. Nutrient/TOR-dependent regulation of RNA polymerase III controls tissue and organismal growth in *Drosophila*. *The EMBO journal*, 31(8), pp.1916–1930.
- Martin, F.A. & Morata, G., 2006. Compartments and the control of growth in the *Drosophila* wing imaginal disc. *Development (Cambridge, England)*, 133(22), pp.4421–4426.
- McBrayer, Z. et al., 2007. Prothoracicotropic hormone regulates developmental timing and body size in *Drosophila*. *Developmental cell*, 13(6), pp.857–871.
- Meissner, G.W. et al., 2016. Sex-specific regulation of *Lgr3* in *Drosophila* neurons. *Proceedings of the National Academy of Sciences of the United States of America*, 113(9), pp.E1256–65.
- Miguel-Aliaga, I., Thor, S. & Gould, A.P., 2008. Postmitotic specification of *Drosophila* insulinergic neurons from pioneer neurons. R. Nusse, ed. *PLoS biology*, 6(3), p.e58.
- Minakuchi, C., Namiki, T. & Shinoda, T., 2009. Krüppel homolog 1, an early juvenile hormone-response gene downstream of Methoprene-tolerant, mediates its anti-metamorphic action in the red flour beetle *Tribolium castaneum*. *Developmental*

Biology, 325(2), pp.341–350.

Minakuchi, C., Namiki, T., et al., 2008. RNAi-mediated knockdown of juvenile hormone acid O-methyltransferase gene causes precocious metamorphosis in the red flour beetle *Tribolium castaneum*. *The FEBS journal*, 275(11), pp.2919–2931.

Minakuchi, C., Zhou, X. & Riddiford, L.M., 2008. Krüppel homolog 1 (Kr-h1) mediates juvenile hormone action during metamorphosis of *Drosophila melanogaster*. *Mechanisms of development*, 125(1-2), pp.91–105.

Minkoff, C. & Wilson, T.G., 1992. The competitive ability and fitness components of the Methoprene-tolerant (Met) *Drosophila* mutant resistant to juvenile hormone analog insecticides. *Genetics*, 131(1), pp.91–97.

Mirth, C., Truman, J.W. & Riddiford, L.M., 2005. The role of the prothoracic gland in determining critical weight for metamorphosis in *Drosophila melanogaster*. *Current biology : CB*, 15(20), pp.1796–1807.

Mirth, C.K. & Riddiford, L.M., 2007. Size assessment and growth control: how adult size is determined in insects. *BioEssays*, 29(4), pp.344–355.

Mirth, C.K. et al., 2014. Juvenile hormone regulates body size and perturbs insulin signaling in *Drosophila*. *Proceedings of the National Academy of Sciences of the United States of America*, 111(19), pp.7018–7023.

Mirth, C.K., Truman, J.W. & Riddiford, L.M., 2009. The Ecdysone receptor controls the post-critical weight switch to nutrition-independent differentiation in *Drosophila* wing imaginal discs. *Development (Cambridge, England)*, 136(14), pp.2345–2353.

Miura, T., 2005. Developmental regulation of caste-specific characters in social-insect polyphenism. *Evolution & development*, 7(2), pp.122–129.

Moore, A.W. et al., 2000. A genomewide survey of basic helix-loop-helix factors in *Drosophila*. *Proceedings of the National Academy of Sciences*, 97(19), pp.10436–10441.

Mora, A. et al., 2004. PDK1, the master regulator of AGC kinase signal transduction. *Seminars in Cell & Developmental Biology*, 15(2), pp.161–170.

- Morante, J. & Desplan, C., 2011. Dissection and staining of *Drosophila* optic lobes at different stages of development. *Cold Spring Harbor protocols*, 2011(6), pp.652–656.
- Morata, G. & Ripoll, P., 1975. Minutes: mutants of *drosophila* autonomously affecting cell division rate. *Developmental Biology*, 42(2), pp.211–221.
- Moreno, E., 2008. Is cell competition relevant to cancer? *Nature reviews. Cancer*, 8(2), pp.141–147.
- Moreno, E. & Basler, K., 2004. dMyc Transforms Cells into Super-Competitors. *Cell*, 117(1), pp.117–129.
- Morrison, T., 2012. *The Regulation of Insulin-like Growth Factor 1 by Growth Hormone via Stat5b*,
- Myers, E.M., Yu, J. & Sehgal, A., 2003. Circadian control of eclosion: interaction between a central and peripheral clock in *Drosophila melanogaster*. *Current biology : CB*, 13(6), pp.526–533.
- Møller, A.P., 1997. Developmental stability and fitness: a review. *The American naturalist*, 149(5), pp.916–932.
- Møller, A.P. & Thornhill, R., 1997. A meta-analysis of the heritability of developmental stability. *Journal of Evolutionary Biology*, 10(1), p.1.
- NIJHOUT, H.F., 1981. Physiological Control of Molting in Insects. *American Zoologist*, 21(3), pp.631–640.
- Nijhout, H.F., 2003. The control of body size in insects. *Developmental Biology*, 261(1), pp.1–9.
- Nijhout, H.F. & Williams, C.M., 1974. Control of moulting and metamorphosis in the tobacco hornworm, *Manduca sexta* (L.): cessation of juvenile hormone secretion as a trigger for pupation. *The Journal of experimental biology*, 61(2), pp.493–501.
- Nilsson, O., 2003. Localization of estrogen receptors-alpha and -beta and androgen receptor in the human growth plate at different pubertal stages. *Journal of Endocrinology*, 177(2), pp.319–326.

- Nitabach, M.N. et al., 2006. Electrical hyperexcitation of lateral ventral pacemaker neurons desynchronizes downstream circadian oscillators in the fly circadian circuit and induces multiple behavioral periods. *The Journal of neuroscience : the official journal of the Society for Neuroscience*, 26(2), pp.479–489.
- Niwa, R. et al., 2008. Juvenile hormone acid O-methyltransferase in *Drosophila melanogaster*. *Insect Biochemistry and Molecular Biology*, 38(7), pp.714–720.
- Niwa, R. et al., 2010. Non-molting glossy/shroud encodes a short-chain dehydrogenase/reductase that functions in the “Black Box” of the ecdysteroid biosynthesis pathway. *Development (Cambridge, England)*, 137(12), pp.1991–1999.
- Okamoto, N. et al., 2009. A fat body-derived IGF-like peptide regulates postfeeding growth in *Drosophila*. *Developmental cell*, 17(6), pp.885–891.
- Oldham, S. & Hafen, E., 2003. Insulin/IGF and target of rapamycin signaling: a TOR de force in growth control. *Trends in cell biology*, 13(2), pp.79–85.
- Ou, Q., Magico, A. & King-Jones, K., 2011. Nuclear receptor DHR4 controls the timing of steroid hormone pulses during *Drosophila* development. D. S. Schneider, ed. *PLoS biology*, 9(9), p.e1001160.
- Palmer, A.R., 1994. Fluctuating asymmetry analyses: a primer. In *Developmental Instability: Its Origins and Evolutionary Implications*. Contemporary Issues in Genetics and Evolution. Dordrecht: Springer Netherlands, pp. 335–364.
- Palomero, T. et al., 2007. Mutational loss of PTEN induces resistance to NOTCH1 inhibition in T-cell leukemia. *Nature medicine*, 13(10), pp.1203–1210.
- Parker, N.F. & Shingleton, A.W., 2011. The coordination of growth among *Drosophila* organs in response to localized growth-perturbation. *Developmental Biology*, 357(2), pp.318–325.
- Partch, C.L., Green, C.B. & Takahashi, J.S., 2014. Molecular architecture of the mammalian circadian clock. *Trends in cell biology*, 24(2), pp.90–99.
- Parvy, J.-P. et al., 2005. A role for betaFTZ-F1 in regulating ecdysteroid titers during post-embryonic development in *Drosophila melanogaster*. *Developmental Biology*, 282(1),

pp.84–94.

- Pasco, M.Y. & Léopold, P., 2012. High sugar-induced insulin resistance in *Drosophila* relies on the lipocalin Neural Lazarillo. A. W. Shingleton, ed. *PLoS one*, 7(5), p.e36583.
- Pasquali, R., 2006. Obesity, fat distribution and infertility. *Maturitas*, 54(4), pp.363–371.
- Pecasse, F. et al., 2000. Krüppel-homolog, a Stage-Specific Modulator of the Prepupal Ecdysone Response, Is Essential for *Drosophila* Metamorphosis. *Developmental Biology*, 221(1), pp.53–67.
- Pettigrew, R. & Hamilton-Fairley, D., 1997. Obesity and female reproductive function. *British Medical Bulletin*, 53(2), pp.341–358.
- Poodry, C.A. & Woods, D.F., 1990. Control of the developmental timer for *Drosophila* pupariation. *Roux's archives of developmental biology : the official organ of the EDBO*, 199(4), pp.219–227.
- Potter, C.J., Pedraza, L.G. & Xu, T., 2002. Akt regulates growth by directly phosphorylating Tsc2. *Nature cell biology*, 4(9), pp.658–665.
- Price, J.L. et al., 1998. double-time is a novel *Drosophila* clock gene that regulates PERIOD protein accumulation. *Cell*, 94(1), pp.83–95.
- Prober, D.A. & Edgar, B.A., 2000. Ras1 Promotes Cellular Growth in the *Drosophila* Wing. *Cell*, 100(4), pp.435–446.
- Pursley, S., Ashok, M. & Wilson, T.G., 2000. Intracellular localization and tissue specificity of the Methoprene-tolerant (Met) gene product in *Drosophila melanogaster*. *Insect Biochemistry and Molecular Biology*, 30(8-9), pp.839–845.
- Quinn, L. et al., 2012. Steroid Hormones in *Drosophila*: How Ecdysone Coordinates Developmental Signalling with Cell Growth and Division. In *Steroids - Basic Science*. InTech.
- Rahn, P., 1972. [Investigations on the development of complete and divided imaginal wing discs by implantation in larvae of *Ephesia kühniella* Z]. *Wilhelm Roux' Archiv für*

- Entwicklungsmechanik der Organismen*, 170(1), pp.48–82.
- Rajan, A. & Perrimon, N., 2012. Drosophila cytokine unpaired 2 regulates physiological homeostasis by remotely controlling insulin secretion. *Cell*, 151(1), pp.123–137.
- Raser, J.M. & O'Shea, E.K., 2005. Noise in gene expression: origins, consequences, and control. *Science (New York, N.Y.)*, 309(5743), pp.2010–2013.
- Reiff, T. et al., 2015. Endocrine remodelling of the adult intestine sustains reproduction in Drosophila. *eLife*, 4, p.e06930.
- Reinking, J. et al., 2005. The Drosophila nuclear receptor e75 contains heme and is gas responsive. *Cell*, 122(2), pp.195–207.
- Rewitz, K.F. et al., 2009. The insect neuropeptide PTTH activates receptor tyrosine kinase torso to initiate metamorphosis. *Science (New York, N.Y.)*, 326(5958), pp.1403–1405.
- Rewitz, K.F., Yamanaka, N. & O'Connor, M.B., 2013. Developmental checkpoints and feedback circuits time insect maturation. *Current topics in developmental biology*, 103, pp.1–33.
- Rewitz, K.F., Yamanaka, N. & O'Connor, M.B., 2010. Steroid hormone inactivation is required during the juvenile-adult transition in Drosophila. *Developmental cell*, 19(6), pp.895–902.
- Riddiford, L.M., 1993. Hormone receptors and the regulation of insect metamorphosis. *Receptor*, 3(3), pp.203–209.
- Riddiford, L.M. & Ashburner, M., 1991. Effects of juvenile hormone mimics on larval development and metamorphosis of Drosophila melanogaster. *General and Comparative Endocrinology*, 82(2), pp.172–183.
- Riddiford, L.M. et al., 2010. A role for juvenile hormone in the prepupal development of Drosophila melanogaster. *Development (Cambridge, England)*, 137(7), pp.1117–1126.
- Rideout, E.J., Marshall, L. & Grewal, S.S., 2012. Drosophila RNA polymerase III repressor Maf1 controls body size and developmental timing by modulating tRNA^{iMet} synthesis and systemic insulin signaling. *Proceedings of the National Academy of*

- Sciences of the United States of America*, 109(4), pp.1139–1144.
- Rion, S. & Kawecki, T.J., 2007. Evolutionary biology of starvation resistance: what we have learned from *Drosophila*. *Journal of Evolutionary Biology*, 20(5), pp.1655–1664.
- Robertson, F.W., 2009. The ecological genetics of growth in *Drosophila* 6. The genetic correlation between the duration of the larval period and body size in relation to larval diet. *Genetical research*, 4(01), pp.74–92.
- Robinson, B.S. et al., 2010. Crumbs regulates Salvador/Warts/Hippo signaling in *Drosophila* via the FERM-domain protein Expanded. *Current biology : CB*, 20(7), pp.582–590.
- Royes, W.V. & Robertson, F.W., 1964. The nutritional requirements and growth relations of different species of *Drosophila*. *Journal of Experimental Zoology*, 156(1), pp.105–135.
- Rulifson, E.J., Kim, S.K. & Nusse, R., 2002. Ablation of insulin-producing neurons in flies: growth and diabetic phenotypes. *Science (New York, N.Y.)*, 296(5570), pp.1118–1120.
- Sancho, M. et al., 2013. Competitive interactions eliminate unfit embryonic stem cells at the onset of differentiation. *Developmental cell*, 26(1), pp.19–30.
- Saucedo, L.J. et al., 2003. Rheb promotes cell growth as a component of the insulin/TOR signalling network. *Nature cell biology*, 5(6), pp.566–571.
- Scaraffia, P.Y. & Miesfeld, R.L., 2013. Insect Biochemistry/Hormones. In *Encyclopedia of Biological Chemistry*. Elsevier, pp. 590–595.
- Schnebel, E.M. & Grossfield, J., 1986. Pupation-temperature range in 12 *Drosophila* species from different ecological backgrounds. *Experientia*, 42(6), pp.600–604.
- Schubiger, G., 1971. Regeneration, duplication and transdetermination in fragments of the leg disc of *Drosophila melanogaster*. *Developmental Biology*, 26(2), pp.277–295.
- Schubiger, G., Schubiger-Staub, M. & HADORN, E., 1969. [State of determination of imaginal blastemas in embryos of *Drosophila melanogaster* as revealed by mixing

- experiments]. *Wilhelm Roux' Archiv fur Entwicklungsmechanik der Organismen*, 163(1), pp.33–39.
- Selcho, M. et al., 2017. Central and peripheral clocks are coupled by a neuropeptide pathway in *Drosophila*. *Nature communications*, 8, p.15563.
- Service, P.M., 1987. Physiological Mechanisms of Increased Stress Resistance in *Drosophila melanogaster* Selected for Postponed Senescence. *Physiological Zoology*, 60(3), pp.321–326.
- Shabanpoor, F., Separovic, F. & Wade, J.D., 2009. Chapter 1 The Human Insulin Superfamily of Polypeptide Hormones. In *Insulin and IGFs*. Vitamins & Hormones. Elsevier, pp. 1–31.
- Shingleton, A.W., 2010. The regulation of organ size in *Drosophila*: physiology, plasticity, patterning and physical force. *Organogenesis*, 6(2), pp.76–87.
- Shingleton, A.W. et al., 2005. The temporal requirements for insulin signaling during development in *Drosophila*. L. Johnston, ed. *PLoS biology*, 3(9), p.e289.
- Siegal, M.L. & Bergman, A., 2002. Waddington's canalization revisited: Developmental stability and evolution. *Proceedings of the National Academy of Sciences*, 99(16), pp.10528–10532.
- Silva, E. et al., 2006. The tumor-suppressor gene fat controls tissue growth upstream of expanded in the hippo signaling pathway. *Current biology : CB*, 16(21), pp.2081–2089.
- Simpson, P., 1976. Analysis of the compartments of the wing of *Drosophila melanogaster* mosaic for a temperature-sensitive mutation that reduces mitotic rate. *Developmental Biology*, 54(1), pp.100–115.
- Simpson, P. & Morata, G., 1981. Differential mitotic rates and patterns of growth in compartments in the *Drosophila* wing. *Developmental Biology*, 85(2), pp.299–308.
- Simpson, P., Berreur, P. & Berreur-Bonnenfant, J., 1980. The initiation of pupariation in *Drosophila*: dependence on growth of the imaginal discs. *Journal of embryology and experimental morphology*, 57, pp.155–165.

- Sisk, C.L. & Foster, D.L., 2004. The neural basis of puberty and adolescence. *Nature neuroscience*, 7(10), pp.1040–1047.
- Siwicki, K.K. et al., 1988. Antibodies to the period gene product of *Drosophila* reveal diverse tissue distribution and rhythmic changes in the visual system. *Neuron*, 1(2), pp.141–150.
- Slaidina, M. et al., 2009. A *Drosophila* insulin-like peptide promotes growth during nonfeeding states. *Developmental cell*, 17(6), pp.874–884.
- Smith, C.M. et al., 2012. Relaxin-3 null mutation mice display a circadian hypoactivity phenotype. *Genes, brain, and behavior*, 11(1), pp.94–104.
- Smith-Bolton, R.K. et al., 2009. Regenerative growth in *Drosophila* imaginal discs is regulated by Wingless and Myc. *Developmental cell*, 16(6), pp.797–809.
- Stall, G.B., 1986. Anti Juvenile Hormone Agents. *Annual review of entomology*, 31(1), pp.391–429.
- Stern, D.L. & Emlen, D.J., 1999. The developmental basis for allometry in insects. *Development (Cambridge, England)*, 126(6), pp.1091–1101.
- Stocker, H. et al., 2003. Rheb is an essential regulator of S6K in controlling cell growth in *Drosophila*. *Nature cell biology*, 5(6), pp.559–565.
- Storelli, G. et al., 2011. *Lactobacillus plantarum* promotes *Drosophila* systemic growth by modulating hormonal signals through TOR-dependent nutrient sensing. *Cell metabolism*, 14(3), pp.403–414.
- Sun, G. & Irvine, K.D., 2011. Regulation of Hippo signaling by Jun kinase signaling during compensatory cell proliferation and regeneration, and in neoplastic tumors. *Developmental Biology*, 350(1), pp.139–151.
- Szabad, J. & Bryant, P.J., 1982. The mode of action of “discless” mutations in *Drosophila melanogaster*. *Developmental Biology*, 93(1), pp.240–256.
- Tabata, T. & Kornberg, T.B., 1994. Hedgehog is a signaling protein with a key role in patterning *Drosophila* imaginal discs. *Cell*, 76(1), pp.89–102.

- Taghert, P.H. & Shafer, O.T., 2006. Mechanisms of clock output in the *Drosophila* circadian pacemaker system. *Journal of biological rhythms*, 21(6), pp.445–457.
- Talbot, W.S., Swyryd, E.A. & Hogness, D.S., 1993. *Drosophila* tissues with different metamorphic responses to ecdysone express different ecdysone receptor isoforms. *Cell*, 73(7), pp.1323–1337.
- Tanenhaus, A.K., Zhang, J. & Yin, J.C.P., 2012. In vivo circadian oscillation of dCREB2 and NF- κ B activity in the *Drosophila* nervous system. P. H. Taghert, ed. *PLoS one*, 7(10), p.e45130.
- Tatar, M. et al., 2001. A mutant *Drosophila* insulin receptor homolog that extends life-span and impairs neuroendocrine function. *Science (New York, N.Y.)*, 292(5514), pp.107–110.
- Tatar, M., Bartke, A. & Antebi, A., 2003. The endocrine regulation of aging by insulin-like signals. *Science (New York, N.Y.)*, 299(5611), pp.1346–1351.
- Thummel, C.S., 1996. Flies on steroids--*Drosophila* metamorphosis and the mechanisms of steroid hormone action. *Trends in genetics : TIG*, 12(8), pp.306–310.
- Thummel, C.S., 1995. From embryogenesis to metamorphosis: the regulation and function of *Drosophila* nuclear receptor superfamily members. *Cell*, 83(6), pp.871–877.
- Thummel, C.S., 2001. Molecular mechanisms of developmental timing in *C. elegans* and *Drosophila*. *Developmental cell*, 1(4), pp.453–465.
- Thummel, C.S., 1990. Puffs and gene regulation ? molecular insights into the *Drosophila* ecdysone regulatory hierarchy. *BioEssays*, 12(12), pp.561–568.
- Tissenbaum, H.A. & Ruvkun, G., 1998. An insulin-like signaling pathway affects both longevity and reproduction in *Caenorhabditis elegans*. *Genetics*, 148(2), pp.703–717.
- TRUMAN, J. & RIDDIFORD, L., 2002. Insect Developmental Hormones and Their Mechanism of Action. In *Hormones, Brain and Behavior*. Elsevier, pp. 841–873.
- Truman, J.W. & Riddiford, L.M., 1974. Hormonal Mechanisms Underlying Insect Behaviour. In *Advances in Insect Physiology*. Elsevier, pp. 297–352.

- Tyler, D.M. & Baker, N.E., 2007. Expanded and fat regulate growth and differentiation in the *Drosophila* eye through multiple signaling pathways. *Developmental Biology*, 305(1), pp.187–201.
- Valen, L.V., 1962. A Study of Fluctuating Asymmetry. *Evolution*, 16(2), p.125.
- Vallejo, D.M. et al., 2015. A brain circuit that synchronizes growth and maturation revealed through Dilp8 binding to Lgr3. *Science (New York, N.Y.)*, 350(6262), p.aac6767.
- Vosshall, L.B. et al., 1994. Block in nuclear localization of period protein by a second clock mutation, timeless. *Science (New York, N.Y.)*, 263(5153), pp.1606–1609.
- WADDINGTON, C.H., 1942. CANALIZATION OF DEVELOPMENT AND THE INHERITANCE OF ACQUIRED CHARACTERS. *Nature*, 150(3811), pp.563–565.
- Wagner, A., 2008. Robustness and evolvability: a paradox resolved. *Proceedings of the Royal Society B: Biological Sciences*, 275(1630), pp.91–100.
- Wang, M.-H. et al., 2004. Environment-dependent survival of *Drosophila melanogaster*: a quantitative genetic analysis. *Aging cell*, 3(3), pp.133–140.
- Wang, S., Baumann, A. & Wilson, T.G., 2007. *Drosophila melanogaster* Methoprene-tolerant (Met) gene homologs from three mosquito species: Members of PAS transcriptional factor family. *Journal of insect physiology*, 53(3), pp.246–253.
- Warren, J.T. et al., 2006. Discrete pulses of molting hormone, 20-hydroxyecdysone, during late larval development of *Drosophila melanogaster*: correlations with changes in gene activity. *Developmental dynamics : an official publication of the American Association of Anatomists*, 235(2), pp.315–326.
- Wheeler, D.E. & Nijhout, H.F., 2003. A perspective for understanding the modes of juvenile hormone action as a lipid signaling system. *BioEssays*, 25(10), pp.994–1001.
- Wieschaus, E. & Gehring, W., 1976. Clonal analysis of primordial disc cells in the early embryo of *Drosophila melanogaster*. *Developmental Biology*, 50(2), pp.249–263.
- Wigby, S. et al., 2010. Insulin signalling regulates remating in female *Drosophila*.

- Proceedings of the Royal Society B: Biological Sciences*, 278(1704), pp.424–431.
- WIGGLESWORTH, V.B., 1934. Factors Controlling Moulting and “Metamorphosis” in an Insect. *Nature*, 133(3367), pp.725–726.
- WIGGLESWORTH, V.B., 1954. Secretion of Juvenile Hormone by the Corpus Allatum of Calliphora. *Nature*, 174(4429), pp.556–556.
- Willecke, M. et al., 2006. The Fat Cadherin Acts through the Hippo Tumor-Suppressor Pathway to Regulate Tissue Size. *Current Biology*, 16(21), pp.2090–2100.
- Wilson, T.G., 2005. Interaction Between Hormonal Signaling Pathways in *Drosophila melanogaster* as Revealed by Genetic Interaction Between Methoprene-tolerant and Broad-Complex. *Genetics*, 172(1), pp.253–264.
- Wilson, T.G. & Fabian, J., 1986. A *Drosophila melanogaster* mutant resistant to a chemical analog of juvenile hormone. *Developmental Biology*, 118(1), pp.190–201.
- Wilson, T.G., DeMoor, S. & Lei, J., 2003. Juvenile hormone involvement in *Drosophila melanogaster* male reproduction as suggested by the Methoprene-tolerant²⁷ mutant phenotype. *Insect Biochemistry and Molecular Biology*, 33(12), pp.1167–1175.
- Xie, X.-J. et al., 2015. CDK8-Cyclin C Mediates Nutritional Regulation of Developmental Transitions through the Ecdysone Receptor in *Drosophila*. D. S. Schneider, ed. *PLoS biology*, 13(7), p.e1002207.
- Xu, T. et al., 1995. Identifying tumor suppressors in genetic mosaics: the *Drosophila* *lats* gene encodes a putative protein kinase. *Development (Cambridge, England)*, 121(4), pp.1053–1063.
- Yamanaka, N., Marqués, G. & O'Connor, M.B., 2015. Vesicle-Mediated Steroid Hormone Secretion in *Drosophila melanogaster*. *Cell*, 163(4), pp.907–919.
- Yamanaka, N., Rewitz, K.F. & O'Connor, M.B., 2013. Ecdysone control of developmental transitions: lessons from *Drosophila* research. *Annual review of entomology*, 58(1), pp.497–516.
- Yamanaka, N., Romero, N.M., et al., 2013. Neuroendocrine control of *Drosophila* larval

- light preference. *Science (New York, N.Y.)*, 341(6150), pp.1113–1116.
- Yang, C.-H. et al., 2008. Drosophila egg-laying site selection as a system to study simple decision-making processes. *Science (New York, N.Y.)*, 319(5870), pp.1679–1683.
- Yao, T.P. et al., 1992. Drosophila ultraspiracle modulates ecdysone receptor function via heterodimer formation. *Cell*, 71(1), pp.63–72.
- Yasuyama, K. et al., 2006. Synaptic connections between eyelet photoreceptors and pigment dispersing factor-immunoreactive neurons of the blowfly *Protophormia terraenovae*. *The Journal of comparative neurology*, 494(2), pp.331–344.
- Yoshii, T. et al., 2009. The neuropeptide pigment-dispersing factor adjusts period and phase of Drosophila's clock. *The Journal of neuroscience : the official journal of the Society for Neuroscience*, 29(8), pp.2597–2610.
- Yoshiyama, T. et al., 2006. Neverland is an evolutionally conserved Rieske-domain protein that is essential for ecdysone synthesis and insect growth. *Development (Cambridge, England)*, 133(13), pp.2565–2574.
- Yoshiyama-Yanagawa, T. et al., 2011. The Conserved Rieske Oxygenase DAF-36/Neverland Is a Novel Cholesterol-metabolizing Enzyme. *Journal of Biological Chemistry*, 286(29), pp.25756–25762.
- Yue, T., Tian, A. & Jiang, J., 2012. The Cell Adhesion Molecule Echinoid Functions as a Tumor Suppressor and Upstream Regulator of the Hippo Signaling Pathway. *Developmental cell*, 22(2), pp.255–267.
- Zehring, W.A. et al., 1984. P-element transformation with period locus DNA restores rhythmicity to mutant, arrhythmic *Drosophila melanogaster*. *Cell*, 39(2 Pt 1), pp.369–376.
- Zhang, C. et al., 2015. The ecdysone receptor coactivator Taiman links Yorkie to transcriptional control of germline stem cell factors in somatic tissue. *Developmental cell*, 34(2), pp.168–180.
- Zheng, X. et al., 2003. TGF- β Signaling Activates Steroid Hormone Receptor Expression during Neuronal Remodeling in the Drosophila Brain. *Cell*, 112(3), pp.303–315.

Žitňan, D. et al., 2007. Complex steroid–peptide–receptor cascade controls insect ecdysis.
General and Comparative Endocrinology, 153(1-3), pp.88–96.

